AN INVESTIGATION INTO THE SUSPENDED SEDIMENT FLUX AND DYNAMICS OF THE MGENI ESTUARY, DURBAN

by

ROHAIDA ABED

Submitted in fulfillment of the academic
requirements for the degree of
Master of Science in the
School of Environmental Sciences,
University of KwaZulu-Natal,
Durban

August 2009

ABSTRACT

This dissertation focuses on both a hydrodynamic and geomorphological study of the Mgeni Estuary. Within the hydrodynamic study, the channel discharge, suspended sediment fluxes and estuary bed sediment characteristics and dynamics were established. Within the geomorphological study, cross-shore topographical surveying of the lower estuary region, measurement of slope angles and surface sediment characteristics were established. The results of this study illustrate strong seasonal variability.

Maximum channel discharges, suspended sediment concentrations and fluxes occur during the summer months, as a result of large amounts of rainfall. Furthermore, maximum suspended sediment concentrations and fluxes occur during spring tides, as a result of a greater tidal range, which enhances bed sediment re-suspension via concomitant increased turbulence. Generally, maximum fluxes occur along the flood tide and ebb tide, during spring tides and neap tides, respectively, which suggest that the estuary is a sink for marine sediment during spring tides and an exporter of sediment during neap tides. The estuary bed sediments are very well sorted and predominantly classified as near-symmetrical, as a result of strong tidal currents that constantly transport and re-work the sediments. On average, the bed sediments are medium sand and in all probability are largely derived from the marine environment. Estuary bed sediments contain negligible mud and organic contents, which as research suggests, is common in such high-energy estuary mouths.

Apart from the seasonal variability, the survey profiles and surface sediments illustrate alongshore and cross-shore variations. The profiles become flatter and finer from the Beachwood Mangroves section of the barrier towards the estuary mouth in the south, as a result of sheltering due to the engineered groyne, conforming to Bascom (1959) and Komar's (1998) sheltered and exposed coasts concept. The survey profiles conform to the summer and winter profiles put forward by Dardis and Grindley (1988). The winter profiles consist of higher, distinct berms and berm crests, as well as vertical erosional faces, whilst the summer profiles are lower, flatter, and consist of unclear berms and berm crests. Sediments are coarsest along the lagoonward slope and finest within the estuary. A strong, positive correlation was generated between slope angle and mean grain size. Despite the low organic contents, the estuary sediments consist of the highest values of organic matter, with the beach and barrier sediments displaying negligible amounts. Thus, the Mgeni can be classified as a very dynamic and active zone.

PREFACE

The experimental work described in this dissertation was carried out in the School of Environmental Sciences, University of KwaZulu-Natal, Durban, from February 2007 to August 2009, under the supervision of Dr. S. Pillay.

These studies represent original work by the author and have not otherwise been submitted in any form for any degree or diploma to any tertiary institution. Where use has been made of the work of others it is duly acknowledged in the text.

FACULTY OF SCIENCE AND AGRICULTURE

DECLARATION 1 - PLAGIARISM

I, ……Rohaida Abed……..……., declare that

1. The research reported in this thesis, except where otherwise indicated, is my original research.

2. This thesis has not been submitted for any degree or examination at any other university.

3. This thesis does not contain other persons' data, pictures, graphs or other information, unless specifically acknowledged as being sourced from other persons.

4. This thesis does not contain other persons' writing, unless specifically acknowledged as being sourced from other researchers. Where other written sources have been quoted, then:
   a. Their words have been re-written but the general information attributed to them has been referenced
   b. Where their exact words have been used, then their writing has been placed in italics and inside quotation marks, and referenced.

5. This thesis does not contain text, graphics or tables copied and pasted from the Internet, unless specifically acknowledged, and the source being detailed in the thesis and in the References sections.

Signed: ……

As the candidate's supervisor I have/have not approved this thesis/dissertation for submission.

Signed: …… Name: …… Date: ……

TABLE OF CONTENTS

LIST OF FIGURES

LIST OF TABLES

LIST OF ABBREVIATIONS

EKZNW	Ezemvelo KwaZulu-Natal Wildlife
LOI	Loss on Ignition
MAR	Mean Annual Runoff
SANHO	South African Navy Hydrographic Office
SAWS	South African Weather Services
SOER	State of the Estuaries Report
SSC	Suspended Sediment Concentration
TOCE	Temporarily Open Closed Estuary
WRC	Water Research Commission
XS	Cross-section

ACKNOWLEDGEMENTS

Firstly, thank you to my guiding light, God, who has given me strength and courage throughout my project and for keeping us safe and free from getting washed out to sea in the high-energy river that is the Mgeni. Also, big up to the angels on my side!

To my entire family, especially my parents and my sister, I thank you from the bottom of my heart for helping me with every aspect of my project from field sampling to lab work, and for always encouraging and supporting me. I would also like to thank my parents for affording me the opportunity to do what I love, I am forever grateful. To my sister, Nadia, thank you for always listening to me go on about my project all the time, now you are probably the most estuary clued-up 15 year old out there. Thanks also to my grandparents, for the support.

This project would seriously not have been possible without the enormous help I received from my family and friends, during both my fieldwork and lab work. My sincerest appreciation goes out to my dad, mum, sister, uncles Ravi, Kercy, Collin, aunts Shen and Rachel, and to my truckload of cousins, Adiel, Ameer, Nathaniel, Irshaad ("I dropped the sample"), Rayhaan and Muji.

To my friends, who also came out in full force, be it rain or shine (both in the field and lab), I thank you all immensely: Zar (Kamza), Cherry, Devendri, Jam, Cass, Sarah, Becky, Jayshree, Davina, Kirsten, Arshad, Vicks, Dhiren, Kyle, Nitesh, Shezi, Mbuso, Jon and Jono. You peeps are the best and most helpful peeps I know, and I am forever grateful. I would especially like to thank Devendri, Cherry, Cass, Kyle, Zar, Arshad and Becky for helping me with transporting and carrying my samples to the lab. Devendri and Cass, I will never forget our UKZN Main Gate "Do You Know The Rules" incident, when we were trying to bring our samples up to the lab. Nor will I forget the many fun field adventures.

To my supervisor, Dr. S. Pillay, I thank you immensely for your guidance, expertise, and assistance with my project, and for organizing funding for my second semester. I would also like to thank the UKZN Graduate Assistance for providing a scholarship for two years of my study. Mr. Isaac Abboy of the Department of Environmental Sciences, I truly thank you for all your help throughout my project, with lab procedures and field equipment. My sincerest gratitude goes out to Tirusha Thambiran, who gave her time so generously to proof read my project and for guiding me. To Professor Gerry Garland (G), I thank you very much for your help and for always replying to several of my queries regarding my project. You have been an inspiration and your extensive knowledge of the coast has urged me to work whole heartedly. Many thanks to Andrew Green

and Suzanne Garden, who readily assisted and guided me, especially with field work planning. Thanks also to Kerry Philp for providing help and advice whenever it was needed.

I would like to sincerely thank Felicia Tiba of Umgeni Water for providing me with water quality data for the Mgeni River, as well as Glenda Swart and Mzukisi Gwata of the South African Weather Services for providing weather data, and the Hydrographer of the South African Navy for providing tide tables and tide information for the coastline of Durban. I am grateful to Basil Pather of Ezemvelo KZN Wildlife Beachwood Mangroves Reserve for permitting access to the Mgeni Estuary mouth. I would also like to thank Andrew Mather and Godfrey Vella of the Ethekwini Municipality, as well as Andre Theron of CSIR Stellenbosch for providing beach sediment data and for replying to my several queries. Thanks also to Professor Derek Stretch of Civil Engineering for providing me with relevant information. I am very thankful to Professor Andrew Kindness for allowing me use of the Chemistry Lab at Howard College. Thanks also to Mrs. Naidoo and Mr. Miler of the chemistry department for assisting me with acquisition of equipment.

I would also like to thank my Uncle Laz for allowing me use of his printer.

Overall, it's like I waited my whole life for this day, for real, so to everyone who has helped me with my project, I cannot thank you enough and I am very grateful. Also, despite the poor condition of the Mgeni Estuary, in terms of litter and water quality, to me it will always be my favourite estuary and I really hope that the pollution decreases.

Big up to 5Fm Music for rocking the republic and keeping me sane during my long hours in the lab.

Peace out!

CHAPTER 1:
INTRODUCTION

1.1. Background

The South African coastline, which spans approximately 3000 km (Morant and Quinn, 1999; Schumann, 2003), contains an abundance of estuaries. Whitfield (2000) documented about 250 estuaries along the South African coastline. Throughout South Africa, estuaries collectively comprise a total area of 70 000 ha, thus making these coastal features highly productive and significant (Turpie *et al*., 2002; Scharler and Baird, 2005). Furthermore, estuaries are considered to play a major role in the geomorphology of the coast (Cooper *et al*., 1999; Cooper, 2001).

Coastal systems such as estuaries are classified as highly productive ecosystems, as they contain economic, aesthetic and recreational value (Breen and McKenzie, 2001; Cooper, 2001; Smakhtin, 2004; Scharler and Baird, 2005). Estuaries provide numerous goods and services (Breen and McKenzie, 2001; Cooper, 2001; Hay, 2007), both on an anthropogenic and environmental scale. These environmental benefits include erosion control, water supply, waste treatment and sediment supply to the surrounding beaches, sandbars and sand banks (Breen and McKenzie, 2001).

"*Environmental sensitivity*" has increased over the past few years, along with the general interest in estuaries (Allanson and Baird, 1999, p.1). Morant and Quinn (1999) indicate that, excluding the influence of catchment land uses and activities, estuaries are regarded as pressurized due to the high-wave energy and rugged coastline of South Africa. As a result, estuaries are classified as sheltered regions along this coastline and are therefore under pressure as they are favoured and form a prime area for many residential, industrial and recreational developments (Morant and Quinn, 1999; Breen and McKenzie, 2001; Schumann, 2003; Scharler and Baird, 2005). As large amounts of people flock to these sensitive ecosystems, their activities and developments negatively impact and weaken the natural status and functioning of the estuaries (Schumann, 2003; Scharler and Baird, 2005). These anthropogenic influences range from freshwater abstraction within catchments to water pollution and harbour developments (Morant and Quinn, 1999; Scharler and Baird, 2005). Estuaries are receptors of water derived from its catchments; hence it reflects catchment land uses (Morant and Quinn, 1999; Scharler and Baird, 2005). Therefore, poor land use practices and catchment management may result in ultimate deterioration and degradation of estuaries. Turpie *et al*. (2002) points out that estuaries are classified as one of the most vulnerable ecosystems in South Africa.

The obvious value of estuaries in terms of their provision of several goods and services makes it vital that the users of estuaries obtain a firm understanding of the resultant impacts on these sensitive systems. Thus, there is major research interest on a global scale, dedicated to understanding the structure and functioning of estuaries (Green, 2004), making estuaries an important area of study. There are various areas of research that occur within estuaries ranging from the assessment of estuarine conservation priority, carried out by Turpie *et al*. (2002), the management of estuaries, performed by Morant and Quinn (1999); Breen and McKenzie (2001) and Hay *et al*. (2005), to the geomorphology and sedimentology of estuaries as documented by Cooper (1991a; 1993; 2001; 2002); Cooper *et al*. (1999) and Beck *et al*. (2004). Allanson and Baird (1999) explain that over the years, estuarine research has shifted from a focus on the ecology of estuarine plants and animals, towards processes within the water column, surface sediments, as well as nutrients and particles.

Sediments are transported within, deposited in and eroded from estuaries (Hay *et al*., 2005). Sediment is constantly changing and has practical value, since sediment supply from estuaries to the nearshore zone, as well as from the nearshore zone to estuaries is essential to sustain beaches and the surrounding regions. Schumann (2003) indicates that understanding sediment movement and the physical processes that influence it within the coastal zone is important for good management practices.

1.2. Motivation for study

Estuaries are important in South Africa as they provide several environmental and economic benefits, as well as form a favoured area for recreational and commercial services (Schumann, 2003). The Mgeni River is hydrologically important as it forms a source of water for both Durban and Pietermaritzburg (Begg, 1978).

"*Sedimentary processes are natural and defining features of South African estuaries*" (Hay *et al.*, 2005, p.3), highlighting the sheer importance of sediment within estuaries. Sediment deposited within estuaries structures the fundamental base for the estuarine environment, and the type of sediment deposited, plays an important role in classifying the nature of these systems (Hay *et al*., 2005). The transport of fine grained suspended sediments is vital within estuaries, as they form a mode for which nutrients and pollutants are transported (Chen *et al*., 2006; Hossain *et al*., 2004).

It is evident that the geomorphology of KwaZulu-Natal estuaries is well researched (Green, 2004). There are several works relating to the sediment dynamics of the Mgeni Estuary, such as Blackshaw (1985); Cooper and Mason (1987); Cooper (1991a; 1993; 2001; 2002); Garland and

Moleko (2000) and Ngetar (2002). The Mgeni Estuary is well understood and has a good information record, according to Whitfield (2000); however most of these studies are focused mainly on the upper regions of the Mgeni. Research indicates that there is a lack of published information directly relating to lower barrier and estuarine environment, including the mouth or inlet of the Mgeni Estuary, with the exception of Cooper and Mason (1987) and Cooper (1991a; 1993), which is situated within the lower extent of the estuary, seaward bound of the M4 Bridge.

In contrast, there is a paucity of published literature that directly relates to the sediment supply and dynamics of the Mgeni Estuary inlet. Clearly, a research gap exists on the sediment flux, channel discharges, as well as geomorphological and sedimentological characteristics within this particular region of the Mgeni Estuary. Therefore, such research will contribute to a greater awareness and understanding of the natural functioning of the Mgeni mouth, as well as other estuaries and beaches, in terms of geomorphology, sediment supply, sediment movements and characteristics.

In order to achieve this, it is important to perform a study that deals with the discharge and suspended sediment input and output of the Mgeni Estuary inlet, which supplies the surrounding beaches, barrier and sandbars. Municipalities are reliant on beaches because they increase tourism and ultimately feed the economy; hence a study of this nature is justifiably important.

1.3. Aim

This research aims to quantify and assess the discharge and suspended sediment flux of the Mgeni Estuary inlet, as well as to study the geomorphology of the lower Mgeni, including an investigation of the concomitant implications on the sediment dynamics and geomorphology.

1.4. Objectives

The objectives of this study, work in conjunction with the aim, and are as follows:

1. To quantify the discharge and suspended sediment, input and output from the Mgeni Estuary, during specific conditions, as follows:
    - mouth state,
    - seasonal variations,
    - tidal cycles, and
    - extreme events (floods and droughts).

2. To assess the contribution of suspended sediment flux to the nearshore/beach and estuarine environments, under the specified conditions.
3. To investigate the sediment dynamics of the Mgeni Estuary, in terms of the current velocity, suspended and estuarine bed sediment, hence sediment movement.
4. To determine the sediment and geomorphological characteristics of the estuarine, barrier and coastal environment, through topographical surveying.
5. To study the concomitant implications for coastal and estuarine geomorphology, such as erosion and accretion.

The fulfillment of the above-mentioned research objectives will allow the overall understanding of the discharge and suspended sediment dynamics of the Mgeni Estuary mouth, as well as shed light onto whether the system is an overall importer or exporter of suspended sediment, and the geomorphological and sedimentological characteristics of the estuarine, barrier and beach environments.

1.5. Structure of Dissertation

Chapter Two outlines the physical site characteristics of the selected study area, which is the Mgeni Estuary, Durban. Chapters Three and Four includes a summary of the findings of past research carried out in the Mgeni Estuary, and outlines the literature and theoretical concepts pertaining to this study. The main theoretical concepts outlined include the coastal zone, sediments and flows, estuaries, beaches, as well as the processes that influence and shape these coastal features. Chapter Five includes the main fieldwork methods, laboratory analysis techniques and data analysis techniques adopted throughout the study sampling period, which comprised two fieldwork components such as the geomorphological study and hydrodynamic study. Chapter Six presents the results and discussion of the geomorphological study; including topographical survey profiles, beach gradient and sediment textural and compositional characteristics. Chapter Seven presents the results and discussion of the hydrodynamic study; including channel discharge, suspended sediment concentrations and fluxes, as well as estuary bed sediment textural and compositional characteristics. Chapter Eight outlines the sediment and hydrodynamic characteristics of the downstream inlet of the Mgeni, including an analysis of the geomorphology of the lower estuary through aerial and digital photography. Chapter Nine outlines the conclusions of the study, followed by limitations and recommendations for future research.

CHAPTER 2:
REGIONAL SETTING

2.1. Introduction

The Mgeni Estuary, located towards the north of Durban, formed the study area of this research. The estuary is a large system (Cooper, 1991a; 1993); therefore the area of study in this research was focused on the Lower Mgeni, which entails the estuarine and coastal region that lies seaward bound of the M4 Bridge, which is illustrated below in Figure 2.1.

Figure 2.1. Aerial photograph illustrating the study area, with particular reference to the lower estuary, seaward of the M4 Bridge (Ethekwini Municipality, 2008).

2.2. Locality

2.2.1. Mgeni Estuary

The Mgeni Estuary is situated 5 km north of Durban, at approximately 29° 48' S and 31° 02' E (Begg, 1978; 1984). The Mgeni River flows through the north of Durban, where it enters the Indian Ocean (Cooper, 1991a; 1993; Garland and Moleko, 2000). Figure 2.2 (Page 6), illustrates the locality of the Mgeni Estuary. The inlet of the Mgeni Estuary is bounded by an artificial groyne on its southern bank (Cooper, 1991a; 1993). The estuary contains tidal and salinity variations that extend 2.5 km upstream, within its lowest course (Cooper and Mason, 1987; Cooper, 1991a; 1993). The estuary is positioned in a narrow alluvial valley, which is constricted by bedrock (Cooper, 1993).

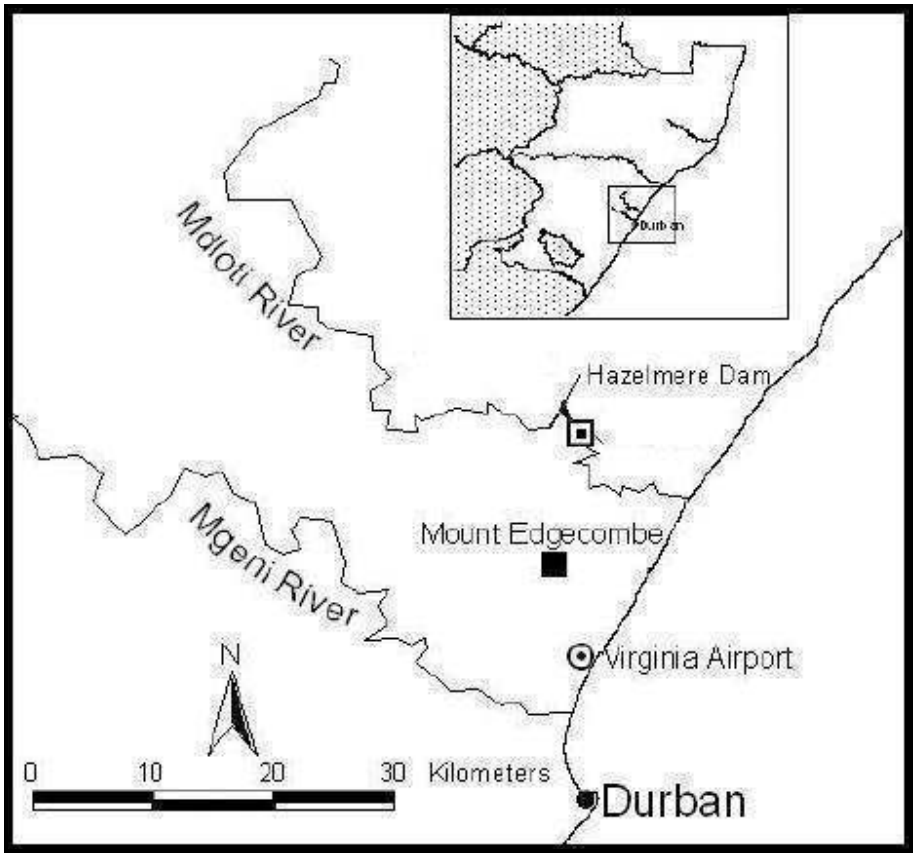

Figure 2.2. Locality map of the Mgeni Estuary, illustrating the Virginia Airport and the Mdloti River in the north (Garden and Garland, 2005).

The concave coastline between the Durban Harbour mouth and the town of Umhlanga Rocks is classified as a wide sandy beach, known as the Durban Bight (Cooper, 1991b). The sandy beach towards the south of the Mgeni Estuary (Begg, 1978; Cooper, 1995a) previously contained a vegetated dune cordon, which is presently damaged due to road construction (Cooper, 1995b). The stretch of beach positioned between the Mgeni and the Durban Harbour is the most anthrogenically influenced section along the KwaZulu-Natal coastline (Cooper, 1991b).

The estuary is highly accessible, owing to several bridges and roads that surround it (Begg, 1978). There are access roads to the mouth along the southern bank (Begg, 1978), as well as to the entrance of the Beachwood Mangroves on the northern side, which leads onto the beach, estuary and barrier. There are four major bridges located across the Mgeni Estuary system namely the, Ellis Brown Viaduct (M4 Bridge), Athlone Bridge, Connaught Bridge, as well as a railway bridge, located above the Connaught Bridge (Begg, 1978; Ngetar, 2002). Figure 2.3 (Page 7) illustrates the bridges present across the Mgeni Estuary.

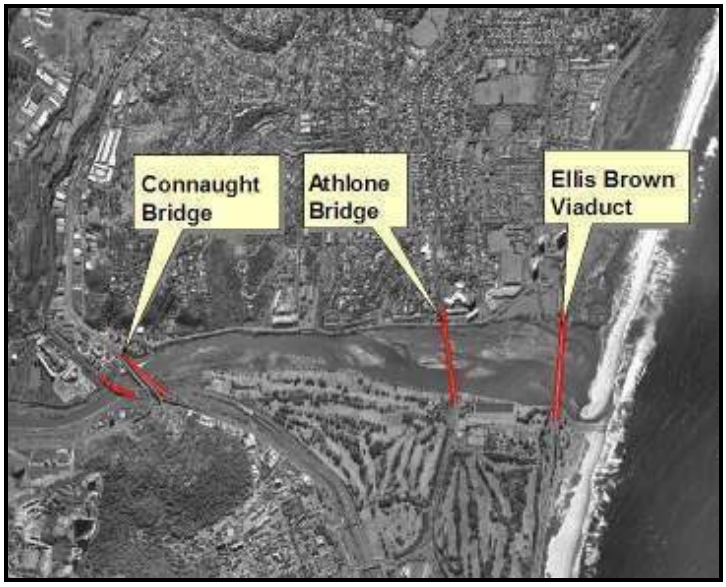

Figure 2.3. The bridges across the Mgeni Estuary (Ngetar, 2002).

2.1.2. Beachwood Mangroves

The Beachwood Creek is positioned to the north of the estuary mouth (Leuci, 1998). The creek extends in a southerly direction, parallel to the coastline behind a coastal vegetated dune (Cooper, 1986; Leuci, 1998), for nearly 2 km where it enters the estuary (Leuci, 1998). According to Leuci (1998), the Mgeni-Beachwood estuarine system formed as a barrier island complex, with the Beachwood Creek forming the remainder of an earlier coastal lagoon. Extensive mangrove species are present within the region (Leuci, 1998), which is susceptible to washover activity as a result of low dunes and strong waves (Cooper, 1986). The Beachwood Mangroves is sheltered from floods of the Mgeni, as a result of its location clear of the main channel, as well as the strength and steadiness offered by the mangroves (Leuci, 1998). Figure 2.1 (Page 5) illustrates the position of the Beachwood Tidal Creek and Mangroves region.

2.3. Climate

South Africa is subdivided into a wet eastern section and a dry western section (Schumann *et al*., 1999; Schumann, 2003). Since the Mgeni Estuary is located within the province of KwaZulu-Natal, the climate of the region is classified as subtropical, consisting of overall warm, wet summers and cool, dry winters (Cooper, 1990; Allanson and Baird, 1999; Tyson and Preston-Whyte, 2000; Green *et al*., 2004). The subtropical nature of the province is influenced by the northerly South Indian Anticyclone and an easterly tropical flow (Allanson and Baird, 1999), which causes deep weathering of the underlying lithologies within the catchment (Cooper, 1993). The

rainfall throughout South Africa is classified as seasonal (Schumann *et al*., 1999), with high rainfall occurring in summer (Cooper, 1993), including fairly frequent flood events (Schumann *et al*., 1999; Garden, 2003).

The KwaZulu-Natal coast is dominated by southwesterly and northeasterly winds (Cooper, 1986; Schumann *et al*., 1999). In summer, frontal systems travel offshore along the KwaZulu-Natal coastline, which tends to experience easterly winds linked with the Indian Ocean anticyclone (Schumann *et al*., 1999). Cooper (1991a) and Schumann *et al*. (1999) explain that generally the winds are strongest during October and November, and are the weakest during June. According to Cooper (1991a), winds from the north and north west occur mainly in winter, with flows extending below 7.2 $m.s^{-1}$. Additionally, Berg winds are characteristic features of coastal climates, and are understood to be highly widespread in late winter and spring (Tyson and Preston-Whyte, 2000). Berg winds cause high maximum temperatures in winter, along the east coast of South Africa (Tyson and Preston-Whyte, 2000).

In terms of the flood history of the Mgeni, flows that exceed 500 m^3/sec have been documented (Begg, 1978). In 1856, approximately 661 mm to 675 mm of rain fell during a four day period, which caused water levels of the estuary to ascend to 6 m (Begg, 1978; Mather *et al*., 2003). This intense rainfall resulted in bank overtopping of the Mgeni River, which consequently redirected its course by flowing southwards into the Durban Bay (Mather *et al*., 2003). Comparatively, Cyclone Domoina, which occurred during January 1984, is classified as one of the most distinct weather-producing features that occurred in KwaZulu-Natal, which generated greater than 500 mm of rainfall over a five day period (Tyson and Preston-Whyte, 2000).

The September 1987 flood, which occurred as a result of the formation of a cut-off low (Cooper, 1993; Tyson and Preston-Whyte, 2000), is classified as a one in 120 year, large magnitude flood (Badenhorst *et al*., 1989; Cooper, 1991a; 1993). During this flood, the mouth of the Mgeni had increased largely in width due to the erosion of the barrier across the mouth (Cooper, 1990). On 26 September 1987, KwaZulu-Natal experienced extremely heavy rainfall, which lasted five days cumulating 800 mm of rainfall, with the flood peak of the Mgeni, occurring two days later (Badenhorst *et al*., 1989; Cooper, 1993). The peak discharge of the 1987 flood in the Mgeni was estimated between 10 000 $m^3\ s^{-1}$ and 10 800 $m^3\ s^{-1}$ (Badenhorst *et al*., 1989; Cooper, 1991a). During this flood, the water level of the Mgeni stretched 5 m above the normal high tide level, causing the mangrove swamp in the north and the low lying land to the south to be completely inundated (Badenhorst *et al*., 1989; Cooper, 1991a; 1993), as is illustrated in Figure 2.4 (Page 9). As a result, the seawater within the estuary was completely flushed out, and a plume was created, which spanned approximately 2 km into the Indian Ocean (Badenhorst *et al*., 1989;

Cooper, 1991a; 1993). At this time, suspended sediment concentrations of 5698 mg/l were measured 3 km upstream from the mouth (Cooper, 1991a; 1993).

Figure 2.4. An aerial photograph illustrating the Mgeni Estuary in flood: 29 September 1987 (Ezemvelo KwaZulu-Natal Wildlife, EKZNW, 1987).

During 19 and 20 March 2007, Durban experienced an extreme, one in 18 year storm event that was driven by outstandingly high tidal levels and large storm waves that stood greater than 8 m in height (Breetzke *et al*., 2008). The impacts were felt across 350 km of the KwaZulu-Natal coastline, which were severe and massive amounts of erosion and property damage (Breetzke *et al*., 2008). The barrier of the Mgeni Estuary was completely flattened as a result of these severe erosive storm waves. Experts indicate that the eroded sediment from the coastline was consequently removed and deposited vast distances offshore into deep regions, with the possibility of it never returning to the beaches (Breetzke *et al*., 2008).

2.4. Coastal Hydrodynamics

According to Allanson and Baird (1999) and Whitfield (2000) the estuaries along the South African coastline are categorized into three main biogeographical regions, in the form of the subtropical (Kosi Bay Estuary in KwaZulu-Natal to Mbashe Estuary in Eastern Cape), warm-temperate (Mendu Estuary in Eastern Cape to Silwermyn Estuary in False Bay), and the cool-temperate regions (Krom Estuary in the Cape Peninsula to Orange River Mouth on the Northern Cape coast). Along the subtropical zone, the rivers are classified as perennial with strong seasonal variations, which in turn influences the geomorphology of estuaries along the coastline (Cooper *et al*., 1999).

2.4.1. Continental Shelf

The continental shelf along the KwaZulu-Natal coastline stretches about 100 m in depth (Cooper, 1991a). Garden (2003) explains that the transportation of sediment along the coastline is influenced by several factors, such as the continental shelf morphology and dimensions, as well as Agulhas and wave generated currents. The continental shelf along the KwaZulu-Natal coastline is narrow and spans between 7 km and 40 km wide, which widens to a maximum along the northern section of the coast, in the vicinity of the Tugela River (Cooper, 1990; 1991a).

2.4.2. Currents

According to Tyson and Preston-Whyte (2000), the South Equatorial Current in the Indian Ocean divides around the east coast of Madagascar and flows towards the north and south. The southward flowing water forms the Mozambique Current, which flows along the western region of the Mozambique Channel (Tyson and Preston-Whyte, 2000). However, the Agulhas Current flows southwards along the east coast of South Africa (Cooper and Mason, 1987; Cooper, 1991a; Tyson and Preston-Whyte, 2000), from the northern KwaZulu-Natal and Mozambique border towards the poles, forming a large scale oceanographic feature within the region (Ramsay, 1994; Tyson and Preston-Whyte, 2000). The Agulhas Current flows at the edge of the continental shelf, approximately greater than 90 km offshore, and obtains the majority of its water from a "*large recirculation gyre in the South-West Indian Ocean*" (Tyson and Preston-Whyte, 2000, p.220).

2.4.3. Swell Regime and Tides

The coastline of KwaZulu-Natal is categorised as wave-dominated, with a high-energy (Cooper, 1990; 1991a; 1993; 1994; 2001). Rossouw (1984) and Schumann *et al*. (1999) point out that the prevailing swell approach direction along the KwaZulu-Natal coast is south to south-south-westerly. Additionally, according to Cooper (1991a; 1993; 1994) and Schumann *et al*. (1999), at Durban, the main direction of wave approach is east-south east to south east, with the major wave heights derived from south-south east to south west, and the lowest recorded from the east to east-south east directions.

Rossouw (1984) and Schumann *et al*. (1999) add that the wave heights generally decrease in a northerly direction along both the east and west coasts of South Africa. The highest waves occur during winter and the lowest waves occur during summer, however this trend decreases from the west coast to the east coast (Rossouw, 1984).

Rossouw (1984) measured wave heights at Port Zimbali and Richards Bay situated along the KwaZulu-Natal coast, which ranged between 0.5 m and 4.49 m, and 0 m and 4.99 m, respectively. Rossouw (1984) found that at these stations, the wave heights were generally higher during summer than winter. Garden and Garland (2005) expand that waves between 2 m and 3.49 m were common throughout the year, although waves below 0.99 m were restricted to winter and autumn. The KwaZulu-Natal coast contains a median wave height and median wave period of 1.49 m and 10.70 s, respectively (Cooper, 1991a; 1993; 1994).

The tides along the coast of KwaZulu-Natal are classified as semi-diurnal (Cooper, 1990; 1991a; 1993; Schumann *et al*., 1999; Schumann, 2003). The coastline of Durban consists of a mean neap and a mean spring tidal range of 0.50 m and 1.72 m, respectively (Cooper, 1991a; 1993; 1994). Cooper (1990) states that the mean tidal range equates to 1.80 m. Cooper (1990; 1993; 1994) draws from the mean tidal ranges, that the KwaZulu-Natal coastline is classified as microtidal (Davies, 1964 in Cooper 1993), or low mesotidal according to Hayes (1979).

2.4.4. Longshore Drift

According to Kinmont (1961), the direction of the littoral drift is north easterly along the coastline of Durban, and the southward flowing warm Mozambique Current slightly stimulates this drift as an eddy current. However, Schoonees (2000) asserts that the direction of the net longshore transport of sediment along the coast of Durban is predominantly northward. The littoral current flows approximately 4.83 km to 6.44 km offshore, and is largely influenced by dominant wind patterns and directions (Kinmont, 1961).

Along the Durban coastline, the longshore sediment transport is disrupted by the harbour entrance, as well as the north and south breakwaters, which results in the deposition of all of the transported sediment along the sand trap positioned directly south of the harbour entrance (Schoonees, 2000). As a result, the Durban Bight, located to the north of the harbour is inclined to erosion (Mather *et al*., 2003; Schoonees, 2000). Therefore, in order to combat the erosion along the Durban Bight, dredging of the accumulated sand from the southern sand trap, followed by pumping of the sand directly onto the beaches of Durban, forms as part of the Sand Bypassing Scheme aimed at nourishing the beaches (Schoonees, 2000; Mather *et al*. 2003).

According to Mather *et al*. (2003), the overall rate of the longshore transport of sediment has been researched by many authors; hence there are several variations in the results. The long term mean annual net longshore transport of sand at the Durban Sand Trap and along the Durban Bight is 500 000 m^3/year and 300 000 m^3/year, respectively (CSIR, 1996 in Schoonees,

2000). However, Mather *et al.* (2003) found that the longshore sediment transport rate along the coast ranges between 450 000 m^3 to 650 000 m^3. Along certain sections of the coastline of KwaZulu-Natal, longshore sediment transport reaches between 500 000 m^3 and 800 000 m^3 (Schumann, 2003).

2.4.5. Sea Levels

According to Cooper (1986), the coast of KwaZulu-Natal was subjected to a post-Pleistocene sea level rise, which resulted in the submergence of the coastline, resulting in narrow stretches of beaches that contain closed or semi-closed estuaries and lagoons, through the development of sand spits. The most recent shoreline fluctuation that influenced the coastal morphology took place about 15 000 years ago, when the sea level dropped to 120 m (Dingle and Rogers, 1972 in Cooper, 1991b). Thereafter, within the following 10 000 years, the sea level rose during the Flandrian Marine Transgression, to approximately 1.5 to 2.0 m above its previous level (Yates *et al*., 1985 in Cooper, 1991b). According to Cooper (1991b), the sea level thereafter fell to its present level, which is understood to be on the rise again. The stretch of coast within the vicinity of the Mgeni Estuary is categorised as regressive (Cooper, 1986).

Since 1937, the shoreline between Umhlanga Rocks and the Mgeni Estuary has undergone both transgression and regression, between 10 and 53 m, on a short-term scale (Cooper, 1991b). However, the shoreline at the Mgeni Estuary mouth underwent erosion on a long-term scale, at a rate of -2.61 m/year since 1937, which was caused by the influence of the engineered groyne (Cooper, 1991b), which is explained in Section 2.7 of this chapter.

2.5. Regional Geology

The catchment geology of the Mgeni contains various rock types (Begg, 1978; Cooper and Mason, 1987), such as Karoo sedimentary rocks, Jurassic and Tertiary sediments and volcanics, and granites (Cooper and Mason, 1987). Ecca and Beaufort Group lithologies are confined to the upper section of the catchment area (Cooper, 1991a; Leuci, 1998). The lithologies comprise mainly of "*fine-grained lacustrine and fluvial sedimentary rock*" (Cooper, 1991a, p.44), with several Late Jurassic Karoo Dolerite intrusions (Cooper, 1991a; Leuci, 1998), that overlie Dwyka Tillite (Cooper, 1991a). Within the middle section of the catchment, the river flows across a Proterozoic granite-gneiss complex that is weathered and found in the Valley of a Thousand Hills (Cooper, 1991a), which generates most of the sand found in the catchment (Cooper and Mason, 1987).

Downfaulted Ecca and Dwyka rocks are found further downstream, over which the river cuts (Cooper, 1991a). The Mgeni channel flowed through its widest section across the Ecca rocks located at the Springfield Flats region (Cooper and Mason, 1987). However, the continual expansion of the Mgeni channel was restricted as a result of resistant rocky outcrops of Dwyka Tillite, located within the region of the Connaught Bridge (Cooper and Mason, 1987). Within the vicinity of the coastline, alluvium is confined to the Springfield Flats and lower valley, with exposed Tertiary and Pleistocene coastal deposits on the sides of the valley and at the coast (Cooper, 1991a, 1993). According to Ngetar (2002), unconsolidated sediments in the form of beach sand dominates the mouth of the estuary. The bedrock underlying the estuary is said to be shale, with evident fracturing and weathering (Begg, 1978). The subsurface of the Mgeni is composed of alternating lagoonal, marine and fluvial sediment which overlies a basal conglomerate (Cooper and Mason, 1987).

2.6. Catchment Characteristics

2.6.1. Catchment Topography

The Drakensberg mountain range forms a large watershed and an influencing topographical feature, from which the main permanent rivers flow towards the Indian Ocean (M^{c}Cormick *et al*., 1992). There are 55 minor perennial, 10 secondary and 9 major perennial rivers present in KwaZulu-Natal (M^{c}Cormick *et al*., 1992). Hence, there are approximately 74 rivers that flow towards the Indian Ocean (Cooper, 1990), forming a large quantity of estuaries and lagoons along the coast (Begg, 1978; 1984), which spans approximately 570 km in length (Cooper, 1990).

Together with the topography and climate of the province, high sediment yields and erosion rates are estimated for the coastline (M^{c}Cormick *et al*., 1992, Garden, 2003). The coastal region of KwaZulu-Natal is distinguished by a steep hinterland with a small coastal plain that drains several short rivers, and generates high sediment yields and a perennial fluvial discharge, with seasonal variations (Cooper, 1991a; 1993; 1994). In addition, the coastline of KwaZulu-Natal is characterised by sandy beaches, which form due to high fluvial sediment yield that sustains the beaches and barrier environments, which develop across the inlets of estuaries (Cooper, 1990).

2.6.2. Catchment Area, River Length and Gradient

In terms of size, the Mgeni River system contains the fourth largest catchment along the KwaZulu-Natal coastline (Badenhorst *et al*., 1989). The Mgeni River flows from the Drakensberg Mountains to the Indian Ocean (Cooper and Mason, 1987; Cooper, 1991a; 1993; Garland and

Moleko, 2000), and rises to an altitude of 1889 m (Cooper, 1991a; 1993), stretching between 252 km and 300 km from the coastline (M^{c}Cormick *et al*., 1992; Cooper, 1991a; 1993; Garland and Moleko, 2000; WRC, 2002). The catchment area of the Mgeni River ranges between 4385 km^2 and 5850 km^2 (Begg, 1978). Cooper (1991a; 1993) states that the Mgeni River covers a catchment area of approximately 4400 km^2. However, Kienzle *et al*. (1997) states that the Mgeni catchment stretches approximately 4387 km^2 in area.

According to Cooper (1991a; 1993), the general gradient of the Mgeni River is 1:132. This hydraulic river gradient links with the youthful stage of the Davisian cycle of erosion, during which the dominant activities are river incision and sediment transportation (Ngetar, 2002). On the other hand, the lower section of the estuary contains a slight gentle gradient of 1: 550 (Cooper, 1991a; 1993), which renders this section a transport and deposition environment (Ngetar, 2002).

2.6.3. Dams

The Mgeni River is a highly regulated system with several large dams, weirs and small farm dams that were constructed with the main aim of water supply, which generates several adverse impacts on the functioning and health of the river itself (WRC, 2002). The Mgeni catchment and the neighbouring Msunduze catchment collectively contain about 129 registered dams (WRC, 2002). There are 5 major dams constructed on the Mgeni River, with a collective capacity ranging between 745.90 million m^3 and 753.00 million m^3 (Kienzle *et al*., 1997; WRC, 2002). These dams take the form of the Midmar, Albert Falls, Henley, Nagle and Inanda Dams (Begg, 1978; Cooper, 1991a; 1993; Kienzle *et al*., 1997; WRC, 2002). Table 2.1 below, illustrates the dams, dates of construction and capacity.

Table 2.1. The details of dam construction on the Mgeni River system.

Name of Dam	Year of Construction	Total Capacity	Source
Henley	1942	Unknown	Begg (1978)
Nagle	1950	20.8 x 10^6 m^3	Begg (1978)
Midmar	1963	172 x 10^6 m^3	Begg (1978)
Albert Falls	1975	261 x 10^6 m^3	Begg (1978)
Inanda	1988	241 x 10^6 m^3	Garland and Moleko (2000)

Research indicates that the Inanda Dam was constructed in 1988 and it is positioned about 30 to 32 km upstream of the Mgeni mouth (Cooper, 1991a; 1993; 2001; Garland and Moleko, 2000). Since the construction of the Inanda Dam, the amount of water and sediment delivered to the coastline and estuary, as well as flooding and high flow events have been minimised (Cooper, 1993; Garland and Moleko, 2000; Ngetar, 2002). Whitfield (2000) explains that due to

impoundments in the catchment, the Mgeni is classified as a temporarily open/ closed estuary (TOCE), despite being previously classified as a permanently open estuary. Furthermore, the Mgeni Estuary was previously opened for greater than 90 % of a year; however the establishment of the Inanda Dam causes the estuary to be closed for long periods of time (Cooper, 2001). The mouth of the estuary is understood to close episodically, as a result of the southward extending spit or low fluvial flows (Cooper and Mason, 1987; Garland and Moleko, 2000).

2.6.4. Hydrology and Sediment Yield

The catchment below the Inanda Dam covers an area of approximately 395 km^2 (Cooper, 1991a; 1993; Garland and Moleko, 2000). According to Cooper (1993), prior to the construction and closure of the Inanda Dam, the area below the four major dams contained a catchment area of 1700 km^2. The tributaries located above the dam flow into the Inanda Dam, where the outflow and dam discharge is controlled by the dam officials (Ngetar, 2002). Therefore, the Inanda influences the lower catchment and subsequently the estuary (Ngetar, 2002). In terms of the hydrological network, the Mgeni River below the Inanda is classified as a third order stream (Ngetar, 2002). The tributaries joining below the Inanda Dam are understood to generate sediment yield that contributes towards the Mgeni River channel (Garland and Moleko, 2000; Ngetar, 2002). According to Garland and Moleko (2000), the main tributaries of the Mgeni River below the Inanda Dam, include the Nzinyati, Molweni, Aller and Palmiet Rivers.

The mean precipitation of the Mgeni catchment ranges between 410 mm and 1450 mm annually (WRC, 2002). Begg (1978) states that the Mgeni generates a mean annual runoff of approximately 707 x 10^6 m^3, however the WRC (2002) indicates that the mean annual runoff varies between 72 mm and 680 mm. According to Begg (1978), the mean annual flow of the Mgeni River, between 1958 and 1961, was determined to be 12.5 m^3/sec to 13 m^3/sec. Seasonal variations in flow were evident, with a mean summer and winter flow of 18.4 m^3/sec and 6.5 m^3/sec, respectively (Begg, 1978). The annual sediment yield of the Mgeni drainage basin is 1.6 x 10^6 tonnes (NRIO (1986) in Cooper, 1991a). With the establishment of five dams within the Mgeni catchment, the amount of sediment delivered to the coast, especially bedload is thus decreased (Cooper, 1991a; 1993; Garland and Moleko, 2000). Cooper (1991a) calculated the average total suspended sediment load of the estuary as 53 295 tonnes per year.

2.7. Estuarine Characteristics and Geomorphology

The total area of the Mgeni Estuary, inclusive of Beachwood Mangroves, during a spring tide equals to approximately 48 ha (Begg, 1978). During a spring tide in 1972, the axial length of the

estuary was calculated via a salinity survey, which stretched to 2.50 km (Begg, 1978). The total width of the estuary near the mouth was measured in 1978 during a spring tide by Begg (1978), which resulted in a width of 600 m, with the entrance of the Beachwood Creek channel stretching approximately 20 m wide. However upon actual measurement, the total width of the channel cross-section that was studied in January 2008 to July 2008, ranged between 75 m to 90 m.

The middle region of the Mgeni Estuary channel contains a large central island, with dimensions approximately 300 m wide and 2 km in length (Begg, 1978). The upper section of the estuary is characterised as a distinct single flowing channel, which is bounded on the north side by a relatively steep bank, whereas the southern bank is a gentle low lying area (Cooper and Mason, 1987). The channel splits into a northern and southern channel around a central elevated island about 1.2 km from the Connaught Bridge (Cooper and Mason, 1987). Visual observations in 2008 concluded that the island is widest between the Athlone and M4 Bridges. Within the region of the Ellis Brown Viaduct, the two separate channels join, which consequently flows southward towards the sea following a sand spit (Cooper and Mason, 1987).

Begg (1978) indicates that during a spring tide, the depth of the estuary is 2.50 m, and during the ebb of a neap tide, the depth ranges between 0.75 m and 2.00 m. Furthermore, the mean depth of the Mgeni calculated during the period from September 1979 to August 1981 was 0.72 m (Begg, 1984). In 2008, water depths were calculated for the selected channel cross-section within the study area, during the period of January 2008 to July 2008, on a spring and neap basis, in which the water levels reached a maximum of 2.30 m during high tide.

Begg (1978) affirms that during winter, when the river flow is minimal, as well as during a high spring tide, the water may be classified as clear. Visual observations throughout the period of January 2008 to July 2008 concluded that the mouth of the estuary comprised a significant degree of clearness during the spring tide, at peak high tide. However, as the tide turns, and the marine influence wanes towards low tide, the water becomes less clear, especially when there has been a prior rainfall. According to Begg (1978), the salinity levels at the mouth of the Mgeni are extremely high, however under large river flows; the salinity levels decrease. Additionally, the salinity levels within the Mgeni Estuary tend to fluctuate with the tidal state and the volume of fluvial discharge (Cooper and Mason, 1987).

The sediments along the northern bank are mainly rich in organics, while the sediments are more uniform within the vicinity of the mouth, as a result of turbulence and marine influence (Begg, 1978). The texture and composition of the sediments in the estuary will be discussed in Chapters Six, Seven and Eight. Normally, the Mgeni Estuary sandbar is generally classified as a southward

accreting spit (Begg, 1978; Cooper, 1986; 1991b). However, under certain conditions, spit growth in a northward direction can take place (Begg, 1978). According to Begg (1978) and Cooper (2001), as well as based on visual observations, flood tidal deltas, bars and sandbanks are evident within the mouth of the estuary.

The mouth of the Mgeni Estuary contains engineered stabilisation in the form an artificial groyne (Cooper and Mason, 1987; Cooper, 1986; 1991a; 1993), which was developed in the early 1900s, prior to 1931 (Cooper, 1991a; b). The groyne is positioned on the southern bank and enables an open mouth except when the fluvial discharge is significantly low (Cooper and Mason, 1987; Garland and Moleko, 2000). According to Cooper (1986; 1991a) and Cooper and Mason (1987) the groyne was developed with the aim of mouth stability, as well as a precautionary measure towards tidal scour. Additionally, Cooper (1991b) explains that the groyne does not only disrupt the natural flow of sediment from the south, but it takes the form of a headland, as well. Therefore, it causes wave refraction within the region, which results in scouring of the bank furthermost north of the estuary mouth (Cooper, 1991a, 1993). This stabilisation of the mouth enables deposition on the southern side and erosion on the northern side of the groyne (Cooper, 1991a, b; Breetzke *et al*., 2008), which is illustrated below in Figure 2.5. This process is comparable to that linked with the natural rock outcrops present at river mouths towards the northern regions of the coast (Cooper, 1991b), and is explained in detail in Chapters Three and Six.

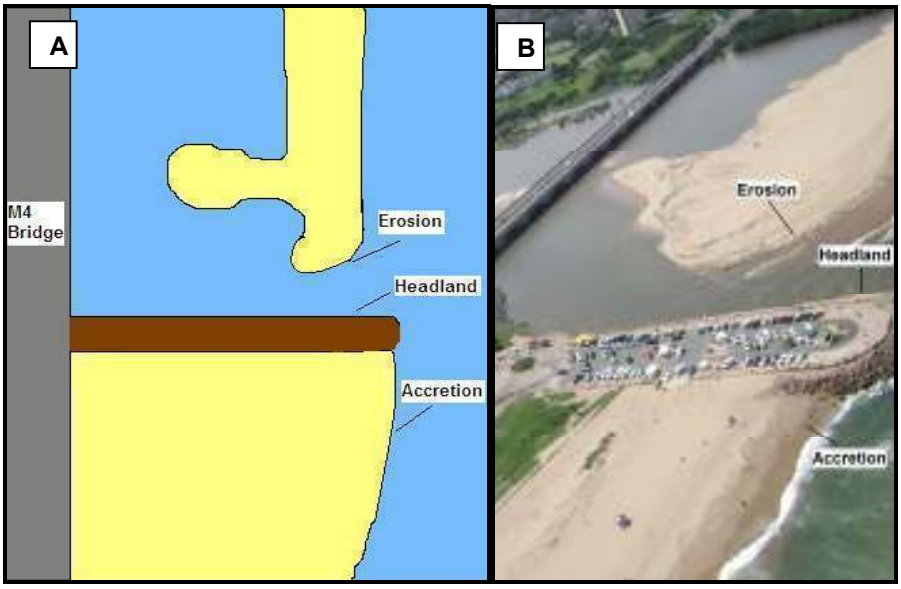

Figure 2.5. A) Schematic diagram of the erosion and accretion along the shoreline at the Mgeni, B) Aerial photograph illustrating the accretion and erosion around the groyne at the Mgeni (Jaganath, 2008).

Leading up to the construction of the groyne, past data stated that the Mgeni previously flowed behind a large sand barrier into the Durban Bay (Begg, 1978; Cooper and Mason, 1987; WRC, 2002). Begg (1978) adds that the mouth of the estuary was located approximately 4 km away from its present position, in the direction of the Durban Bay. However, the estuary mouth was manually breached at its current mouth location, as a result of flooding, malaria and damage risks (Begg, 1978). In 1984, the mouth was reported as being permanently open for the past 15 years (i.e. since 1969), as a result of the establishment of the groyne (Begg, 1984). Begg (1984) affirms that, with analysis of 1937 aerial photography, the mouth of the Mgeni was then found at Beachwood, in a northerly direction from its current position, which confirms that the groyne is a definite controlling factor of the characteristics and status of the mouth and sandbar (Begg, 1984).

2.8. Catchment Land Uses

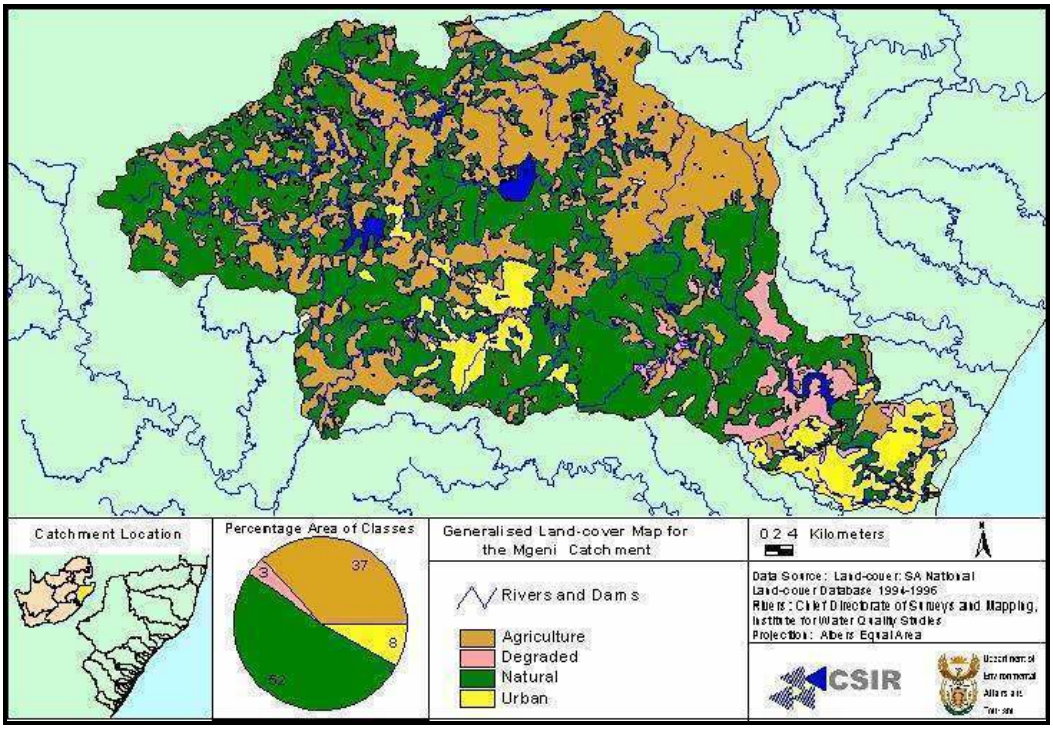

Figure 2.6. The generalized land cover of the Mgeni Catchment (SOER, 2001).

The Mgeni flows through various land cover and land use zones, such as industrial and residential areas of Durban and Pietermaritzburg (Begg, 1984; Leuci, 1998). Figure 2.6 above indicates the generalized land cover of the Mgeni catchment. Within the catchment of the Mgeni, the main land use that occurs is intensive farming of fruits, sugar and crops (Begg, 1978). Harrison *et al*. (2001) explains that in the Mgeni Catchment, 37 % of the land cover is categorized as agriculture, ranging from sugar cane cultivation, commercial forestry, to subsistence farming,

whereas 3 % of the catchment contains degraded shrubland and bushland. Furthermore, 52 % of the catchment is classified as natural, which comprises forest and bushland, with 8 % of the land being classified as urban, including mainly residential, commercial and industrial developments (Harrison *et al*., 2001).

2.9. Estuary Land Uses and Human Impacts

The Mgeni is considered as an urban river within its lower course (Garland and Moleko, 2000), which makes it susceptible to anthropogenic activities and hence several negative impacts (Cooper and Mason, 1987; Garland and Moleko, 2000). Considering its proximity to Durban, the estuary is susceptible to negative human impacts (Cooper and Mason, 1987; Garland and Moleko, 2000). However the estuary contains a strong conservation potential and status due to the Beachwood Mangroves, hence it is definitely recognized (Begg, 1978). Presently, the Beachwood Mangroves forms part of the Ezemvelo KZN (KwaZulu-Natal) Wildlife Conservation Areas. The Beachwood Mangroves provides several benefits to the estuary, as well as humans, as it forms an educational facility, promotes awareness, and positively contributes to the productivity and biodiversity of the estuary itself (Begg, 1978; Demetriades, 2009).

The Mgeni is a major supplier of water to both the Durban and Pietermarizburg Metropolitan areas (Kienzle *et al*., 1997). The Mgeni Estuary is an important resource in terms of recreation and environmental benefits (Begg, 1978; Garland and Moleko, 2000). The estuary is an area of many water sports, such as canoeing, rafting, boating as well as fishing, bird watching, angling and bait collection (Begg, 1978; 1984).

The Mgeni River channel above the head of the estuary is canalised (Cooper and Mason, 1987; Garland and Moleko, 2000), which eliminates a floodplain zone above the Connaught Bridge (Demetriades, 2009). According to Begg (1984), the Mgeni Estuary underwent canalisation during 1982, which generated a great deal of concern regarding the threats of floods, although massive impoundments along the Mgeni have been believed to ease flood peaks. Canalisation may influence the water quantity and quality of the estuary due to impermeable surfaces that drain industrial and residential runoff.

The estuary contains the Springfield Industrial Park, which lines the upper estuary region in the vicinity of the Connaught Bridge, residential and commercial areas along the northern and southern banks, as well as the sand mining site and sewage works (Demetriades, 2009). The southern bank of the Mgeni holds several different land uses, such as a golf course, model yacht pond, restaurants and several recreational facilities (Begg, 1978). These activities and estuary

uses definitely influence the natural functioning of the estuary by impacting and changing the water quantity in the estuary due to discharges and runoff into the estuary, which may in turn influence the water quality, as such inflows may contain nutrients and pollutants (Demetriades, 2009).

Recently, there have been several reports and newspaper articles regarding the water quality of the Mgeni Estuary. de Boer (2008) reported in the Daily News, about the sewage leaks into the Mgeni. The water quality of the system has deteriorated over time, considering that that the Mgeni once was contained good water quality (Begg, 1978). The main cause of this deterioration is the ongoing pollution of the system, via several sources, such as sewage discharge, informal settlements and industry (Begg, 1978; 1984; WRC, 2002).

However, the sediments located within the lower regions of the Mgeni are considered as a major resource to the municipality (Garland and Moleko, 2000). The fluvial sediment supply to the surrounding beaches enables beach build up and provides material through direct extraction from the channel bed (Garland and Moleko, 2000). The latter generated a mounting sand mining industry within the Mgeni (Garland and Moleko, 2000). A study performed by Demetriades (2007) concerning sand mining within the estuaries of KwaZulu-Natal, found that sand mining operations were still in existence along the Mgeni River, upstream of the estuary. According to Demetriades (2007) sand mining occurs within three localities along the Mgeni, such as above the N2 Bridge, within the Springfield region, and in rural areas further upstream. The collective volume of sand extracted between two operating contractors in 1997, equated to 210 000 tonnes (Garland and Moleko, 2000). Garland and Moleko (2000) state that continued sand mining will cause changes in the estuary, as a result of the reduction in sediment delivery.

CHAPTER 3: THEORETICAL BACKGROUND: THE COASTAL ZONE AND BEACHES

This chapter reviews and discusses the literature and theoretical concepts that structures the body of knowledge of coastal geomorphology, upon which this research is based. Initially, the existing literature and past research pertaining to the Mgeni Estuary, in terms hydrology, sedimentology and coastal and estuarine geomorphology is reviewed and analysed. Secondly, the coastal zone is discussed, followed by an account of sediments and the processes involved in sediment movement within the coastal zone. Thereafter, the theoretical concepts pertaining to beaches, such as classification, processes and morphology are discussed.

3.1. Review of Past Research

There are several published works covering estuarine and coastal geomorphology, focusing on estuaries as single entities regarding their form, processes and structures, as well as part of a larger scale coastal system. In South Africa, investigations and research on estuaries is remarkably significant, especially those concerning geomorphology (Green, 2004). Estuaries are considered to be imperative features contributing to, and influencing the coastal geomorphology of South Africa (Cooper, 2001), as mentioned in Chapter One.

In South Africa, past research exists copiously, with Begg's (1978; 1984) survey of 73 KwaZulu-Natal estuaries forming a well-known piece of literature referenced by many researchers. Begg (1978; 1984) carried out a comprehensive survey of these systems, including their geomorphological, chemical, biological and physical characteristics. Cooper (1990; 1991a; 1993; 1994; 1995b; 2001; 2002) studied several systems along the KwaZulu-Natal coastline, dealing with an overall classification of estuaries, as well as their response to flooding and sedimentation. Additionally, Schumann (2003) expanded on marine sedimentation of the Eastern Cape estuaries and Harrison *et al*. (2000) produced an estuarine classification scheme for South African estuaries. Shoreline changes and sea level rise along the KwaZulu-Natal coast were studied by Cooper (1991b; 1995a). Recently, Wright *et al*. (2000) studied the Cenozoic evolution of the northern KwaZulu-Natal water bodies, Stretch and Zietsman (2004) studied the hydrodynamics of the Mhlanga and Mdloti estuaries, and Beck *et al*. (2004) and Beck (2005) studied sediment transport in South African estuaries. Therefore, the geomorphology and physical characteristics of South African estuaries is well-covered.

However, closer to the extent of this study, the Mgeni Estuary is no exception relating to the abundance of published literature and research within KwaZulu-Natal. The Mgeni Estuary is a

system that is well researched, in terms of geomorphology (Cooper, 1991a; 1993; Cooper and Mason, 1987), and chemical (Kienzle *et al*., 1997) and biological characteristics, with research spanning back to 1985 (Cooper, 1991a). Blackshaw (1985) analysed the beach and fluvial sediments of the lower region of the Mgeni River. Cooper (1986; 1991a; 1993; 2001) and Cooper and Mason (1987) have produced intensive studies that are fully dedicated to the geomorphology and sedimentology of the Mgeni Estuary and Beachwood Mangroves. Garland and Moleko (2000) and Ngetar (2002) have collectively studied pre- and post-dam sedimentary impacts of the Inanda on the Mgeni Estuary.

With the above said, there is a noticeable gap that lies in the literature and past research concerning the Mgeni Estuary. This gap lies in the form of a specific locality of the Mgeni Estuary, as well as the aspect of suspended sediment flux. Overall the Mgeni Estuary has been studied mainly within its upper to middle reaches, however the lower reaches, including the mouth has been rarely studied in the past. Therefore, there seems to be a paucity of published literature, directly relating to the geomorphology and sediment characteristics of this lower reach and mouth of the Mgeni Estuary. This is stated with the exception of the work produced by Blackshaw (1985), Cooper (1991a; 1993) and Cooper and Mason (1987). Furthermore, to date, published literature regarding the quantification of suspended sediment flux of the Mgeni Estuary and the Mgeni inlet does not exist. Therefore, there is a clear lack of information pertaining to this particular aspect of sediment dynamics within this specific region of the estuary. However, Theron (2007) points out that regardless of the availability of the abovementioned literature, there is a remarkable lack of published work concerning the hydrodynamics, morphology and sediment dynamics of the South African estuaries, thus the amount of relevant information on these aspects is poor. Hence, as discussed in Chapter One, this gap in literature provides motivation for this research study.

3.2. The Coastal Zone

3.2.1. Introduction

According to Haslett (2000), coasts are unique environments, encompassing the interaction of the land, sea and the atmosphere. Coasts are dynamic and constantly changing (King, 1972; Davis, 1978; Haslett, 2000), as a result of processes of erosion, transport and deposition (Haslett, 2000). The coastal zone, also termed the littoral zone, is classified as a highly composite geomorphic system that encounters several different processes (Dardis and Grindley, 1988). The coast comprises several different zones or components (Bird, 2000). Masselink and Hughes (2003) explain that the term coastal is somewhat uncertain, because several different authors may

define it differently, in terms of its boundaries and overall extent. Haslett (2000) states that the coastal zone is a spatial region that stretches between the land and sea. Comparatively, Masselink and Hughes (2003) describe the coastal zone as the region that stretches to the limit of which coastal processes extended during the Quaternary geological period, comprising the coastal plain, shoreface and continental shelf. Haslett (2000); Bird (2000) and Hill (2004) describe the coastal zone as the region between the landward boundary of marine influence and the seaward boundary of the influence of the land. The landward boundary of marine influence may take the form of the head of an estuary, a cliff or the ground situated at the back of a lagoon or coastal dune system (King, 1972; Davis, 1978; Bird, 2000).

The coastal zone is divided according to morphological changes (Komar, 1998; Haslett, 2000), into the backshore, foreshore, inshore and offshore regions (Komar, 1998; Haslett, 2000; Hill, 2004), as is illustrated in Figure 3.1 below. The backshore zone stretches from the high water mark to the landward boundary of marine influence (Davis, 1978; Hill, 2004), and tends to elevate above the levels of normal high tide (King, 1972; Bird, 2000), however it is susceptible to changes that occur during storms (Hill, 2004). The foreshore zone extends from the low water mark to the high water mark and is a significant zone for marine processes (Hill, 2004). At high tide and low tide, the foreshore zone is inundated and uncovered, respectively (King, 1972; Bird, 2000). The inshore zone extends seaward from the foreshore to the zone where waves break (breaker zone) (Komar, 1998). The offshore zone is a fairly flat section of the profile (Komar, 1998), which extends away from the wave base, wherein wave activity is fairly inadequate and mainly takes the form of fine sediment deposition (King, 1972; Haslett, 2000; Hill, 2004). The wave base is the region it which the water is adequately deep and waves do not influence the land and water below it (Haslett, 2000; Masselink and Hughes, 2003; Hill, 2004).

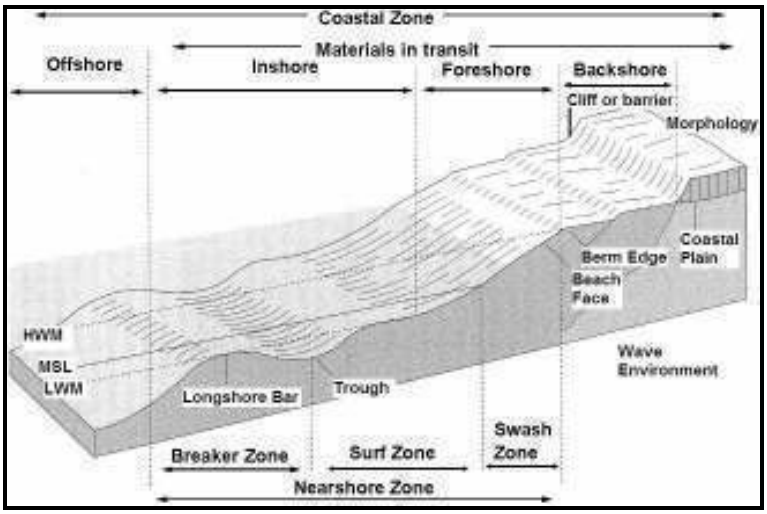

Figure 3.1. The components of the coastal zone (Hill, 2004).

The shore zone is divided into the breaker zone, surf zone and swash zone, according to various wave types and processes (Komar, 1998; Haslett, 2000; Hill, 2004), as illustrated in Figure 3.1 (Page 23). These zones together form the nearshore zone (Bird, 2000; Haslett, 2000), which fluctuates with the rising and falling tides (Bird, 2000), and stretches from the shoreline to the sea, to a point offshore where waves break (Komar, 1998). The breaker zone, where waves break, is bounded by the offshore zone (Komar, 1998; Bird, 2000; Hill, 2004). The surf zone is located between the breaker line and swash zone (Komar, 1998; Beck *et al*., 2004), wherein breaking waves obtain an increase in wave energy due to a reduction in the gradient (Bird, 2000; Hill, 2004). The swash zone is positioned along the upper section of the shore and contains broken waves in the form of swash and backwash, respectively (Komar, 1998; Bird, 2000; Hill, 2004).

3.2.2. Coastal Processes

The coastal system consists of numerous sections that are interlinked and also controlled by factors that operate beyond the boundaries of the coastal zone (Masselink and Hughes, 2003). Woodroffe (2002) explains that coastal features are subjected to and influenced by several processes, such as wave, sedimentary, tidal, oceanic, wind and fluvial processes. Masselink and Hughes (2003) highlight the most important processes as hydrodynamic, in form of waves, tides and currents, and aerodynamic, in the form of wind. The coastal processes focused on in this research include tides and waves, which will be addressed within the relevant sections, further in this chapter and in Chapter Four.

3.2.3. Sediments in the Coastal Zone

3.2.3.1. Fluid Properties, Flows and the Boundary Layer

Sediments are significantly important in the coastal zone, as they build and sustain beaches. Masselink and Hughes (2003) explain that sediments within the coastal zone can either be derived from external environments or can be locally produced. In addition, features within the coastal zone occur as a result of erosion and deposition of sediments (Masselink and Hughes, 2003). Therefore, sediment transport and movement plays a large and vital role within the coastal environment.

However, fluids such as wind, fresh water and salt water, waves and currents (Allen, 1994; Masselink and Hughes, 2003), play an imperative role in the transportation of sediments (Woodroffe, 2002). Fluids generally apply forces onto sediments and provide momentum, which allows the sediments to initially move and maintain motion (Masselink and Hughes, 2003). Most

fluids display a natural resistance to flow (Allen, 1994; Masselink and Hughes, 2003), and are known as viscous fluids (Masselink and Hughes, 2003).

There are two significant types of flows identified within a moving fluid, in the form of laminar and turbulent flows (Tucker, 1981; Allen, 1994; Woodroffe, 2002; Masselink and Hughes, 2003; Schumann, 2003). Laminar flow is defined as a one-directional, uniform movement flow (Pethick, 1984; Dyer, 1986; Gordon *et al*., 1992; Masselink and Hughes, 2003). Laminar flows contain streamlines and thin layers of lamina that are straight, ordered, flow separately and do not mix together (Allen, 1994; Woodroffe, 2002; Masselink and Hughes, 2003). Laminar flow takes place under conditions of low flow velocities and high viscosities (Woodroffe, 2002; Schumann, 2003). Molecular viscosity creates adequate forces that withstand deformation of flow, so the fluid flow remains unmixed (Allen, 1994; Woodroffe, 2002; Masselink and Hughes, 2003).

Turbulent flow is described as the movement of fluid parcels that flow mainly in one direction (Masselink and Hughes, 2003), however is characterised by random movements of particles as a result of turbulence in the flow, which creates eddies (Tucker, 1981; Pethick, 1984; Dyer, 1986; Woodroffe, 2002; Schumann, 2003). Thus, turbulent flows contain streamlines that are entangled (Allen, 1994), and occurs under conditions of a high velocity and low viscosity (Woodroffe, 2002). The inertial forces cause the fluid to accelerate significantly, resulting in deformation, in which the flow becomes turbulent and mixed (Masselink and Hughes, 2003; Schumann, 2003).

The boundary layer theory states that the friction that occurs between a relatively moving fluid and a solid boundary, such as the sea bed or the bed of an estuary, is constrained to a single thin layer known as the boundary layer (Dyer, 1986; Allen, 1994; Masselink and Hughes, 2003). According to Schumann (2003), the shear caused as a result of the fluid flowing over the boundary generates stress within this interface and consequently influences the velocity profile within the water column, which within a schematic boundary layer rises from zero at the bottom to a constant value outside the layer.

3.2.3.2. Modes of Sediment Movement

There are three modes of sediment transport, such as wash load, suspended load and bedload (Tucker, 1981; Selley, 1982; Dyer, 1986; 1995; Hardisty, 1990; Gordon *et al*., 1992; Reid and Frostick, 1994; Masselink and Hughes, 2003). Wash load contains the finest sediment fractions, which is generally classed as fine clays and dissolved material (Gordon *et al*., 1992; Reid and Frostick, 1994; Masselink and Hughes, 2003). These fine particles remain in constant suspension (Gordon *et al*., 1992; Masselink and Hughes, 2003), caused by turbulence and generally do not

require a high velocity in order to be transported, thus are transported by all flow velocities (Gordon *et al*., 1992; Dyer, 1995). The vertical profile of wash load concentrations illustrates a uniform pattern (Dyer, 1995).

Sediment grains are transported as bedload along the bed of an estuary or river (Tucker, 1981; Selley, 1982; Gordon *et al*., 1992; Reid and Frostick, 1994; Masselink and Hughes, 2003). Masselink and Hughes (2003) explain that continuous contact with the bed is achieved through traction and irregular contact with the bed is achieved through saltation. Traction is a transportation process by which the sediment grains slide or roll along the bed (Tucker, 1981; Selley, 1982; Masselink and Hughes, 2003; Schumann, 2003), and is characterised as a fairly slow mode of transport, which occurs while weak currents move sands or strong currents move larger pebbles and boulders (Masselink and Hughes, 2003). During saltation the sediment grains bounce or hop along the bed, and it occurs as moderate currents move sand or as strong currents move gravel and pebbles (Tucker, 1981; Gordon *et al*., 1992; Masselink and Hughes, 2003; Schumann, 2003). Sediments transported as bedload, initially move along the bed through traction and saltation (Dyer, 1995; Schumann, 2003); however as the flow velocity increases, ripples and dune bedforms tend to form (Dyer, 1995).

Suspension occurs as a result of the erosion of bed particles (Dyer, 1995; Schumann, 2003), which initially move and flow in the direction of the main current due to turbulence in the fluid (Dyer, 1995; Yang, 1996; Masselink and Hughes, 2003; Schumann, 2003). Turbulence maintains the sediments in suspension for a significantly large distance and long period of time (Selley, 1982; Reid and Frostick, 1994; Yang, 1996; Schumann, 2003). Sediment transport in several natural rivers occurs mainly as suspended load (Yang, 1996). Sediments transported as suspended load tend to make irregular contact with the bed; however they mainly travel in suspension (Masselink and Hughes, 2003). Sediment particles less than 150 μm in size are immediately transported in suspension, whilst larger particles are transported firstly as bedload, until higher velocities permits transport in suspension (Dyer, 1995). The transport pathways of suspended sediments are different from those of saltation due to turbulence which causes non-uniform movements (Masselink and Hughes, 2003). Sediments are transported as suspended load when moderate currents move silts or strong currents move sands (Masselink and Hughes, 2003).

The density of water within a water column increases due to the suspended sediment (Schumann, 2003). The generalised trend is that as the flow intensity and velocity increases, the concentration of particles transported in suspension increases, along with the mean grain size (Dyer, 1995). The vertical profile of suspended load indicates a nature of grading, where the

higher concentrations and large sediment grain sizes are positioned close to the estuary bed (Dyer, 1995). However in reality, when currents decrease in speed, the turbulence tends to decrease as well, which causes sediment deposition out of suspension at a corresponding settling velocity, which is dependent on the size, shape and density of the grains, as well as the remaining turbulence (Schumann, 2003). Generally, small sized sediment particles tend to take a longer time period to settle than larger, coarser sediment grains (Schumann, 2003).

3.2.3.3. Sediment Grain Movement, Transport and Dynamics

In order for a fluid to transport a sediment particle, the fluid itself needs to be in motion (Allen, 1985). Fluid properties related to sediment dynamics include mass, acceleration, velocity and stress (Masselink and Hughes, 2003). The dynamic action of sediment within a moving fluid is highly influenced and determined by the grain size of the sediment, the mechanics and physical nature of the fluid and the velocity of the current (Allen, 1994; Dyer, 1995; Yang, 1996; Woodroffe, 2002; Masselink and Hughes, 2003; Schumann, 2003). Grain sizes greater than 63 μm have the ability to behave on an individual basis, whilst grain sizes less than 63 μm, do not have the ability to move individually, due to the cohesive nature of these fine sediments, in which the movement depends on bulk sediment properties such as floc size and water content (Masselink and Hughes, 2003). Therefore, sediment transport depends on the physical properties of both the fluid and the sediment particles (Allen, 1985; Woodroffe, 2002).

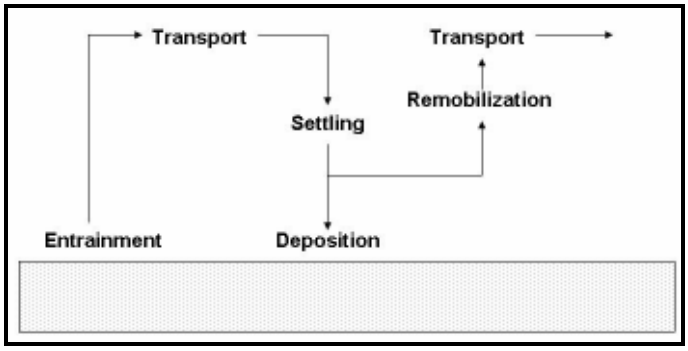

Figure 3.2. A schematic diagram illustrating the small scale processes that permit sediment transport (Redrawn from Masselink and Hughes, 2003).

The processes of sediment entrainment and re-suspension are linked to the forces that act on sediment grains by the current (Allen, 1994; Masselink and Hughes, 2003). The forces that act on sediment grains at rest on a bed are lift, drag and weight forces (Allen, 1985; 1994; Pye, 1994; Yang, 1996; Masselink and Hughes, 2003). Therefore, in order for sediment grains to move, the collective shear stress, drag and lifting forces applied by the fluid must be sufficient in order to

surmount the gravitational, cohesive and frictional forces that maintain the sediment grains on the bed (Blackshaw, 1985; Schumann, 2003). Accordingly, this threshold is the critical shear stress, which basically is at a minimum for the smallest and lightest sediment grains that tend to move foremost (Schumann, 2003). Masselink and Hughes (2003) point out that the localised movement of sediments is controlled by small-scale processes, in the form of entrainment, transport, settling and deposition, which collectively generates the movement of sediments, which encompasses the process of sediment dynamics, as is illustrated in Figure 3.2 (Page 27).

Bascom (1959) and Schumann (2003) indicate that as sediments are transported away from its source, the mean particle size tends to decrease, which is indicative of fining down the transport pathway. Therefore, finer sediments of bedload and suspended load generally tend to be transported over longer distances than coarser sediment particles, which lead to a process known as gradation of sediment (Schumann, 2003).

3.2.3.4. Models for Calculation of the Sediment Transport Rate

Masselink and Hughes (2003, p.129) define the sediment transport rate as "*the mass of sediment transported per unit cross-sectional area of flow per unit time*". Calculating sediment transport, particularly in estuaries, is considered a complicated task, since several equations and formulae for bedload and suspended load transport rates exist in the literature, Allen (1985); Dyer (1986), Yang (1996); Masselink and Hughes (2003), Schumann (2003); Beck *et al*. (2004); Beck (2005). Furthermore, Hjulstrom (1935) in Yang (1996) created a graph known as the Hjulstrom Curve, in order to illustrate the relationship between the sediment grain size and the average flow velocity for erosion, transport and sedimentation. In addition, Beck *et al*. (2004) and Beck (2005) focus on sediment transport in estuaries within South Africa, in which several sediment transport formulae are discussed and analysed.

3.3. Beaches

3.3.1. Introduction

Beaches are classified as the most changeable landforms that consist of a dynamic nature and are constantly undergoing rapid changes (King, 1972; Davis, 1978; Komar, 1998; Woodroffe, 2002), as sand undergoes continuous shifting by waves, nearshore currents and winds (Komar, 1998). Beaches are described as an accumulation of wave influenced loose sediment (King, 1972; Davis, 1978; Komar, 1998; Bird, 2000; Haslett, 2000; Woodroffe, 2002; Masselink and Hughes, 2003), in the form of sand, gravel and boulders (Komar, 1998; Bird, 2000; Haslett, 2000;

Masselink and Hughes, 2003), positioned around the margin of wave action along marine, lacustrine and estuarine shorelines (Bird, 2000; Masselink and Hughes, 2003). Despite their unconsolidated composition, beaches are still able to remain intact along coastlines with strong wave energies (Pethick, 1984; Haslett, 2000). Beaches thus have the ability to change their shape according to different wave energies (Pethick, 1984, Haslett, 2000). Beaches stretch from the low tide level of a spring tide, to the landward point that forms a boundary such as cliffs, dunes or vegetation (Komar, 1998; Masselink and Hughes, 2003), or the upper boundary of wave action (Davis, 1978). Masselink and Hughes (2003) point out that in most cases, beaches consist of disturbances in the general concave-upward profile shape, as a result of several small-scale morphological features in the form of beach cusps, berms and nearshore bars. The nearshore currents that act within the coastal zone are essential to the dynamics of beaches, as they generate and control the transport of beach sediments, which effectively outlines the beach morphology (Masselink and Hughes, 2003).

3.3.2. Beach Sediments

Beaches may be dominated by coarse or fine sediments of varying proportions and uniformity (Bird, 2000). Beaches acquire sediment derived from numerous sources (Bird, 2000; Schumann, 2003). According to Beck *et al*. (2004) and Theron (2007), the sediment located closely inshore and at estuary mouths, is generally derived from fluvial sources and the abrasion of rocks and shells along the shore. However, the sediment that is transported into estuaries is generally derived from beaches and dunes (Schumann, 2003). Hence, coarser fluvial sediments generally dominate the adjacent river mouth region (Bird, 2000), whilst the resultant finer sediments tend to be transported over greater distances along the shore and further offshore (Bird, 2000; Schumann, 2003; Beck *et al*., 2004; Theron, 2007). Dune and beach erosion, offshore sources, as well as larger rivers, forms the major source of marine sediment into estuaries and the inshore area (Bird, 2000; Beck *et al*., 2004; Theron, 2007). Figure 3.3 (Page 30) indicates the sources and losses of sediment to and from beaches, respectively. Beck *et al*. (2004) and Theron (2007) state that once these sediments finally reach the coastal zone via numerous sources as stated above, they become exposed to several coastal processes, which generates them into marine sediments.

Beaches that obtain their sediment from fluvial sources occur as a result of sand and gravel that are transported downstream as fluvial bedload towards the mouth of the river, where it enters the nearshore system and is moved along the coast by waves (Bird, 2000; Beck *et al*., 2004; Theron, 2007). Alternatively this sediment can be transported out to sea or deposited on the beach, where it may be reworked by waves and currents (Bird, 2000; Schumann, 2003), and may develop

deltas, spits or extended beaches (Bird, 2000). Generally, the sediments found along beaches, undergo constant movement due to wave, current and wind action (Beck *et al*., 2004; Theron, 2007).

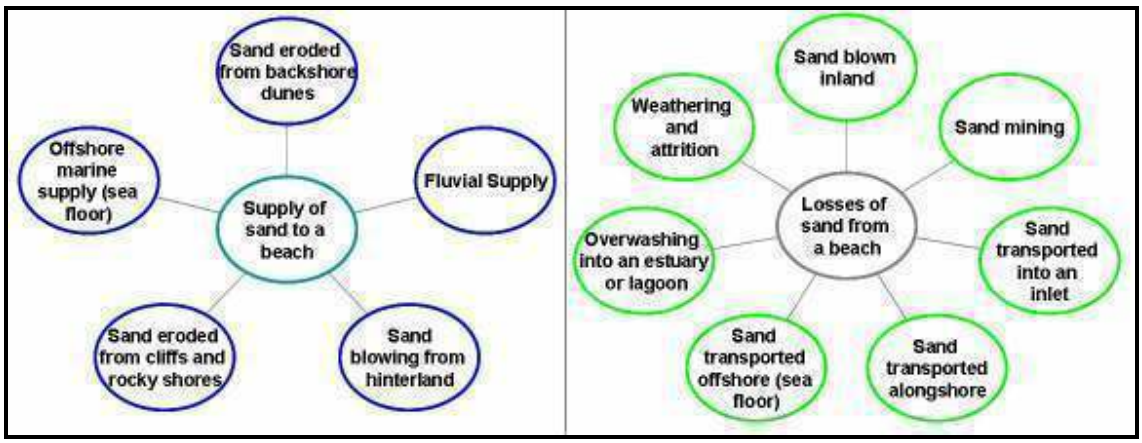

Figure 3.3. Various sources and losses of sand from a beach (Adapted from Bird, 2000).

The sediment found on the beaches of South Africa are usually classified as sand, ranging from very fine sand to very coarse sand (Schumann, 2003), which is classified as marine sediment that is non-cohesive (Woodroffe, 2002; Schumann, 2003). Beach or marine sediments are generally composed of quartz, feldspar and heavy minerals (Komar, 1998), and contains sand, shell fragments, gravel, small amounts of mud particles (Davis and FitzGerald, 2004), and approximately 25 % to 50 % of biogenic fragments that are made up of broken mollusc shells (Schumann, 2003). Sand and gravel particles positioned along beaches are mainly angular or sub-angular which becomes rounded in shape as a result of abrasion by waves (Bird, 2000). The sediments that withstand abrasion for a significant period of time include quartz or quartzite grains (Schumann, 2003). Hence, the sand transported into estuaries, sourced from beaches and dunes are composed of inorganic and biogenically-derived components (Schumann, 2003).

3.3.3. Beach Classification

The classification of beaches allows the study of beach morphodynamics and beach change (Masselink and Hughes, 2003). Sandy beaches are classified according to slope, which controls the amount of energy reaching the shoreline and influences the beach configuration and morphology (Masselink and Hughes, 2003; Davis and FitzGerald, 2004). Figure 3.4 (Page 31) illustrates a general classification of sandy beaches, in which these beaches are subdivided according to slope, into steep and gentle gradient beaches, and are further classified as

reflective, intermediate and dissipative beaches, as well as according to their distinctive morphology (Bird, 2000; Masselink and Hughes, 2003; Davis and FitzGerald, 2004).

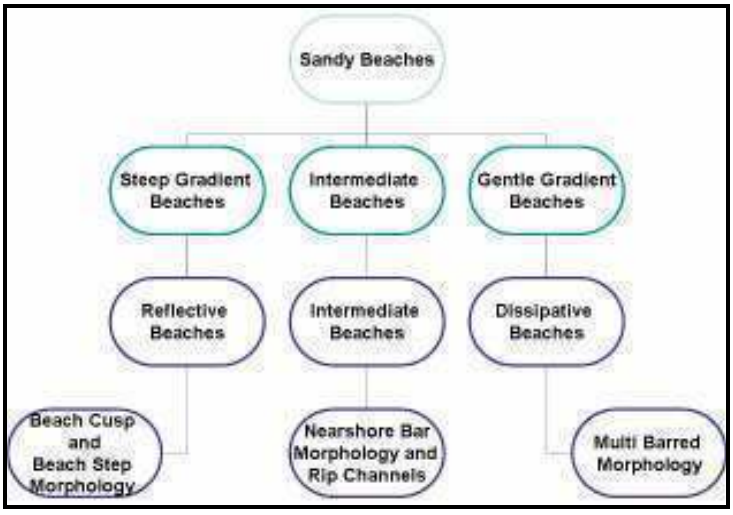

Figure 3.4. A summary of beach classification of sandy beaches (Derived from Bird, 2000 and Masselink and Hughes, 2003).

Steep beaches usually do not contain a wide surf zone; hence waves break directly onto the beachface either as plunging or surging waves (Komar, 1998; Bird, 2000; Masselink and Hughes, 2003), resulting in a large proportion of the incident wave energy to be reflected back towards the sea from the shoreline, thus these beaches are termed reflective (Komar, 1998; Bird, 2000; Woodroffe, 2002; Masselink and Hughes, 2003; Beck *et al*., 2004; Davis and FitzGerald, 2004; Theron, 2007). Reflective beaches are usually steep, sandy, composed of coarse sediment (Bird, 2000; Beck *et al*., 2004; Davis and FitzGerald, 2004; Theron, 2007), and contain high berms that limit barrier overwash (Cooper *et al*., 1999). These beaches are characterised by low waves (Bird, 2000), surging breakers (Beck *et al*., 2004; Theron, 2007), and beach cusp and step morphology (Bird, 2000; Masselink and Hughes, 2003).

Gentle gradient, low elevation beaches contain a wide surf zone, with several lines of spilling breakers (Komar, 1998; Cooper *et al*., 1999; Bird, 2000; Masselink and Hughes, 2003; Beck *et al*., 2004). Therefore, large amounts of the wave energy are dissipated gradually and further away from the shoreline due to extensive breaking as a result of the morphology, terming these beaches dissipative (Komar, 1998; Bird, 2000; Woodroffe, 2002; Masselink and Hughes, 2003; Beck *et al*., 2004; Davis and FitzGerald, 2004; Theron, 2007). Dissipative beaches are linked to steep waves and fine sands (Bird, 2000), characterised by multi-barred morphology (Bird, 2000; Masselink and Hughes, 2003), and are generally associated with back barrier connections to the sea, through shallow overwash or overspilling (Cooper *et al*., 1999).

Intermediate beaches contain both reflective and dissipative conditions (Masselink and Hughes, 2003), and various morphological types (Komar, 1998), as they are dynamic and typically contain nearshore bar morphology, with rip channels (Masselink and Hughes, 2003; Davis and FitzGerald, 2004). Several beaches along the east coast of South Africa are classified as intermediate beaches, with traverse bars and rips (Dardis and Grindley, 1988). However, intermediate to reflective beaches are likely to occur along the northern Natal coast, which are composed mainly of coarse sediments (Dardis and Grindley, 1988), and exposed to decreased wave energy (Cooper *et al*., 1999).

3.3.4. Beach Processes: Nearshore Currents

As waves reach the shoreline and consequently break, currents of many types are generated, depending on the wave and beach conditions (Komar, 1998). Within the surf zone, incident waves gradually disperse their energy as a result of the wave breaking process (Masselink and Hughes, 2003). An amount of this energy is utilised to create nearshore currents and sediment transport (Masselink and Hughes, 2003). The nearshore current strength tends to increase, as the incident wave energy increases; hence the strongest currents occur during storms (Masselink and Hughes, 2003). Nearshore currents have a strong ability to transport vast amounts of sediment (Komar, 1998; Bird, 2000; Masselink and Hughes, 2003), as a result of their large current velocities and mixing motion generated by breaking waves, which amplifies the entrainment of sediment (Masselink and Hughes, 2003). There are three types of currents generated by waves within the nearshore zone, such as longshore currents, bed return flow and rip currents (Komar, 1998; Masselink and Hughes, 2003; Davis and FitzGerald, 2004). Longshore, cross-shore and aeolian transport of sediment occurs concurrently, therefore sediment transport in the nearshore zone near estuary mouths, occurs as a result of the complex wave and current systems within the zone (Beck *et al*., 2004).

3.3.4.1. Longshore Currents

Longshore currents flow parallel to the shoreline within the surf zone (Davis, 1978; Komar, 1998; Bird, 2000; Schumann, 2003; Masselink and Hughes, 2003; Davis and FitzGerald, 2004). These currents are predominantly powered by waves that flow into the surf zone and approach the shore at oblique angles (Davis, 1978; Bird, 2000; Haslett, 2000; Masselink and Hughes, 2003). Longshore currents illustrated in Figure 3.5 (Page 34), are capable of attaining velocities higher than 1 m/s (Masselink and Hughes, 2003), and are enhanced within or near the breaker zone (Hardisty, 1994). The power of these currents increase as the incident wave energy and wave

approach angle increase (Bird, 2000; Woodroffe, 2002; Masselink and Hughes, 2003; Beck *et al*., 2004; Davis and FitzGerald, 2004).

The waves approaching the beach at oblique angles break and push the sediment into suspension generating the longshore drift via an oblique or traverse movement of sediment up the beachface with the swash, which flows back straight down the beach as backwash (Komar, 1998; Bird, 2000; Haslett, 2000; Schumann, 2003). This zig-zag motion of sediment on the beachface, results in sediment being transported as suspended load along the shore in the same direction of the longshore currents (Bird, 2000; Haslett, 2000; Schumann, 2003; Beck *et al*., 2004), until transport is inhibited via a sediment trap (Haslett, 2000). The collective effects of longshore currents, zig-zag motion and oblique wave approach results in the longshore drift (Bird, 2000), which is also termed littoral drift (Hardisty, 1994; Bird, 2000; Davis and FitzGerald, 2004).

Therefore, longshore currents are significant in the transport of sediment, generally transporting large amounts thereof (Davis, 1978; Dardis and Grindley, 1988; Hardisty, 1994; Schumann, 2003; Davis and FitzGerald, 2004), which is extremely significant in terms of the sediment budget (Masselink and Hughes, 2003). Sediment traps include headlands, embayments, spits and deep sea sinks (Hardisty, 1994; Haslett, 2000; Schumann, 2003), and can also take the form of anthropogenic formations such as groynes and breakwaters (Hardisty, 1994; Schumann, 2003). In the case of flow obstruction of the longshore current by sediment traps such as groynes and breakwaters, sediment accretion tends to take place on the updrift side, whereas erosion and beach narrowing occurs on the downdrift side (Hardisty, 1994; Beck *et al*., 2004; Breetzke *et al*., 2008), since the sediment that formerly fed the downdrift beach is now blocked due to the presence of the groyne (Beck *et al*., 2004). The dynamics of longshore drift around a groyne is similar to that around an estuary mouth, however to a lesser extent (Beck *et al*., 2004). If waves tend to approach the shore from a certain direction more frequently, then the overall resultant drift will be in one direction. Several coastal features develop as a result of the longshore drift of sediment, such as spits that develop across the mouths of estuaries, particularly along the east coast of South Africa (Dardis and Grindley, 1988), cuspate forelands, barrier islands and tombolos (Dardis and Grindley, 1988; Komar, 1998).

3.3.4.2. Bed Return Flow

Bed return flow, also termed the undertow, is a mean flow near the bed that is directed offshore, which forms a component of a vertically-segregated circulation of water, where the onshore flow is restricted to the upper section of the water column and the offshore flow is restricted to the bottom (Masselink and Hughes, 2003). In general, the velocities of the bed return flow range

between 0.1 m/s and 0.3 m/s, however during extreme wave conditions the velocities may stretch to 0.5 m/s (Masselink and Hughes, 2003; Davis and FitzGerald, 2004). Bed return flow occurs as a result of the water that flows onshore by breaking waves, which essentially supplies the return flow (Masselink and Hughes, 2003), as is illustrated in Figure 3.5 below.

3.3.4.3. Rip Currents

Rip currents and rip heads are longshore features that develop when the waves break parallel to the shoreline (Haslett, 2000). Rip currents are relatively strong, narrow currents that flow through channels in a seaward direction within the surf zone (Hardisty, 1994; Komar, 1998; Masselink and Hughes, 2003; Schumann 2003; Davis and FitzGerald, 2004), which influences the average longshore transport of sediment (Schumann, 2003). Rip currents develop distinct channels of concentrated offshore flow (Haslett, 2000), that intersect the longshore bars (Pethick, 1984). These currents are supplied by symmetrical longshore transport of water from either sides of the rip (Hardisty, 1994; Komar, 1998; Haslett, 2000; Davis and FitzGerald, 2004), which increase in velocity from zero at the middle of the two rips, to a maximum before entering the rip channel (Hardisty, 1994; Komar, 1998).

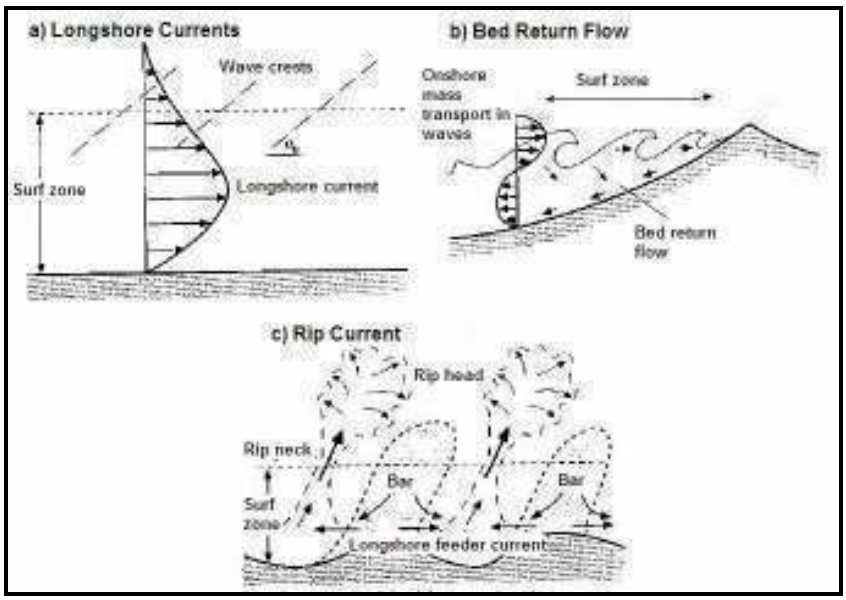

Figure 3.5. a) Longshore currents, b) bed return flow and c) rip currents within the nearshore zone (Masselink and Hughes, 2003).

Schumann (2003) explains that rip currents form a vital component in the nearshore cell circulation system. Within the cell circulation system, there is an onshore movement of water between the rip currents, a high velocity, offshore movement of water within the rip currents

known as the rip neck, and longshore feeder currents that flow in between the rips and the onshore flow, transferring water into the rip (Komar, 1998; Haslett, 2000; Masselink and Hughes, 2003). Masselink and Hughes (2003) indicate that the highest current velocities tend to occur within the rip neck, wherein they may stretch up to 2 m/s during storms, and range between 0.5 m/s and 1 m/s under normal conditions. Figure 3.5 (Page 34) illustrates rip currents in the nearshore zone.

Therefore, the abovementioned wave generated currents occur concurrently and do not take place individually (Hardisty, 1994; Masselink and Hughes, 2003; Beck *et al*., 2004). For instance, under conditions of waves breaking at an angle to the shoreline, longshore currents and cell circulation system with rip currents are generated (Masselink and Hughes, 2003), hence sediment transport can be fairly complicated (Beck *et al*., 2004). However, bed return flow constantly occurs under breaking waves, although it is less distinct under increased cell circulation in the nearshore (Masselink and Hughes, 2003). The longshore currents and cell circulations, work together with waves to create longshore bars and troughs by moving around the sediment (Komar, 1998). Thus, marine sediment transport relies on both wave and tide conditions as it continually changes in direction and position in the nearshore (Beck *et al*., 2004).

3.3.5. Beach Morphology

Bird (2000) explains that as beach sediments are transported along the beach from one area to the next, via waves and currents, the resultant shape of the beach changes. The currents that are created by wind, waves and tides, transport sediment offshore, onshore and alongshore, as the tide fluctuates. This movement of sediment enhances erosion and accretion, which ultimately influences the shape and morphology of beaches, which also displays changes due to fluctuating tides. As the tide rises, the depth of the water increases, which generates stronger waves, resulting in the fine sediment being removed from the beachface, however along the falling tide, a layer of fine sediment tends to be deposited (Bird, 2000).

3.3.5.1. Swash Morphology

The swash zone is classified as a high energy environment and forms part of the upper region of the beach that contains intermittent wet and dry cycles (Komar, 1998; Masselink and Hughes, 2003). Sediment transport within the swash zone occurs as a result of the onshore and offshore flow of the water, which is known as uprush and backwash, respectively (Komar, 1998; Masselink and Hughes, 2003). The morphological features related to the movement of swash are the berm,

beachface, beach steps and beach cusps (Masselink and Hughes, 2003). The profile of the swash zone, as well as the associated morphological features is displayed below in Figure 3.6.

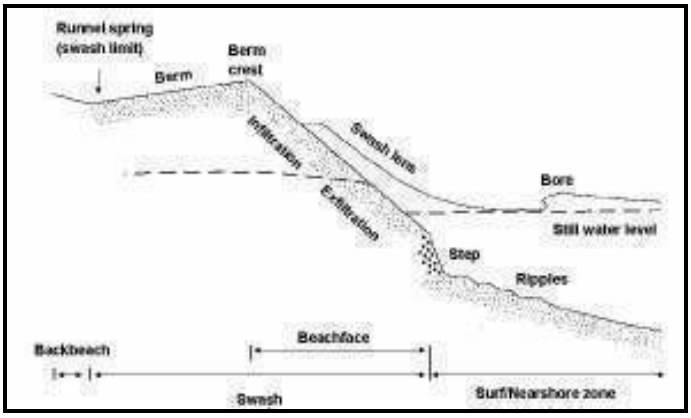

Figure 3.6. The swash zone and beachface morphology (Masselink and Hughes, 2003).

The mean grain size within the swash zone is generally indicative of the energy level of the wave conditions (Komar, 1998). As the swash uprush travels up the beachface, it decreases in intensity and velocity due to friction and percolation, hence the largest particles are deposited first (Komar, 1998; Masselink and Hughes, 2003), which results in the grain size decreasing along the beachface (Komar, 1998). Finer sediment particles are generally found within the upper regions of the swash zone, where the flow velocity is low, however coarser particles are found lower down in line with the plunge point, which contains the highest energy and velocity (Bascom, 1959; 1960; Komar, 1998). The swash uprush is powered by wave energy, whilst the backwash, which also plays an important role in the swash zone, is powered by gravity (Komar, 1998). The velocity of the swash uprush decreases towards the upper region of the swash zone, whilst the velocity of the backwash increases towards the plunge point, where it reaches its greatest velocity at the base of the swash zone (Komar, 1998). Therefore, there is a general fining of sediments in an upward direction along the beachface within the swash zone (Komar, 1998), which indicates that the sediment sorting and mean grain sizes of the swash zone are a function of velocity.

- ***Beachface***

According to Komar (1998) and Masselink and Hughes (2003), the beachface is the steep and planar upper section of the beach profile that is inclined to swash zone processes. Significant proportions of sediment are moved along the beachface, both in an upward and downward direction, as a result of the uprush and backwash, correspondingly (Masselink and Hughes, 2003). The beachface is classified by temporary zones of fine and coarse sediment, as well as small scale features in the form of ridges, terraces and cusps (Bird, 2000).

- ***Berm***

The berm is identified as an almost flat lying section of the beach that is positioned landward of the beachface (Davis, 1978; Komar, 1998; Masselink and Hughes, 2003). It is formed through accretion by sediments that are moved onshore and accumulate within this region or at the landward boundary of wave action (Bascom, 1959; 1960; Komar, 1998; Bird, 2000; Masselink and Hughes, 2003). The berm is classified as an early form of defence for the beach, as it protects the backbeach and coastal dunes from erosion during moderate waves and the initial part of storms (Masselink and Hughes, 2003).

Berms are not present along beaches that are undergoing erosion, as the upper foreshore and backshore are constant with slope (Bascom, 1959; 1960; Davis, 1978; Dardis and Grindley, 1988). Certain beaches, specifically gravel beaches, consist of several berms at different levels of elevation (Masselink and Hughes, 2003), such as those beaches found along macrotidal coastlines (Bird, 2000). However, along microtidal coastlines, a single swash built berm is generally present (Bird, 2000). The berm crest is a point on the berm that divides it from the beachface (Masselink and Hughes, 2003), and symbolises the seaward boundary of the berm with a rapid change in slope (Davis, 1978). On coarse grained beaches, the berm crest is well-defined due to the extremely steep beachface and almost flat back-beach, however on fine grained beaches; the berm crest tends to be unclear due to comparable gradients of the beachface and the backbeach (Komar, 1998; Masselink and Hughes, 2003).

The berm height is highly influenced by the maximum height to which sediment is moved by the uprush of the wave (Masselink and Hughes, 2003). As the wave height or wave period increases, the vertical run-up increases, hence the berm increases in elevation (Komar, 1998; Masselink and Hughes, 2003). Hence, berms and beachfaces are fairly dynamic, as they contain a rapid reaction to fluctuating wave conditions (Masselink and Hughes, 2003). Overtopping of the berm crest and subsequent deposition of the sediment in a pool of water above the berm crest are required to allow vertical accretion of the berm (Masselink and Hughes, 2003). However, vertical erosion of the berm is also permitted by overtopping of the berm crest (Bascom, 1959; Masselink and Hughes, 2003; Stretch and Zietsman, 2004). Sediment grain size, sediment and wave characteristics, as well as aeolian transport are related to the development and size of berms (Bird, 2000; Theron, 2007). Berms also play a role in estuary mouth closure and breaching, overwash into estuaries, and seepage of water landward or seaward into an estuary and the ocean, respectively (Zietsman, 2004; Stretch and Zietsman, 2004; Theron, 2007).

- ***Beach Step***

Masselink and Hughes (2003) define the beach step as a small, underwater scarp that is positioned at the base of the beachface, which may vary in height from a few centimetres to larger than a metre. Beach steps generally consist of the coarsest sediment found within the beach and are therefore most well defined on steep, coarse sediment and gravel beaches (Bascom, 1959; Masselink and Hughes, 2003). Beach steps form as a result of the interaction between the backwash and the incoming wave, which generates a backwash vortex that develops seaward of the shoreline during the backwash cycle that ultimately erodes the bed and forms a rotation directed landward along the bed (Masselink and Hughes, 2003).

- ***Beach Cusps***

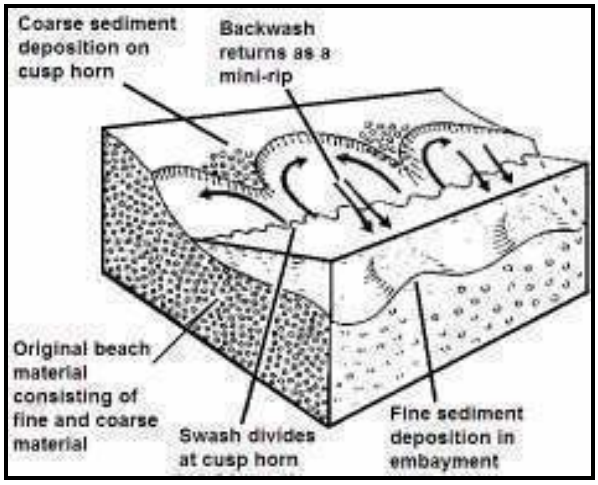

Figure 3.7. The morphology of beach cusps (Masselink and Hughes, 2003).

Beach cusps are periodic features that form along shorelines as a result of swash action (Bird, 2000; Masselink and Hughes, 2003), and are significant features of beach morphology (Beck *et al*., 2004; Theron, 2007). Cusps generally form along shorelines that obtain a wave approach parallel to the coastline, as opposed to oblique angles (Komar, 1998; Bird, 2000), and tend to form well on sand and gravel beaches (Komar, 1998; Bird, 2000; Masselink and Hughes, 2003). In general, beach cusps display a regular pattern in terms of spacing and contain a crescent-like plan form (Pethick, 1984; Hardisty, 1994; Komar, 1998; Masselink and Hughes, 2003; Theron, 2007). The morphology of such features includes gentle, shallow and fine grained seaward facing cusp embayments, as well as steeper gradient, coarse grained, seaward pointing cusp horns (Pethick, 1984; Bird, 2000; Masselink and Hughes, 2003). Figure 3.7 above illustrates the details of beach cusps.

3.3.6. Beach Profile

Bird (2000) and Theron (2007) explain that beach profiles are linked to beach sediment characteristics and wave conditions. Pethick (1984) explains that the beach profile stretches from the landward boundary of wave action to the seaward boundary that is the depth at which shoaling waves form. Beach profiles are highly influenced by wave action, particularly the motions of swash and backwash (Bird, 2000; Theron, 2007). The swash and backwash are in turn influenced by the sediment grain size and beach permeability (Pethick, 1984; Bird, 2000; Masselink and Hughes, 2003). Certain authors identify beach profiles based on environmental controls, such as summer and winter profiles (Bascom, 1959; 1960; King, 1972; Komar, 1998), storm and normal profiles (Pethick, 1984), and storm and swell profiles (Komar 1983; Dardis and Grindley, 1988). Bird (2000) explains that the typical beach profile consists of an upper beach, which is elevated above normal high tide levels, a middle section, which contains a steep slope, and a lower section, which contains a gentle gradient (Bird, 2000).

The most significant aspect of the morphology of beach profiles is their overall gradient, which is the mean slope between the seaward and landward boundaries (King, 1972; Pethick, 1984; Bird, 2000; Masselink and Hughes, 2003). Pethick (1984) explains that beach profiles are classified as either steep or shallow, and over time a particular beach may vary between a steep and shallow profile. Moreover within a range of beaches, certain beaches may be classified as steeper than others (Pethick, 1984). For instance, shingle beaches may be steeper than sand beaches (King, 1972; Pethick, 1984). Bascom (1960) established beach slope angles that range from 1:41 to 1:8 in Half Moon Bay in California. There are three significant factors that influence beach profiles, including waves, sediment variability and sediment transport processes (Pethick, 1984). The slope of the beachface profile is related to the wave breaking type, power of the backwash and amount of nearshore currents (Komar, 1998; Theron, 2007).

3.3.6.1. Beach Profiles, Wave Variability and Wave Energy

According to Haslett (2000) and Masselink and Hughes (2003), beaches are exceptional natural coastal defences, considering the way in which they react to wave energy. Pethick (1984) states that there is a strong relationship between wave type and beach profile gradient. Haslett (2000) states that beaches generally contain fairly steep gradients under normal fair-weather wave conditions, since the wave energy is generally reflected back towards the sea.

According to Bird (2000) and Haslett (2000), steep beach gradients occur due to the swash and backwash action. During fair-weather or calmer conditions, which are characterised by spilling

breakers (Bird, 2000), there tends to be an extended period of time between successive waves, as the backwash flows towards the sea prior to the next breaking wave (Haslett, 2000). The energy of the swash is greater than that of the backwash, therefore under normal fair-weather conditions, the swash transports more sediment up the beach than the backwash transports downwards (Bird, 2000; Haslett, 2000). Consequently, the beach undergoes accretion via sediment movement and deposition up the beach, rather than seaward (Haslett, 2000; Schumann, 2003).

Therefore low, flat, low-energy, swell fair-weather waves are termed constructive waves that generate steep berm-type beach profiles, which build up a wide berm and enable the steep beachface to prograde towards the sea (Bascom, 1959; 1960; King, 1972; Dardis and Grindley, 1988; Pethick, 1984; Haslett, 2000; Masselink and Hughes, 2003; Schumann, 2003). These steep profiles are also known as swell profiles (Bascom, 1959; Dardis and Grindley, 1988; Pethick, 1984; Haslett, 2000) or convex profiles (Bird, 2000; Masselink and Hughes, 2003). Swell profiles occur mainly during the winter season along the east coast of South Africa (Dardis and Grindley, 1988). Therefore, swells cause beach accretion, which develops steep beach profiles (Bascom, 1959; Dardis and Grindley, 1988; Masselink and Hughes, 2003).

Storm waves contain a larger wave height and greater wave steepness than swell waves, as well as a higher range of periods, which ensures that waves break more frequently, resulting in larger amounts of water displaced onto the beachface, ultimately causing erosion, especially at the beach step (Schumann, 2003). Beach profiles are lowered or decrease in slope, as a result of extremely strong wave conditions, which enables the dissipation of wave energy due to a larger surface area specifically during storms (Bascom, 1959; 1960; Bird, 2000; Haslett, 2000; Schumann, 2003). During storms, plunging and surging storm waves generally contain a limited swash and a greater backwash with large offshore orbital velocities that contain a prolonged duration, which enables erosion of sediment from the beach and a dominant overall offshore transport of sediment (Bascom, 1959; 1960; Bird, 2000; Haslett, 2000; Masselink and Hughes, 2003; Schumann, 2003). Storm waves generally remove finer sands from the beach and transports coarse sand to the berm and backshore, with onshore winds transporting it landward (Bird, 2000).

Therefore, high, steep, destructive storm waves tend to generate flatter, shallower bar-type beaches, as a result of erosion of the beachface and berm, and the movement of the sediment towards the sea (Bascom, 1959; 1960; King, 1972; Pethick, 1984; Dardis and Grindley, 1988; Bird, 2000; Haslett, 2000; Masselink and Hughes, 2003; Schumann, 2003), which facilitates the development of a longshore bar, through offshore deposition as the wave current velocity

decreases (Bascom, 1959; 1960; Pethick, 1984; Dardis and Grindley, 1988; Schumann, 2003). These profiles are known as storm profiles (Bascom, 1959; Pethick, 1984; Dardis and Grindley, 1988; Haslett, 2000) or concave profiles (Bird, 2000; Masselink and Hughes, 2003). Storm profiles generally occur within the summer months or the wet season along the east coast of South Africa (Dardis and Grindley, 1988). Therefore, higher wave energies caused by storm waves, lower the gradient of the beachface slope (Dardis and Grindley, 1988). Steep beaches may transform into shallow beaches, through an elimination of the berm and the formation of a longshore bar (Bascom, 1959; 1960; Pethick, 1984). Storm and swell profiles are illustrated below in Figure 3.8. Hence, the beach profiles clearly illustrate seasonal variations.

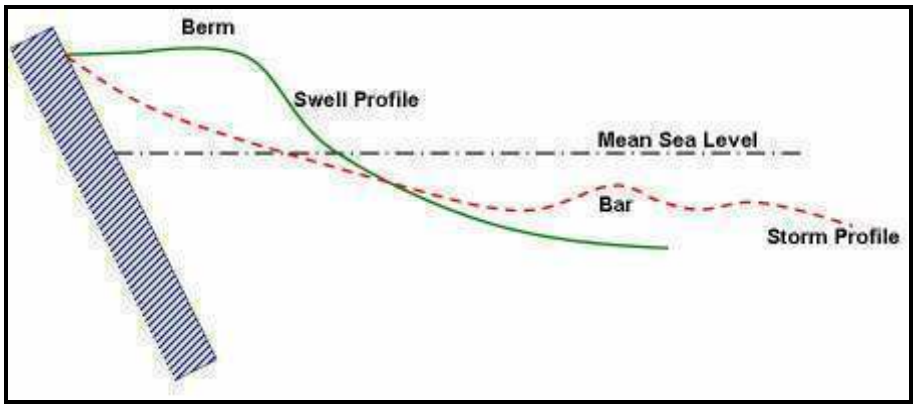

Figure 3.8. Storm and Swell Profile (Redrawn from Pethick, 1984).

Pethick (1984) asserts that there is a relationship between waves, breakers and beach profile gradients. King (1972) established a strong relationship between wave steepness and beach gradient. Bird (2000) points out that deep water waves with a steepness lesser than 0.025, create constructive or spilling breakers. Comparatively, destructive or plunging waves are created by a greater wave steepness ratio (Bird, 2000). Theron (2007) adds that an increase of the beach profile slope generates more rigorous surf conditions, which results in an increase in sediment entrainment and availability for transportation into an estuary mouth. Therefore, the slopes of beach profiles usually reflect the energy distribution throughout the coastline (Komar, 1998; Theron, 2007). However, although these correlations to beach gradient are significant, Pethick (1984) states that there are several other factors that are involved in the gradient of beach profiles, such as sediment particle size and wave approach angles.

3.3.6.2. Beach Profiles and Sediment Size

According to Pethick (1984), the relationship between beach profile gradient and sediment size is extremely well documented. Bird (2000); Masselink and Hughes (2003) and Theron (2007) add

that there is a relationship between beach gradient and sediment size, as these variables are interlinked. The steepness of the beachface slope is governed and influenced by the wave energy and mean grain size or sediment coarseness (Dardis and Grindley, 1988), which the latter is indicative of the wave energy dissipation and the strength of turbulence within the region (Komar, 1998). Bascom (1959; 1960) worked in Half-Moon Bay in California, which according to Pethick (1984) contains a great variability in sediment particle sizes and beach gradients throughout its length. Bascom (1959) established a significant relationship between sediment grain size and beach gradient. The general trend indicates that steep beaches are composed of larger sediment grain sizes, whilst shallow beaches are composed of finer sediment sizes (Bascom, 1959; 1960; Pethick, 1984; Bird, 2000). Although there are several other factors and dynamics involved in the relationship between grain size and beach gradient, it is clear that as one variable changes, so does the other (Pethick, 1984).

The relation between beach gradient and sediment size is linked to the rate of percolation or infiltration of various grain sizes (King, 1972; Pethick, 1984; Bird, 2000; Masselink and Hughes, 2003; Schumann, 2003), which is described as the rate at which water flows through sediment (Pethick, 1984). The rate of percolation is at a maximum for coarse grained sediment (Pethick, 1984; Masselink and Hughes, 2003). For instance on a shingle or gravel beach, as the swash travels up the beach, large amounts of water and energy from the surface flow is lost through percolation and friction, and as a result the amount of backwash is greatly decreased (King, 1972; Pethick, 1984; Bird, 2000; Masselink and Hughes, 2003; Schumann, 2003). Consequently, this causes a landward build up of swash-piled sediment, which results in accretion and an enlarged beach gradient (Pethick, 1984; Bird, 2000; Schumann, 2003), which creates a higher erosive power of the backwash (Dardis and Grindley, 1988).

Fine grained beaches generally contain small rates of percolation due to a decreased permeability, which causes the force and amount of swash and backwash to be relatively equal (King, 1972; Pethick, 1984; Bird, 2000). Along fine grained sediment beaches, the gravitational force that acts downslope causes an offshore sediment transport, which results in erosion of the upper beach and the deposition of a longshore bar, with an overall reduction in the beach gradient (Pethick, 1984). Therefore, shingle and coarse grained beaches contain higher percolation rates and tend to be steeper than fine grained sand beaches (King, 1972; Schumann, 2003).

Furthermore, sediment sorting and mean grain size play an important role in the rate of percolation and hence beach gradient (Pethick, 1984). Beaches with poor sediment sorting contain less percolation and shallow beach profiles, whilst beaches with well sorted sediments of

the same grain size contain steeper beach profiles (Pethick, 1984). Therefore, the slope angle decreases with a decrease in sediment grain size, due to several aspects such as percolation, volumes of backwash and swash, as well as sediment sorting (King, 1972; Pethick, 1984).

3.3.6.3. Beach Profiles and Sediment Transport

According to Pethick (1984), beach profiles transform and adjust largely due to the influence of sediment transport processes. Masselink and Hughes (2003) point out that there is a limited potential for the overall transport of sediment towards the shoreface. Generally, tide- and wind-driven currents are insufficient in order to transport and entrain sediment; however waves generally contain larger velocities, thereby sufficiently transporting and entraining sediment (Masselink and Hughes, 2003). There are three main factors that add to the overall transport of sediment towards the shoreface, which include wave-current interaction, wave asymmetry and bed morphology (Masselink and Hughes, 2003).

There has long been a documented link between flow asymmetry and sediment transport (Pethick, 1984). Importantly, wave orbital velocities are in charge of sediment transport (Schumann, 2003). As waves undergo shoaling, they become non-linear and asymmetrical, by containing sharper crests and long, shallow troughs, as they progress into shallower areas (Masselink and Hughes, 2003; Schumann, 2003). Pethick (1984) identifies a hypothesis that involves the transport of sediment and asymmetrical sediment thresholds under waves, which is known as the null-point hypothesis. This hypothesis states that higher onshore velocities of shorter durations tend to transport large and small sediment grains onshore, however lower offshore velocities of prolonged periods tend to transport only fine sediments towards the sea (Pethick, 1984; Masselink and Hughes, 2003; Schumann, 2003), as illustrated below in Figure 3.9.

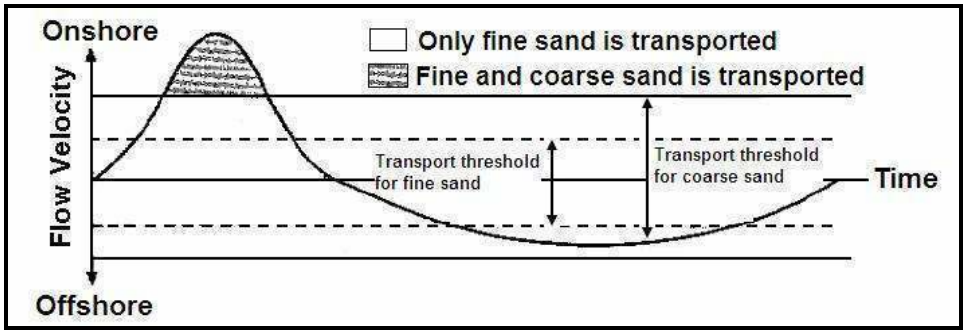

Figure 3.9. The influence of onshore wave asymmetry on sediment transport (Masselink and Hughes, 2003).

Hence, there tends to be an overall offshore movement of fine sediments (Pethick, 1984), and an onshore transport and deposition of coarser sediment particles (Masselink and Hughes, 2003). Masselink and Hughes (2003) explain that the onshore transport of sediment is generally greater than the offshore sediment transport, since transport is linked to the flow velocity to the power of three. However, due to the asymmetry of the velocity and duration, the finer sediments tend to travel a greater distance offshore than onshore (Pethick, 1984). Therefore, the swash contains larger velocities for a short period of time, whereas the backwash contains a lower velocity for a longer period of time, as a result of movement enhanced by the gravitational force (King, 1972; Pethick, 1984; Masselink and Hughes, 2003).

3.3.7. Beach Plan and Longshore Shape

Beaches generally differ according to their shape alongshore, in addition to their variations in profile (Haslett, 2000; Woodroffe, 2002). The plan of a beach is linked to wave patterns, as well as the trend of the coastline, such as the location and occurrence of headlands (Bird, 2000). Beaches vary alongshore as a result of the variation in the longshore drift of sediment and currents (Haslett, 2000). The beach plan or longshore shape is classified as a two-dimensional form of morphology (Pethick, 1984). Research indicates that beaches are commonly straight and smooth-curved (Davis, 1978; Beck *et al*., 2004). Additionally, beaches vary in plan view in terms of their beach outlines and the rhythmic morphologies within them, which include cusps (Figure 3.7: Page 38), crescentic bars and rip current circulations (Pethick, 1984; Komar, 1998; Woodroffe, 2002; Beck *et al*., 2004). Beach plans differ in the form of open beaches, pocket beaches, zeta-form beaches (Davis, 1978; Pethick, 1984; Bird, 2000), and swash-aligned or drift-aligned beaches (Bird, 2000; Woodroffe, 2002; Masselink and Hughes, 2003).

According to Bascom (1959) and Komar (1998), beaches illustrate alongshore sorting based on the exposure to the open ocean. Bascom (1959) and Komar (1998) explain that exposed beaches are generally coarser and steeper than sheltered beaches. Exposed beaches experience the high energy of the open ocean, and responds by changing its morphology (Bascom, 1959). Sheltered beaches experience lesser wave energies and tend to be fine grained and gentle (Bascom, 1959). Sheltered beaches usually contain rocky headlands or groynes, which alter and reduce the wave energy reaching the coastline (Bascom, 1959; Cooper, 1991a, b; 1993; Breetzke *et al*., 2008), as is the case in the Mgeni Estuary. Komar (1998) adds that a section of beach may contain coarser sediments on one end and finer sediments dominating the other end, as a result of higher wave heights within the coarse section of the coast.

CHAPTER 4: THEORETICAL BACKGROUND: ESTUARIES AND FLUXES

This chapter aims to discuss and review the literature and theoretical concepts which structures the body of knowledge of coastal and estuarine geomorphology, upon which this research is based. An outline of the theoretical concepts pertaining to estuaries is discussed, including a description of the definitions, classifications and the physical processes within estuaries. Estuarine morphology, tidal processes and the dynamics of sediment within these coastal features are included within this chapter, as well as sediment discharge and sediment fluxes.

4.1. Introduction

According to Masselink and Hughes (2003), estuaries are fairly modern, unique coastal features that were formed during the end of the last postglacial marine transgression, through which river valleys were inundated as a result of the associated sea level rise. Since this period, estuaries have continued to infill their valleys with sediment (Masselink and Hughes, 2003). Estuaries form in a transitional zone between the land and sea, and therefore form at the boundary between the marine and terrestrial zone, thus are exposed and susceptible to processes derived from both environmental extremes (Cooper *et al*., 1999; Cooper, 2001). As a result, these coastal features develop into fairly dynamic environments, which experience geomorphological change ranging from instantaneous to progressive, in the form of floods and sediment infilling, respectively (Cooper, 2001). Therefore, several types of estuaries occur (Masselink and Hughes, 2003), which consist of various physical processes, morphological patterns and sediment characteristics.

4.2. Estuary Definitions

Estuaries are complex (Pethick, 1984); ephemeral (Dalrymple *et al*., 1992), coastal features and this has given rise to several definitions (Perillo, 1995). Essentially, the word "*estuary*" is derived from "*aestus*", a Latin word, meaning "*of tide*" (Perillo, 1995, p.18). Pritchard (1952) in Pethick (1984, p.167) defines an estuary as "*a semi-enclosed coastal body of water which has a free connection with the open sea and within which sea water is measurably diluted with fresh water derived from land drainage*". According to Pethick (1984); Dalrymple *et al*. (1992) and Perillo (1995), this definition is one that is commonly utilised by coastal scientists, although it is broad, whilst focusing on sea water intrusion and dilution, as opposed to the influence of tides.

Day (1980) critically analysed Pritchard's definition, arguing that it did not consider those typical South African and South Australian estuaries that contain a sandbar across its mouth, which are

temporarily closed or blind, as well as the complete salinity nature of estuaries. Therefore, Day (1980, p.198) suggests that an estuary, in a South African context, is a "*partially enclosed coastal body of water which is either permanently or periodically open to the sea, and within which there is a measurable variation of salinity due to the mixture of sea water with fresh water derived from land drainage*". According to Cooper (2001) this definition considers the distinctive non-permanent characteristic of several estuary mouths in South Africa, thereby incorporating those systems that are hypersaline or dry for long periods of time.

Dalrymple *et al*. (1992, p. 1132) put forward a geologically based definition of an estuary as "*the seaward portion of a drowned valley system which receives sediment from both fluvial and marine sources and which contains facies influenced by tide, wave and fluvial processes. The estuary is considered to extend from the landward limit of tidal facies at its head to the seaward limit of coastal facies at its mouth*". However, Perillo (1995) argues that this definition stresses on the estuarine forming factor of sea-level rise, whilst omitting many other estuarine forming factors.

Therefore, Perillo (1995, p.26) developed a new definition of an estuary, as "*a semi-enclosed coastal body of water that extends to the effective limit of tidal influence, within which sea water entering from one or more free connections with the open sea, or any other saline coastal body of water, is significantly diluted with fresh water derived from land drainage, and can sustain euryhaline biological species from either part or the whole of their life cycle*". This definition includes bar built estuaries, salt water intrusion and the influence of tides, which are significant and responsible for the mixing of marine and fluvial water by tidal energy, and the transport and deposition of sediments (Perillo, 1995).

Therefore, several definitions of estuaries exist, based on salinity, geology, geomorphology and sedimentology. Although most of the definitions are important, the definition created by Dalrymple *et al*. (1992) is considered as most relevant to this study, as it considers the geomorphology and sediment patterns under the influence of tides, upon which this study is focused. In relation, the Mgeni Estuary is positioned in an alluvial valley (Cooper, 1993) along the KwaZulu-Natal coastline, which was subjected sea level regressions and transgressions (Cooper, 1991b). Day's (1980) definition is considered as equally important, since it defines estuaries in terms of South African conditions and also considers the influence of waves and tides, which are significant.

4.3. Estuarine Classification

Estuaries exist as several different types, based on palaeo-valley patterns, mouth conditions and the amount of infilling (Masselink and Hughes, 2003), hence many estuary classifications exist.

4.3.1. Physiographic classification: Shape

Pethick (1984) explains that the morphology of estuaries is highly influenced by its shape, which in turn is based on and influenced by their inherited river valley. The morphological classification of estuaries includes the following four types of estuaries, namely bar-built estuaries, drowned river valleys, rias and fjords (Pritchard, 1952 in Pethick, 1984).

- ***Bar-built estuaries***

Bar-built estuaries, also known as coastal lagoons, form along coasts with a low relief, and limited tidal ranges and fluvial discharge (Perillo, 1995). The bars may take the form of offshore spits or barrier islands (Dyer, 1973; 1997; Pethick, 1984).

- ***Drowned river valleys***

Drowned river valleys formed during the last glaciation phase when the sea level rose (Dyer, 1973; 1997; Pethick, 1984), and they contain open mouths and no tidal attenuation (Green, 2004).

- ***Rias***

Rias are inlets that are formed under drowning of deeply divided unglaciated valleys by the rising sea levels (Pethick, 1984; Bird, 2000).

- ***Fjords***

Fjords occur due to drowning of glacial troughs, which results in exceptionally deep estuaries that flow along parallel courses bounded by steep rocky walls (Pethick, 1984; Bird, 2000). Fjords only develop in high mountainous regions and generally contain an underwater sill across the mouth, which inhibits tidal intrusion (Dyer, 1973; 1997; Pethick, 1984; Perillo, 1995; Bird, 2000).

4.3.2. Tidal Range Classification: Tidal Processes and Estuary Shape

Tidal range is considered a major controlling factor of estuarine processes (Pethick, 1984). Hayes (1979) classified estuaries into three groups according to tidal range and described the depositional shape and morphology of each. Hayes (1979) divided estuaries into microtidal, mesotidal and macrotidal environments.

- ***Microtidal Estuaries***

Microtidal estuaries form along coastlines with a tidal range less than 2 m (Hayes, 1979; Pethick, 1984; Bird, 2000). These estuaries are mainly dominated by fluvial discharge and waves driven

by wind within the estuary mouth region (Pethick, 1984; Perillo, 1995; Bird, 2000). Microtidal coastlines, such as the South African coastline (Schumann *et al*., 1999; Cooper, 2001; Schumann, 2003; Beck *et al*., 2004), contain large flood-tidal deltas and small ebb-tidal deltas (Hayes, 1979). These estuaries may develop a salt-wedge, (Pethick, 1984; Perillo, 1995; Bird, 2000), and generally contain dominant depositional features (Hayes, 1979; Pethick, 1984; Perillo, 1995; Bird, 2000).

- ***Mesotidal Estuaries***

Mesotidal estuaries occur along coastlines containing a tidal range between 2 m and 4 m (Hayes, 1979; Pethick, 1984). Mesotidal coastlines usually demonstrate both wave and tidal influences (Hayes, 1979). However, the tidal influence is strong (Bird, 2000), and greater than marine and fluvial influences (Perillo, 1995). Mesotidal estuaries contain two characteristic features in the form of meandering tidal channels in its upper region and two delta deposits in the mouth region (Pethick, 1984). Ebb-tide deltas are larger than flood-tide deltas, which are positioned seaward and landward of the mouth, respectively (Hayes, 1979; Perillo, 1995).

- ***Macrotidal Estuaries***

Macrotidal estuaries are found along coastlines with a tidal range in excess of 4 m (Hayes, 1979; Pethick, 1984; Perillo, 1995; Bird, 2000). These coastlines are mainly influenced by medium wave energy and tidal currents that stretch a great distance inland (Hayes, 1979; Pethick, 1984; Bird, 2000). These estuaries do not contain barrier islands (Hayes, 1979), and ebb-tide deltas due to large, dominant tidal currents (Pethick, 1984; Perillo, 1995), however they do contain dominant salt marshes, intertidal flats (Hayes, 1979; Perillo, 1995; Bird, 2000), and linear sand bars within the mouth that form parallel to the direction of the tidal flow (Pethick, 1984; Perillo, 1995).

4.3.3. Evolutionary Sedimentary Facies Classification: Estuarine classification in terms of dynamics and facies zonation

Dalrymple *et al*. (1992) classified estuaries into wave- and tide-dominated estuaries, which are discussed in terms of energy distributions, morphological components and facies distributions. Ideally wave- and tide-dominated estuaries can be categorized into three zones, termed the outer, central and inner zones, according to the physical processes taking place within them (Dalrymple *et al*., 1992). The outer zone mainly experiences marine processes such as waves and tides, the central zone is classified as low-energy due to the balance between tidal and river currents, and the inner zone is classified as river dominant (Dalrymple *et al*., 1992). The inner and outer zones of estuaries are therefore dominated by sediment transport, as they contain the highest energy (Dalrymple *et al*., 1992; Masselink and Hughes, 2003).

4.3.3.1. Wave-dominated Estuaries

Wave-dominated estuaries contain limited tidal influences and strong wave energy, which collectively generate an alongshore and onshore movement of sediment into the estuary mouth, that results in the formation of a subaerial barrier or submerged sand bar, which reduces the wave energy entering the estuarine system (Dalrymple *et al*., 1992). Narrow inlets exist within the outer zone (Masselink and Hughes, 2003), and tidal influence does not extend to the head of the estuary, which is mainly influenced by fluvial input (Perillo, 1995). These estuaries contain two points of maximum energy, positioned at the head and mouth of the estuary, since river energy decreases down an estuary due to a drop in the hydraulic gradient, and marine energy decreases up an estuary due to the barrier or sand bar, respectively (Dalrymple *et al*., 1992).

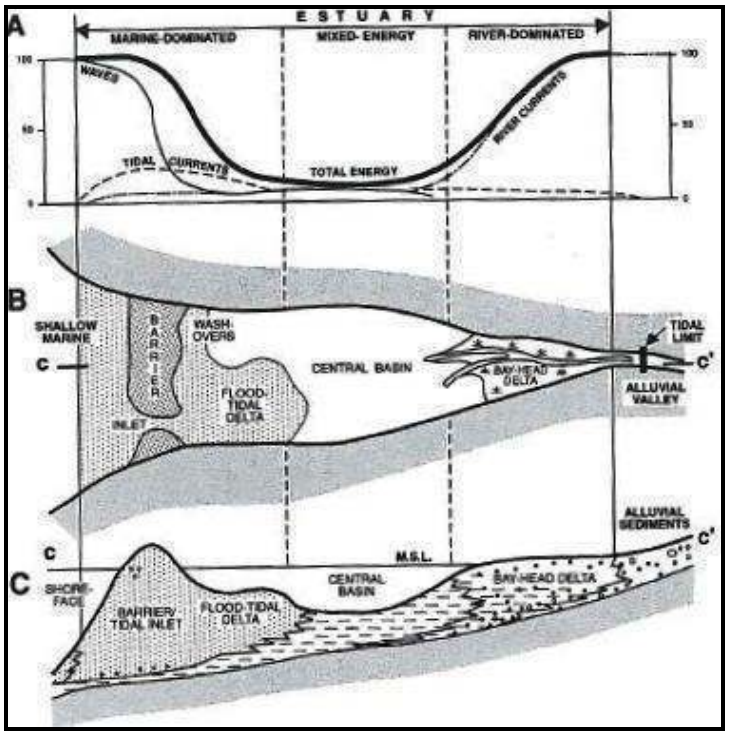

Figure 4.1. A wave-dominated estuary (a) Energy regime, (b) An idealised plan view of the morphology, (c) A longitudinal profile of sedimentary facies (Dalrymple *et al*., 1992).

The morphology and facies distributions of wave-dominated estuaries is linked to bar-built or microtidal estuaries (Perillo, 1995), and flood-dominated estuaries, as they contain an overall influx of marine sediment due to dominant flood tides (Beck *et al*., 2004). In terms of lithofacies, most wave-dominated estuaries adopt a tripartite pattern, ranging from coarse to fine to coarse, from the estuary mouth to the head (Dalrymple *et al*., 1992). A body of marine sand occurs at the mouth, containing washover fans, flood-tidal deltas and transgressive subtidal shoals, whilst fine

sediment dominates the central zone and fluvially derived coarse sand and gravel accumulate at the head of the estuary, developing a bay-head delta (Dalrymple *et al*., 1992). The shallow central basin may develop into a mud basin; however it generally contains several traverse tidal channels, in which the main process is bed sediment re-suspension by waves (Dalrymple *et al*., 1992; Perillo, 1995; Masselink and Hughes, 2003). Figure 4.1 (Page 49) indicates the energy regime, morphology and sedimentary facies within a wave-dominated estuary.

4.3.3.2. Tide-dominated Estuaries

Tidal currents contain a higher energy than wave energy at the mouth of a tide-dominated estuary (Dalrymple *et al*., 1992; Perillo, 1995), which generally contain characteristic elongated, linear sand bars that form several tidal channels that decrease the wave energy (Dalrymple *et al*., 1992; Masselink and Hughes, 2003). Tide-dominated estuaries are generally identified by a funnel shape, which causes the ensuing flood-tide to travel into a gradual smaller channel area, which causes an increase in the speed of the flood-tide (Dalrymple *et al*., 1992; Dyer, 1997). As the flood-tide current travels up the estuary, the tide energy decreases to an overall minimum at the limit of tidal influence due to friction exceeding convergence, however comparatively fluvial energy reduces as it flows towards the sea (Dalrymple *et al*., 1992).

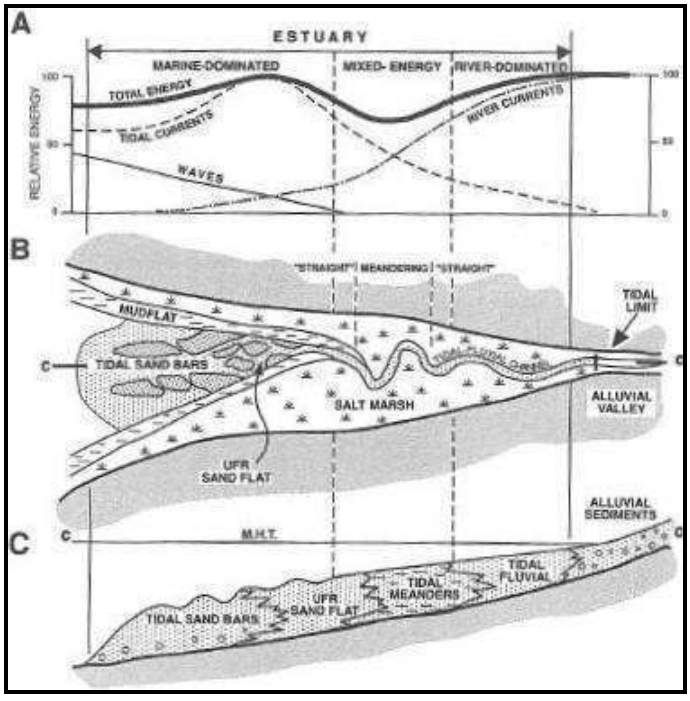

Figure 4.2. A tide-dominated estuary (a) Energy regime, (b) An idealised plan view of the morphology, (c) A longitudinal profile of sedimentary facies (Dalrymple *et al*., 1992).

According to Dalrymple *et al*. (1992), the sedimentary facies distribution in tide-dominated estuaries is not as distinct as those present in wave-dominated estuaries, since tidal energy travels further up the estuary than wave energy. Sand dominates the tidal channels positioned along the longitudinal axis of the estuary, whilst the point of minimum energy is characterised by the deposition of the finest sands, with muddy sediments occupying the tidal flats and marshes (Dalrymple *et al*., 1992). The central zone is dominated by fine sediment deposition (Perillo, 1995; Masselink and Hughes, 2003), and contains low-energy and patterns of progressive meandering and straight channels (Dalrymple *et al*., 1992). The inner zone does not contain bay-head deltas (Dalrymple *et al*., 1992), due to a strong tidal influence throughout the central zone and part of the inner zone (Masselink and Hughes, 2003). Figure 4.2 (Page 50) indicates the energy regime, estuary morphology and sedimentary facies within a tide-dominated estuary.

4.3.4. South African Classification of Microtidal Estuaries on a Wave Dominated Coastline

This morphological conceptual classification was documented with the aim of incorporating the differences and geomorphological variability between South African estuaries (Cooper *et al*., 1999; Harrison *et al*., 2000, Cooper, 2001). The morphology of South African estuaries varies according to climate, fluvial discharge, coastal gradient, catchment hinterland gradient, fluvial sediment input and sedimentary characteristics of both the coastal and fluvial zones (Cooper, 2001). Hence, the South African coastline displays several types of estuaries, each consisting of different and distinct sedimentary environments and geomorphological units (Cooper, 2001).

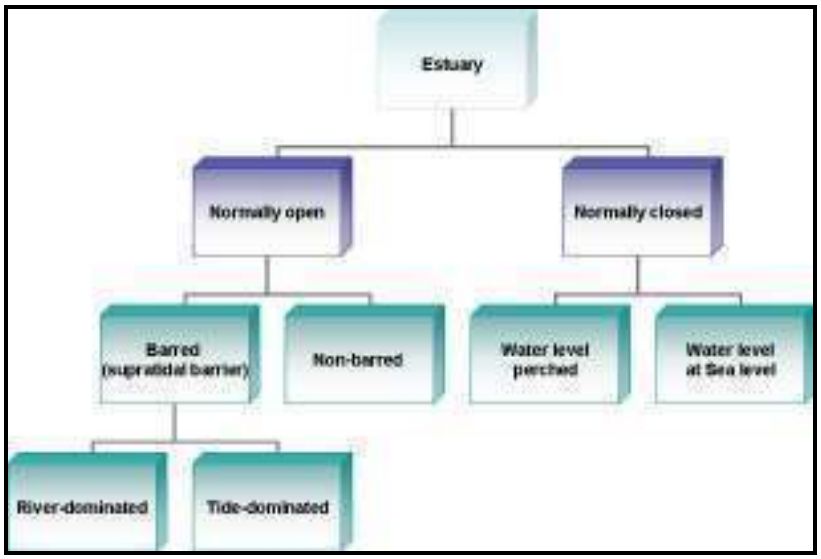

Figure 4.3. Morphodynamic conceptual classification of microtidal South African estuaries (Redrawn from Harrison *et al*., 2000 and Cooper, 2001).

The most distinct variation between South African estuaries is the linkage to the sea, therefore estuaries are initially classified as normally open or normally closed, in which the latter contains a barrier across the inlet (Harrison *et al*., 2000; Cooper, 2001). This classification between normally open and normally closed estuaries is most evident in KwaZulu-Natal (Harrison *et al*., 2000; Cooper, 2001), as estuaries are grouped according to those that they are open for more than 70 % and less than 30 % of the time (Begg, 1984). Normally open estuaries are additionally sub-divided into barred open and non-barred open systems (Harrison *et al*., 2000; Cooper, 2001). This conceptual classification is illustrated in Figure 4.3 (Page 51).

- ***Normally Open Estuaries***

According to Harrison *et al*. (2000) and Cooper (2001), non-barred open estuaries are fairly infrequent and remain open with no sediment accumulation at the inlet. Usually estuaries present along a high energy coastline are susceptible to close under certain extreme wave conditions, therefore the presence of non-barred estuaries along the coastline of South Africa is considered as unusual (Cooper, 2001). However, non-barred open estuaries may contain an intertidal sand barrier at the mouth of the estuary that may be classified as the surface of a flood-tidal delta, which reduces incoming wave action, creating a calm environment in the estuary (Harrison *et al*., 2000; Cooper, 2001).

Barred open estuaries generally vary in dimensions and the amount of river discharge, and distinctively contain significant deposition of sediment across the mouth in the form of a supratidal barrier with a surface channel (Harrison *et al*., 2000; Cooper, 2001). These estuaries generally contain short barriers that minimize the discharge volume by barrier seepage (Cooper, 2001). Harrison *et al*. (2000) further divides barred open estuaries according to their size, into those that contain a Mean Annual Runoff (MAR) greater than and lesser than 15×10^6 m^3. Smaller barred open estuaries that contain small tidal prisms, sustain their open status through fluvial discharge and rarely contain flood tidal deltas (Harrison *et al*., 2000; Cooper, 2001). Larger barred open estuaries are divided into two further categories, namely river- and tide-dominated estuaries (Cooper, 1993; 2001; Cooper *et al*., 1999; Harrison *et al*., 2000).

- ***River-dominated Estuaries***

Dalrymple *et al*. (1992) argued that the classification of estuaries into a fluvially-dominated category is pointless, since the river does not influence the morphology of estuaries. However, Cooper (1993; 1994; 2001; 2002) explains that river-dominated estuaries are important classifications of estuaries. These estuaries are most distinct and well formed within KwaZulu-

Natal (Cooper, 1993; 1994; 2001; Cooper *et al*., 1999; Harrison *et al*., 2000). River-dominated estuaries generally contain inadequate tidal prisms in order to maintain an open mouth against the nearshore tidal currents, wave action and sediment transport that close the estuary inlet (Cooper *et al*., 1999; Harrison *et al*., 2000; Cooper, 2001; 2002). These estuaries occur as a result of their constricting morphology in terms of steep gradients and high sediment supplies, as well as via sedimentation and infilling of prior tide-dominated estuaries (Cooper *et al*., 1999; Cooper, 2001; 2002). Fluvial sediments and facies dominate the system (Cooper *et al*., 1999; Cooper, 2001; Beck *et al*., 2004), which stretch towards the barrier and together with increased bed levels, hinder the amount of tidal input, creating an intertidal or shallow back-barrier region (Cooper *et al*., 1999; Harrison *et al*., 2000; Cooper, 2001; 2002; Beck *et al*., 2004). However, marine sediment may enter these systems via barrier overwash (Cooper, 1986; Cooper *et al*., 1999).

Additional fluvial sediment is transported via the infilled estuary to the nearshore zone, where it undergoes dispersal, and it is under these conditions that river-dominated estuaries are considered as suppliers of sediment to the coastal zone, as opposed to sinks for marine sand (Cooper, 2001; 2002). Thus, fluvial flow is the main factor that sustains the open nature of these estuaries; hence drought conditions may influence the mouth state, causing them to close for long periods (Harrison *et al*., 2000; Cooper, 2001). However, dam construction within a river catchment may also influence the amount of river discharge and sediment delivery to estuaries, which is true for the Mgeni Estuary (Garland and Moleko, 2000; Harrison *et al*., 2000, Cooper, 2001). Due to the establishment and closure of the Inanda Dam, the Mgeni Estuary tends to be closed for long periods of time, considering that it previously remained open for more than 90 % of the year (Cooper, 1993; 2001). Seasonal floods play major roles in river-dominated estuaries, by removing and eroding most of the deposited sediment throughout the estuarine channel, which results in channel deepening (Harrison *et al*., 2000; Cooper, 2001; 2002; Beck *et al*., 2004). The September 1987 flood event caused the channel, and the entire vegetated, mangrove barrier island of the Mgeni Estuary to be completely eroded (Cooper, 2001; 2002).

- ***Tide-dominated Estuaries***

According to Green (2004), the classification of tide-dominated estuaries put forward by Harrison *et al*. (2000) and Cooper (2001) is different to that put forward by Dalrymple *et al*. (1992), because the arrangement of facies follows that of Dalrymple *et al*. (1992) wave-dominated estuaries. Tide-dominated estuaries are classified as those that contain adequate tidal prisms, which are able to uphold their estuary inlets through tidal flows against the sediment transport by

longshore and wave-driven currents (Cooper, 2001; 2002). Tide-dominated estuaries contain a different morphological pattern compared to river-dominated estuaries.

According to Cooper (2001; 2002), estuaries that are tide-dominated display a facies arrangement parallel to that of a microtidal barrier environment, as described by Hayes (1979). Cooper (2001) describes the facies arrangement of these estuaries as tripartite, displaying marine influx at the mouth, fluvial sediment input at the head, and low-energy suspension settling in the middle section. Ebb-tidal delta formation is negligible due to high wave action (Cooper, 2001; 2002), although transgressive flood-tidal deltas within the estuary inlet are distinct and well formed (Harrison *et al*., 2000; Cooper, 2001; 2002). These flood-tidal deltas are formed as a result of the overriding influence of the flood-tide, which causes sediment suspension through wave action as the tide progresses upstream and sediment deposition as the wave action wanes (Harrison *et al*., 2000; Cooper, 2001; 2002). Estuarine protruding coarse grained fluvial deltas are positioned upstream and a deep region is located landward of the flood-tidal deltas (Harrison *et al*., 2000; Cooper, 2001).

Fluvial floods also play a major role in the morphology of tide-dominated estuaries, such that the flood-tidal deltas are fully eroded (Harrison *et al*., 2000; Cooper, 2001; 2002). However, tide-dominated estuaries may possibly close due to the impact of large scale marine events (Cooper, 2001). Generally, tide-dominated estuaries are identified as sinks of marine sediment, due to the prevailing force of the flood-tide at the estuary inlet (Cooper, 2001; 2002). The morphological plan views of normally open barred river- and tide-dominated estuaries, as well as non-barred open estuaries are displayed below, in Figure 4.4.

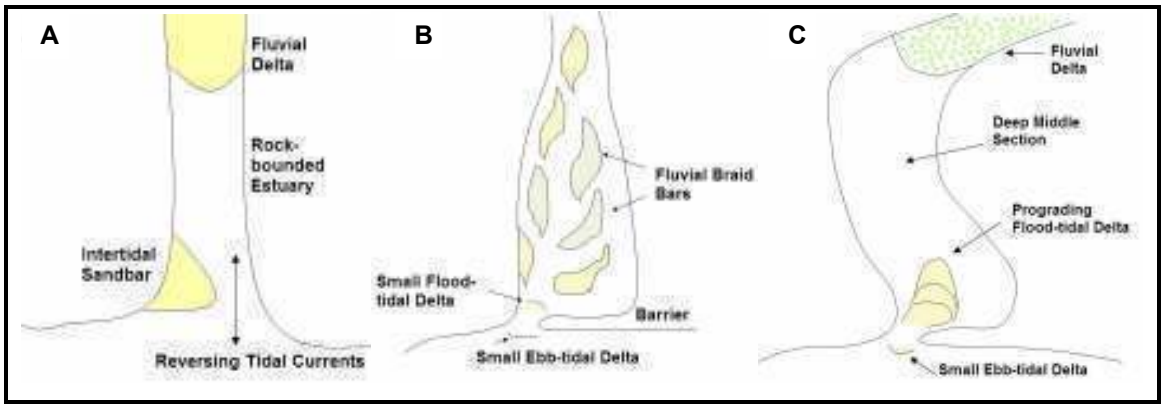

Figure 4.4. The morphology of a (A) non-barred open estuary, (B) barred open river-dominated estuary, (C) barred open tide-dominated estuary, plan view (Redrawn from Harrison *et al*., 2000; Cooper, 2001; Cooper, 2002).

Hence, river- and tide-dominated estuaries are different in terms of morphology and facies arrangements (Cooper, 2001). According to this classification, the Mgeni Estuary contains a MAR greater than 15 x 10^6 m^3, is normally opened, barred and river-dominated (Harrison *et al*., 2000).

- ***Normally closed Estuaries***

According to Harrison *et al*. (2000) and Cooper (2001), normally closed estuaries are divided into perched and non-perched estuaries, based on the water level within the back-barrier region of the estuary, in relation to the water level of the open sea. Perched closed estuaries contain relatively elevated berms that form due to the accumulation of coarse barrier sediment and low wave energy, which trap large amounts of water behind them, at levels exceeding most high tides. These trapped water bodies are at equilibrium with the inputs (fluvial input, rainfall and barrier overwash), and the outputs (evaporation, evapotranspiration and seepage through the barrier) (Harrison *et al*., 2000; Cooper, 2001).

Non-perched closed estuaries are those that lack a high elevated berm and distinct surface channel, which are trapped behind a barrier at or close to high tide level (Harrison *et al*., 2000; Cooper, 2001). The beaches fronting these estuaries generally contain a low gradient profile that in conjunction with the absence of a high berm and high wave energy, results in regular occurrences of barrier overwash (Harrison *et al*., 2000; Cooper, 2001). The lower regions of non-perched estuaries are dominated by marine sand, whereas the upper regions are dominated by fluvial sand (Cooper, 2001).

4.4. Estuarine Morphology

Estuaries experience alternating incoming flood tide currents and outgoing ebb tide currents, which also includes significant changes in current velocity throughout the tidal cycle (Cooper *et al*., 1999; Bird, 2000; Beck *et al*., 2004). The morphology of estuaries is indicative of the interaction between the capacity of the tidal channels and the volume of incoming and outward flowing water by tidal fluctuations (Bird, 2000). Estuarine morphology is linked to climate, hinterland topography, sediment supply, coastal lithology and hydrodynamic processes, in the form of fluvial flow, flood tidal currents, wave action, and chemical and biological processes, all of which illustrate variations (Cooper *et al*., 1999; Bird, 2000; Harrison *et al*., 2000).

4.4.1. Tidal Channels, Zones and Flows

- ***Subtidal, Intertidal and Supratidal Zones***

Masselink and Hughes (2003) identify three types of tidal channels and zones within estuaries, specifically termed the subtidal, intertidal and supratidal zones. The subtidal zone is the channel positioned below the level of mean low water, which is submerged during all times, transports water throughout the entire tidal cycle and contains the highest energy levels. The intertidal zone is positioned between the levels of mean high and mean low water, is exposed and submerged during the tidal cycle, and contains overall moderate energy levels. The supratidal zone is located within the channel above mean high water and is exposed for the majority of the tidal cycle, with the exception of spring tidal conditions, during which it is inundated. This exposed nature of the supratidal zone yields an exceptionally low energy regime (Masselink and Hughes, 2003).

- ***Ebb and Flood Channels***

Bird (2000); Beck *et al*. (2004) and van Niekerk (2007) identify tidal channels, in addition to those described above by Masselink and Hughes (2003). These channels are identified as ebb and flood channels (Bird, 2000; Beck *et al*., 2004; Beck, 2005; van Niekerk, 2007). Ebb channels are those that are meandering (Beck *et al*., 2004), which contain an overall output flow of fluvial sediment and water (Dyer, 1994; Bird, 2000). Ebb channels develop around the flood-tide sand bank (van Niekerk, 2007), and generally become broadened out and shallower towards the sea (Bird, 2000). These channels are linked to the main estuarine channel to the side of the mouth, which causes sheltering against the incoming sediment due to the berm (van Niekerk, 2007).

Flood channels contain an incoming flow of marine sediment and water (Dyer, 1994; Bird, 2000). During the flood tide, the incoming flow tends to travel across the adjacent exposed banks, which results in the formation of a flood channel that is directed headward within the main channel (Dyer, 1994; Beck *et al*., 2004; van Niekerk, 2007). Flood channels become shallower towards the land (Bird, 2000), and the maximum velocities decrease as the channel cross-section increases (Dyer, 1994). The sediment delivered to the estuary via the flood-tidal channel mainly results in the formation of a flood-tide sand bar or bank within the inlet (van Niekerk, 2007).

Therefore, the main estuary channel is divided into two, unstable flow channels, known as the ebb and flood channels (Bird, 2000; Beck *et al*., 2004; Beck, 2005; van Niekerk, 2007). In most cases the ebb and flood channels intersect flow paths, and it is at this point where shoaling occurs (Beck *et al*., 2004; Beck, 2005). Sand tends to be deposited in the flood channel during

the ebb-tide, whilst being deposited in the ebb channel during the flood-tide (Beck *et al*., 2004; Beck, 2005). van Niekerk (2007) adds that the interaction between the ebb and flood tidal channels influences the mouth state of estuaries, thus if the ebb channel remains remarkably sheltered, then the estuary is likely to adopt an open mouth state. Figure 4.5 below illustrates the patterns and positions of the ebb and flood channels, in a specific estuarine inlet.

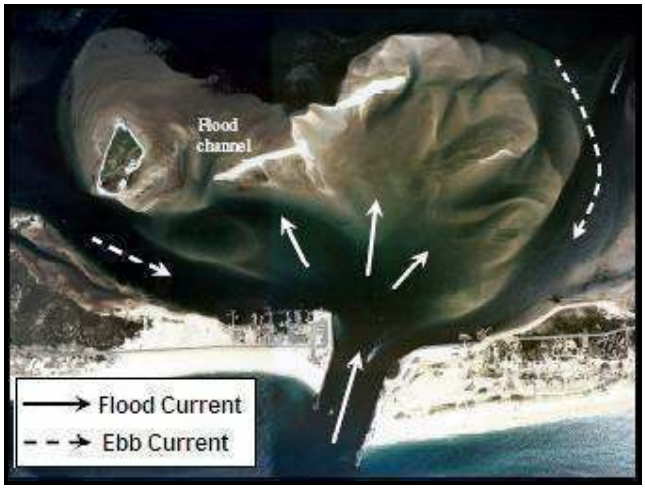

Figure 4.5. Flood and ebb channels in the Shinnecock Inlet in USA (Walton, 2002 in Beck *et al*., 2004).

- ***Ebb- and Flood-Dominated Estuaries and the Influence on Sedimentation***

Tide-dominated estuaries are divided into ebb- and flood-dominated based on tidal channels and dominant estuarine flows (Beck *et al*., 2004; Beck, 2005). Flood- and ebb-dominated estuaries are related to the prevalence of flood and ebb currents (Masselink and Hughes, 2003; Beck *et al*., 2004). Dyer (1995; 1997) and Masselink and Hughes (2003) explain flood dominance in a shallow frictionless estuary generally occurs due to the deep section under the crest of the tidal wave moving faster than the shallow water under the trough of the tidal wave, which may cause the crest to overtake the trough. Dyer (1997) further explains that flood dominance also occurs as a result of bottom friction which decelerates the movement of water at low water in relation to high water. Flood-dominated estuaries contain a flood tide or a rising tide that is larger in velocity and magnitude and shorter in duration than the ebb tide (Dyer, 1995; 1997; Masselink and Hughes, 2003; Beck *et al*., 2004). This results in a peak flood current that is greater than the peak ebb current, rendering the system flood-dominant (Beck *et al*., 2004).

Dyer (1997) explains that ebb dominance occurs in estuaries as a result of the interaction between deep channels and shallow water regions, as well as various frictional distributions

during the tide. An estuary is classified as ebb-dominant if it contains extensive tidal flats, which influences the water surface area and the cross-sectional area of the estuary (Schumann *et al*., 1999; Beck *et al*., 2004). Ebb dominance results in an ebb tide or falling tide that is larger and stronger in velocity and magnitude, as well as shorter in duration than the flood tide (Dyer, 1997; Masselink and Hughes, 2003; Beck *et al*., 2004). Generally, the peak ebb current is greater than the peak flood current, rendering the system ebb-dominant (Beck *et al*., 2004).

Hence, ebb- and flood-dominated estuaries are dependent on the mouth state of the estuary and the occurrence of tidal flats (Beck *et al*., 2004). These types of estuaries are related to, and play a significant role in sedimentation patterns (Beck *et al*., 2004). Flood- and ebb-dominated estuaries generally display an overall movement of sediment landward or seaward respectively, and a small difference in velocity and magnitude of either the ebb or flood tide, can generate a large difference in the overall amount of sediment transported in and out of the estuary by each tide (Masselink and Hughes, 2003). Ebb-dominated estuaries are composed mainly of fluvial sediment and limited amounts of marine sediment, whereas flood-dominated estuaries are mainly composed of marine sediment (Masselink and Hughes, 2003; Beck *et al*., 2004).

4.5. Estuarine Processes

Processes within estuaries include those that influence the morphology and sediment transport (Masselink and Hughes, 2003); however the processes focused on in this study are tides and tidal currents.

4.5.1. Tides

Tides are the rise and fall of the surface of the ocean, as a result of the gravitational attraction of the earth, moon and sun (King, 1972; Dyer, 1986; Schumann *et al*., 1999; Komar, 1998; Bird, 2000; Haslett, 2000; Masselink and Hughes, 2003; Beck *et al*., 2004; Davis and FitzGerald, 2004; Beck, 2005). The moon, due to its closeness, and the sun, due to its large mass, are the bodies that generate tides (Komar, 1998; Masselink and Hughes, 2003; Davis and FitzGerald, 2004). These tidal oscillations are not distinct within the deep waters of the ocean, but are extremely evident along shallow coastlines, estuaries and funnel-shaped embayments (Schumann *et al*., 1999; Masselink and Hughes, 2003; Davis and FitzGerald, 2004). The ebb and flow mechanism of the tide is responsible for sea level changes along the coastline, which generates tidal currents (Bird, 2000). Tides significantly shape and form the morphology of estuaries (Masselink and Hughes, 2003), and are important for sediment transport processes (Dyer, 1986; 1995, 1997).

4.5.2. Spring and Neap Tides

Masselink and Hughes (2003) describe the generation of the spring and neap tidal cycle through solar and lunar interaction in which the sun moderates and amplifies the tides, and the magnitudes of the solar and lunar bulges vary according to the various phases of the moon. Spring tides occur during syzygy, when the earth, moon and sun are in collective alignment (Masselink and Hughes, 2003), and the tidal bulges of the moon and sun are aligned as well (Komar, 1998; Masselink and Hughes, 2003; Davis and FitzGerald, 2004), producing a collective and enlarged tidal range (Komar, 1998; Bird, 2000; Masselink and Hughes, 2003; Schumann, 2003; Davis and FitzGerald, 2004; Beck *et al*., 2004). Spring tides occur during a new moon and a full moon (Komar, 1998; Masselink and Hughes, 2003; Davis and FitzGerald, 2004), and are the largest tides, containing the highest high tides and lowest low tides, compared to lunar tides (Masselink and Hughes, 2003; Davis and FitzGerald, 2004).

Neap tides occur during quadrature (Komar, 1998; Bird, 2000; Masselink and Hughes, 2003; Davis and FitzGerald, 2004), when the moon is perpendicular to the earth in relation to the sun (Komar, 1998; Masselink and Hughes, 2003), and the tides are out of phase and opposed; producing an overall reduced tidal range (Komar, 1998; Bird, 2000; Masselink and Hughes, 2003; Davis and FitzGerald, 2004; Schumann, 2003; Beck *et al*., 2004). Neap tides display a small tidal range and small tides (Komar, 1998; Bird, 2000; Masselink and Hughes, 2003; Davis and FitzGerald, 2004). Spring tides are 20 % above the average tidal range, while neap tides are 20 % below the average tidal range (Komar, 1998). Stronger and faster tidal currents occur during spring tides as opposed to neap tides, because a higher volume of water is transported (Bird, 2000; Davis and FitzGerald, 2004; Theron, 2007). Consequently, the ability to transport sediment within an estuary during neap tides is reduced, however higher amounts of sediment transport occur during spring tides (Dyer, 1995; Kitheka *et al*., 2005; Theron, 2007).

4.5.3. Tidal Amplitude and Tides in Estuaries

Theron (2007) explains that the ocean tide is the main, significant hydraulic force in an estuary, apart from river discharge. Tidal currents occur as a result of tidal fluctuations (Bird, 2000), and the variation of tidal amplitude and phase throughout the estuary influences the current velocities (Dyer, 1997). Tidal elevations within estuaries are very important as they influence the potential of currents to transport sediment; hence it influences the sediment flux (Dyer, 1995; 1997; Theron, 2007). Tides provide energy that enables mixing of fluvial and estuarine water, the re-suspension and transportation of sediments, creation of bedforms and scouring channels, and the redistribution of sediments (Wells, 1995; Dyer, 1997).

Tidal progression involves the development of periodic water level oscillations and currents caused by a hydraulic gradient present between the water levels outside of the estuary and within (Pethick, 1984; Schumann *et al*., 1999; Masselink and Hughes, 2003). As the tide moves up an estuary, the water level in front of the wave transforms from low to high and the water level at the back of the wave transforms from high to low (Pethick, 1984; Masselink and Hughes, 2003). According to Masselink and Hughes (2003), flood and ebb tide currents are experienced equally throughout an entire tidal period. As the water level outside the inlet becomes higher than the water inside, the water surface grades into the estuary, which generates the flood tide current (Schumann *et al*., 1999; Masselink and Hughes, 2003; Davis and FitzGerald, 2004). This gives rise to the tidal prism, which is described as the overall volume of water that enters the estuary on the flood tide (Schumann *et al*, 1999; Schumann, 2003; Masselink and Hughes, 2003), which is proportional to the cross-sectional area of the inlet (Dyer, 1994). As the water level of the ocean decreases on a falling tide and becomes lower than the water level inside, then the water surface grades out of the estuary, which generates the ebb tide current (Schumann *et al*., 1999; Masselink and Hughes, 2003; Davis and FitzGerald, 2004).

Estuary channels generally become shallower and narrower as they progress further away from the coast (Masselink and Hughes, 2003), which is known as the funneling effect (Dyer, 1995). Frictional effects caused by the estuary bed, channel edges, as well as the funneling effect can cause the tide within the estuary to change substantially (Schumann *et al*., 1999; Dyer, 1995). Considering that wave energy is directly proportional to the wave height (Pethick, 1984), when a tidal wave travels up the estuary, frictional effects cause the wave energy to decrease, as well as the wave height and amplitude (Pethick, 1984; Schumann *et al*., 1999). This decrease in wave energy causes the tide to flatten and disappear as it moves inland (Pethick, 1984).

4.5.4. Tidal Currents: Velocity-Stage Relationships

Pethick (1984); Bird (2000) and Masselink and Hughes (2003) explain that theoretically, maximum velocities of an advancing tide at the mouth of an estuary are encountered at high and low water, with current reversal and zero velocities occurring during mid-tide, which renders the current slack, which is illustrated in Figure 4.6 (Page 61). However, Pethick (1984) and Bird (2000) explain that at the head of the estuary, maximum flow velocities take place at mid-tide, whereas zero velocities occur at high water and low water. Research indicates that when the tide enters an estuarine channel, the relationship between velocity, current direction and tidal stage intensifies (Pethick, 1984).

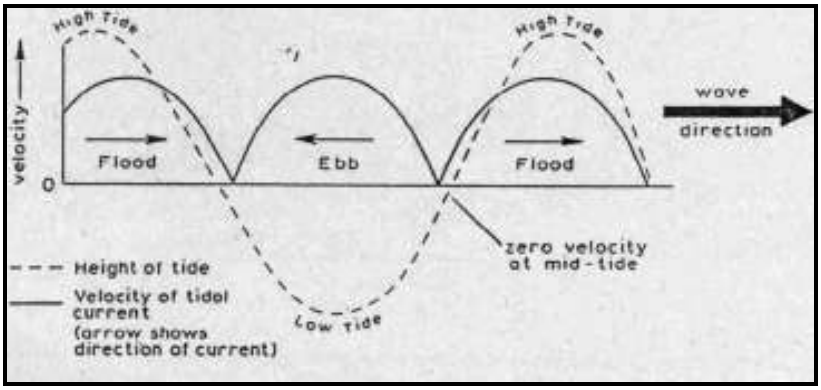

Figure 4.6. Tidal-stage velocity regime at the mouth of an estuary, illustrating slack water and current reversal at mid-tide, with maximum velocities attained at high and low water (Pethick, 1984).

However, Pethick (1984) asserts that in reality, the velocity-stage relationships do not relate to its theoretical counterpart. Bird (2000) reasons that the velocity pattern is changed in reality, based on the fractional reflection of the tidal wave, which obscures the generalised theoretical pattern, as it impedes the upstream progression of the high tide or crest of the tidal wave. Pethick (1984) maintains that in most estuaries the reversal of the current and zero velocities or slack water, does not occur at mid-tide, which is three hours before and after high water. Instead, slack water occurs within a range of one and two hours after high and low tide (Pethick, 1984; Masselink and Hughes, 2003). Additionally, Masselink and Hughes (2003) explain that the highest current velocities are experienced just after mid-tide.

Conversely, Redfield (1950) in Pethick (1984) notes that the tides located in proximity to the estuary mouth and the sea, encounter slack or zero velocities closer to mid-tide than those further landward. This occurs as a result of the reflectance of energy as the tide travels up an estuary, which generates a seaward bound wave that counters the oncoming tide (Pethick, 1984; Masselink and Hughes, 2003). The formation of a standing wave would occur if all of the energy of the incoming tide was reflected (Pethick, 1984). However, the tidal patterns within the vicinity of the estuary mouth are classified as progressive, whereas standing tidal patterns are dominantly displayed at the head of the estuary, considering that most of the reflection takes place within this region (Masselink and Hughes, 2003).

4.5.5. Standing and Progressive Waves

The rise and fall of water in connection to the ebb tide and flood tide current is controlled by the behaviour of the tide as either a standing or progressive wave (Masselink and Hughes, 2003). Progressive tides occur in straight and lengthened estuarine channels, in which no reflection

takes place (Masselink and Hughes, 2003). Progressive tides are produced under conditions of total frictional dissipation of the travelling tidal wave before it reaches the reflective boundary, or if the length of the estuarine channel is adequate or unlimited (Dyer, 1997; Masselink and Hughes, 2003). Under such circumstances, the tidal current and amplitude will be in phase, meaning that maximum flood currents would take place at high tide (Dyer, 1997; Masselink and Hughes, 2003).

However, in a frictionless or an idealized estuarine channel that is straight and contains a vertical boundary at the head, a tidal wave will enter the estuary and advance towards the head, where it will be reflected down the estuary (Dyer, 1995; 1997; Masselink and Hughes, 2003). If the time of this progression and reflection of the wave equals to the tidal period, then it will meet and interact with the next tidal wave that enters the estuary from the sea (Pethick, 1984; Dyer, 1997; Masselink and Hughes, 2003). This results in a standing wave system, in which maximum velocities occur at mid-tide, whilst slack water occurs at both high and low tide (Pethick, 1984; Masselink and Hughes, 2003). Standing tides occur when the tide progresses up an estuary and encounters reflective boundaries, such as channel margins, bends and an increase in bed elevation (Masselink and Hughes, 2003).

4.5.6. Tidal Asymmetry and Tidal Lag

- ***Tidal Asymmetry***

Pethick (1984) and Schumann *et al*. (1999) explain that as the tidal wave travels up the estuary, an increase in asymmetry of the tide is encountered. Masselink and Hughes (2003) describe this process of tidal asymmetry as a key feature of long estuaries, termed tidal distortion. Tidal distortion includes a shortened rising tide and lengthened falling tide, which occurs as a result of steepening of the wave front as the tide travels up the estuary (Masselink and Hughes, 2003). Hence, the flood tide or leading edge of the tide steepens and the ebb tide flattens (Pethick, 1984). Research indicates that there are several causes attributed to tidal asymmetry. Schumann *et al*. (1999) explain that shallow depths and estuary mouth constrictions lead to tidal distortion and asymmetry. However, the difference between the wave velocity of the crest and trough of the tidal wave is highlighted as a major cause (Pethick, 1984; Masselink and Hughes, 2003).

- ***Ocean Tide and Estuary Tide***

According to Schumann (2003) and Beck *et al*. (2004), at high tide the cross-sectional area of the mouth of the estuary is considerably large, which allows a large exchange of water between the estuary and ocean, and results in a small tidal lag time and a small difference in elevation

between the ocean and estuary. However, as the tide approaches low tide and falls, the cross-sectional area of the estuary mouth becomes small, which increases the frictional force on the ebb tide. Consequently, the estuarine ebb tide continues to flow as a result of friction, even though the ocean tide has completed the ebb phase and has turned into the rising tide, resulting in a large lag time between the ocean and estuary. Therefore, the estuary tide takes a longer time to ebb than flood (Schumann, 2003; Beck *et al*., 2004).

4.6. Estuary Hydrodynamics: Stratification, Mixing and Residual Currents

The mixing of salt and fresh water is important in the hydrodynamics and sediment transport in estuaries, as mixing processes generate currents in addition to tides and river flows (Pethick, 1984; Schumann *et al*., 1999; Bird, 2000; Masselink and Hughes, 2003), known as residual currents (Pethick, 1984). The fundamental factor that governs the mixing of salt and fresh water is that sea water is denser than fresh water (Dyer, 1986; Pethick, 1984; Schumann *et al*., 1999). Mixing of salt and fresh water is determined by molecular diffusion and turbulent mixing (Schumann *et al*., 1999; Masselink and Hughes, 2003). There are three types of estuarine circulation, such as salt wedge or stratified, partially mixed and fully mixed or well mixed estuaries (Dyer, 1973; 1995; Pethick, 1984; Schumann *et al*., 1999; Masselink and Hughes, 2003).

Salt wedge estuaries contain a limited tidal range and a large fluvial flow that is inadequate to displace the underlying salt water body or to create turbulent mixing, which creates a salt wedge whereby the more dense salt water covers the bottom of the estuarine channel, which is overlain by fresh water (Dyer, 1973; 1986; 1995; 1997; Pethick, 1984; Bird, 2000; Masselink and Hughes, 2003), as illustrated in Figure 4.7 (Page 64). The salinity contours stretch horizontally, forming a halocline (Dyer, 1997; Masselink and Hughes, 2003). Sediments in salt wedge estuaries are mainly fluvially-derived and deposited sediment grain sizes increase towards the land, displaying a unique coarsening upstream pattern (Dyer, 1979; Pethick, 1984; Bird, 2000). Cooper and Mason (1987) recorded a salt wedge extending to the Athlone Bridge in the Mgeni Estuary.

Partially mixed estuaries are characterised by a minimal fluvial input and a large tidal range (Pethick, 1984), which causes the estuary to become less stratified (Dyer, 1995; 1997; Bird, 2000), as illustrated in Figure 4.7 (Page 64). These estuaries contain adequate tidal energy to generate greater internal waves and shear along the halocline (Masselink and Hughes, 2003), resulting in significant mixing (Dyer, 1973; 1995; 1997; Pethick, 1984; Masselink and Hughes, 2003). Partially mixed estuaries are mainly composed of marine sediment (Pethick, 1984), and the deposited sediments create a fining upstream pattern (Pethick, 1984; Bird, 2000), which is characteristic of most tidal environments, converse to salt-wedge estuaries (Pethick, 1984).

Fully mixed estuaries contain very strong dominant tidal currents and low fluvial inputs through a limited river flow (Dyer, 1973; Pethick, 1984), as illustrated in Figure 4.7 below. Fully mixed estuaries form under conditions of extremely effective mixing, thus the vertical salinity variation is completely diminished (Dyer, 1973; 1995; Masselink and Hughes, 2003). However, estuaries that are very wide, in excess of 0.5 km, experience lateral salinity variations throughout its width (Pethick, 1984; Dyer, 1995), causing the fluvial flow and marine flow to travel in different directions (Masselink and Hughes, 2003). Large amounts of marine sediments are deposited in the plane of the sea water flow, whereas minimal amounts of fluvial sediment are deposited in the plane of the fresh water flow (Pethick, 1984). Estuaries may be classified as partially mixed or stratified during neap tides or periods of enlarged river inputs, however under conditions of an increasing tidal range, such as during spring tides, estuaries may be classified as well mixed (Dyer, 1995; 1997).

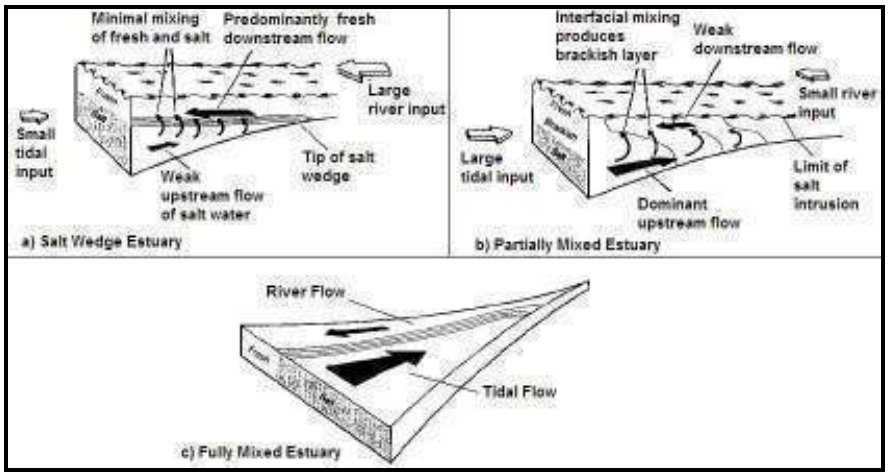

Figure 4.7. a) Salt-wedge or stratified estuary, b) Partially mixed estuary, c) Fully mixed estuary (for northern hemisphere) (Pethick, 1984 in Masselink and Hughes, 2003).

4.7. Fluvial Sediments

Fluvial sediment is derived from parent rivers and catchments (Allen, 1985; Reid and Frostick, 1994; Schumann, 2003). The nature of the sediment transported by the river depends on the characteristics of the drainage regions and the type of sediment source, which includes the type of rocks within the catchment (Bird, 2000; Beck *et al*., 2000; Theron, 2007). Estuaries are influenced by the sediment yield derived from large catchments, which vary according to climate, as well as catchment land use and degradation, in the form of deforestation and urbanization (Beck *et al*., 2004). The sediment transported downstream is classified as a heterogeneous mixture due to the different sources of catchment derived sediment of various grain sizes (Dyer, 1995). However, sediment sorting occurs with the flow due to the different modes of

transportation of fine and coarse sediments (Dyer, 1995). Fluvial sediment is carried into estuaries via freshwater inflow at the head (Allen, 1985; Schumann, 2003), and characteristically comprises of very fine sand, silt and clay, as well as granular bedload (Reid and Frostick, 1994; Schumann, 2003, Davis and FitzGerald, 2004). Most of the fine sediments are kept in suspension (Reid and Frostick, 1994; Bird, 2000; Schumann, 2003), and contain a cohesive nature, which leads to a build up of fine sediments within the upper section of the estuary (Woodroffe, 2002; Schumann, 2003).

4.8. Estuarine Sediments

Estuaries are coastal features that display active sedimentation (Bird, 2000), and form a pathway in which sediment is transported from rivers to the sea (Dyer, 1995). However, sediments are continually being transported into and out of estuaries from marine and fluvial sources, respectively (Bird, 2000; Schumann, 2003). Estuaries contain three main sediment sources, such as the sea, river input and sediment generated within an estuary which is mainly composed of organic material (Cooper *et al*., 1999). These systems attain marine sediment from the advancing flood tide, barrier overwash and wind transport (Cooper *et al*., 1999). Fine, fluvial suspended load (Bird, 2000) is transported into the estuary where it is mixed with marine sediment (Dyer, 1995). Estuaries are characterised by high suspended sediment concentrations, however large portions of coarse sediments may be deposited within estuaries and along the flood plain (Dyer, 1979; 1995). Fine sediments found within estuaries usually consist of sediment grains smaller than 2 μm and are predominantly composed of clay minerals illite, kaolinite and montmorillonite, which collide and flocculate, forming large aggregates particularly within sea water (Dyer, 1979).

Dyer (1979) documents that coarse sediments found within estuaries are commonly comprised of sand and gravel particles. Within the river-dominated section of the estuary, coarse bedload sediment is transported downstream to the limit of salt water intrusion since maximum currents are equivalent on both the ebb and flood tides at this point. Hence, maximum flood currents move landward, by which it transports bedload sediment to a region in which the velocities do not surpass the threshold for that specific grain size. Consequently, the general trend in an idealised estuary indicates that the sediment grain size tends to decrease further upstream (Dyer, 1979).

4.9. Sediment Transport in Estuaries

According to Beck *et al*. (2004), the transport of sediment within an estuary is similar to that within a river, except that in an estuary, current reversal occurs during a tidal cycle. The movement of sediment within estuaries is largely influenced by circulation patterns in terms of salinity, tidal flow

and fluvial discharge (Dyer, 1979), as well as the interaction between waves and currents (Beck *et al*. 2004; Theron, 2007). According to Beck *et al*. (2004), during the tidal cycle, sediment transport is nil or minimal when the tide reverses as a result of generally low flow velocities during this period, which tends to increase once the tide has turned.

As sediment enters the estuary head or the fluvial section of the estuary, the tides play an important role in sediment transport (Dyer, 1995). Over a tidal cycle, the amount of sediment transported into and out of an estuary is unbalanced (Bate *et al*., 2002), because as a tidal wave travels up a shallowing channel, the tidal asymmetry increases along with differences in ebb and flood tide velocities (Pethick, 1984). Due to tidal asymmetry, flood-dominated estuaries display an overall upstream influx and transportation of sediment (Schumann *et al*., 1999; Bird, 2000; Schumann, 2003), which contributes largely to the growth and accretion of sand flats and mudflats within the upper intertidal zone (Bird, 2000, Schumann, 2003). Comparatively, an overall seaward transportation of sediment in ebb-dominated estuaries (Schumann *et al*., 1999; Bird, 2000), results in a significant amount of scouring of sediments and erosion in the mid-tide zone, which creates a steep intertidal profile and narrow low tide channels (Bird, 2000). South African estuaries are characteristically prone to obtaining higher sediment loads on the flood tide than the ebb tide, which results in the build up of sediment in the mouth, causing a natural blockage and the development of flood-tidal deltas, such as those along the south coast (Bate *et al*., 2002).

Sediments are transported in estuaries as bedload and suspended load (Schumann, 2003; Davis and FitzGerald, 2004). Finer sediments are generally transported in suspension within residual flows (Dyer, 1979; Bird, 2000), and remain mobile and in suspension during high flow velocities by turbulence (Dyer, 1995). Suspended sediment is characteristic of low-energy and sheltered environments (Davis and FitzGerald, 2004). As fluvial suspended sediment is carried from the river into the estuary, it will generally start to settle when entering the estuary, however due to its fine nature; it may only settle when it is further down the estuary (Dyer, 1995; Masselink and Hughes, 2003). However, within the upper section of the estuary, the strong flowing high-energy tidal currents generate mixing, which re-suspends the sediment and hence increases the suspended sediment concentrations (Dyer, 1995).

Therefore, during slack water or low velocities the fine suspended sediments undergo settling, deposition and consolidation, however these sediments have a tendency to be eroded, re-suspended and transported in the direction of the averaged tidal flow during the following tidal cycle when the velocity increases (Dyer, 1979; 1995). Bird (2000) explains that as the finer sediment transport decreases due to a decreasing flow velocity, sand is deposited along the bed, which may result in the formation of sand flats. Coarser sediments are commonly transported

along the bed and mainly influenced by strong currents, principally transported in the direction of the maximum currents (Dyer, 1979; 1995; Bird, 2000).

Since spring tides obtain higher velocities than neap tides, it is understood that greater amounts of sediment transport occur during spring tides than neap tides (Dyer, 1995; Bird, 2000; Davis and FitzGerald, 2004; Kitheka *et al*., 2005; Theron, 2007). During spring tides, suspended sediment concentrations are comparatively high in the estuary due to strong currents that erode large amounts of sediment from the bed and maintain it in suspension (Dyer, 1995; Masselink and Hughes, 2003). However, during neap tides the tidal amplitude and peak current velocities are reduced, which are insufficient to re-erode and re-suspend sediment, which results in reduced suspended sediment concentrations (Dyer, 1979; 1995). Therefore, erosion and high suspended sediment concentrations occur during spring tides, however deposition and low suspended sediment concentrations occur during neap tides (Dyer, 1995; Bird, 2000; Davis and FitzGerald, 2004; Kitheka *et al*., 2005; Theron, 2007).

High sediment transport rates throughout the sediment grain size range are restricted to large significant discharge events (Dyer, 1995, Cooper, 2002), whilst only fine sediments are transported during significantly low flow rates (Dyer, 1995). Therefore, the tidal cycle results in fluctuations of the water surface and current velocities, which influences the average suspended and bedload transport (Dyer, 1995).

4.10. Sediment Discharge

According to Dyer (1986), the sediment yield of a catchment is dependent on the geology, topography and climate. In most cases, the sediment yield does not equal the amount of sediment that is discharged into an estuary because large amounts of sediments are deposited within the lower course of the river. The annual sediment discharge varies according to several factors, the main factor being climate and weather patterns. In regions of subtropical climates, the maximum discharge tends to occur during summer months, whilst the regions in temperate latitudes obtain maximum discharge during winter months (Dyer, 1986).

The relationship between sediment concentration and water discharge has been well documented (Dyer, 1986; Gordon *et al*., 1992). In most cases, high flow discharges generate high sediment concentrations (Dyer, 1986). According to Dyer (1986), the relationship between these two variables can be illustrated in the form of a rating curve, such that:

$$C = a Q^b \quad 4.1$$

Where,

C = suspended sediment concentration (mg/l)

Q = flow rate (m^3/s)

a = constant that ranges between 0.004 and 80 000

b = exponent that ranges between 0.0 and 2.5

Therefore, by plotting suspended sediment concentrations against flow discharges, a relationship between the two becomes apparent, which is a useful component in estuarine and coastal sediment dynamics (Dyer, 1986; Mangelsdorf *et al*., 1990). In relation, Thomas (1988); Lindsay *et al*. (1996), Kleinhans and Brinke (2001) established a link between channel discharge and suspended sediment concentrations.

4.11. Suspended Sediment Fluxes

Lapidus and Winstanley (1990, p.222) define flux as the "*rate of flow of fluid, particles or energy*". Based on research, it is clear that some authors refer to suspended sediment flux as the suspended sediment discharge or load. These terms are synonymous based on their identical measured units, in the form of mass per unit time. However, for purposes of this research, the term suspended sediment flux will be used. According to McCave (1979), the flux of an estuarine section is calculated by the multiplication of the current speed and suspended sediment concentration. Therefore, it is the amount of sediment that passes through an estuarine cross-section per unit time (McCave, 1979). Certain controls exist for suspended sediment concentrations and therefore for fluxes, hence analysis of sediment budgets are somewhat complicated (McCave, 1979).

Several research papers have been published and several works have been carried out on a global scale dedicated to suspended sediment fluxes. In South Africa, however, published literature regarding suspended sediment fluxes is significantly limited. Schubel (1972); Kjerfve (1979); McCave (1979); Pillay (1981); Uncles *et al*. (1985); Childers and Day (1990); Dyer (1995; 1997); Dyer *et al*. (2000); Geyer *et al*. (2001); McKee *et al*. (2002); Yang *et al*. (2004); Ganju *et al*. (2005); Kao *et al*. (2005); Kitheka *et al*. (2005) and Ganju and Schoellhamer (2006); Gardner and Kjerfve (2006); Wang *et al*. (2007), form just some of the referenced work based on suspended sediment fluxes. Furthermore, Allen (1985); Gordon e*t al*. (1992); Nikora and Goring (2002) and Wall *et al*. (2008) form some of the work focused on suspended sediment discharges. Locally, suspended sediment fluxes and discharges have been studied by McCarthy *et al*. (1991); Beck *et*

al. (2004) and Beck (2005). These authors have suggested and used several various methods to calculate suspended sediment flux. Therefore, there are several ways to calculate the suspended sediment flux, which tends to become complicated as each method contains different variables, which is discussed in Chapter Five.

McCave (1979) explains that as the tidal range increases, the flux tends to increase as well. In most suspended sediment flux studies, fluxes were higher on spring tides than neap tides, as a result of greater flow velocities and sediment re-suspension due to turbulence, as found by Uncles *et al*. (1985); Dyer *et al*. (2000); Geyer *et al*. (2001); Kitheka *et al*. (2005) and Wall *et al*. (2008). Furthermore, it is established that higher suspended sediment concentrations and fluxes occur due to increased velocities and wave activity, which enhance bed sediment re-suspension, as found by Dyer *et al*. (2000); Ridderrinkhof *et al*. (2000); Geyer *et al*. (2001); Kitheka *et al*. (2005); Theron (2007). Additionally, Kitheka *et al*. (2005) established that suspended sediment concentrations and fluxes generally display seasonal variability, peaking during the wet seasons, particularly at the beginning with an abundant loose sediment availability (Kitheka *et al*., 2005).

Yang *et al*. (2004) performed a study in the Yangtze River in China, dealing with the anthropogenic influences on the suspended sediment flux into the river. Accordingly, it was found that fluvial sediment flux influences and controls river morphology such as delta formation and evolution, as well as the sediment transport in estuarine and coastal regions. Additionally, it was established that human activities influence the estuarine suspended sediment flux, for example dam construction reduces the suspended sediment flux in an estuary, whereas land-use change in the form of deforestation increases the flux within an estuary (Yang *et al*., 2004).

4.12. Conclusion

There are several factors and processes that occur within the coastal zone. The coastal zone is indeed a broad environment, whereby the features are interlinked by sediment, which is essential within the coastal zone. Estuarine, marine and beach sediments are different in composition, size and source. Estuaries and beaches are vital features within the coastal zone and comprise several definitions and classifications. Beaches are dynamic and constantly changing. The role of tides within estuaries is vital in sediment transport and discharge. Estuarine morphology plays an important role in the movement of sediment, as well as the shape of estuaries. Estuaries and beaches are therefore important, dynamic features within the coastal zone.

CHAPTER 5:
RESEARCH METHODOLOGY

This chapter outlines the methods adopted for the fieldwork and laboratory analysis, throughout this research. Various data were gathered in the field, which included two main approaches of sampling methods and procedures. Fieldwork incorporated both a hydrodynamic and geomorphological study, in which different types of samples were collected. Laboratory analysis spanned a number of different tests and procedures and a photographic analysis of the estuary mouth was also undertaken within this research timeframe.

5.1. Sampling Procedure

The study area of this research forms the Lower Mgeni Estuary mouth inlet system, including the estuary, barrier, spit and beach environments, stretching seaward from the M4 Bridge or Ellis Brown Viaduct, as illustrated in Figure 2.1 (Chapter 2). Access to the Mgeni Estuary and barrier was granted by the officials of the Beachwood Mangroves Nature Reserve, managed by Ezemvelo KZN Wildlife. Discharge measurements, topographical surveying and sediment samples were collected from the Mgeni Estuary in a series of sequential fieldtrips. As mentioned above, two types of fieldtrips were conducted, during which different methods and procedures were adopted.

5.1.1. Hydrodynamic Study

The hydrodynamic study included the direct measurement of the estuary channel discharge, as well as the collection of estuary bed and suspended sediment samples. It must be clearly noted from the outset that the inlet channel of the Mgeni Estuary is a fast-flowing system and that sampling within the channel itself is not recommended via wading, due to safety constraints. A boat is required in order to sample within the main channel. However, during this research, wading was carried out in a suitable cross-section at the innermost part of the channel, a small distance further up from the main inlet channel, as illustrated in Figure 5.1 (Page 72).

5.1.1.1. Discharge Measurement

The estuary channel discharge was directly measured by the velocity-area method outlined by Gordon *et al*. (1992). Barnes (1999); Zietsman (2004); Stretch and Zietsman (2004); Beck (2005) and Lawrie (2007) have adopted similar methods of calculating and measuring discharge. A single cross-sectional area was chosen, which was positioned between 29° 48.653 S and 31°

02.344 E and the groyne, and approximately 75 m from the M4 Bridge and 185 m from the coastline, as illustrated in Figure 5.1 (Page 72). This estuarine cross-section was selected as it was fairly straight, uniform and unobstructed by rocks and vegetation. The estuarine channel cross-section was sampled every two hours, from approximately 8 am to 4 pm, throughout a spring and neap tidal cycle, which was repeated on a seasonal basis, from January 2008 to July 2008. Table 5.1 below shows the sampling dates, tides and seasons for the hydrodynamic sampling period.

Table 5.1. The sampling period of the hydrodynamic study for discharge measurement, collection of sediment samples in the Mgeni Estuary, on a spring-neap tidal cycle and seasonal basis.

	Date	Tide	Season
1	12 January 2008	Four days after Spring Tide	Summer
2	8 February 2008	One day after Spring Tide	
3	11 February 2008	Four days after Spring Tide	
4	16 February 2008	Two days after Neap Tide	
5	21 February 2008	Spring Tide	
6	12 May 2008	Neap Tide	Autumn
7	20 May 2008	Spring Tide	
8	26 June 2008	Neap Tide	Winter
9	3 July 2008	Spring Tide	

However, due to technical and logistical constraints, in the form of poor weather conditions and lack of entry access to the sampling site, field sampling was, on occasion, postponed to a few days later than the actual spring or neap tide, when the conditions were conducive for fieldwork. Rain occurred on 8 February 2008, which caused the sampling process to be stopped and postponed. Furthermore, sampling on 21 February 2008 intersected with a small-scale flooding event as a result of significant rainfall on 19 February 2008, which caused high, strong flows in the estuary that were not favourable for wading and the completion of the total cross-sectional width. Specifically, 46.80 mm and 4.40 mm of rainfall occurred on 19 and 20 February 2008, respectively (South African Weather Services, SAWS, 2008).

The average cross-sectional length was approximately 80 m, with the starting point of the cross-section positioned on the inlet beachface of the estuary and the end point located at the engineered groyne (Figure 5.1, Page 72).

Figure 5.1. Aerial photograph illustrating the estuarine cross-section for discharge measurements and sediment sampling (Year: 2008).

The time at which discharge measurements commenced and concluded along the cross-section, was noted down in order to correlate the time to the tide tables acquired from the South African Navy Hydrographic Office (SANHO) (2008), to derive the tidal status within each sampling day.

Initially, a rope was pegged and strung across the cross-section at right angles to the flow, which allowed measurement and recording of the channel width. The width of the cross-section was divided into 15 m intervals and at each interval the channel width, depth of the water, and the flow velocity were measured along the vertical. The channel depth and flow velocity were measured with a measuring staff and current meter, respectively. The flow velocity was measured for the majority of the fieldwork with the SEBA Universal Current Meter F1, which is a propeller type current meter. However, due to a malfunction of the latter, the YSI Sontek Flowtracker Handheld Acoustic Doppler Velocimeter (ADV) was utilised for the remainder of the fieldwork, as illustrated in Figure 5.2 below.

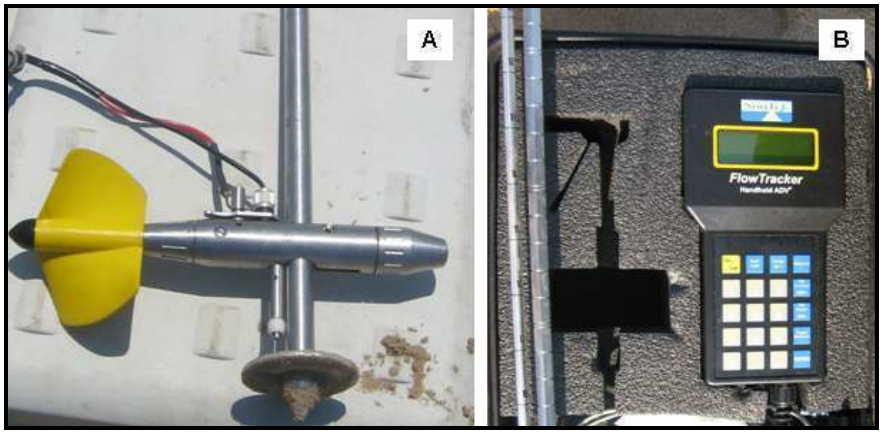

Figure 5.2. A) SEBA Universal Current Meter F1 and B) YSI Sontek FlowTracker.

Kjerfve (1979) explains that the measurement of estuarine velocity is classified into three different types or categories such as eulerian, lagrangian and indirect measurements. Within this study, eulerian flow velocity measurements were made with a current meter, which include the measurement of the flow velocity as a function of time, at a certain point within the fluid (Kjerfve, 1979; Dyer, 1997). The mean flow velocity was measured with the current meter that was attached to a rod, at a single point along the depth of the vertical, at approximately 0.4 D or four-tenths of the total depth measured from the bottom of the estuary bed (Gordon *et al*., 1992). Flow velocity was measured at a single point along each vertical because the channel cross-section was fairly wide and measurements had to be made quickly (Gordon *et al*., 1992), since the objective of this study is to determine the influence of tidal fluctuations on estuarine channel discharge and sediment characteristics. The measurement duration for both current meters was set at 30 seconds. Figure 5.3 (Page 74) shows hydrodynamic sampling in the Mgeni Estuary,

along the channel cross-section, on 12 May 2008. Therefore at each vertical, the channel width, total water depth and current meter readings were noted, which is illustrated in Figure 5.4 (Page 75). Additional width and water depth measurements were noted at places of rapid changes in topography within the cross-section, as advised by Gordon *et al*. (1992).

Figure 5.3. Hydrodynamic sampling on 12 May 2008.

5.1.1.2. Sediment Sampling

In conjunction with the velocity, channel width and water depth measurements; a water-sediment sample (suspended sediment) and an estuary bed sediment sample were collected along each vertical. The suspended sediment samples were collected in 2 litre plastic sample bottles, at 0.8 D or eight-tenths of the total depth measured from the bottom of the estuary bed, along each vertical. The sediment sizes smaller than 0.063 mm are generally evenly distributed throughout the cross-section (Gordon *et al.*, 1992), hence samples taken at this point are understood to be representative of the suspended sediment concentrations throughout the cross-sectional profile.

Sediment samples were collected from the estuary bed along each vertical by diving, as similarly performed by Cooper (1994) in the Mvoti Estuary. The estuary bed sediment samples were collected in 250 ml plastic sample bottles. The suspended and estuary bed sediment samples were sealed, labelled according to the time, tide and sample point number, and transported back to the laboratory at the University of KwaZulu-Natal for analysis. A total of 124 estuary bed sediment samples and 164 suspended sediment samples were collected throughout the sampling period. Figure 5.4 (Page 75) illustrates the sampling strategy adopted for the hydrodynamic study.

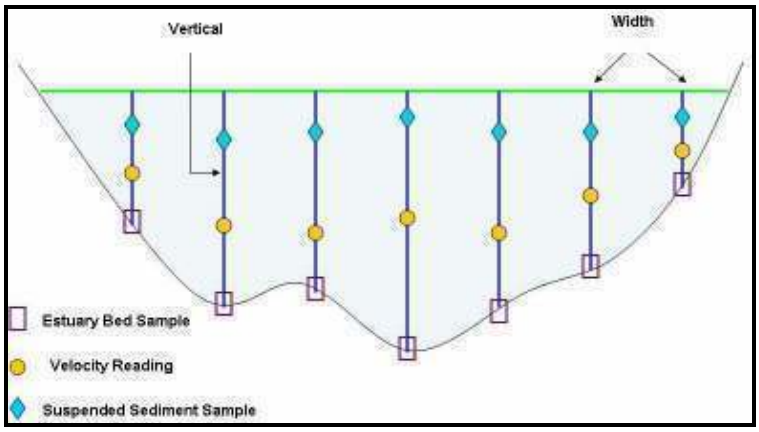

Figure 5.4. A schematic diagram illustrating the sampling strategy for the measurement of channel discharge and collection of sediment samples.

It must be mentioned at the outset that the velocity readings and sediment samples were collected via wading into the estuary, hence when conditions became unsafe and risky due to increased rapid, strong flows; the sampling process was put on hold. Therefore, in some cases cross-sectional profiles were plotted until the middle of the channel.

5.1.2. Geomorphological Study

The geomorphological study included topographical surveying of the barrier, as well as the measurement of beach slope angle and the collection of surface sediment samples.

Table 5.2. The sampling period of the geomorphological study for surveying and collection of sediment samples along the barrier of the Mgeni Estuary, on a seasonal basis.

	Date	Season
1	29 November 2007	Early Summer
2	20 March 2008	Autumn
3	21 June 2008	Winter

5.1.2.1. Surveying

Surface sediment sample points along the barrier of the Mgeni Estuary were surveyed on a seasonal basis, incorporating summer, autumn and winter. Table 5.2 illustrated above, shows the seasonal sampling period of the geomorphological study. During the sampling period, the barrier region lacked the presence of dunes and vegetation. The barrier stretches approximately 425 m

southwards from the Beachwood Tidal Creek towards the mouth of the estuary, which includes a barrier extended sandbar (explained in Chapter Eight) and a recurved spit. The barrier was surveyed by standard methods with a dumpy level and staff, along a set of traverse lines running perpendicular to the coastline. The relative elevation and the distance away from the staff were recorded, in order to plot the survey profiles. Each transect stretched from the base of the M4 Bridge towards the swash zone, which led to the identification of various significant geomorphological zones, such as the estuary, lagoonward slope, berm and swash zone, as previously researched by Garden (2003) and Garden and Garland (2005).

The first transect was positioned beyond the Beachwood Mangroves Tidal Creek in the north, and the final transect was situated within the vicinity of the estuary mouth in the south. Survey transects were plotted at intervals of approximately 100 m (Figures 5.6 to 5.8). However, survey transects on the preliminary fieldtrip of 29 November 2007, were plotted between 50 m and 80 m intervals. However, it was later decided that subsequent surveying transects should be plotted at 100 m intervals, which adequately represents the topography and sediment characteristics of the barrier. Figure 5.5 below shows the surveying sampling procedure.

Figure 5.5. A) Surveying the berm on 29 November 2007, B) The slope of the swash zone on 21 June 2008.

5.1.2.2. Sediment Sampling

In conjunction with surveying the barrier, surface sediment samples were systematically collected along each transect. These sediment samples were collected with a sand auger, at a sample interval of 20 m. The upper 15 cm of surface sediment was collected, which equated to about 500g, which were placed in plastic bags, sealed and labelled according to the transect and sample number, and transported back to the laboratory at the University of KwaZulu-Natal for analysis. Each auger hole or sediment sample point was positioned with a Magellan SporTrak Handheld GPS, which is accurate to 3 m, in order to generate maps illustrating the positions of the sediment sample points (Figure 5.6 to Figure 5.8, Page 77 to Page 79).

Figure 5.6. Surveying and GPS sediment sample points on 29 November 2007.

Figure 5.7. Surveying and GPS sediment sample points on 20 March 2008.

Figure 5.8. Surveying and GPS sediment sample points on 21 June 2008.

It must be noted that the GPS malfunctioned on 21 June 2008; therefore the sample points were positioned using the M4 Bridge as a guide. A total of 135 surface sediment samples were collected along 15 transects, throughout the seasonal sampling period, from November 2007 to June 2008.

5.1.2.3. Beach Slope Angle Measurement

Additionally, the slope angle was measured adjacent to each auger sample point, with a Smart Tool Leveller, illustrated below in Figure 5.9. The use of the Smart Tool is restricted to dry surfaces; therefore the slope angle was measured only on dry sand along the barrier and berm. The slope angle was measured and noted down correspondingly, in order to calculate the gradient.

Figure 5.9. The Smart Tool Leveller used to measure the beach slope angle.

5.2. Laboratory Work

The laboratory analysis included a number of different tests such as particle size analysis, organic content and suspended sediment concentration. The procedures for each test are described below, and illustrated in a schematic flow diagram below, in Figure 5.10.

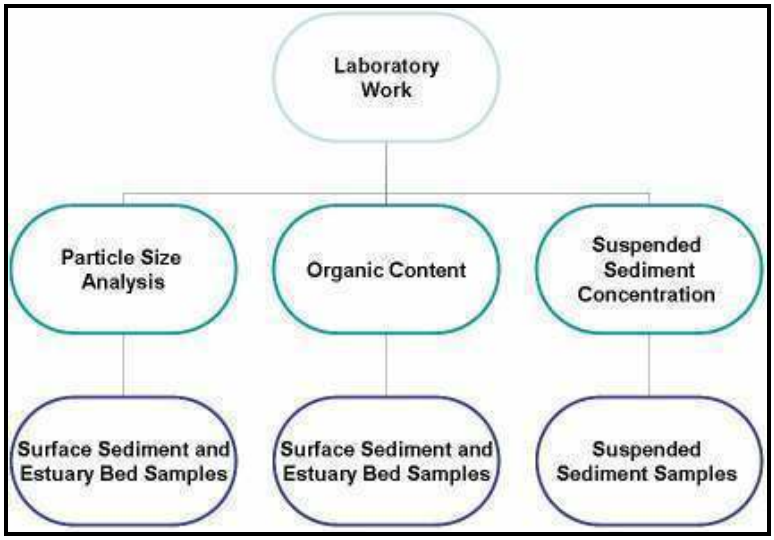

Figure 5.10. A flow diagram illustrating the entire laboratory work procedures.

5.2.1. Particle Size Analysis

Particle size analysis was performed on the estuary bed and surface sediment samples, in order to determine the grain size distribution of the sediment within the estuary and barrier regions. These two sets of samples were analysed separately, although with the same method. The analysis of the particle size distribution was carried out by standard dry sieving techniques, as outlined by Buller and McManus (1979); Dyer (1986) and Gordon *et al.* (1992), which is understood to be a common, simple method (Buller and McManus, 1979; Gordon *et al.*, 1992), appropriate for marine and estuarine sediment (King, 1972). It is suggested that for gravel samples, approximately 10 kg of sediment is required, whereas for coarse sands, approximately 100 g to 250 g is required (Buller and McManus, 1979).

Sample preparation was carried out as outlined by Buller and McManus (1979) and Green (2004), and is illustrated in Figure 5.11 (Page 82). Firstly, the sample was mixed and approximately 400 g of each surface sediment sample and approximately 80 g of each estuary bed sample was measured out in a pre-weighed beaker. Thereafter, the sediment samples were placed in beakers and oven dried for 24 hours, at 105 °C (Buller and McManus, 1979; Heiri *et al.*, 2001). Subsequently, the samples were removed from the oven and placed in a desiccator for approximately 30 minutes. The sediment samples were then mixed in a pestle and mortar, with the aim of disaggregation of the samples after drying, without breaking up and crushing the actual grains (Gordon *et al.*, 1992).

The samples were then manually sieved through a 2 mm sieve in order to establish the gravel fraction. However, the gravel fraction was not quantified as a result of its small, negligible quantities, especially within the estuary bed sediment samples. A possible reason for this lack in gravel and coarse particles within the region owes to the establishment of the Inanda Dam, which traps the coarse sediment particles behind the dam, ultimately fining the sediment reaching the lower estuary (Garland and Moleko, 2000; Ngetar, 2002). Once this was completed, the remaining samples were then split in a riffle box until a representative sediment sample was achieved. Half of the split sample was reserved for dry sieving and the remaining portion was stored in a desiccator for the determination of the organic content.

Dry sieving was followed for approximately 250 g of surface sediment and 40 g of estuary bed sediment, which were each passed through a set of sieves. Six sieves of aperture sizes 2 mm, 1 mm, 0.5 mm, 0.25 mm, 0.125 mm and 0.063 mm, with a catching pan at the base and sieve cover at the top, were placed in ascending order in an automated sieve shaker (Buller and McManus; 1979; Gordon *et al.*, 1992; Bird, 2000).

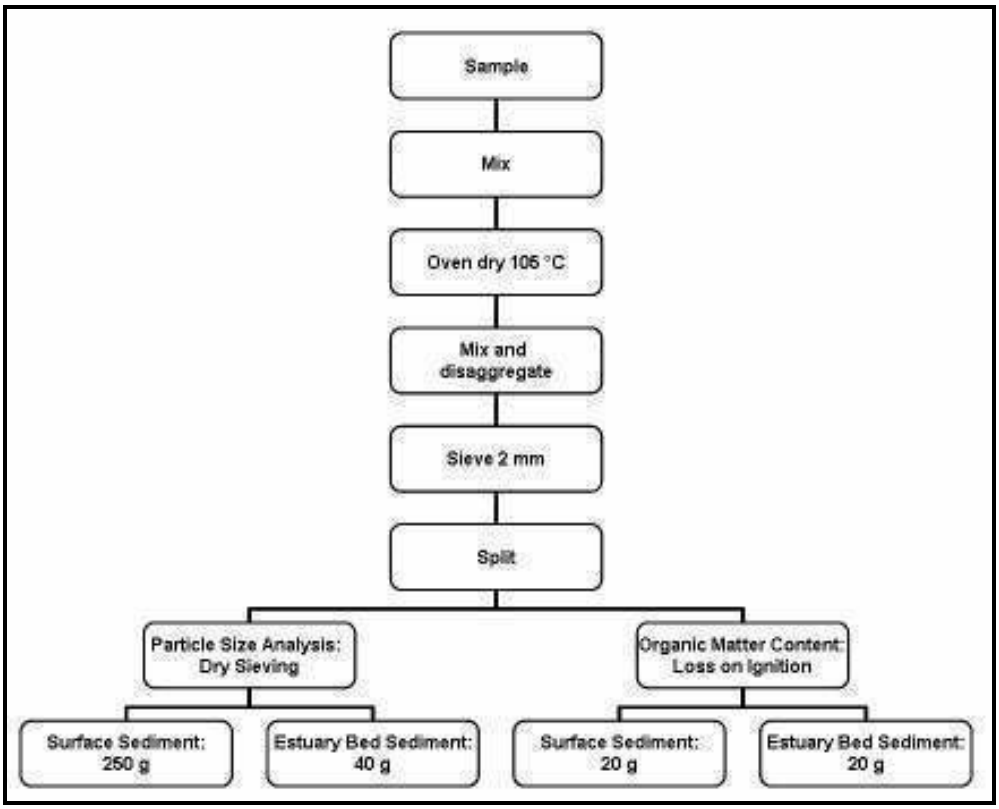

Figure 5.11. A flow diagram illustrating the laboratory analysis of the surface sediment and estuary bed sediment samples.

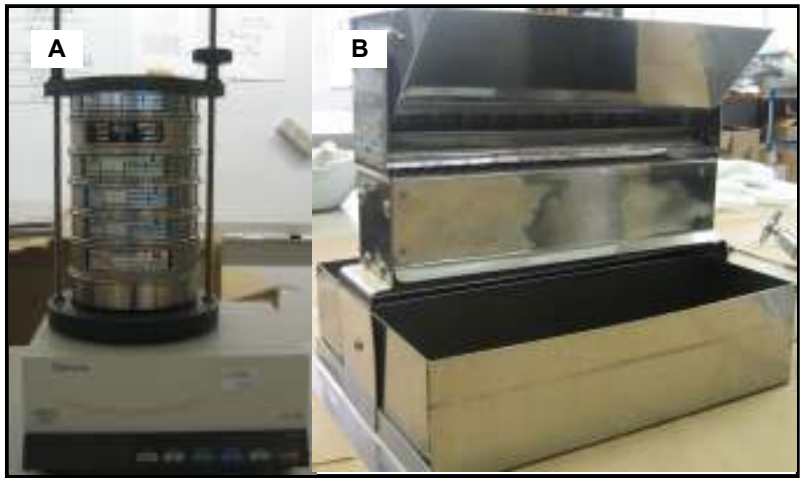

Figure 5.12. A) The mechanical sieve shaker and B) The riffle box sample splitter.

Each sample was mechanically sieved for approximately 10 minutes and the remaining sediment obtained within each sieve size was transferred with a sieve brush to pre-weighed weigh boats. Each weigh boat containing the sieved sediment was then weighed on an electronic balance,

capable of accuracy to two decimal places or 0.01 g. The resultant sediment weights of each corresponding sieve aperture size were noted in a table as the mass retained. Subsequently, the percentage of the total weight of the sieved sediment was calculated and recorded, as suggested by Buller and McManus (1979); Dyer (1986); Gordon *et al*. (1992). From this the percentage finer than each specific grain size was calculated, as suggested by Dyer (1986) and Gordon *et al*. (1992). All of the data were stored and analysed in an electronic database. Figure 5.12 (Page 82) shows the sieve shaker and riffle box sample splitter used in the laboratory.

5.2.2. Organic Matter Content

The organic matter content or the weight percentage of organic matter of the sediment samples was established by the method of loss on ignition (LOI), as outlined by Heiri *et al*. (2001). LOI is classified as a common method utilised to generate the organic content of sediments (Heiri *et al*., 2001). Cooper (1991a) suggests that the LOI method is efficient in that it eliminates the bound water from clays and that it is a fairly quick procedure, especially when large sample sizes are obtained from the field.

The remaining split estuary bed sediment and surface sediment samples were used in the LOI test (Figure 5.11, Page 82). Approximately 20 g of each sediment sample was weighed and placed into pre-weighed crucibles, and then oven dried for one hour at 105 °C. Thereafter, each sample was placed in a desiccator for 30 minutes and subsequently weighed, with the weight being recorded correspondingly. Thereafter each crucible containing the sediment was placed in a muffle furnace set at approximately 450 °C for 12 hours. Subsequently, the crucibles were weighed and recorded as the weight after combustion. Prior to the sediments being placed into the oven and furnace, simple visual analysis was performed in order to note the descriptive characteristics of the sediments, such as the sediment texture, presence of biogenic and shell fragments, as well as the occurrence of leaves or sticks. This was carried out in order to substantiate and provide reasons for the percentage of organics achieved within each sample once LOI was completed.

5.2.3. Suspended Sediment Concentration

The concentrations of the suspended sediment samples were determined through the method of filtration, as outlined by McCave (1979); Mangelsdorf *et al*. (1990) and Gordon *et al*. (1992). The method of determining sediment concentration involves the filtration of a known volume of well-agitated sediment-water mix and the subsequent weighing of the filters (McCave 1979; Gordon *et al*., 1992). Each suspended sediment sample was filtered through Whatman Ashless, slow fine

crystalline filter papers, with a diameter of 5.5 cm. The samples were filtered via a process of suction, with the use of a vacuum pump and line. Approximately five Buchner flasks and funnels were run off a single vacuum line. Each flask was secured with clamps to ensure no spillages, as illustrated in Figure 5.13 below. Each filter paper was pre-weighed on an electronic scale balance accurate to 3 decimal places or 0.001 g, with each weight being recorded. Prior to filtration, each 2 litre sample was vigorously agitated to ensure an even distribution of sediment suspended throughout the sample. Subsequently, approximately 500 ml of each fully mixed 2 litre sample was accurately measured out in a measuring cylinder, in order to prevent clogging of the filter paper by filtering a larger volume of sediment.

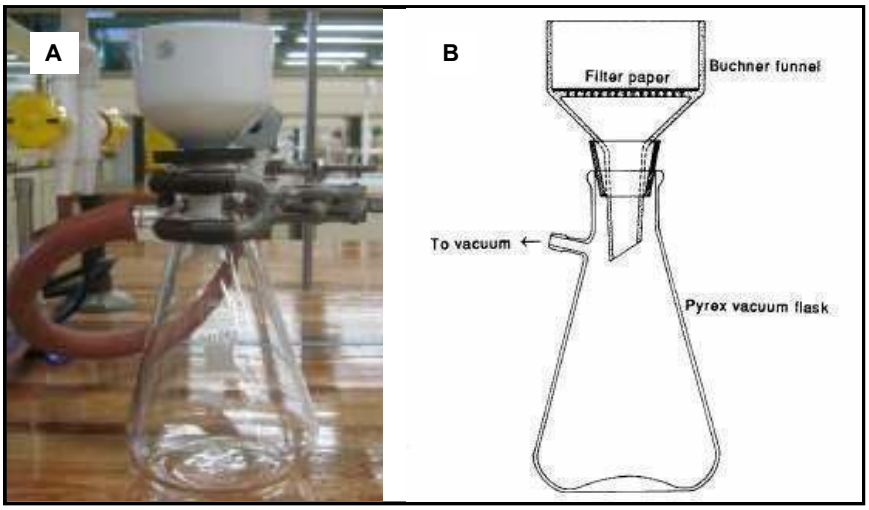

Figure 5.13. Apparatus utilised for vacuum sediment filtration A) Buchner funnel and flask, with linkage to vacuum line and B) Diagram illustrating the apparatus used for vacuum sediment filtration (Gordon *et al.*, 1992).

Thereafter the pre-weighed filter paper was placed into the Buchner funnel and the vacuum was switched on a moderate level. The 500 ml sample was then steadily filtered though the filter paper and once completed, was allowed to remain under suction for approximately five minutes, to make certain that most of the moisture was removed. Subsequently, each filter paper with the filtered sediment was removed from the funnel and placed in a large plastic box, with the cover not firmly placed over to allow circulation as suggested by McCave (1979). McCave (1979) strongly asserts that oven drying and desiccation of filter papers before and after filtration is inaccurate and should be avoided because once the filter paper is removed from the desiccator to the scale balance, it rapidly attracts moisture from the air, hence altering its weight. Therefore, McCave (1979) recommends drying the filters in air within Petri dishes. The filter papers and sediment were dried for 24 hours and subsequently weighed and recorded. The suspended

sediment concentration was then calculated. Filtration was carried out on approximately 164 suspended sediment samples. Dried filter papers are illustrated below in Figure 5.14.

Figure 5.14. Filter papers with sediment once filtration, drying and weighing was completed.

5.3. Data Analysis

Data analysis includes the calculation of the estuary channel discharge, plotting of the survey profiles, statistical analysis of dry sieving data, and the calculation of the organic matter content and suspended sediment concentration.

5.3.1. Discharge Calculation

The discharge is calculated in line with the velocity-area method of measuring discharge in the field, as outlined by Gordon *et al*. (1992), which involves the establishment of the cross-sectional channel area, as well as the average flow velocity. Therefore, the discharge is calculated as follows, as established by Gordon *et al*. (1992):

$$\mathbf{Q = V \times A} \qquad \mathbf{5.1}$$

Where,

Q = discharge (m^3/s or cumecs)

V = average velocity (m/s)

A = cross-sectional area of the channel water (m^2).

Each width, total depth and current meter velocity reading was recorded in an electronic database. Correspondingly, channel cross-sectional profiles were plotted with the depth and width readings, within a Microsoft Excel database. Thereafter, the SEBA Universal Current Meter readings were converted from clicks to current velocities in cm/s, as specified within the SEBA current meter documentation. The YSI Sontek Flowtracker Handheld ADV generates and displays instantaneous current velocities in cm/s, thereby omitting the need for conversions. Each average velocity was then converted to m/s as specified by the equation utilised to calculate discharge.

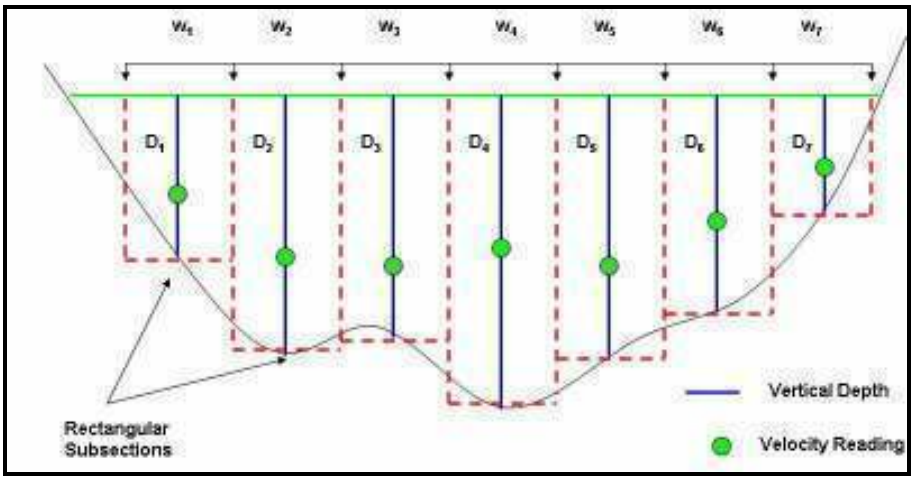

Figure 5.15. The components involved in discharge calculation, including the rectangular subsections, subsection width and depths and the velocity readings (Redrawn and adapted from Gordon *et al*., 1992).

The channel cross-sectional profiles were subdivided into several rectangular subsections according to each vertical, which is illustrated in Figure 5.15 above. The average velocity of each vertical and the area of each rectangular subsection were then multiplied together in order to establish the discharge of each subsection (Equation 5.1). Subsequently, each subsectional discharge within the entire cross-section was added up to generate the total discharge for the cross-section, by means of the following equation, as derived by Gordon *et al*. (1992):

$$\mathbf{Q = w_1D_1v_{mean1} + w_2D_2v_{mean2} + \ldots + w_nD_nv_{mean\ n}} \qquad \mathbf{5.2}$$

Where,

Q = discharge (m^3/s)

w = width (m)

d = water depth (m)

v_{mean} =average velocity (m/s).

Discharge calculations were completed for the entire hydrodynamic study sampling period, on a seasonal neap-spring tidal cycle. Approximately 4 cross-sectional profiles were generated in a sampling day, which yielded a corresponding channel discharge. These cross-sectional profiles were analysed in terms of shape and area, in order to establish variations with the fluctuating tide, as well as spring and neap tides. The velocities and discharges were analysed in order to determine the maximum and minimum values, which were linked to the type of tide and season. Rainfall data for the sampling period were provided by the South African Weather Service in 2008. The rainfall data was utilised in order to ascertain the influence that rainfall plays on the channel discharge.

5.3.2. Survey Profiles

Survey data were placed into an electronic database, in which relative conversions were applied in order to generate the cumulative distance and the relative elevation which were used to plot the survey profiles. These survey profiles were analysed and differentiated in order to establish seasonal variations, in terms of topography and profile shape. Several sediment characteristics were established and assessed in terms of the different geomorphological zones present within the survey profiles.

5.3.3. Beach Gradient

The beach gradient was established by the measurement of the beach slope angle. The beach gradient is the tangent of the slope angle (Pethick, 1984; Masselink and Hughes, 2003), illustrated below in Equation 5.3. The gradient was analysed within the different geomorphological zones across the barrier, in order to reveal various trends and differences. The link between sediment grain size and beach gradient was determined and analysed by the establishment of scatter-plots, as this interrelation is known to be distinct and significant (Pethick, 1984). Bascom (1959; 1960) illustrated the relationship between sediment grain size and beach slope angle.

Beach Gradient = tan (beach slope angle) **5.3**

5.3.4. Particle Size Distribution and Statistical Analysis

Particle size analysis data were displayed graphically by cumulative frequency curves, which enable a comparison between and classification of samples (Dyer, 1986; Gordon *et al*., 1992). Cumulative frequency curves were plotted on semi-logarithmic graphs, whereby the grain size (mm) was placed on a logarithmic x-axis and the percentage finer than each specific grain size

was placed on a linear y-axis (Gordon *et al*., 1992). Several statistical parameters of each particle size distribution were established and derived from the graphical cumulative frequency curves, which include the mean, median, standard deviation or sorting, skewness and kurtosis (Buller and McManus, 1979; Pethick, 1984; Dyer, 1986; Gordon *et al*., 1992; Pye, 1994; Bird, 2000 and Masselink and Hughes, 2003).

The various statistical formulae that were utilised in order to analyse the particle size distribution of the samples, includes the following Equations 5.4 to 5.7 derived by Folk and Ward (1957) in Masselink and Hughes (2003) and Equation 5.8 derived by Folk and Ward (1957) in Lewis and McChoncie (1994):

$$\textbf{Median} = \textbf{Ø50} \qquad \textbf{5.4}$$

$$\textbf{Mean} = \frac{\textbf{Ø16 + Ø50 + Ø84}}{\textbf{3}} \qquad \textbf{5.5}$$

$$\textbf{Sorting} = \frac{\textbf{Ø84 – Ø16}}{\textbf{4}} + \frac{\textbf{Ø95 - Ø5}}{\textbf{6.6}} \qquad \textbf{5.6}$$

$$\textbf{Skewness} = \frac{\textbf{Ø16 + Ø84 - 2Ø50}}{\textbf{2(Ø84 – Ø16)}} + \frac{\textbf{Ø5 + Ø95 - 2Ø50}}{\textbf{2 (Ø95 – Ø5)}} \qquad \textbf{5.7}$$

$$\textbf{Kurtosis} = \frac{\textbf{Ø95 – Ø5}}{\textbf{2.44 (Ø75 – Ø25)}} \qquad \textbf{5.8}$$

From Equations 5.4 to 5.8 listed above, the symbol Ø or phi with an adjacent number, such as Ø50, denotes the grain size at that specific percentile derived from the frequency curve. In order to statistically analyse the particle size distribution, data was interpolated or derived from the cumulative frequency curves, as explained by Buller and McManus (1979); Dyer (1986); and Mangelsdorf *et al*. (1990). Therefore, the relevant percentiles were extended parallel to the x-axis until the point of intersection with the frequency curve, where the corresponding grain size value was extended downwards and read off the x-axis, which was labelled as the grain size in mm. The relevant percentiles used for statistical analysis of each sediment sample were the 5^{th}, 16^{th}, 25^{th}, 50^{th}, 75^{th}, 84^{th} and 95^{th}, as outlined by the statistical equations above. The grain sizes relative to the corresponding percentile values derived from the cumulative frequency curves were converted from millimetres to phi values, in order to carry out various statistical analyses (Pethick, 1984; Pye, 1994; Masselink and Hughes, 2003). The phi grain size is represented in the

Udden-Wentworth Scale, which is a commonly utilised scale (Dyer, 1986), that represents the grade scales of sediment classes and sizes (Pethick, 1984; Dyer, 1986), which is shown below in Table 5.3. The conversion of grain size from millimetres to the phi scale was achieved with the following equation, known as the phi grain size or the phi scale, as indicated by Buller and McManus (1979); Pethick (1984); Dyer (1986); Pye (1994) and Masselink and Hughes (2003):

$$\text{Ø} = -\log_2 D \qquad 5.9$$

Where,

Ø = phi grain size

D = grain size in mm

Table 5.3. Udden-Wentworth Scheme illustrating grain size classification and grain sizes in mm and phi (Redrawn from Dyer, 1986).

mm	Phi	Class Terms
		Boulders
256	-8	Cobbles
128	-7	
64	-6	Pebbles
32	-5	
16	-4	
8	-3	
4	-2	Granules
2	-1	Sand: very coarse
1	0	coarse
0.5	1	medium
0.25	2	fine
0.125	3	very fine
0.062	4	Silt: coarse
0.031	5	medium
0.016	6	fine
0.008	7	very fine
0.004	8	Clay

Once the grain sizes corresponding to the relevant percentiles were derived from each frequency curve, the values were input into the abovementioned equations for median, mean, sorting, skewness and kurtosis. These statistical measures were calculated for each sediment sample. The median particle size was calculated by reading off the corresponding grain size value that the 50th percentile intersected with the frequency curve. Mangelsdorf *et al*. (1990) explains that the median particle size is a central value, which indicates the sediment size at which 50 % or half of the sediments are finer or coarser (Mangelsdorf *et al*. 1990; Ngetar, 2002). Conversely, the mean grain size indicates the most frequent or common sediment grain size (Masselink and Hughes,

2003). Pethick (1984) explains that the mean of the sediment particles is indicative of the size of the force, exerted by wind or water that enables the sediment grains to move. The mean and median are measures of central tendency (Buller and McManus, 1979).

Sorting, also termed standard deviation (Pethick, 1984; Dyer, 1986; Bird, 2000) is defined as the assessment of the spread of the grain size about the mean (Buller and McManus, 1979; Dyer, 1986; Gordon *et al*., 1992). It is a measure of the extent of scatter of the sediment particles (Buller and McManus, 1979). The sorting of sediment particles is governed mainly by the variation of sediment particle sizes at the source, including the processes that occur during transport and deposition (Pethick, 1984; Masselink and Hughes, 2003). The sorting of sediments are classified into various classes by Folk and Ward (1957) in Masselink and Hughes (2003), as illustrated in Table 5.4 below.

Table 5.4. The different classes of sediment sorting (Folk and Ward, 1957 in Masselink and Hughes, 2003 (Redrawn).

	Sorting Scale (Ø scale)
< 0.35	Very well sorted
0.35 to 0.50	Well sorted
0.50 to 0.71	Moderately well sorted
0.71 to 1.00	Moderately sorted
1.00 to 2.00	Poorly sorted
> 2.00	Very poorly sorted

The skewness is a measure of the extent of symmetry (Buller and McManus, 1979; Mangelsdorf *et al*., 1990), and indicates the symmetry displayed by the grain size distribution (Masselink and Hughes, 2003). Pethick (1984) puts forward that the skewness of a sediment particle size distribution is significantly indicative of the history of the sediment sample. Skewness reduces the symmetry of a particle size distribution curve about the mean (Dyer, 1986). The skewness of sediments are classified into various classes by Folk and Ward (1957) in Masselink and Hughes (2003), as illustrated in Table 5.5 (Page 91).

Table 5.5. The different classes of sediment skewness (Folk and Ward, 1957 in Masselink and Hughes, 2003).

	Skewness Scale
> +0.30	Strongly fine skewed
+0.30 to +0.10	Fine-skewed
+0.10 to -0.10	Nearly symmetrical
-0.10 to -0.30	Coarse skewed
< -0.30	Strongly coarse skewed

Kurtosis is the measure of the extreme variation from the normal within the limits of the particle size distributions (Dyer, 1986). It is an assessment of the extent of peakedness of the grain size distributions (Buller and McManus, 1979). Kurtosis is related to the sorting, as well as the regularity or normality of the particle size distribution (Dyer, 1986). Table 5.6 below illustrates the kurtosis scale as indicated by Folk and Ward (1957) in Dyer (1986). These statistical measures were completed and analysed for the estuary bed and surface sediment samples.

Table 5.6. The different classes on the kurtosis scale (Folk and Ward, 1957 in Dyer, 1986).

	Kurtosis Scale
< 0.67	Very Platykurtic
0.67 to 0.90	Platykurtic
0.90 to 1.11	Mesokurtic
1.11 to 1.50	Leptokurtic
1.50 to 3.00	Very leptokurtic
> 3.00	Extremely leptokurtic

5.3.5. Organic Matter Content

Once the process of loss on ignition was completed for the sediment samples, the relevant weights were recorded in an electronic database, which allowed calculation of the percentage of organics. The oven dried weight and the burnt weight or weight of the sample subsequent to the furnace, was recorded and used to calculate the organic matter content. The organic matter content was calculated with an equation, adapted from Heiri *et al*. (2001). The equation is stated as follows:

$$LOI_{450} = ((DW_{105} - DW_{450})/DW_{105})*100 \quad 5.10$$

Where,

LOI_{450} = LOI at 450 °C (%)

DW_{105} = Dry weight of the sample after oven at 105 °C, before combustion in furnace (g)

DW_{450} = Dry weight of the sample after furnace heating at 450 °C (g).

The percentage of organic matter was then graphically illustrated in order to indicate the variations within the different regions within the estuary and barrier. The organic content was linked with the mean grain size and mud content of the sediments, in order to establish a trend, as carried out by Cooper and Mason (1987); Grobbler (1987) and Cooper (1991a).

5.3.6. Suspended Sediment Concentration

Once the vacuum filtration process was completed and the relevant weights and volumes were recorded, the sediment concentration was calculated, as outlined by Gordon *et al*. (1992). The volume of the sediment-water mix, mass of the filter and the mass of the dried filter with the sediment was recorded. The sediment concentration was calculated with the following equation, as established by Gordon *et al*. (1992):

$$Cs = \frac{(M_{FS}) - (M_F)}{V_{SW}} \times 10^3 \quad 5.11$$

Where,

Cs = sediment concentration (mg/l)

M_{FS} = mass of the dried filter paper and sediment (g)

M_F = mass of the filter paper before filtration (g)

V_{SW} = volume of sediment-water mix (l).

The sediment concentrations were then graphically illustrated according to the fluctuating tide (flood or ebb), the type of tide in terms of springs and neaps, and lastly in terms of the season. From this, the sediment concentrations were compared based on these parameters, in order to establish trends, variations, and minimum and maximum values. In conjunction with the analysis of the sediment concentrations, the associated channel discharge and average velocity were also correlated to the sediment concentration by plotting these parameters against each other in a scatter-plot in order to establish a trend.

5.3.7. Suspended Sediment Flux

In order to calculate the net fluxes through the estuary, measurements need to be taken at several points along the estuary (Kjerfve, 1979; Dyer, 1997), which then need to be averaged in order to correspond to the complete variation across the cross-section channel (Dyer, 1997). Dyer (1997) explains that the salt flux through an estuarine cross-section is determined by the multiplication of both the salinity and the flow velocity across the cross-section. Wang *et al*. (2007) describes the suspended sediment flux as the multiplication of the current velocity and the suspended sediment velocity. Gardner and Kjerfve (2006) carried out a study on the tidal fluxes of nutrients and suspended sediments in the Winyah Bay in South Carolina, where the instantaneous flux of suspended sediment was calculated by obtaining the product of the instantaneous concentrations and the channel discharges, which is measured in unit mass per unit time, in g/s. Kitheka *et al*. (2005) calculated net cross-sectional suspended sediment fluxes (kg/s) in the Tana Estuary in Kenya, similar to that of Gardner and Kjerfve (2006). Pillay (1981) calculated sediment flux by multiplying the cross-sectional area, averaged velocity and averaged concentration.

Sediment discharge is defined as the "*amount of sediment moving past a cross-section over some period of time*" (Gordon *et al*., 1992, p.294). The sediment discharge is measured in units of mass per unit time, such as kg/s (Gordon e*t al*., 1992). In relation, Kao *et al*. (2005) carried out a study in the mountainous rivers in Taiwan and established the suspended sediment load as the suspended concentration multiplied by the channel discharge, ultimately measured in mass per unit time. Similarly, Schubel (1972) calculated the suspended sediment discharges in the Susquehanna River in Maryland, and Wall *et al.* (2008) calculated instantaneous sediment discharges in the Hudson River in New York, parallel to that of Kao *et al*. (2005). Parallel to these aforementioned works, Uncles *et al*. (1985) established the suspended sediment transport through an estuarine cross-section by the multiplication of the suspended sediment, velocity and channel cross-sectional subsection rectangular area, which was measured in kg/s.

Beck *et al*. (2004) and Beck (2005) performed a study in the Goukou Estuary in the Western Cape of South Africa, focussed on the sediment transport through a tidal cycle, with the objective to quantify the amount of sediment moving into the estuary. The total amount of sediment transported through the cross-section was calculated by integrating the suspended sediment concentrations and the average velocities obtained throughout the cross-sectional area (Beck, 2005). However, calculation of the total sediment flux throughout the cross-section was measured through multiplying the average velocity, channel area (water depth and dimensions) and the suspended sediment concentrations, measured in mass per unit time, in g/s (Beck, 2005).

Based on the reviewed literature in Chapter Four and the various methods available to calculate sediment flux, as explained above, assessment has led to the following method used to calculate the suspended sediment of the estuary. The simplest and most relevant method of calculating the suspended sediment flux was adopted in this research, based on the manner in which the suspended sediment samples and velocity readings were collected in the field. The most relevant methods outlined is that carried out by Schubel (1972); Uncles *et al*. (1985); Gordon *et al*. (1992); Beck *et al*. (2004); Beck (2005) and Kao *et al*. (2005). It was deemed that the calculation of an instantaneous suspended flux, through the product of instantaneous velocity and suspended sediment concentrations and the rectangular subsection area illustrates much variation. Therefore, average values of both velocity and suspended sediment concentrations were utilised.

The suspended sediment flux was calculated as the product of the average channel velocity, average suspended concentration and total cross-sectional area. The cross-sectional area was calculated in the same manner in which it was calculated for the channel discharge, as outlined by Gordon *et al*. (1992). The vertical flow velocities and suspended sediment concentrations were averaged for the entire cross-sectional area. Therefore, the suspended sediment flux was calculated with Equation 5.12 below:

$$\mathbf{F = A \times V \times C} \qquad \mathbf{5.12}$$

Where,

F = Suspended Sediment Flux (g/s)

A = Cross-sectional Area (m^2)

V = Cross-sectional Average Velocity (m/s)

C = Cross-sectional Average Suspended Sediment Concentration (g/m^3)

The suspended sediment flux is therefore measured in unit mass per unit time. The suspended sediment flux was calculated for each sampled cross-section for each various stage of the tide. Thereafter, these tidal fluxes were compared between the various tidal stages, springs and neaps, as well as seasons.

5.3.8. Descriptive and graphic analysis of the estuary mouth

Throughout the sampling period, several photographs were taken of the mouth of the estuary, in order to note the mouth state and morphological characteristics between spring and neap tides. Each photograph was descriptively analysed in order to establish differences and variations within the estuary mouth during these different periods, in order to illustrate trends during the

sampling period. Aerial photographs from August 2003 to August 2008 were also analysed in order to establish the various morphological patterns of the lower estuary and mouth.

5.4. Conclusion

Several methods have been adopted to collect and analyse the data in this study. The fieldwork comprised a hydrodynamic study and a geomorphological study. The hydrodynamic study included the direct measurement of channel discharge and the collection of estuary bed sediment and suspended sediment, which was measured and sampled every two hours on a spring and neap tidal cycle, as well as on a seasonal basis. The geomorphological study included topographical surveying of the barrier and collection of surface sediment samples. The laboratory work included particle size analysis through dry sieving, organic matter content by loss on ignition and suspended sediment concentration via vacuum filtration. The data were analysed using several different methods, such as statistically and graphically. A photographic analysis of the estuary mouth was also undertaken in order to study the morphology and establish links and trends in the tidal phases.

CHAPTER 6:
RESULTS AND DISCUSSION: GEOMORPHOLOGICAL STUDY

This chapter presents the results and discussion of the geomorphological study, which comprised topographical surveying, measurement of slope angle and sediment sampling, as explained in Chapter Five. Initially, the results of the surveying study will be presented, followed by a discussion of the shape and gradient of the profiles, as well as the seasonal variability. Subsequently, the results of sediment texture, distribution and statistics, as well as the organic content are presented, followed by a detailed discussion, which highlights seasonal variability.

6.1. Survey Data

Survey profiles were plotted from the data obtained during the fieldwork performed along the barrier or spit bar of the Mgeni. During the fieldwork period, the barrier of the Mgeni remained laden with debris in the form of driftwood, litter and plastic bottles. Fourteen survey profiles were plotted and these illustrate different geomorphological zones or environments, each displaying distinguishing physical characteristics, extending from the estuary to the swash zone. Four geomorphological zones were identified, in the form of the estuary, lagoonward slope, berm and swash zone, as identified by Garden (2003) and Garden and Garland (2005). A schematic diagram of the barrier of the Mgeni, indicating the four geomorphological zones, is shown below in Figure 6.1.

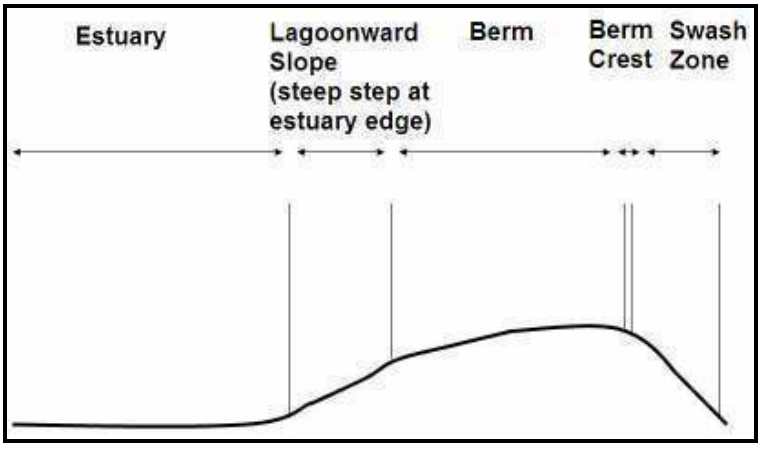

Figure 6.1. Schematic diagram illustrating a typical barrier profile of the Mgeni (Adapted from Garden, 2003 and Garden and Garland, 2005).

Generally, throughout the surveying period, the estuary zone displays a planar topography, containing the lowest elevations and slope angles, except where depressions were present. The

lagoonward slope zone extends from the estuary edge to the berm and generally contains high slope angles and coarse sediment. The estuary edge was characterized by a distinct steep sloping step. Parallel to the theories outlined in Chapter Three, the berm was identified as a relatively flat-topped region that is almost horizontal or dips very gently towards the land, and is positioned landward of the beachface. The parameters of the swash zone are often difficult to determine (Garden, 2003), and has been defined for the Mgeni as the region positioned along the beachface, forming part of the foreshore that is exposed to typical swash processes in the form of wave uprush and backwash (Masselink and Hughes, 2003). Steep gradients mainly dominate the swash zone.

The survey profiles display seasonal variations in terms of the overall shape, height and gradient. Each profile is displayed below in seasonal order and discussed in terms of the overall shape, maximum elevation, barrier width, slope angle and gradient. The barrier width was measured from the estuary edge (steep step) to the last sample point in the swash zone. Slope angles and gradient data for the complete survey period are displayed and discussed below. It must be noted that apart from low tide periods, slope angle readings could not be collected within the estuary because the SmartTool could not be submerged in water.

6.1.1. 29 November 2007: Early Summer Profiles

In summer, the barrier was surveyed and sampled approximately 20 m into the estuary from the estuary edge to the swash zone, with the exception of Profile C. Profile C was surveyed approximately 100 m into the estuary, within which two samples were collected. Samples C1 and C2 were collected approximately 100 m and 15 m into the estuary, respectively, in order to avoid high water levels in a depression within the estuary. Sampling occurred two days prior to a neap tide on the tidal cycle, therefore the tidal levels were considered somewhat moderate.

Profiles A and G are located approximately 30 m south of the Beachwood Tidal Creek and 40 m north of the estuary mouth, respectively. Generally, the profiles display variation in shape with the progression from the Beachwood Mangroves towards the Mgeni mouth in the south. Throughout the surveying sampling period, sampling on the barrier extended sandbar precluded sampling within the estuary zone because it extended under and beyond the M4 Bridge, which forms the boundary of the study area, as shown in Figure 2.1 in Chapter Two. The details of the formation of the barrier extended sandbar are discussed in Chapter Eight. The profiles surveyed on 29 November 2007 are displayed in Figure 6.2 (Profiles A to F) and Figure 6.3 (Profile G).

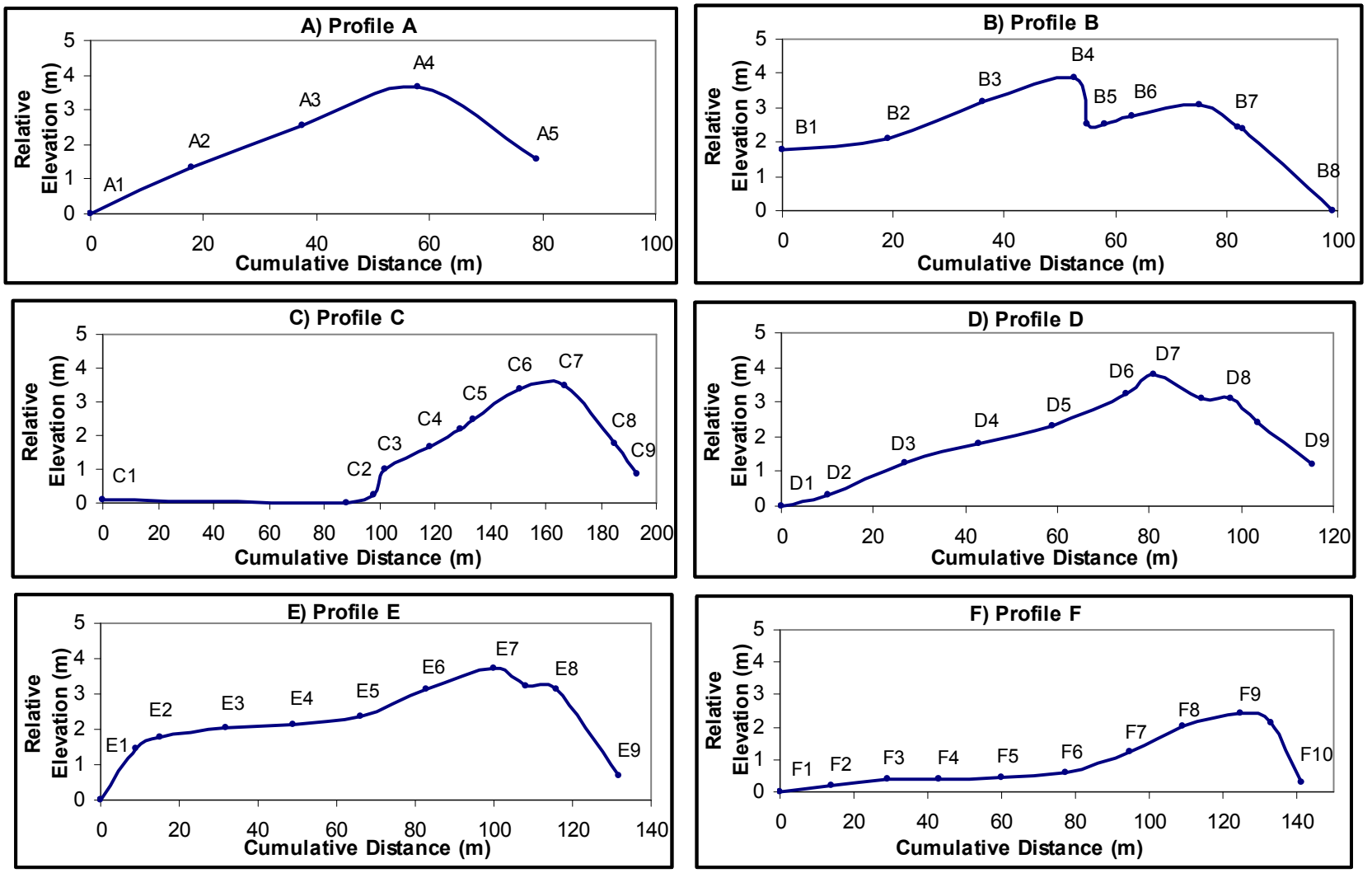

Figure 6.2. A) Profile A, B) Profile B, C) Profile C, D) Profile D, E) Profile E and F) Profile F.

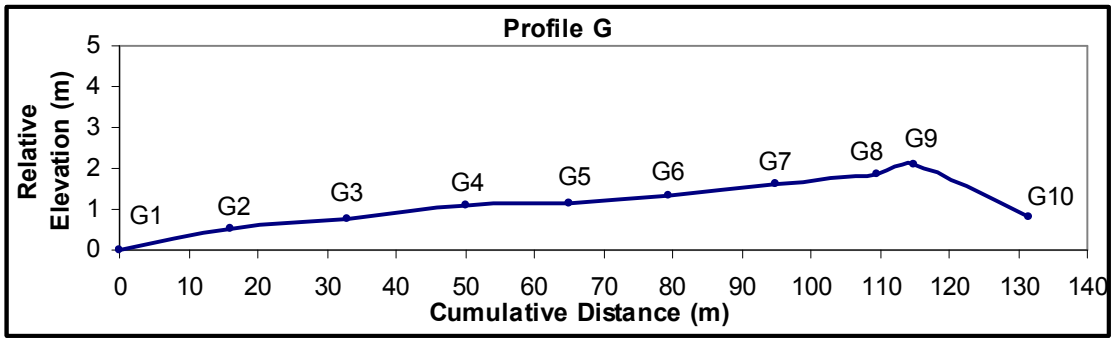

Figure 6.3. Profile G.

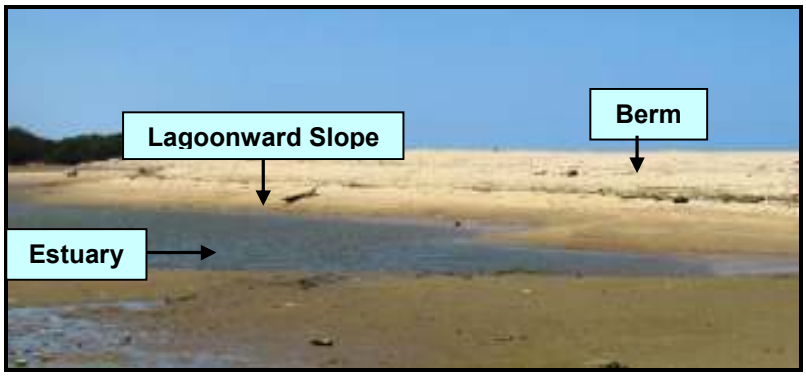

Figure 6.4. Photograph showing the estuary, lagoonward slope and berm of the Mgeni barrier on 29 November 2007, viewed northwards from the barrier extended sandbar.

Figure 6.4 above shows the estuary, lagoonward slope and berm along the barrier of the Mgeni on 29 November 2007. In general, the profiles display alongshore variations in shape, with the progression from the Beachwood Mangroves to the estuary mouth in the south. The profiles plotted north of the barrier extended sandbar, Profiles A to E, are similar in shape and gradient. The only minor difference exists in Profile B, which contains two berms. Profiles F and G, plotted on the barrier extended sandbar are similar in shape and gradient. Overall, the profiles illustrate an alongshore flattening and widening pattern towards the mouth of the estuary in the south, which is illustrated above in Figures 6.2 and 6.3, as well as in Table 6.1 (Page 100). Table 6.1 (Page 100) shows the barrier width and maximum elevation, as well as the geomorphic zone that it intersects with along each surveyed profile. The barrier width for each profile increases from 61.00 m along Profile A to 141.20 m along Profile F, becoming wider towards the estuary mouth from the Beachwood Mangroves section.

The maximum elevation of each profile varies from 2.11 m along Profile G to 3.89 m along Profile B. The points of maximum elevation intersect completely with the berm. Therefore along each profile, the berm represents the highest point of elevation. The maximum elevation generally

decreases from Profile A to Profile G, causing the profiles to become lower from the Beachwood Mangroves towards the estuary mouth in the south. Conversely, the estuary zone forms the point of minimum elevation; hence it is classified as the lowest zone along each profile, whilst the berm is classified as the highest zone along each profile.

Table 6.1. Barrier width and maximum elevation of each profile: 29 November 2007.

Profile	Barrier Width (m)	Maximum Elevation (m)	Point of Maximum Elevation	
A	61.00	3.64	A4	Berm
B	80.00	3.89	B4	Berm
C	95.00	3.46	C7	Berm
D	105.50	3.79	D7	Berm
E	123.00	3.75	E7	Berm
F	141.20	2.45	F9	Berm
G	131.50	2.11	G9	Berm Crest

On 29 November 2007, the measured slope angles vary from 0.10° to 11.80° throughout the barrier. Profiles A to D contain steep, linear lagoonward slope and swash zones, which incline landward and seaward, respectively. Profile E shows slight variation from this trend, as it contains a relatively gentle lagoonward slope zone and a steep swash zone. Overall, Profiles A to E contain linear, planar lagoonward slope and swash zones, with significantly gentle and slightly landward dipping berms, with the exception of Profile B. Profiles F and G are remarkably similar, as they are positioned on the barrier extended sandbar and are classified as the lowest and gentlest profiles throughout the barrier, containing a low, gentle berm and steep, linear swash zone. Additionally, the berm along Profiles E and F contains a relatively flat lower section and a gentle, landward dipping upper section. Berm crests are generally evident along each profile but are distinct when the swash zone is well defined and steep. The steep step at the estuary edge is most distinct in Profiles C and E.

Table 6.2 (Page 101) shows the maximum and minimum slope angles and gradients for each surveyed profile. Maximum slope angles along each profile vary from 5.80° to 11.80°, along the swash zone of Profile E and the lagoonward slope of Profile B, respectively. Therefore, the swash zone and lagoonward slope contain the steepest angles throughout the barrier. The swash zone mainly contains the steepest angles throughout each profile, with the exception of the lagoonward slope which contains the steepest angles along Profiles B to D.

Table 6.2 (Page 101) shows that the minimum slope angles occur entirely along the berm of each profile. Minimum slope angles vary between 0.10° to 3.20°, along the berm of Profiles B and F,

and the berm of Profile A, respectively. Minimum slope angles along the berm fall below 3.20°, therefore it contains significantly low slope angles and gradients, hence it is classified as the flattest, gentlest section along each profile throughout the barrier.

Table 6.2. Maximum and minimum slope angles and gradients along each surveyed profile: 29 November 2007.

Sample Point	Geomorphic Zone	Maximum Slope Angle (°)	Maximum Gradient (°)
A5	Swash Zone	9.20	0.160
B2	Lagoonward Slope	11.80	0.210
C3	Lagoonward Slope	9.50	0.170
D2	Lagoonward Slope	7.30	0.130
E9	Swash Zone	5.80	0.100
F10	Swash Zone	9.10	0.160
G10	Swash Zone	6.10	0.110
Sample Point	**Geomorphic Zone**	**Minimum Slope Angle (°)**	**Minimum Gradient (°)**
A4	Berm	3.20	0.060
B6	Berm	0.10	0.002
C6	Berm	1.60	0.030
D8	Berm	0.40	0.010
E4	Berm	0.20	0.003
F5	Berm	0.10	0.002
G5	Berm	0.20	0.003

The average slope angle for the berm along each profile is displayed below in Table 6.3. The table reveals a trend which shows that the average slope angle of the berm for each profile decreases from the Beachwood Mangroves towards the mouth of the estuary, with the exception of Profile C, which illustrates a slightly higher average slope angle than Profile B. This means that on average, the berm flattens and becomes gentler towards the estuary mouth.

Table 6.3. Average slope angle of the berm along each profile: 29 November 2007.

Profile	Average Slope Angle (°) of the Berm
A	3.30
B	2.10
C	2.60
D	1.95
E	1.64
F	1.59
G	1.54

6.1.2. 20 March 2008: Autumn Profiles

Surveying fieldwork on 20 March 2008 extended 20 m from the M4 Bridge within the estuary, as opposed to sampling in November 2007, which began 20 m into the estuary from the estuary edge (Figure 5.7 in Chapter Five). This change in sampling strategy was adopted for the remaining sampling period, in order to collect more samples within the estuary and to ensure a greater understanding of the sediment characteristics and topography. Sampling took place one day before a spring tide, indicating an enlarged tidal range. Profiles A and D occur approximately 45 m south of the Beachwood Tidal Creek and 60 m north of the inlet, respectively. The profiles surveyed on 20 March 2008 are displayed below from Figures 6.5 to 6.8.

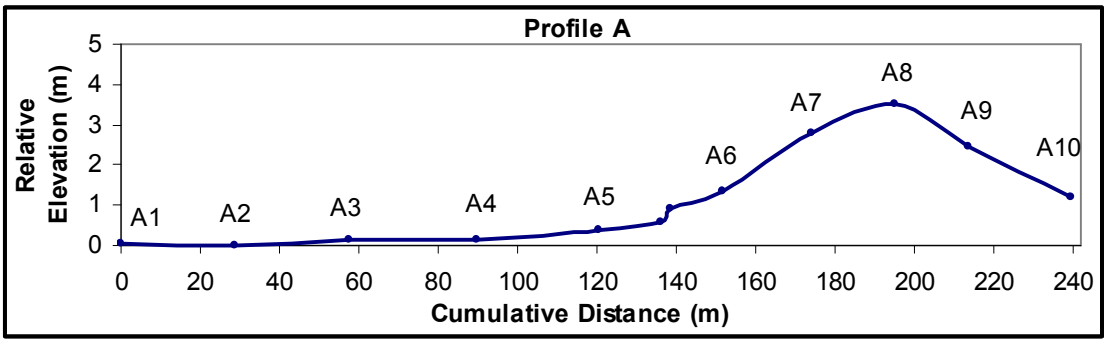

Figure 6.5. Profile A

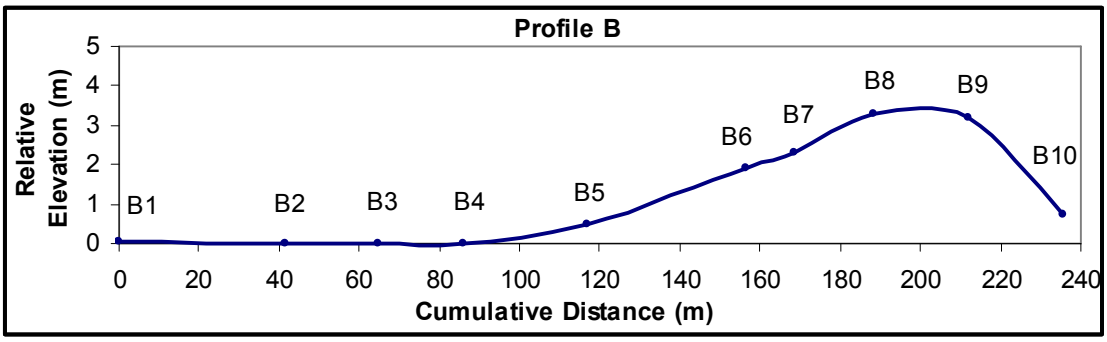

Figure 6.6. Profile B

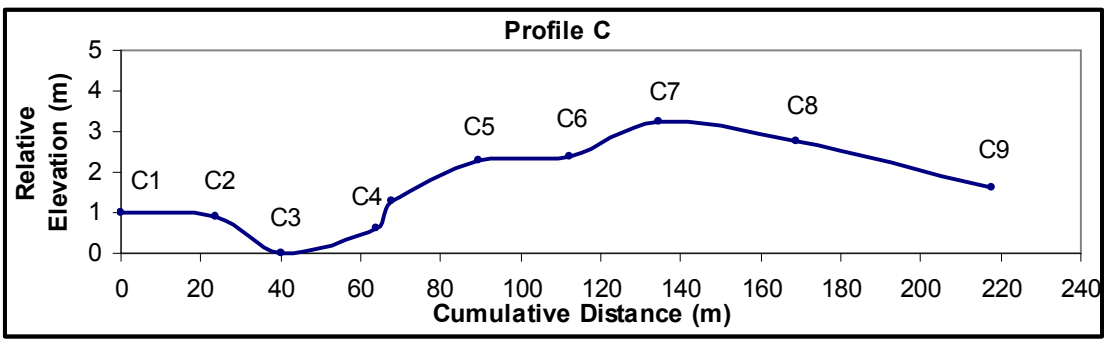

Figure 6.7. Profile C

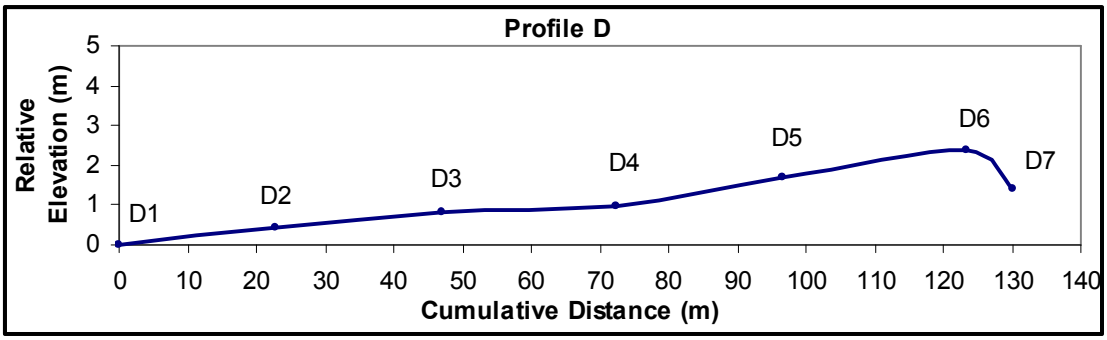

Figure 6.8. Profile D

Similar to the profiles surveyed and plotted on 29 November 2007, these profiles illustrate alongshore variations in shape and gradient, from the Beachwood Mangroves section towards the estuary mouth. Profiles A to C are positioned north of the barrier extended sandbar, whilst Profile D intersects with the barrier extended sandbar. Profiles A and B are remarkably similar in shape, however the remaining profiles illustrate variations. The profiles generally become flatter and lower from the Beachwood Mangroves section to the estuary mouth in the south, which is illustrated in the surveyed profiles in Figures 6.5 to 6.8 above, and Table 6.4 below. Table 6.4 indicates the barrier width and the points of maximum elevation of each profile surveyed on 20 March 2008. The barrier width ranges from 100.70 m to 149.80 m, along Profiles A and B, respectively. The width of the barrier lacks an alongshore widening pattern as evident on 29 November 2007, and instead it fluctuates in width from the Beachwood Mangroves to the estuary mouth in the south.

Table 6.4. Barrier width and maximum elevation of each profile: 20 March 2008.

Profiles	Barrier Width (m)	Maximum Elevation (m)	Point of Maximum Elevation	
A	100.70	3.50	A8	Berm
B	149.80	3.30	B8	Berm
C	104.20	3.22	C7	Berm Crest
D	110.00	2.37	D6	Berm Crest

From Table 6.4 above, maximum elevation of each profile varies from 2.37 m to 3.50 m, along Profiles D and A, respectively. Hence, the profiles become lower alongshore, as the maximum elevation along each profile decreases from Profile A to Profile D, from the Beachwood Mangroves towards the estuary mouth in the south. The berm is completely dominated by points of maximum elevation, indicating that the berm is the highest point along each profile. Conversely, the estuary predominantly contains points of minimum elevation, forming the lowest point along each profile.

The slope angles measured on 20 March 2008 vary from 0.00° to 6.80°. Profiles A and B contain an almost flat, linear estuary zone; steep, linear swash zones; relatively planar, gentle landward dipping berms; and fairly gentle lagoonward slopes. Profile C is very different in comparison to Profiles A and B, as it contains an undulating estuary region, as opposed to the previous general trend of a flat linear estuary. The estuary zone along Profile C contains a dip in the bed which results in a depression that is almost 1.50 m deep. Profile C contains an anomalously gentle, planar swash zone in comparison to the previous profiles, and the berm consists of a lower horizontal section and a gentle, landward dipping upper region. Profile D is similar to the profiles plotted on the barrier extended sandbar in November 2007. Profile D is gentle, shallow and almost linear, and contains a gentle lagoonward slope and berm, with a slightly steeper swash zone. Profiles A and C contain a distinct step at the estuary edge. Berm crests are most distinct along Profiles A, B and D.

Table 6.5 below, shows the maximum and minimum slope angles and gradients for each profile surveyed on 20 March 2008. Maximum slope angles range from 3.80° along the berm of Profile C to 6.80° along the swash zone of Profile D. Therefore, the berm and swash zone contain maximum slope angles equally throughout the barrier. The berm is the steepest section along Profiles A and C, whilst the swash zone is the steepest section along Profiles B and D.

Table 6.5. Maximum and minimum slope angles and gradients along each surveyed profile: 20 March 2008.

Sample Point	Geomorphic Zone	Maximum Slope Angle (°)	Maximum Gradient (°)
A8	Berm Crest	6.40	0.11
B10	Swash Zone	5.00	0.09
C7	Berm	3.80	0.07
D7	Swash Zone	6.80	0.12
Sample Point	**Geomorphic Zone**	**Minimum Slope Angle (°)**	**Minimum Gradient (°)**
A6	Lagoonward Slope	0.40	0.010
B9	Berm	0.00	0.000
C1	Estuary	0.10	0.002
D2	Lagoonward Slope	0.50	0.010

Table 6.5 above, shows minimum slope angles along each profile that vary from 0.00° along the berm of Profile B to 0.50° along the lagoonward slope of Profile D. Minimum slope angles along each profile occur within various geomorphological zones, as the lagoonward slope, berm and estuary collectively contain minimum slope angles along each profile. The lagoonward slope is

classified as the gentlest section along Profiles A and D. The berm and estuary are classified as the gentlest section along Profiles B and C, respectively.

The average slope angle of the berm along each profile is displayed below in Table 6.6. A trend is revealed which states that with the exception of Profile B, the average slope angle of the berm along each profile decreases from the Beachwood Mangroves towards the mouth of the estuary. Therefore, on average the berm decreases in steepness from the Beachwood Mangroves region towards the estuary mouth.

Table 6.6. Average slope angle of the berm along each profile: 20 March 2008.

Profile	Average Slope Angle (°) of the Berm
A	5.00
B	1.38
C	2.50
D	2.25

6.1.3. 21 June 2008: Winter Profiles

In winter, sampling took place three days after a spring tide within the tidal cycle, indicating that the tidal range was waning towards a neap tide, hence the tides were considered somewhat moderate. Profile A is positioned approximately 60 m south of the Beachwood Tidal Creek and Profile D is located 40 m north of the Mgeni mouth. Overall, the profiles follow similar trends and patterns to the autumn surveys. Figures 6.9 to 6.12 illustrated below, show the topographical profiles surveyed on 21 June 2008.

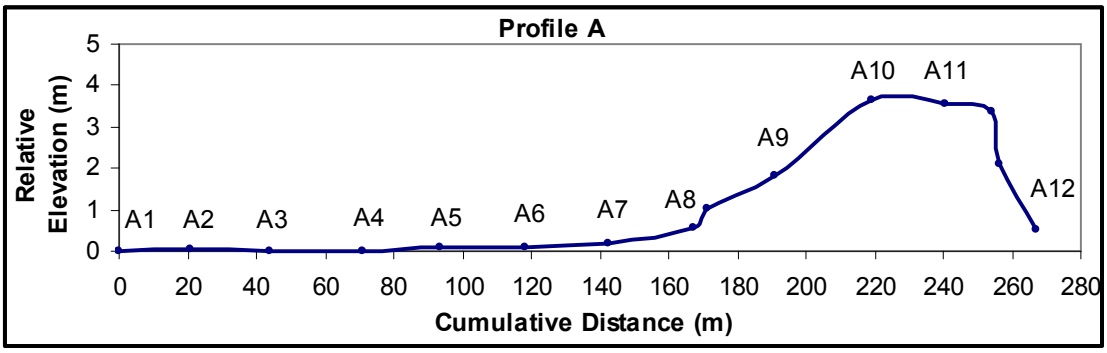

Figure 6.9. Profile A.

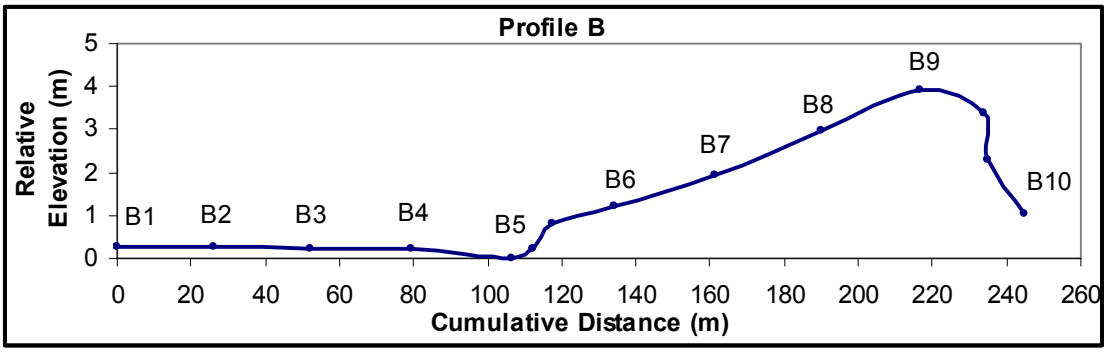

Figure 6.10. Profile B.

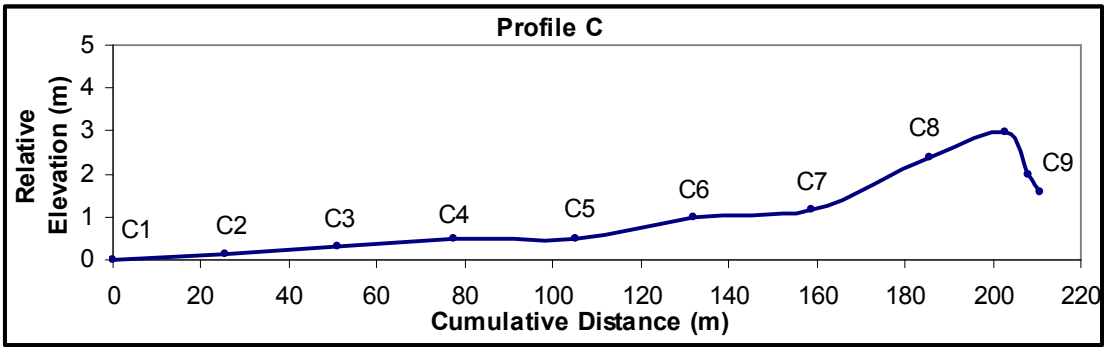

Figure 6.11. Profile C.

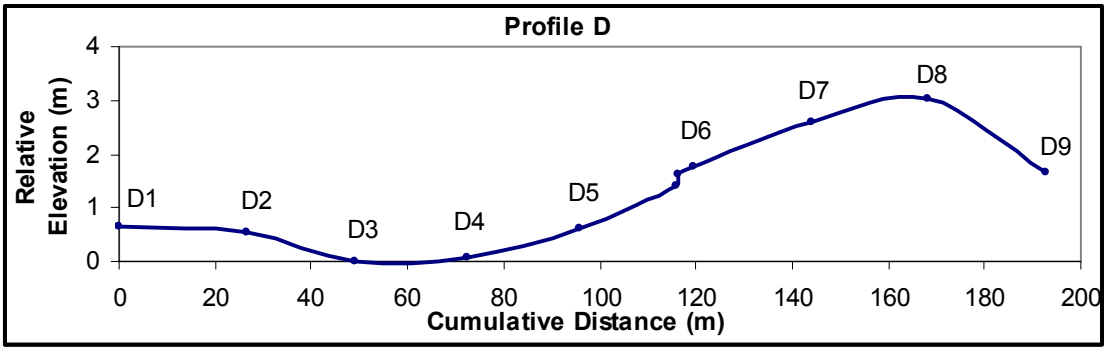

Figure 6.12. Profile D.

These surveyed profiles demonstrate alongshore variations in shape and gradient, similar to those depicted for the 29 November 2007 and 20 March 2008 profiles. Profiles A and B are plotted north of the barrier extended sandbar, whereas Profile C intersects with the barrier extended sandbar, and Profile D is positioned south of the barrier extended sandbar and traverses a section of the estuary inlet. Profiles A and B are remarkably similar in shape, whilst Profiles C and D show slight variations. It is clear that the profiles generally become lower in elevation from the Beachwood Mangroves towards the estuary mouth. Figure 6.13 (Page 107) shows the various geomorphological zones and elements of the barrier on 21 June 2008.

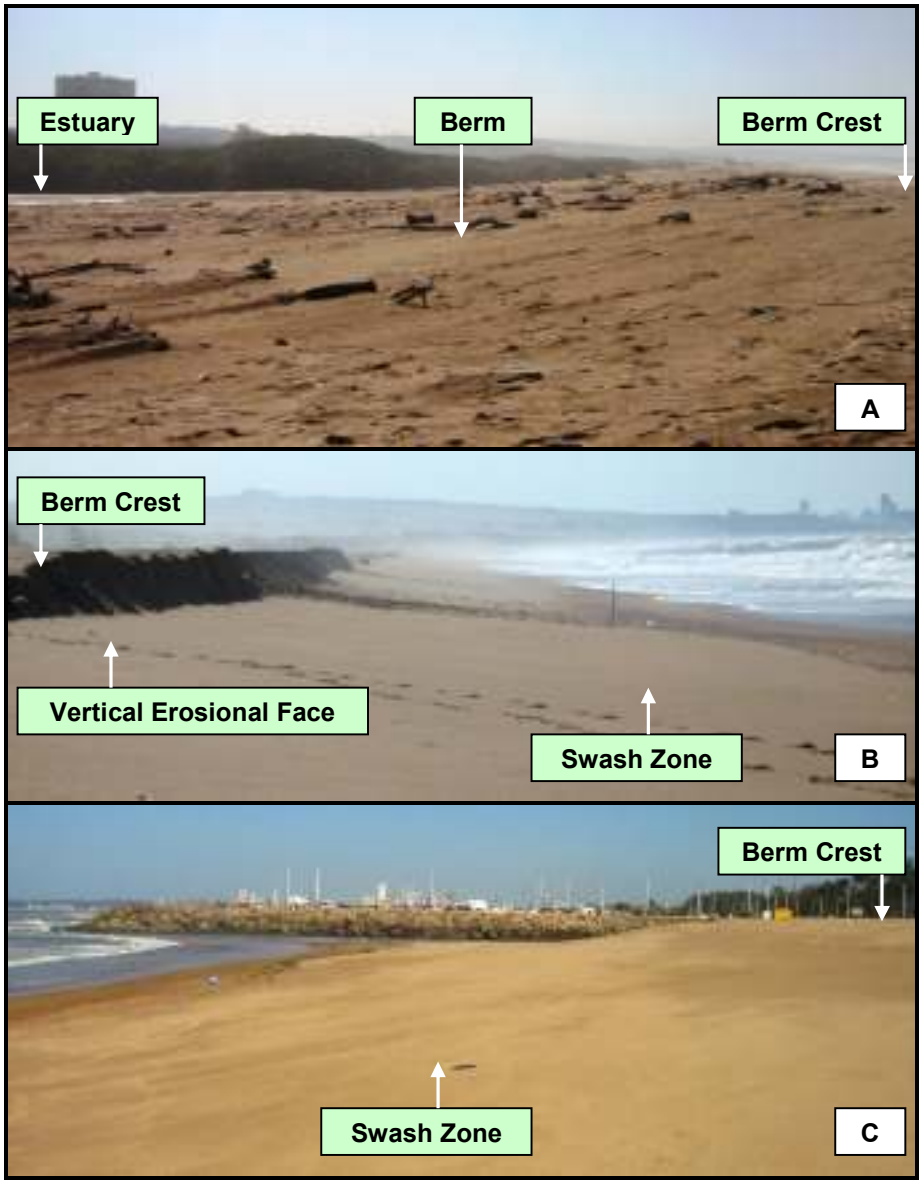

Figure 6.13. Photograph showing the A) estuary, berm and berm crest viewed northwards from the berm, B) berm crest, swash zone and vertical erosional face viewed northwards from the swash zone and C) berm crest and swash zone viewed southwards towards the estuary mouth from the swash zone (Photographs taken by researcher).

Table 6.7 (Page 108) indicates the barrier width and maximum elevation for each profile surveyed along the barrier on 21 June 2008. The barrier width varies from 76.40 m along Profile D to 210.80 m along Profile C. It is clear that the barrier width increases from Profile A (95.70 m) to Profile C (210.80 m), from the Beachwood Mangroves section to the barrier extended sandbar. However, the barrier width decreases further towards Profile D, since it traversed a part of the inlet, hence was exposed to erosive forces such as waves and tides.

Table 6.7. Barrier width and maximum elevation of each surveyed profile: 21 June 2008.

Profile	Barrier Width (m)	Maximum Elevation (m)	Point of Maximum Elevation	
A	95.70	3.65	A10	Berm
B	127.00	3.91	B9	Berm
C	210.80	2.99	Extra Reading	Berm Crest
D	76.40	3.02	D8	Berm Crest

Table 6.7 above shows that the maximum elevation varies from 2.99 m along the berm crest of Profile C to 3.91 m along the berm of Profile B. It is clear that the profiles generally decrease in maximum elevation from the Beachwood Mangroves section towards the estuary inlet, especially from Profiles B to D. The berm is dominated by points of maximum elevation along each profile, indicating that the berm is the highest point along each profile. Conversely, the points of minimum elevation along each profile occur mainly within estuary, which consequently forms the lowest zone along each profile.

The slope angles measured on 21 June 2008 vary from 0.10° to 6.70°. Profiles A and B contain a relatively flat, planar estuary zone, however Profile B contains a slight depression at the estuary edge. Profile A contains a significantly steep, almost linear lagoonward slope and a berm with a distinctively flat upper region and a gentle, landward dipping lower section. Profile B contains a comparatively gentle lagoonward slope and a linear, gentle landward dipping berm. Profile C is relatively gentle, consisting of a berm with a gentle, slightly undulating lower component and a fairly linear, slightly steeper, landward dipping upper component. Profile D consists of a non-linear estuary zone, which contains a very deep depression, almost 0.70 m in depth, with a water level of 1.50 m on the sampling day. In addition, Profile D contains a slightly steep, linear lagoonward slope and a linear, gentle, landward dipping berm. Profiles A to D contain steep, linear and distinct swash zones.

The steep step at the estuary edge is clearly distinct, well defined and consistent throughout Profiles A, B and D. Profile C lacks a steep step at the estuary edge, as it intersects with the barrier extended sandbar. Furthermore, Profile A and Profile B contain a very distinct steep, vertical erosional face at the base of the berm crest on the seaward section, above the upper section of the swash zone. Profile C contains a slight vertical erosional face, which is absent along Profile D. Berm crests are evident throughout Profiles A to D; however they are most distinct along those profiles that contain a distinct vertical erosional face.

Table 6.8 (Page 109) indicates the maximum and minimum slope angles and gradient along each surveyed profile. Maximum slope angles vary from 3.00° along the swash zone of Profile D to

6.70° along the swash zone of Profile A. It is clear that along each profile, the swash zone is completely dominated by maximum slope angles and gradients, which classifies this zone as the steepest section along the barrier. Furthermore, the swash zone illustrates an alongshore decrease in maximum slope angle and gradient from Profile A to Profile D, from the Beachwood Mangroves section towards the estuary mouth in the south. Therefore, the swash zone becomes flatter alongshore towards the estuary mouth.

Table 6.8. Maximum and minimum slope angles and gradients along each surveyed profile: 21 June 2008.

Sample Point	Geomorphic Zone	Maximum Slope Angle (°)	Maximum Gradient (°)
A12	Swash Zone	6.70	0.12
B10	Swash Zone	6.60	0.12
C9	Swash Zone	6.30	0.11
D9	Swash Zone	3.00	0.05
Sample Point	**Geomorphic Zone**	**Minimum Slope Angle (°)**	**Minimum Gradient (°)**
A11	Berm	1.40	0.02
B6	Lagoonward Slope	0.30	0.01
B9	Berm	0.30	0.01
C3	Berm	0.10	0.002
D7	Berm	1.00	0.02

Table 6.8 above, indicates that minimum slope angles range from 0.10° along the berm of Profile C to 1.40° along the berm of Profile A. Minimum slope angles mainly occur on the berm of each profile, indicating that the berm is the flattest section along the profile. However, Profile B contains minimum slope angles along both the berm and lagoonward slope zones. Therefore, the lagoonward slope also forms as part of the flattest section along Profile B. Therefore, the swash zone is classified as the steepest section along each profile, whilst the berm is classified as the gentlest section along each profile.

The average slope angles of the berm for each profile are displayed in Table 6.9 (Page 110). The average slope angles of the berm fall below 1.85° and with the exception of Profile D, the berm decreases in slope towards the barrier extended sandbar. Therefore, the berm becomes gentler towards the estuary mouth. Furthermore, Profile D illustrates a certain degree of deviation from the established trend, as a result of its locality and proximity to the estuary mouth. Consequent to traversing through the inlet, the average slope angle of the berm along Profile D tends to be higher, due to its direct exposure to waves and tides within the inlet.

Table 6.9. Average slope angle of the berm along each profile: 21 June 2008.

Profile	Average Slope Angle (°) of the Berm
A	1.85
B	1.53
C	1.21
D	1.70

6.1.4. Discussion: Survey and Gradient Data

The resultant surveys plotted from the survey data for the complete sampling period illustrate alongshore variations in shape and gradient from the Beachwood Mangroves section of the barrier towards the estuary mouth in the south. The plotted profiles illustrate seasonal variations as well, hence are different in shape and gradient between each season. Therefore, the plotted profiles show variations in overall shape and gradient between each transect and between each season.

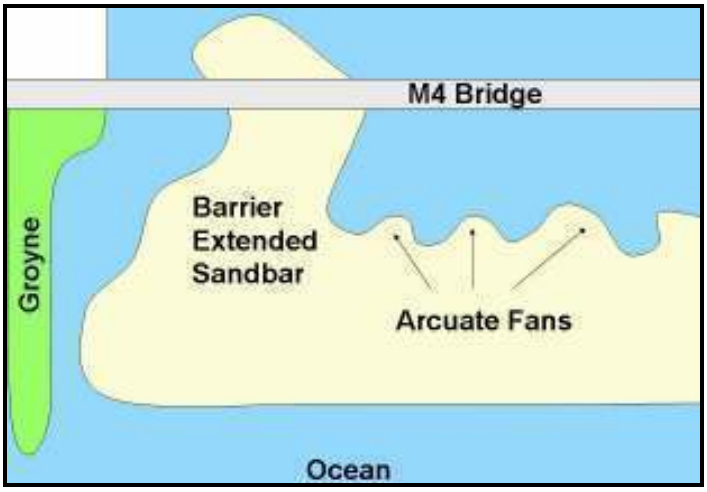

Figure 6.14. Schematic morphological outline of the Mgeni Estuary, specifically along the estuary edge, indicating arcuate fans and the barrier extended sandbar or re-curved spit.

Throughout the sampling period, the steep step at the estuary edge was distinctly present mainly along the profiles plotted north of the barrier extended sandbar. Within this region, the estuary edge contains a very distinctive morphological outline. In plan form, the estuary edge undulates and is punctuated with several micro-scale cusps and arcuate fans, depicted schematically in Figure 6.14 above. These fans were also identified in the Mdloti Estuary by Garden (2003) and Garden and Garland (2005); and in the Mvoti Estuary by Le Vieux (2007). Along the boundary of the estuary and lagoonward slope, these fans are interspersed by cusp formations.

This undulating or meandering morphological outline of the estuary, in the form of cusps and fans, occurs as a result of the flow of water and sediment through the estuary as the tide turns, rides and falls. As the sediment is transported along with the flow and the changing tide, different flow velocities ensure sediment deposition and erosion. It is believed that these cusps, positioned in between the fans, are regions of erosion and undercutting, which results in the steep step at the estuary edge. In addition, this type of erosion may take the form of rill erosion, by which marine water seeps through the barrier, derived from waves during high tide (Reineck and Singh, 1980; Le Vieux, 2007). Rill erosion was identified in the Kosi Estuary by Green (2004) and the Mvoti Estuary by Le Vieux (2007).

Profile B, plotted on 29 November 2007, formed the only profile that contains two berms. A probable reason for the profile shape is that the barrier along Profile B previously contained a single berm, however due to high wave energies; swash uprush possibly overtopped the original berm crest, which caused the water and sediment to pond in a slight depression on the berm, which ultimately created a runnel at the swash limit. Eventually the water level of the runnel possibly reached capacity and seeped through the berm crest, which ultimately resulted in erosion of the berm crest (Komar, 1998), in order to flow towards the sea as backwash. This, therefore, could have generated two berms, in which the swash limit beyond the first berm crest, enhanced accretion along the first berm, as well as erosion and undercutting below the second berm crest, thereby creating a vertical erosional face or scarp, as a result of high wave conditions. Masselink and Hughes (2003), point out that beaches with multiple berms are common along those that are composed of coarse grained sediment and gravel.

Throughout the sampling period, points of maximum elevation along each profile occur completely along the berm, indicating that the berm is the highest point along each profile along the barrier, which is typical of a beach profile and conforms to theories outlined in Chapter Three.

Throughout the sampling period, maximum slope angles occur mainly within the swash zone (especially on 29 November 2007 and 21 June 2008), lagoonward slope and in certain cases along the berm crest. The swash zone forms the steepest section of the profile as it is a complex zone (Dardis and Grindley, 1988), which is exposed to several geomorphological elements. The swash zone is exposed to a range of wave conditions, which generally causes erosion and deposition that both influence the slope, as discussed in Chapter Three.

Conversely, in most cases minimum slope angles intersect mainly with the berm, especially on 29 November 2007 and 21 June 2008, although in certain cases minimum slope angles occur along the lagoonward slope. Therefore, this indicates that the berm is mainly the flattest section of each

profile along the barrier, which conforms to theories outlined in Chapter Three (King, 1972; Davis, 1978; Pethick, 1984; Komar, 1998; Garden, 2003; Masselink and Hughes, 2003).

- ***Alongshore Sorting***

Despite the variations that exist between the profiles, certain similarities exist between the seasons, which entail that the profiles become lower in elevation and flatter from the Beachwood Mangroves section of the barrier towards the estuary mouth in the south. Furthermore, the height of the berm becomes lower with this alongshore progression, causing the berm to become less distinct. Throughout the sampling period, those profiles plotted north of the barrier extended sandbar are classified as similar in shape. The barrier generally tends to become wider towards the region of the Mgeni mouth, which is partly due to the fact that the barrier extended sandbar occurs within the vicinity, specifically about 35 m north of the inlet, which will be discussed Chapter Eight.

However, it is clear that within the inlet region, the barrier and inlet beachface are exposed to erosion. This occurs as a result of a hindrance of the longshore drift of sediment due to the establishment of the engineered groyne, which acts as a rocky headland that generally shelters this region, as well as generates local erosion (Cooper, 1991a; b; Komar, 1998; Breetzke *et al*., 2008), as previously discussed in Chapters Two and Three. This erosion is evident within the mouth region of the Mgeni Estuary, both from aerial photographs and within the results of this study, since the surveyed profiles contain small barrier widths within this region, such as along Profile D (plotted on 21 June 2008), which traversed a section of the inlet channel. The width of the barrier along this profile is limited due to the erosion caused by a hindered longshore sediment supply, as well as erosion by waves and inlet currents. Therefore, the Mgeni inlet region and the barrier region closest to the groyne are starved of sediment (Cooper, 1991a; b).

Furthermore, the accretion of the sediment south of the groyne and around the tip of the groyne, changes the underwater profile, which in turn reduces the wave energy reaching the Mgeni inlet, which causes sheltering of the closest region of the barrier and the inlet (Mather, 2009, pers. comm.). Therefore, the barrier closest to the groyne experiences erosion as a result of waves and tides within the inlet, as well as the reduction of sediment supply, through the establishment of the groyne.

In relation, according to Bascom (1959) and Komar (1998), exposed coasts are steep and coarse grained, whilst sheltered coasts that are not exposed to high wave energies, are flat and fine grained, which is parallel to the findings of this research, since the Beachwood Mangroves

(northern) section of the barrier is classified as exposed, whilst the region closest to the estuary mouth in the southern section of the barrier, adjacent to the groyne is sheltered, as discussed above. Furthermore, the major trend in the findings of this research is that the profiles become flatter and lower, from the Beachwood Mangroves region in north towards the Mgeni mouth, in the south, which agrees with Bascom (1959) and Komar's (1998) abovementioned concept. Furthermore, overwash activity from the marine environment into the estuary, as well as estuary overtopping onto the barrier are understood to also reduce the elevation of the berm and barrier (Cooper, 1986; Mather, 2009, pers. comm.). Therefore, the section of barrier closest to the groyne is described as a sheltered region, with local erosion.

- ***Seasonal Variations in Survey Profiles***

The profiles surveyed during summer, autumn and winter display certain variations and trends. The summer profiles are a bit complex because in comparison to the winter profiles, the berm is not as distinct and flat-topped. Throughout the seasonal surveying period, the point of maximum elevation occurs along the berm of Profile B, plotted on 21 June 2008, which reached a height of 3.91 m. In contrast, the lowest value of maximum elevation reached 2.11 m along the berm of Profile G, surveyed on 29 November 2007. Therefore, the lowest maximum elevation occurred in summer and the highest maximum elevation occurred in winter. Average maximum elevation values calculated for each season are 3.30 m, 3.10 m and 3.39 m, for summer, autumn and winter, respectively. Therefore, on average, the profiles plotted during winter are highest, followed by summer and autumn, with the lowest elevation. Thus, the summer profiles are generally lower than the winter profiles by containing lower berms. Higher berms are indicative of increased levels of deposition and accretion (Dardis and Grindley, 1988; Masselink and Hughes, 2003), hence more deposition is taking place during winter, via increased levels of sediment delivered to the barrier. However, in summer the low elevation of the berm makes the estuary more prone to overwashing and overtopping, which both form as breaching mechanisms (Zietsman, 2004).

Despite the fact that the points of maximum elevation were located on the berm of each profile throughout the seasonal survey period, the berms are definitely clearer and higher in winter. Additionally, the steep, vertical erosional face is only present in the profiles plotted during winter. Generally, a vertical erosional face at the base of the berm crest transforms a profile from one that appears gentle, to one that appears steep (Bascom, 1959). Garden (2003) and Garden and Garland (2005) also recorded a vertical erosional face along surveyed profiles in the Mdloti Estuary. Therefore, the winter profiles containing these vertical erosional faces were considered much steeper profiles. Additionally, it was found that the profiles containing vertical erosional

faces generally contain a better developed berm, as opposed to profiles that lacked these morphological features.

Furthermore, the berm contains average slope angles of 2.16°, 2.46° and 1.43°, in summer, autumn and winter, respectively. Hence, the berm is most gentle in winter and steepest in autumn. These results and patterns conform to theory, as the berm is most distinct, meaning that it is flat-topped according to theory and wide during winter (Dardis and Grindley, 1988). The winter profiles contain well defined berm crests as well, which is a characteristic of the winter profiles (Bascom, 1960). As a result, the profiles plotted during winter and summer, generally follow the patterns outlined by literature and conform to theory.

These seasonal profile variations and trends show a remarkable conformability to theoretical concepts and published literature regarding beach profiles, as explained thoroughly in Chapter Three. Dardis and Grindley (1988) explain the seasonality of beach profiles in a South African context, specifically along the east coast. Accordingly, a swell profile (associated with beach accretion, a wide berm and steep inclined beachface slope) mainly occurs during winter on the east coast of South Africa, and a storm profile (associated with beach and berm erosion) occurs during wet summers (Dardis and Grindley, 1988). Bascom (1959) explains that depositional processes generate steep beach profiles, whereas erosional processes cause gentle and flat beach profiles. The findings of this research, as explained above, include that the winter profiles are higher, steeper and contain distinct berms, in comparison to the summer profiles, therefore these profiles adhere to the theoretical concepts of Bascom (1959) and Dardis and Grindley (1988). The distinctness and presence of the berm, berm crest and vertical erosional face were utilised to distinguish between the winter and summer profiles.

The lowest and highest maximum slope angles of the swash zone occur in winter and summer, ranging from 3.00° to 9.20°, respectively. In comparison, the swash zone contains intermediate slope angles and gradients in autumn. With reference to Dardis and Grindley (1988), winter profiles along the east coast of South Africa generally contain steep beachface slopes or swash zones, which is however is not reflected by the results captured in this study. Instead, the summer profiles generally contain steeper swash zones than the winter profiles. It is understood that the foreshore and beachface region is a fairly complex section of the beach, as it exposed to waves, tides and swash uprush and backwash, and is influenced by wave conditions, sediment sorting and grain size (Dardis and Grindley, 1988). Therefore, if the wave conditions are very strong and contain a high energy and erosive power, then the beachface slope generally becomes less steep or gentle (Bascom, 1959; Pethick, 1984; Dardis and Grindley, 1988).

Therefore, it is possible that the wave conditions on 21 June 2008 contained a higher erosive power than that experienced on 29 November 2007 in summer, which reduced the slope angle of the swash zone throughout the barrier. Sampling during summer took place one day before a spring tide and during winter it took place three days after a spring tide. This means that the tides were high and contained a high tidal range in summer. The tidal range and amplitude were reduced during the winter sampling, since the tide was in a waning phase towards a neap tide. However, average swash zone slope angles of 7.55°, 5.90° and 5.65° were calculated for summer, autumn and winter, respectively, which do not display a large range in values between the seasons.

Even though the swash zone is steeper in summer than in winter, it does not question the classification and suitability of the winter profiles, since the swash zone is dynamic and complex (Dardis and Grindley, 1988; Komar, 1998). The profiles plotted during winter contain a vertical erosional face, such that the beach appears much steeper than in summer and autumn (Bascom, 1959). Bascom (1959) explains that berms are generally built and accreted during spring tides due to a high tidal range, in which the tides at high tide overtop the berm crest and enhance deposition and accretion. However, the reduced tidal ranges and tidal levels during neap tides fail to overtop the berm crest, which causes the waves to break and uprush to a point below the berm crest causing erosion at this point, which results in the formation of a vertical erosional face or a steep scarp, as explained by Bascom (1959). Therefore, despite the lower average slope angles of the swash zone, the beach appears steeper in winter as opposed to summer, due to the presence of the vertical scarp. Furthermore, the winter profiles are higher and contain well developed, high, flat, distinct berms and berm crests in comparison to the summer profiles.

6.2. Sediment Texture and Distribution

Surface sediment was collected from the barrier region of the Lower Mgeni Estuary, along cross-shore transects from each geomorphic zone, which displays specific sediment characteristics. The estuarine, barrier and beach sediments were analysed using the methods described in Chapter Five. The results of this sediment analysis are graphically displayed below, in chronological order, followed by an interpretation and discussion.

6.2.1. Gravel Fraction

Gravel (> 2mm) is classified as the coarsest sediment found within the estuary. However, observations within the field and laboratory conclude that the overall amount of gravel and shell fragments within the study area is low. However, gravel and shell fragments were noticeably

confined to the region bordering the mouth of the estuary along the inlet beachface, which did not fall within the boundaries of the sampled area. Garland and Moleko (2000) and Ngetar (2002) established that since the construction and closure of the Inanda Dam, the amount of gravel reaching the Mgeni Estuary has been significantly reduced. Ngetar (2002) explains that due to this reduced fluvial flow and coarse sediment supply, the marine influence at the mouth tends to intensify and increase. Hence, the gravel found along the inlet of the estuary is most likely derived from the marine environment, via the incoming flood tide and overwash from tides and waves. In addition, the gravel and shell fragments tend to dominate the uppermost surface sediment layer.

6.2.2. Sand Fraction and Statistical Parameters

6.2.2.1. Mean Grain Size

The mean grain sizes of the sediment collected at each sample point illustrates large variability, ranging from 0.13 mm to 1.42 mm, which are classified as fine sand and very coarse sand, respectively.

Table 6.10. The mean grain size of each geomorphic zone along each profile throughout the sampling period.

		Mean Grain Size (mm)			
Date	**Profile**	**Estuary**	**Lagoonward Slope**	**Berm**	**Swash Zone**
29-Nov-07	**A**	0.77	0.74	0.54	0.56
	B	0.54	1.42	0.60	0.52
	C	0.57	1.11	0.63	0.47
	D	0.18	0.70	0.56	0.48
	E	0.46	0.85	0.53	0.42
	F	-	-	0.53	0.57
	G	-	-	0.37	0.47
20-Mar-08	**A**	0.31	0.76	0.56	0.55
	B	0.15	0.60	0.62	0.35
	C	0.28	0.66	0.51	0.38
	D	0.40	0.53	0.39	0.31
21-Jun-08	**A**	0.29	0.65	0.45	0.57
	B	0.19	0.65	0.56	0.36
	C	-	-	0.42	0.47
	D	0.38	0.33	0.37	0.52

- ***Estuary***

Table 6.10 (Page 116) indicates the mean grain size of each geomorphic zone along each profile. Table 6.10 (Page 116) shows that the estuary contains sediment with mean grain sizes varying from 0.15 mm to 0.77 mm, which are classified as fine sand and coarse sand, respectively. Fine sand dominates the deep, calm depressions within the estuary, however medium and coarse sand are confined to the estuary region in proximity to the Beachwood Mangroves Tidal Creek. Furthermore, medium sand occurs close to the estuary inlet.

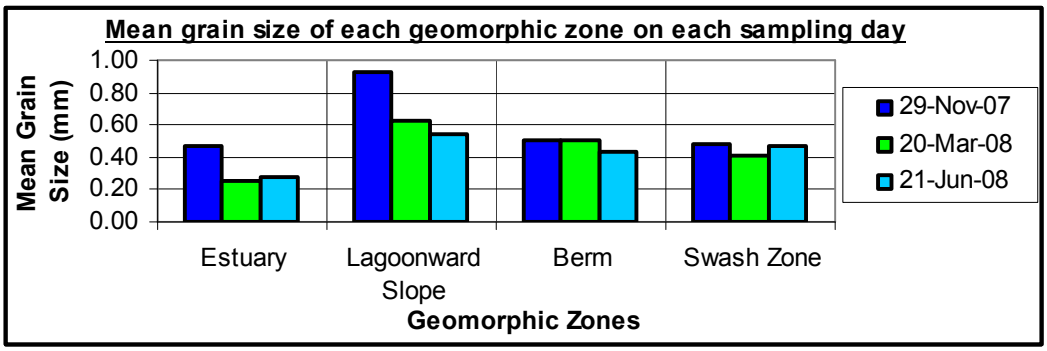

Figure 6.15. Overall mean grain size of each geomorphic zone on each sampling day.

Figure 6.15 illustrated above, shows the overall mean grain size of each geomorphic zone throughout the barrier, for each season. The sediments in the estuary contain a mean grain size of 0.48 mm in summer, which is classified as medium to coarse sand. However, the mean grain sizes of the sediment in the estuary equate to 0.26 mm and 0.28 mm in autumn and winter, respectively, which are both classified as medium sand. Therefore, the estuarine sediments are coarsest in summer and finest in autumn.

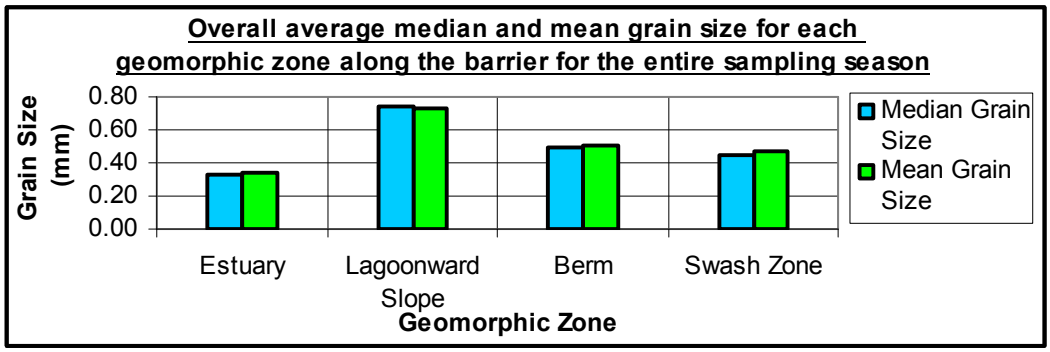

Figure 6.16. Average median and mean grain sizes (mm) for each geomorphic zone along the barrier for the complete sampling period.

Figure 6.16 (Page 117) displays the average median and mean grain sizes of each geomorphic zone throughout the sampling period. Figure 6.16 (Page 117) shows the estuary zone comprises sediment with an overall mean grain size of 0.34 mm, which is classified as medium sand.

- ***Lagoonward Slope***

Table 6.10 (Page 116) shows the lagoonward slope contains sediment with mean grain sizes varying from 0.33 mm to 1.42 mm, which are classified as medium sand and very coarse sand, respectively. The coarsest sediments along the lagoonward slope generally occur within the vicinity of the Beachwood Tidal Creek, whilst the finest sediments generally occur close to the estuary inlet.

Figure 6.15 (Page 117) indicates the lagoonward slope comprises sediment with an overall mean grain size of 0.93 mm in summer, 0.63 mm in autumn, and 0.55 mm in winter, which are collectively classified as coarse sand. Thus, the lagoonward slope contains the coarsest sediments in summer and the finest sediments in winter. Figure 6.16 (Page 117) shows that the sediments on the lagoonward slope contain an overall mean grain size of 0.73 mm, which is classified as coarse sand.

- ***Berm***

Sediments along the berm show large variability in grain size, particularly between sample points. Table 6.10 (Page 116) shows the berm comprises sediment with a mean grain size varying from 0.37 mm to 0.63 mm, which are classified as medium sand and coarse sand, respectively. Generally, the finest sediments along the berm dominate the region close to the estuary mouth, however the coarsest sediments are found within the Beachwood Mangroves section of the barrier. Coarse sediments are also found along the berm bordering the coarse lagoonward slope.

Figure 6.15 (Page 117) shows the berm contains sediment with an overall mean grain size of 0.509 mm in summer and 0.505 mm in autumn, which are both classified as coarse sand. Furthermore, the berm contains sediment with an overall mean grain size of 0.439 mm in winter, which is classified as medium sand. Therefore, the berm contains the coarsest sediments during summer and the finest sediments during winter. In addition, Figure 6.16 (Page 117) indicates that the berm consists of sediment with an overall mean grain size of 0.51 mm, which is classified as coarse sand.

- ***Swash Zone***

Table 6.10 (Page 116) shows that the swash zone contains sediments with mean grain sizes ranging from 0.31 mm to 0.57 mm, which are classified as medium sand and coarse sand, respectively. Overall, the coarsest sediments in the swash zone occur within the Beachwood Mangroves section of the coast, positioned towards the north of the barrier. Medium sand generally dominates the southern section of the barrier; however the region closest to the inlet displays slightly coarser mean grain sizes, evident in winter sampling. Additionally, the sediments within the lower swash zone are generally coarser than the sediments in the upper swash zone, indicating that the mean grain sizes decrease towards the landward section of the beach profile.

Figure 6.15 (Page 117) shows that the sediments in the swash zone display an overall mean grain size of 0.48 mm in summer, 0.41 mm in autumn, and 0.47 mm in winter, which are classified as medium to coarse sand. Therefore, the swash zone contains the coarsest sediments in summer and the finest sediments in autumn. Figure 6.16 (Page 117) shows that the swash zone contains sediment with an overall mean grain size of 0.47 mm throughout the sampling period, which is classified as medium to coarse sand.

Overall, the mean grain sizes of the estuary (particularly in summer), lagoonward slope, berm and swash zone along each profile, tends to decrease from the Beachwood Mangroves section of the barrier in the north towards the estuary mouth in the south. However in some cases, such as within the estuary in autumn and winter, and the swash zone in winter, the mean grain sizes tend to peak at the extremes of the barrier, in the Beachwood Mangroves section and close to the estuary mouth.

Throughout the sampling period and on average, the sediments on the lagoonward slope contain the highest mean grain size, hence is dominated by the coarsest sediments, as illustrated in Figure 6.16 (Page 117). Conversely, the estuary sediments contain the lowest mean grain size, hence is dominated by fine sediments. The berm and swash zone sediments contain the second and third highest mean grain sizes, in which both contain medium to coarse sand. The berm and swash zone are somewhat similar in terms of sediment size, however the berm is slightly coarser as a result of the influence of the coarse grained lagoonward slope zone.

Table 6.11 (Page 120) shows the calculated average median grain sizes, mean grain sizes and skewness for each surveyed profile along the barrier. The mean grain size of each profile along the barrier varies from 0.31 mm to 0.66 mm, which are classified as medium sand and coarse sand, respectively. In general, the coarsest profile mean grain sizes occur within the northern

section of the barrier or north of the barrier extended barrier, within the Beachwood Mangroves section. In summer, the mean grain size of each profile is mainly classified as coarse sand. However, in autumn and winter, the mean grain size of each profile is completely classified as medium sand. Generally, particularly in summer, the mean grain size of each profile decreases alongshore from the Beachwood Mangroves section of the barrier towards the inlet section in the south.

Table 6.11. Average median, mean grain size and skewness of each surveyed profile.

Date	Profile	Median (mm)	Mean (mm)	Skewness
29-Nov-07	A	0.60	0.62	0.11
	B	0.66	0.66	-0.02
	C	0.61	0.62	0.03
	D	0.47	0.50	0.14
	E	0.50	0.52	0.12
	F	0.50	0.54	0.17
	G	0.38	0.38	0.06
20-Mar-08	A	0.41	0.43	0.05
	B	0.39	0.38	-0.18
	C	0.37	0.37	0.05
	D	0.38	0.40	0.11
21-Jun-08	A	0.37	0.38	-0.03
	B	0.31	0.31	0.00
	C	0.41	0.42	0.11
	D	0.38	0.39	0.06

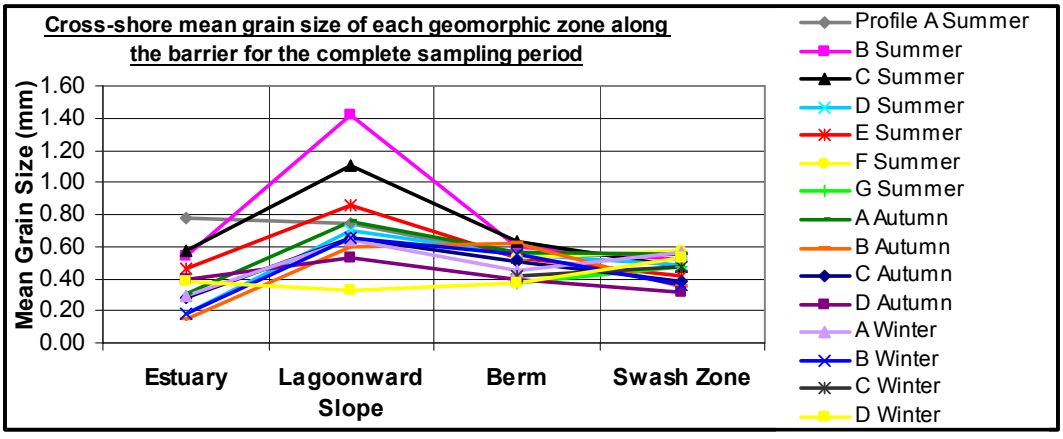

Figure 6.17. Mean grain size of each geomorphic zone along the barrier, perpendicular to the coast for the complete sampling period.

Figure 6.17 (Page 120) indicates the cross-shore variations in mean grain sizes for each geomorphic zone along each profile, perpendicular to the coast from the estuary towards the swash zone. In summer and autumn, the mean grain sizes of the sediment increase from the estuary towards the lagoonward slope, followed by a decrease in mean grain size from the lagoonward slope towards the berm, with a subsequent decrease towards the swash zone. However, in winter, the mean grain sizes of the sediment tend to increase from the estuary to the lagoonward slope, from which it decreases towards the berm, followed by an increase towards the swash zone. Therefore, on average, during summer, autumn and winter, the mean grain sizes peak at the lagoonward slope and generally vary in mean grain size from the lagoonward slope towards the swash zone.

6.2.2.2. Median Grain Size

Throughout the sampling period, the median grain size displays large variability between each sample point along each profile, ranging from 0.17 mm to 1.50 mm. Figure 6.18 below indicates the overall median grain size for each geomorphic zone along each profile. Figure 6.18 shows that median grain sizes of the sediment vary from 0.17 mm to 0.79 mm in the estuary zone, from 0.34 mm to 1.50 mm along the lagoonward slope, from 0.36 mm to 0.64 mm along the berm, and from 0.32 mm to 0.55 mm in the swash zone.

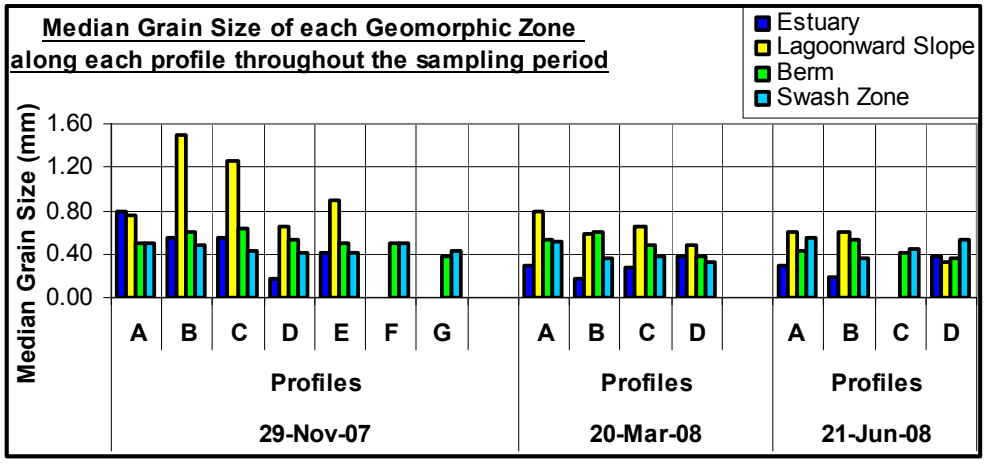

Figure 6.18. The average median grain size of each geomorphic zone along each profile throughout the sampling period.

Figure 6.16 (Page 117) shows that the average median grain sizes calculated for the sediments in the estuary, lagoonward slope, berm, and swash zone for the complete sampling period equate to 0.33 mm, 0.74 mm, 0.49 mm and 0.44 mm, respectively. Hence, the sediments along the lagoonward slope contain the highest median grain size, whilst the estuary contains the lowest,

which indicates that 50 % of the sediments along the lagoonward slope are finer and coarser than 0.74 mm (coarse sand) and 50 % of the sediments in the estuary are finer and coarser than 0.33 mm (medium sand). Furthermore, the sediments along the berm and swash zone contain the second and third highest median grain sizes, respectively.

From Table 6.11 (Page, 120), the median grain size of each profile generally decreases alongshore from the Beachwood Mangroves towards the estuary mouth. The coarsest profile median grain sizes occur within the vicinity of the Beachwood Mangroves section of the barrier.

Figure 6.19 below, illustrates the average median grain size of each geomorphic zone for each season. It is clear that the sediments in the estuary and swash zone contain the highest overall median grain sizes in summer and the lowest in autumn. The sediments along the lagoonward slope and berm contain the highest overall median grain sizes in summer and the lowest in winter.

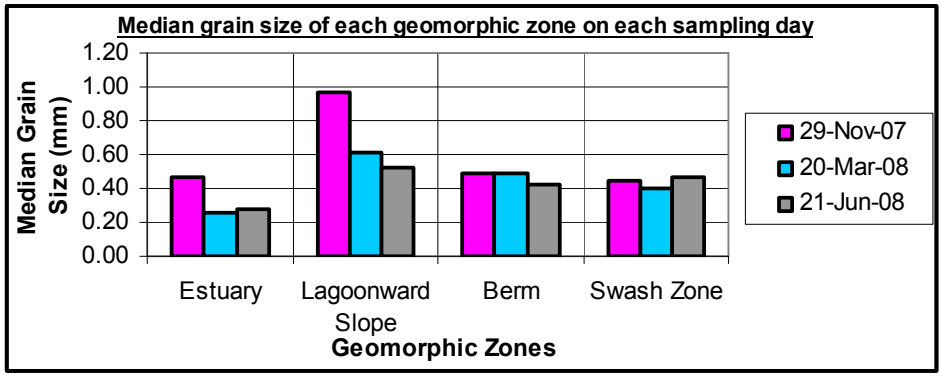

Figure 6.19. Overall median grain size of each geomorphic zone on each sampling day.

6.2.2.3. Sorting

The sediments at each sample point along each profile, and within each geomorphic zone collectively contain sorting values that extend below 0.35 Ø, which is classified as very well sorted. There are several factors attributed to these low sorting values, which will be discussed further on in this chapter.

6.2.2.4. Skewness

The skewness values at each sediment sample point varies from -1.31 to 0.38, which are classified as strongly coarse skewed and strongly fine skewed, respectively. The estuarine

sediments predominately vary between near symmetrical and strongly coarse skewed, indicating no skew and an abundance of coarse sediments, respectively. In the estuary, strongly coarse skewed sediments and coarse skewed sediments mainly occur during autumn and winter, and are restricted to the region close to the Beachwood Tidal Creek. The sediments along the lagoonward slope are mainly coarse to strongly coarse skewed; however some patches of fine skewed sediments occur only during autumn and winter. Coarse skewed sediments occur along the lagoonward slope mainly within the region close to the Beachwood Tidal Creek.

Sediment skewness values for the berm predominantly range between near symmetrical and fine skewed. Patches of coarse skewed sediments occur along the berm mainly in summer and to a small degree in autumn. Sediments along the berm are noticeably coarse skewed in the region bordering the lagoonward slope, which is primarily composed of coarse skewed sediments. However, fine skewed sediments dominate the berm during winter. Sediment skewness in the swash zone mainly varies from near-symmetrical to fine skewed, however the sediments are primarily fine skewed in summer and near-symmetrical in autumn and winter.

The average skewness for each geomorphic zone displays a more generalized pattern in comparison to the sediments at each sample point. Figure 6.20 illustrated below, shows the average skewness of each geomorphic zone along the barrier, throughout the sampling period. From Figure 6.20, the average sediment skewness values of the estuary and lagoonward slope vary from coarse skewed to near symmetrical. Comparatively, the average sediment skewness values of the berm and swash zone range from near symmetrical to fine skewed.

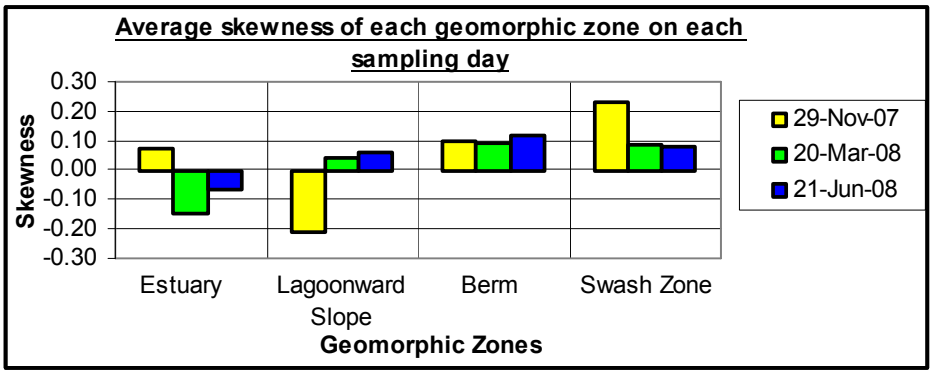

Figure 6.20. Average skewness values of each geomorphic zone on each sampling day.

6.2.2.5. Kurtosis

Figure 6.21 (Page 124) indicates the average kurtosis of each geomorphic zone along the barrier, for each season. The sediments in the estuary, berm and swash zone display mesokurtic curves

in summer, autumn and winter. However, the sediments along the lagoonward slope display mesokurtic curves in summer, and platykurtic curves in autumn and winter.

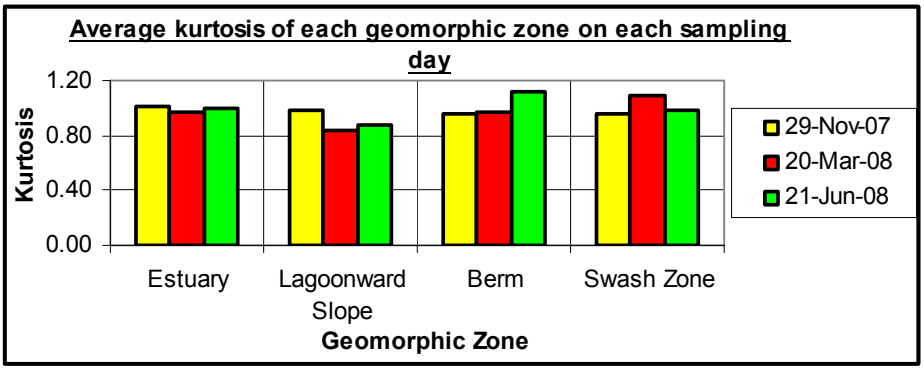

Figure 6.21. Average kurtosis values of each geomorphic zone along the barrier throughout the sampling period.

6.2.2.6. Mean Grain Size and Gradient

The average gradient, slope angle and grain size were calculated for each geomorphic zone, and for each seasonal sampling date. From this data, scatter-plots with trend-lines were established, in which the average gradient and slope angle were plotted against the average grain size for each geomorphic zone, in order to determine a link between these variables. Bascom (1959; 1960); King (1972); Pethick (1984) and Theron (2007) explain that the grain size and beach slope angle are both related, such that coarser beaches are generally steeper. The x variable takes the form of the mean grain size (mm) and the y variable forms either than the average gradient or slope angle (degrees). The scatter-plots in Figure 6.22 A to C (Page 125) indicate the correlation between the seasonal average slope angle and grain size for the lagoonward slope, berm and swash zone, respectively. Figure 6.22 D to F (Page 125) indicates the correlation between the seasonal average gradient and grain size for the lagoonward slope, berm and swash zone, respectively.

According to Burt and Barber (1996), a good fit between the variables occurs if the R^2 value is high, whilst a low R^2 value is indicative of a poor fit between the variables. A strong correlation exists between the average grain size and average slope angles for the lagoonward slope, berm and swash zone (Figure 6.22 A to C), since the R^2 values are high, ranging from 0.6628 (Figure 6.22 B) to 0.9098 (Figure 6.22 C). The correlation between the average grain size and average gradient of the lagoonward slope, berm and swash zone generates slightly higher R^2 values that range from 0.6941 (Figure 6.22 E) to 0.9166 (Figure 6.22 F). Therefore, these high R^2 values indicate that these variables are strongly linked, revealing a positive, linear correlation throughout.

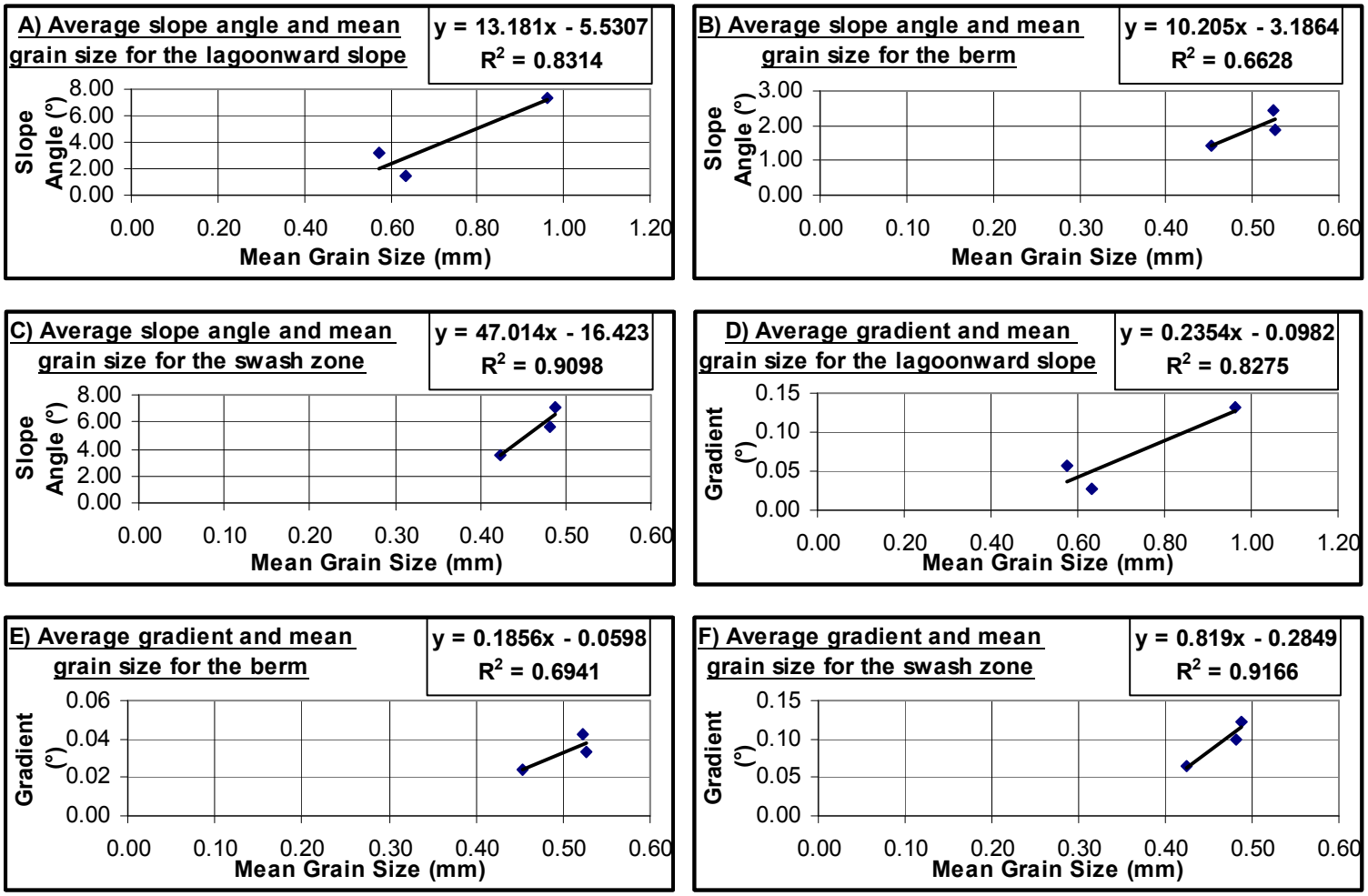

Figure 6.22. Scatter-plots of seasonal average mean grain size and slope angle for the A) lagoonward slope, B) berm and C) swash zone and scatter-plots of the seasonal average mean grain size and gradient for the D) lagoonward slope, E) berm and F) swash zone.

In terms of the R^2 values, the swash zone seems to generate the strongest correlation, followed by the lagoonward slope and berm, which consequently contains the lowest R^2 values. Therefore, based on these scatter-plots and trend lines, it is clear that a strong correlation exists between the mean grain size and the slope angle, as well as the gradient.

6.2.3. Discussion

6.2.3.1. Seasonal Variations in Sediment Characteristics

Seasonal variations in the sediment characteristics and patterns along the barrier occur as a result of variations in rainfall and wave conditions. The rainfall data shown in Figure 6.23 below is sourced from the South African Weather Services (SAWS, 2008), and shows the daily rainfall during November 2007, March 2008 and June 2008. This rainfall data is extracted from the Virginia Station, which is the closest station to the Mgeni Estuary. It must be noted that rainfall data is shown only for the months that sediment sampling occurred in, which will provide simple insight into the influence of rainfall on sediment characteristics of the estuary.

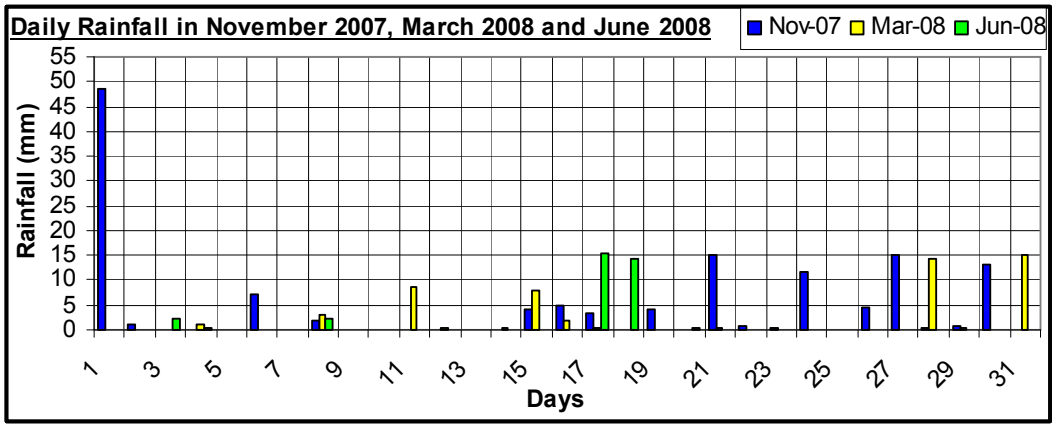

Figure 6.23. The amount of rainfall for each month: November 2007, March 2008 and June 2008. Data sourced from (SAWS, 2008).

Figure 6.23 shows that 136.80 mm of rainfall occurred in November 2007, 53.60 mm in March 2008 and 34.40 mm in June 2008. Therefore, it is evident that the highest rainfall occurred during November 2007, followed consecutively by March 2008 in autumn and June 2008 in winter.

Within each geomorphic zone, the coarsest mean grain sizes occur in summer, ranging between medium to coarse sand. As established above, the highest amount of rainfall occurred during summer. Hence, large amounts of sediments are transported to the estuary during these wet

seasons (Kitheka *et al*., 2005). During summer the fluvial discharges into the estuary generally contain high flow velocities (Hydrodynamic Study, Chapter Seven), which means that it is capable of transporting coarse sediment particles into the estuary (Cooper, 1991a), where it may remain in the estuary or flushed out to the nearshore zone by flooding events (Cooper, 2002), tides and waves.

In addition, as a result of high rainfall in summer, which influences the estuarine water levels, the lagoonward slope and berm become more susceptible to estuary overtopping. As a result, the coarse sediments derived from the catchment and the Beachwood Tidal Creek, tend to overtop onto the lagoonward slope, and may even extend to the berm under extremely high water levels, which is evident in the coarse sediments integrated into the berm.

Based on the storm beach profile concept explained above, the berm, lagoonward slope and estuary are more prone to wave overwash activity in summer when it is exposed to large, erosive storm waves (Dardis and Grindley, 1988), which transports and integrates coarse marine sediments into these regions (backshore region) (Bird, 2000; Schumann, 2003). Therefore, these geomorphic zones contain coarse mean grain sizes during summer, thereby conforming to the abovementioned theories. However, the estuary and swash zone contain slightly higher mean grain sizes in winter than in autumn. This occurs because the estuary experiences a stronger marine influence at the mouth during winter, as explained by Ngetar (2002), which causes more coarse marine sediments to be transported into the estuary (Schumann, 2003). Due to reduced rainfall in winter, the lagoonward slope and berm become less susceptible to estuary overtopping. Therefore, the lagoonward slope and berm contain minimum mean grain sizes during winter.

6.2.3.2. Alongshore Sediment Variations

In most cases, the mean grain sizes of each profile and geomorphic zone illustrate an alongshore decreasing pattern from the Beachwood Mangroves section towards the estuary mouth in the south. The overall alongshore decrease in mean grain size is linked to the engineered groyne which influences wave energy reaching the estuary inlet, sheltering the southern-most region closest to the inlet and groyne, whilst exposing the northern section of the barrier (Beachwood Mangroves) to the open ocean, as previously explained (Bascom, 1959; Cooper, 1991a; b; Breetzke *et al*., 2008). Hence the findings of this research conforms to Bascom (1959) and Komar's (1998) sheltered and exposed beach theoretical concept, since the exposed section of the barrier is coarser than the sheltered region of the coast close to the groyne, which is generally finer (Bascom, 1959; Komar, 1998).

However, certain exceptions exist with regards to this abovementioned alongshore fining trend, which was explained above. The Beachwood Tidal Creek forms a source of sediment to the Mgeni Estuary and according to Cooper and Mason (1987); it contains large amounts of sand within its lower reaches. Cooper (1986) documented frequent overwash activity into the Beachwood Tidal Creek causing it to be dominated by coarse marine sediments. According to Bascom (1959), sediments become finer as its source increases in distance. Therefore, the findings in the Mgeni correspond to this concept put forward by Bascom (1959), since the majority of the mean grain sizes of each profile and geomorphic zone along each profile tend to be highest within the vicinity of the tidal creek. However, in certain instances, such as in the estuary zone in autumn and winter, and in the swash zone in winter, the mean grain sizes tend to peak within the region of the estuary inlet. The estuary inlet is also classified as a source of coarse marine sediment, hence the mean grain sizes tend to peak within this region. Under these conditions, the mean grain sizes illustrate fining towards the middle of the barrier, away from the two sediment sources, especially in the estuary zone.

6.2.3.3. Cross-shore Sediment Variations

The overall mean grain size of the swash zone is generally classified as medium-coarse sand throughout the sampling period. However, individual sediment samples in the swash zone display a decrease in mean grain size up along the swash zone as the flow velocity decreases, which agrees with the theoretical concept put forward by Komar (1998).

However, the overall mean grain sizes peak at the lagoonward slope zone and decrease towards the swash zone. The berm tends to be influenced by the lagoonward slope, as the coarse sediments extend from the lagoonward slope to the extreme landward section of the berm. The estuary zone is influenced by tides, waves and wind, whereas the lagoonward slope is mainly influenced by estuary overtopping and wind action. The berm is mainly influenced by wind (Garden, 2003), estuary overtopping and wave overwash. The swash zone contains several influencing factors such as the flow velocity, swash uprush and backwash, grain size, slope and wind (Komar, 1998). Therefore, these geomorphic zones are influenced by these factors and controls, which are therefore reflected in the mean grain sizes.

6.2.3.4. Median and Mean Grain Size

The median and mean grain sizes for each geomorphic zone along the barrier throughout the sampling period reveal that on average, the lagoonward slope zone contains the coarsest sediments, followed by the berm, swash zone and the estuary, with the finest sediments. This

agrees with the findings of Garden (2003) and Garden and Garland (2005) in the Mdloti Estuary, whereby the lagoonward slope contained the coarsest sediments, followed by the swash zone and berm, which contained more fine grained material than the swash zone.

The lagoonward slope contains the coarsest sediments most probably as a result of coarse marine sediments that overtop the berm by the swash of high waves, which deposit and settle on parts of the berm and may extend to the lagoonward slope and estuary especially under conditions of a steep landward dipping berm, which was documented by Garden (2003). Furthermore, Garden (2003) added that this process leads to the formation of large arcuate fans that punctuate the estuary edge. The coarse sediments deposited into the estuary from the catchment, nearshore zone, as well as from the Beachwood Tidal Creek may also be overtopped onto the lagoonward slope by high water levels and tidal currents in the estuary. The fine sediments along the lagoonward slope may also be susceptible to wind action and winnowed away for dune formation, lagging behind the coarse grained sediments (Lewis and McConchie, 1994; Garden, 2003). Therefore, the lagoonward slope is classified as a lag deposit, dominated by coarse grained sediments.

In general, the berm and swash zone sediments in the Mgeni are somewhat similar, however the sediments along the berm are slightly coarser grained. This is most probably the case as the berm tends to be influenced by both the marine and estuarine environments, rendering it susceptible to estuary overtopping and marine overwashing, respectively, both of which are capable of integrating coarse sediments into the berm. Furthermore, the fine sediments along the berm may generally be transported by wind for dune formation, leaving behind the coarse sediments in certain regions. Therefore, the berm is exposed to coarser sediments than the swash zone. In contrast, the estuary zone contains the finest sediments because of the high mud content sourced from the mangroves, as well as the fine sediments transported to the estuary by fluvial currents, which accumulate in the deep depressions. This conforms to previous studies, as estuarine sediments are typically fine grained as they are composed of silts and clays, forming high mud contents (Cooper and Mason, 1987).

Blackshaw (1985) recorded that the river sediments in the Lower Mgeni Estuary contained mean grain sizes varying from 0.17 mm to 0.44 mm, classified as fine sand to medium sand. Furthermore, Blackshaw (1985) recorded mean grain sizes of beach sediments in the Lower Mgeni to vary between 0.25 mm to 0.41 mm. Le Vieux (2007) established that on average the sediments in the Mvoti Estuary contain a mean grain size of 1.09 mm, which is classified as very coarse sand. Furthermore, Le Vieux (2007) found that the sediments along the berm and swash

zone in the Mvoti barrier are dominated by coarse sand. These findings correspond to the findings in the Mgeni Estuary.

6.2.3.5. Sorting

Tucker (1981) explains that the sorting of sediment is dependent on several factors, such as the sediment source, the grain size of the sediment and the type of depositional mechanisms. Sand sized sediments contain the ability to be easily transported by wind and water, which enables better sorting (Tucker, 1981; 1991). Sediment which is deposited fairly quickly by one transport event is usually rendered as poorly sorted, however sediment that undergoes continual reworking and re-deposition by wind and water is commonly well sorted (Tucker, 1981; Masselink and Hughes, 2003).

Poor sorting means that as transportation and deposition takes place there tends to be minimal selection of the sediment particles, which results in a broad range of sediment grain sizes, whereas well sorted sediment generally undergoes sediment selection such that limited ranges of sediment are transported and deposited (Tucker, 1981; Pethick, 1984; Bird, 2000; Davis and FitzGerald, 2004). Low levels of sorting reveal a fairly uniform sediment sample, such that a small amount of sediment particles tend to be larger or smaller than the mean (Dyer, 1986). Beach sediments are usually well sorted (Tucker, 1981; Bird, 2000; Masselink and Hughes, 2003), whilst fluvial sediments are usually moderately sorted (Selley, 2000).

Throughout the sampling period, the sorting of the sediments in the Mgeni extend below 0.35 Ø, which is classified as very well sorted. This very well sorted sediment is expected of a marine environment and conforms to theory, as there is constant working, reworking and transportation of the sediments throughout the barrier (Tucker, 1981; Masselink and Hughes, 2003). This is particularly the case in the swash zone, where backwash and swash uprush are consistent in constantly reworking the sediment, which results in sorting and selection of the sediment sizes by water. Even the sediments within the estuary are very well sorted, notwithstanding the general calm conditions in certain parts of the estuary, the repeated draining and infilling of the estuary, respectively during low tide and high tide twice a day, ensures that the sediment within the estuary is constantly reworked and sorted by the tidal currents. The sediments along the lagoonward slope and berm are most susceptible to wind and are thus sorted by this mechanism. Therefore, the entire estuary and barrier region of the Mgeni is considered as an extremely active zone, which ensures strong and continual reworking of the sediments, which ultimately generates very well sorted sediments.

Cooper and Mason (1987) established sediment sorting ranging from well sorted to poorly sorted, in the Mgeni Estuary. Furthermore, the sorting of these sediments were extremely variable along the surface, as a result of minor variations in the hydraulic system between transects and sample points (Cooper and Mason, 1987). Blackshaw (1985) found that the beach sediments in the Mgeni varied from moderately sorted to well sorted, whilst the river sediments ranged from very well sorted to moderately well sorted, which agrees in part with the findings of this research.

6.2.3.6. Skewness

Negative skewness indicates that there are more coarse sediments present within log-normally distributed sediment, and conversely positive skewness shows that more fine sediments are present (Buller and McManus, 1979; Tucker, 1981; Pethick, 1984; Lindholm, 1987; Masselink and Hughes, 2003). Symmetrical distributions indicate that the sediment is not skewed (Tucker, 1981). Skewness of a sediment sample can occur as a result of the integration of sediments from two separate sources (Masselink and Hughes, 2003), and it is an indicator of the processes that occur during sediment transport and deposition (Tucker, 1981; Masselink and Hughes, 2003). Beach sediments and those that are subjected to strong wave and tidal action generally display negative skewness (Buller and McManus, 1979; Tucker, 1981; Pethick, 1984; Bird, 2000; Masselink and Hughes, 2003), due to continuous wave action, which re-suspends the finer sediment particles, causing a surplus of coarser sediment present along the bed (Tucker, 1981; Pethick, 1984; Bird, 2000; Masselink and Hughes, 2003). Generally the large proportion of shell fragments present within beach sediments contribute to the negative skewness of these sediments (Masselink and Hughes, 2003). Fluvial sands are generally positively skewed because most of the fine particles in the form of silt and clay remain in the sediment as they are not removed by the river currents (Tucker, 1981).

Throughout the sampling period the calculated skewness of the sediments in the estuary zone ranges from strongly coarse skewed to strongly fine skewed. On average, the sediments within the estuary are near symmetrical in summer and winter, which occurs as a result of the strong tidal currents within the estuary, as suggested by Cooper and Mason (1987). However, coarse skewed sediments in the estuary during autumn, occurs as a result of the excess of coarse sediment present within the vicinity of the Beachwood Tidal Creek. The total rainfall decreases from summer towards autumn, which reduces the amount of flow and sediment delivered to the estuary (Kitheka *et al.*, 2005), hence it causes a build up of coarse sediment in the estuary, where it persists until strong tidal currents are able to transport it out of the estuary. Similarly, Cooper and Mason (1987) found coarse skewed sediment within the Beachwood Tidal Creek.

In most cases, the sediments throughout the lagoonward slope are coarse skewed, especially within the region closest to the tidal creek, which supplies coarse sediment and accounts for the coarse skewness (Cooper and Mason, 1987), as explained above. The lagoonward slope contains coarse skewed sediments in summer and near-symmetrical sediments in autumn and winter, which is linked to the seasonal distribution of rainfall and deliverance of sediments to the estuary, as explained above. Conversely, the berm displays large variation in terms of skewness, generating no distinct patterns. The main transporting mechanism of sediment along the berm is wind. Hence, the presence of patches of coarse skewed sediments along the berm is a possible indicator of the winnowing and removal of fine sediments from the berm for the formation of dunes (Tucker, 1981).

The calculated average skewness of the sediments in the swash zone ranges between near-symmetrical and fine skewed. Blackshaw (1985) states that beach sands are generally negatively skewed, however they may be slightly positively skewed, whilst river sands are predominately positively skewed, which corresponds to the findings of this research. A possible reason for this slight fine skewness in the swash zone is due to a decrease in grain size up the beachface as the swash velocity decreases (Komar, 1998), which causes a surplus of fine sediments within the upper regions. Lewis and McConchie (1994) explain that as sediment is deposited, the resulting deposit may either be coarser or finer grained than the sediment at its source, however it does tend to become better sorted as it is transported and deposited, as well as obtaining a more positive skewness. Therefore, this justifies the slight positive skewness of the sediment within the swash zone.

Blackshaw (1985) calculated that the skewness of the beach sediments in the Mgeni Estuary, which ranged from near symmetrical to positively skewed, and recorded beach sediments with a very positive skew and river sediments ranging between negatively and positively skewed. Le Vieux (2007) established fine skewed sediments in the estuary zone and near symmetrical sediments along the berm in the Mvoti Estuary. The findings of both Blackshaw (1985) and Le Vieux (2007), agrees with the findings of this research.

6.2.3.7. Kurtosis

Kurtosis is an assessment of the extent of peakedness of the grain size distributions (Buller and McManus, 1979, Lewis and McConchie, 1994; Selley, 2000). According to Lindholm (1987), kurtosis deals with the ratio of sorting in the tails and central portions of distribution curves. Leptokurtic curves are extremely peaked, in which the central portion is better sorted than the tails of the distribution curve (Lindholm, 1987; Selley, 2000). Leptokurtic curves contain a surplus

of extreme grain sizes, whereas platykurtic curves contain a shortage of extreme grain sizes (Dyer, 1986). Platykurtic curves contain flat peaks, in which the tails are better sorted than the central portion of the distribution curve (Lindholm, 1987; Selley, 2000). Mesokurtic curves are classified as normal distribution curves that do not contain a shortage or surplus of extreme grain sizes (Dyer, 1986).

On average the calculated kurtosis of the sediments throughout the sampling period ranges from platykurtic (0.67 Ø to 0.90 Ø) to leptokurtic (1.11 Ø to 1.50 Ø). On average, the sediments in the estuary, berm and swash zone display mesokurtic curves, which reflect a normally distributed curve that is not excessively peaked. The sediments along the lagoonward slope range between mesokurtic and platykurtic curves, meaning that the some of the sediments within the lagoonward slope display normally distributed curves, as well as curves that are better sorted in the tails than the central portion.

In comparison, Ngetar (2002) found that the sediments within the upper regions of Mgeni Estuary, above the M4 Bridge, contained a calculated kurtosis ranging between leptokurtic and very leptokurtic. Blackshaw (1985) found that the beach sediments in the Mgeni were generally less peaked than normal in terms of kurtosis, displaying platykurtic curves. However, the kurtosis within the lower Mgeni, within this study, reveals a different pattern, which mostly reflected mesokurtic curves. This means that the sediments in the lower regions of the estuary is normally distributed and sorted throughout the curve, as a result of better sorting mechanisms within the lower regions.

6.2.3.8. Correlation between Mean Grain size, Gradient and Slope Angle

Based on the findings of this research, there is a definite strong, positive correlation between the mean grain size, slope angle and gradient. Therefore, these findings conform to theoretical concepts put forward by Bascom (1959; 1960); King (1972) and Pethick (1984), which explains that as the mean grain size increases, the slope angle increases, hence coarser beaches are generally steeper beaches. This correlation is linked to the amounts of percolation and sediment sorting (King, 1972; Pethick, 1984), as discussed in Chapter Three. The sediments throughout these zones are very well sorted, which consequently influences the slope angles and gradient.

6.3. Organic Matter Content

The organic matter content was calculated for the sediments collected during the fieldwork, by loss on ignition as described in Chapter Five. Loss on ignition was performed only for the

sediment samples collected within the estuary during 29 November 2007, because it was established by visual analysis that the sandy samples of the barrier and beach were composed of a smaller amount of fine particles and mud, hence it was expected that these samples contained low organic contents. However, it was later decided that loss on ignition should be performed for all the samples collected during 20 March 2008 and 21 June 2008, in order to confirm that sandy samples contain less organic content.

The organic content of the sediments throughout the sampling period varies from 0.10 % to 2.93 %. Estuarine sediments collected on 29 November 2007 contain organic contents varying from 0.30 % to 1.15 %. Figures 6.24 and 6.25 below show the organic contents of the sediments along each profile on 20 March 2008 and 21 June 2008, respectively. The organic contents vary from 0.10 % to 2.93 % on 20 March 2008, and from 0.10 % to 1.61 % on 21 June 2008.

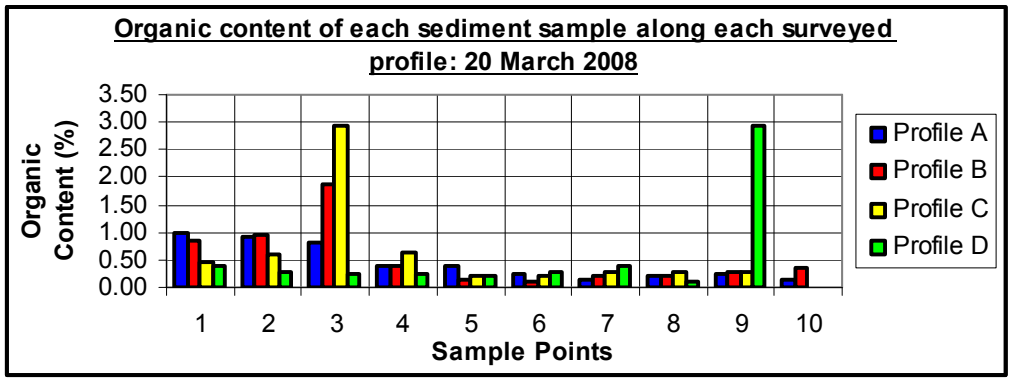

Figure 6.24. Organic content of each sediment sample along each profile: 20 March 2008.

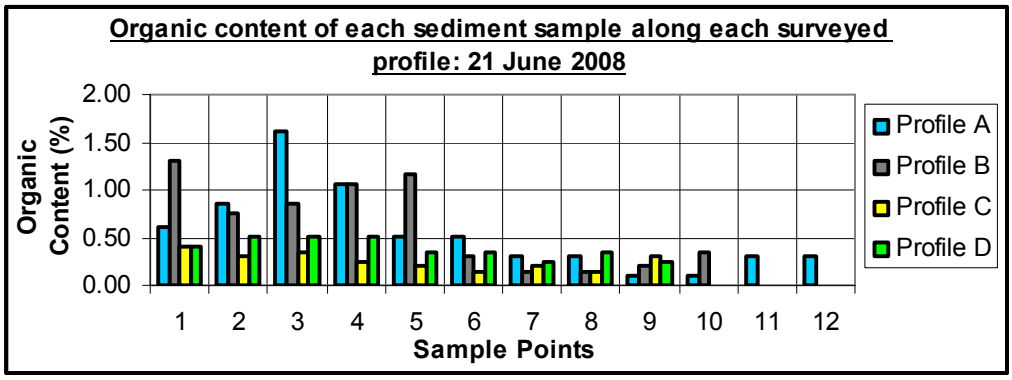

Figure 6.25. Organic content of each sediment sample along each profile: 21 June 2008.

Throughout the sampling period, the estuarine sediments in the Mgeni contain the highest organic contents, especially along those profiles plotted north of the barrier extended sandbar.

The estuary zone closest to the Beachwood Tidal Creek contains substantially high organic contents. The Beachwood Tidal Creek is a source of organic detritus, mud and fine grained sediment to the estuary (Cooper and Mason, 1987); hence the sediments in proximity contain high organic contents. In particular, the sediments within the deep, calm depressions within the estuary hold the highest organic contents, whilst the sediments closest to the estuary mouth contain low organic contents. Generally, the sediments along the swash zone, berm and lagoonward slope contain extremely low organic contents.

Additionally, in most cases the organic contents tend to decrease cross-shore from the estuary towards the swash zone. The estuarine sediments contain the highest organic contents and are generally the finest in comparison with the remaining geomorphic zones. Therefore, the link between mean grain size organic content was sought.

The correlation between the mean grain size and organic matter content was established through scatter-plots and trend lines. Figure 6.26 below, illustrates the link between the mean grain size and percentage of organic matter for the sediments collected on 29 November 2007, which reveals a R^2 value of 0.6217. Figures 6.27 A and B (Page 136) show the correlation between the average grain size and the average organic content of each geomorphic zone on 20 March 2008 and 21 June 2008, respectively. Figures 6.27 A and B reveal R^2 values of 0.6914 and 0.7475, respectively. These are fairly high R^2 values; hence the link between these variables is strong.

A negative or inverse correlation exists between the mean grain size and the organic content throughout. Therefore, it is clearly evident that the mean grain size and the organic content are correlated. The finer the sediments in the estuary tend display an affinity to greater amounts of organic matter, whilst coarser particles contain lower organic contents.

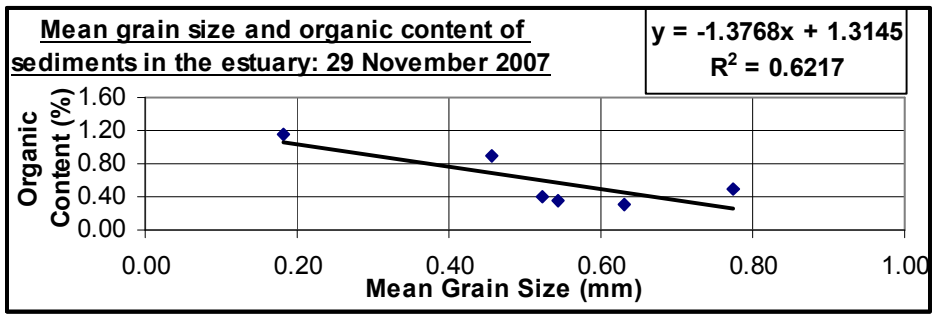

Figure 6.26. Mean grain size and organic content of each sediment sample in the estuary: 29 November 2007.

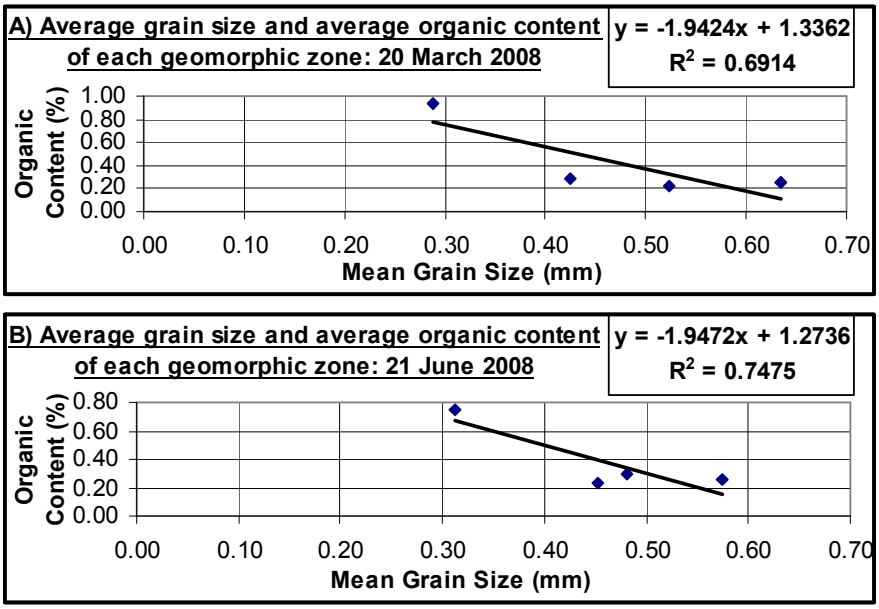

Figure 6.27. Average grain size and average organic content of each geomorphic zone for A) 20 March 2008 and B) 21 June 2008.

This correlation between the mean grain size and organic content analysed above, occurs mainly as a result of the percentage of mud within the sediment. Throughout the sampling period, the estuary sediments, which contain the highest organic contents, contain the highest percentages of mud and the lowest percentages of sand. The samples along the remainder of the barrier, including the marine sediment, contain negligible amounts of mud and large amounts of sand, and these are the samples that contain the lowest amounts of organic matter. In addition, the sediments within low flow velocities regions, particularly in the deep depression north of the barrier extended sandbar, contain high mud contents and subsequently high organic matter contents. Hence, the correlation between mud content and organic content was sought.

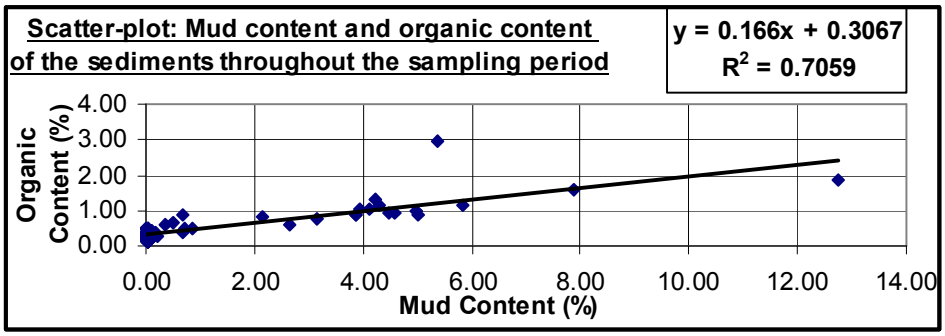

Figure 6.28. The correlation between the mud content and organic content of each sediment sample collected throughout the sampling period.

Figure 6.28 (Page 136) shows the link between the percentage of mud and the organic matter content of the sediments collected throughout the sampling period. The scatter-plot reveals a high R^2 value of 0.7059. Therefore, a strong, positive correlation exists between the percentage mud and the organic content for the sediments throughout the barrier.

6.3.1. Discussion

Throughout the entire barrier and the seasonal sampling period, the organic content reaches a maximum of 2.93 %. In view of this maximum organic content, it is concluded that the organic content of the Lower Mgeni Estuary and barrier is relatively low, considering that Wright (1990) recorded organic contents of up to 20.70 % within the upper regions of the St. Lucia Estuary. More site specific, Cooper and Mason (1987) found that the surface sediment in the upper Mgeni Estuary contained the highest levels of organic carbon, with values reaching up to 12.00 %. Grobbler (1987) also found high organic carbon contents in the surface sediments in the upper Mdloti Estuary, north of Durban, and low values within the lower regions and the mouth of the estuary, which conforms to the findings in this research. In addition, Grobbler (1987) found values of organic carbon reaching 12.40 % in the uMgababa Estuary, south of Durban.

The reason for the low organic content of the sediments within the Lower Mgeni Estuary and barrier is due to the region being a very active zone, which occurs as a result of the high velocity and high energy of the swash zone, as well as the presence of strong marine tidal currents and waves in the inlet, which agrees with the findings of Wright (1990; 1995). The estuary is subjected to low tide draining and high tide inundation twice a day. As a result, the sediment within the estuary is being re-worked and transported most of the time, which dissipates calm and stagnant conditions. However, calm conditions prevail in the deep depression in the estuary, northwards of the barrier extended sandbar, which proves to contain high organic matter contents, since fine sediments and mud are allowed to settle and concentrate. Hence, sheltered and calm regions in the estuary contain the highest organic contents, as opposed to the sediments in the active swash zone.

The sediments collected in the estuary, in proximity to the mangroves contain high organic contents, as a result of the faecal remains of many estuarine organisms, litter produced from the mangroves along the Beachwood Tidal Creek, and plant remains and bacteria which are believed to contribute to the high organic matter content within the estuary, as found by Wright (1990; 1995) in the St. Lucia Estuary, as well as by Cooper and Mason (1987) within the Mgeni Estuary.

The correlation between mean grain size and organic matter content was sought and analysed above, which substantiated the trend that the coarse beach and barrier sediments contain low organic contents. Tucker (1981) explains that the porosity of sediment generally increases as the grain size and sorting increases, and as the amount of clay decreases, therefore beach sands contain high porosities and are highly permeable. Consequently, from this it is understood that fine sediments contain lower porosities than coarse sediments, which means that they are more capable of maintaining organic matter.

This led to the establishment of a positive link between the mud content and organic content of the sediments, since according to Cooper and Mason (1987); mud in the Mgeni Estuary is generally composed of fine quartz particles, clays and organic matter. Mud is a significant constituent of the sediments within an estuary, as it decreases the amount of porosity of the sediment by filling in the spaces in between the larger sediment particles, and thereby increases the cohesive forces between the sediments (Cooper and Mason, 1987). Parallel to the findings of this research, Cooper and Mason (1987) established an almost near linear relationship between the percentage of mud and the organic matter content in the Mgeni Estuary and explained that this relationship occurs due to the production of mud through the disaggregation of organic material. Additionally, Grobbler (1987) and Wright (1990; 1995) found a linear relationship between organic carbon and mud content, within the Mdloti Estuary and St. Lucia Estuary mouth, respectively. Therefore, sediments composed mainly of sand, such as the barrier and beach sediments, contain minor organic contents, whilst sediments with high mud contents contain high amounts of organic matter, which agrees with the findings of Cooper and Mason (1987); Grobbler (1987) and Wright (1990).

6.4. Conclusion

The lower estuary and barrier of the Mgeni, that lies seaward bound of the M4 Bridge, is classified as a fairly active zone. Throughout the sampling period, the inlet of the estuary remained open to the sea, which therefore enabled the transportation of catchment derived sediment to the nearshore zone and the subsequent transportation of marine sediment into the estuary. This region contains a high energy and velocities within the channel reach high values, which will be discussed in the following chapter. Throughout the barrier, shore-perpendicular surveying and sediment sampling was performed, which resulted in the identification of four geomorphological zones, in the form of the estuary, lagoonward slope, berm and the swash zone. In general, the estuary is fairly flat and contains relatively low slope angles, except in cases of deep depressions. The lagoonward slope contains some of the steepest slope angles especially

during summer sampling; however the majority of maximum slope angles occur within the swash zone. The berm is classified as flat, however in most cases it is gently landward dipping.

The survey profiles display alongshore variations in terms of shape, gradient and sediment sizes, with the progression from the Beachwood Mangroves Tidal Creek towards the mouth of the estuary in the south. Generally, the profiles generally become flatter, lower and finer towards the mouth estuary, as a result of the sheltering nature of the engineered groyne (Cooper, 1991a; b; Breetzke *et al*., 2008), as explained by Bascom (1959) and Komar (1998), which also causes erosion along the inlet beachface close to the groyne, as a result of the hindrance of the longshore drift (Cooper, 1991a; b; 1995; Breetzke *et al*., 2008). However, the barrier seemed to widen southwards towards the barrier extended sandbar, along which it was the widest.

Apart from longshore variations, the profiles illustrate seasonal variations, as well. The summer and winter profiles conformed to the theoretical concepts regarding swell and storm profiles put forward by Dardis and Grindley (1988). The summer profiles contain lower elevations, and less distinct berms and berm crests, in comparison to the winter profiles. The profiles plotted during autumn formed the transitory phase, as the profiles change from summer to winter. The winter profiles contain the highest elevations, higher, distinct and flatter berms, with distinct berm crests. The winter profiles appeared much steeper than the summer profiles, as a result of the presence of a vertical erosional face at the base of the berm (Bascom, 1959), above the swash zone.

In terms of the sediment texture and distribution, the sediments within the estuary contain the lowest mean grain size, whilst the sediments along the lagoonward slope characteristically contain the highest mean grain size. On average, throughout the sampling period, the sediments along the lagoonward and berm are classified as coarse sand, whilst the estuarine sediments are classified as medium sand and the sediments in the swash zone are classified as medium-coarse sand. The berm shows large scale variation in mean grain size between sample points and profiles. The swash zone is classified as the most complex (Dardis and Grindley, 1988), and energetic geomorphic zone throughout the study area, as it contains several influencing factors such as swash uprush, backwash, wave velocity, sediment grain size and slope angle.

The Beachwood Tidal Creek and the mouth of the estuary are classified as sediment sources, as they provide sediment to the estuary (Cooper and Mason, 1987). In certain cases there is fining towards the middle of the barrier, away from the sources (Bascom, 1959). In terms of cross-shore variations, the mean grain sizes generally peak at the lagoonward slope zone, and the individual sediment samples collected in the swash zone are generally finer along the upper sections than the lower sections, agreeing with Komar (1998).

The mean grain size of each geomorphological zone is coarsest in summer, which occurs as a result of the rainfall distribution between seasons, which is highest in summer. Therefore in summer, as a result of the large rainfall and consequent fluvial discharges, large amounts of coarse and fine sediments are transported from the catchment to the estuary; hence the largest mean grain sizes occur during this period. A strong, positive correlation between mean grain size, slope angle and gradient was established for the lagoonward slope, berm and swash zone, which conforms to the vast theoretical concepts outlined in Chapter Three.

The sediments throughout the estuary, lagoonward slope, berm and swash zone are very well sorted. This occurs as a result of the high energy and strong sorting mechanisms within the study area. Tidal and fluvial currents, as well as wave action are dominant in the estuary, which constantly re-work and transport the sediments, which efficiently sorts it. The sediments along the lagoonward slope and berm are sorted by wind and water, by estuary overtopping and overwash, which enables good sorting of the sediment.

In terms of skewness, the sediments in the estuary and along the lagoonward slope are mainly coarse skewed close to the Beachwood Mangroves Tidal Creek, which supplies the estuary with sediment (Cooper and Mason, 1987). Near symmetrical sediments dominate the majority of the estuary, as a result of strong tidal currents. The berm displays large variation in skewness ranging from coarse skewed to fine skewed, whilst the sediment skewness in the swash zone varies from near symmetrical to fine skewed, which agrees with past research in the Mgeni. In terms of kurtosis, the estuarine, berm and swash zone sediments contain mesokurtic curves, whilst the lagoonward slope sediments vary between platykurtic and mesokurtic curves.

The estuary sediments display the highest organic contents throughout the sample period, partly due to the Beachwood Mangroves and Tidal Creek which supplies organic material to the estuary (Cooper and Mason, 1987), as well as the calm, deep depressions in the estuary which enhance fine sediment accumulation. Conversely, the barrier and beach sediments display negligible organic contents. A strong, inverse correlation was established between the mean grain size and organic content, which is linked to the porosity and mud content of the sediments (Tucker, 1981; Cooper and Mason, 1987). A strong, positive linear correlation was established between the mud content and organic content, which conformed to previous studies. In general, the organic contents established for the sediments in the Lower Mgeni are very low in comparison to various studies. However, a reason attributed to this low organic content is that the region contains strong tidal flows and is an active zone (Wright, 1990; 1995), which is not susceptible to the accumulation of mud, which generally enhances the organic content with the sediment.

CHAPTER 7:
RESULTS AND DISCUSSION: HYDRODYNAMIC STUDY

This chapter presents the results of the hydrodynamic study carried out in the Mgeni Estuary from January 2008 to July 2008. The displayed results include the estuary channel discharge, suspended sediment flux and statistical results of the estuary bed sediment. This is followed by a complete discussion of the results, in order to establish tidal variations within a sampling day, spring-neap tide variations, as well as seasonal variations.

7.1. Tide Information and Sampling Times

The tide information for the entire hydrodynamic sampling period is supplied by the South African Navy Hydrographic Office (SANHO) (2008). The tidal station for the coast of Durban is situated at the Port of Durban (SANHO, 2008). Based on the tide tables and tidal information, it is clear that the high tide elevations are higher during spring tides than neap tides. Conversely, spring tides contain lower low tides than neap tides. The tides close to spring tides also contain higher high tides than during neap tides.

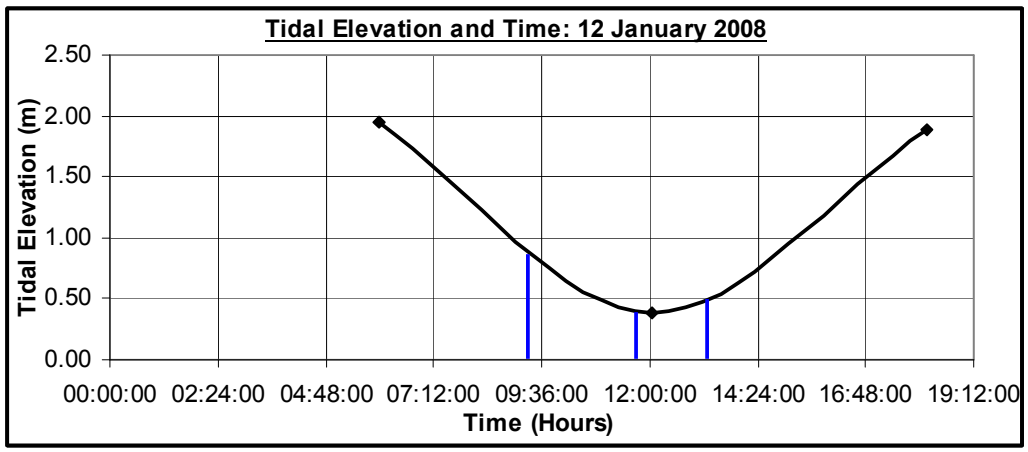

Figure 7.1. The tidal height and times plotted from tidal information (SANHO, 2008), intersected with the sampling times for 12 January 2008.

Figure 7.1 shown above, graphically illustrates the sampling and tide times for 12 January 2008 (SANHO, 2008). The tidal curve in black represents the tidal height and time, whilst the intersecting blue vertical lines indicate the times at which the estuary cross-section was sampled. In terms of the monthly tidal cycle, sampling on 12 January 2008 occurred four days after a spring tide. From Figure 7.1, Profile 1 was sampled during the ebb tide, on the falling limb to peak low

tide, Profile 2 took place on the ebb tide, during the peak low tide and Profile 3 took place on the rising limb to peak high tide, thus on the flood tide. This was carried for the complete sampling period, in order to establish the tidal phase during which the cross-section was sampled. Table 7.1 illustrated below, indicates the sampling times and tide information for the complete sampling period.

Table 7.1. Tidal details for each sampled cross-sectional profile for the complete sampling period.

Season	Date	Profile	Tide	Tidal Details
Summer	**12-Jan-08**	1	Ebb	Falling limb to peak low tide, just after mid-low tide
		2	Ebb	Peak low tide
		3	Flood	Rising limb to peak high tide, just after peak low tide
	8-Feb-08	1	Ebb	Falling limb to peak low tide, after mid-low tide
	11-Feb-08	1	Ebb	Falling limb to peak low tide, after mid-low tide
		2	Flood	Rising limb to peak high tide, just after peak low tide
		3	Flood	Rising limb to peak high tide, before mid-high tide
	16-Feb-08	1	Flood	Rising limb to peak high tide, just before mid-high tide
		2	Flood	Rising limb to peak high tide, just after mid-high tide
		3	Flood	Rising tide, just immediately close to peak high tide
		4	Ebb	Falling limb to peak low tide, before mid-low tide
		5	Ebb	Mid-low tide
		6	Ebb	Falling limb to peak low tide, after mid-low tide
	21-Feb-08	1	Ebb	Peak low tide
		2	Flood	Mid-high tide
		3	Flood	Rising limb to peak high tide, just after mid-high tide
Autumn	**12-May-08**	1	Flood	Rising tide, just immediately after peak high tide
		2	Ebb	Falling limb to peak low tide, just before mid-low tide
		3	Ebb	Falling limb to peak low tide, just after mid-low tide
		4	Ebb	Peak low tide
	20-May-08	1	Ebb	Falling limb to peak low tide, just before peak low tide
		2	Flood	Rising limb to peak high tide, just after peak low tide
		3	Flood	Rising limb to peak high tide, just before mid-high tide
		4	Flood	Rising limb to peak high tide, after mid-high tide
Winter	**26-Jun-08**	1	Flood	Rising tide, just immediately after peak high tide
		2	Ebb	Falling limb to peak low tide, just before mid-low tide
		3	Ebb	Falling limb to peak low tide, just after mid-low tide
		4	Ebb	Shortly after peak low tide
	3-Jul-08	1	Ebb	Falling limb to peak low tide, just before peak low tide
		2	Flood	Rising limb to peak high tide, after peak low tide
		3	Flood	Mid-high tide
		4	Flood	Rising limb to peak high tide, after mid-high tide

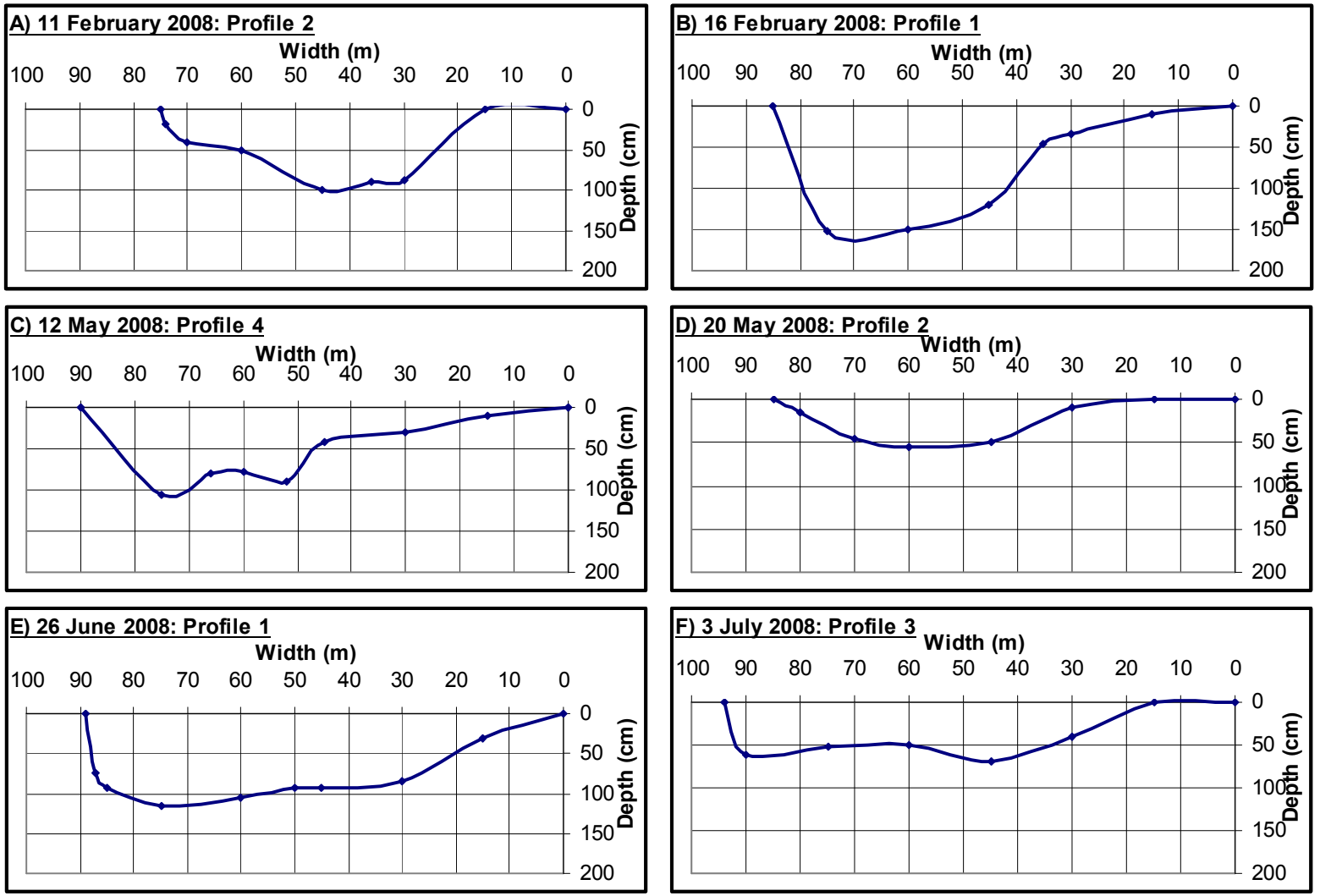

Figure 7.2. Cross-sectional profiles plotted on A) 11-Feb-08, B) 16-Feb-08, C) 12-May-08, D) 20-May-08, E) 26-June-08 and F) 3-July-08.

7.2. Channel Cross-sectional Profiles, Channel Velocity and Discharge

Within this section, the channel profiles plotted along the sampled cross-section are described in terms of width, depth and area. The channel velocity, area and discharge are also illustrated and discussed below. Several cross-sectional channel profiles were plotted and examples of these are displayed in Figure 7.2 (Page 143). The profiles illustrate variations with the tidal phases and spring and neap tides. Generally, the cross-sectional profiles become deeper as the tide rises, and shallower as the tide falls, which consequently influences the cross-sectional area.

Tables 7.2 to 7.4 below, show the cross-section (XS) area, maximum channel depth, minimum channel velocity, maximum channel velocity, average channel velocity and channel discharge for each profile plotted throughout the entire sampling period, from January 2008 to July 2008.

Table 7.2. Cross-sectional area, maximum depth, minimum, maximum and average velocity, and channel discharge for each profile plotted in summer.

Date	Profile	Tide	XS Area (m^2)	Maximum Channel Depth (m)	Minimum Velocity ($cm.s^{-1}$)	Maximum Velocity ($cm.s^{-1}$)	Average Velocity ($cm.s^{-1}$)	Channel Discharge ($m^3.s^{-1}$)
12-Jan-08	1	Ebb	12.42	130	7.13	45.57	18.18	2.99
	2	Ebb	8.98	125	33.10	69.63	54.33	5.13
	3	Flood	38.40	115	1.93	44.53	22.61	8.65
8-Feb-08	1	Ebb	38.75	110	2.97	21.67	11.02	4.48
11-Feb-08	1	Ebb	42.55	115	23.75	70.70	50.60	24.99
	2	Flood	37.82	100	21.67	47.65	29.57	11.64
	3	Flood	52.60	126	21.67	29.98	27.91	15.26
16-Feb-08	1	Flood	69.75	152	2.97	19.59	8.94	7.41
	2	Flood	76.70	230	2.97	6.09	3.83	3.20
	3	Flood	49.30	220	1.93	5.05	2.97	1.54
	4	Ebb	49.55	170	4.01	9.20	6.09	3.33
	5	Ebb	36.30	160	1.93	19.59	8.51	5.01
	6	Ebb	33.75	160	8.16	20.63	14.40	5.56
21-Feb-08	1	Ebb	30.00	125	5.05	47.65	26.35	9.50
	2	Flood	40.65	140	20.63	34.14	25.83	10.41
	3	Flood	61.50	130	12.32	37.26	20.11	13.47

In Table 7.2 above, the cross-sectional channel area varies from 8.98 m^2 to 76.70 m^2. The maximum channel depth varies from 100 m to 230 m. The velocity readings along the channel

vary from 1.93 $cm.s^{-1}$ to 70.70 $cm.s^{-1}$. Average channel velocities range from 2.97 $cm.s^{-1}$ to 54.33 $cm.s^{-1}$, whilst the channel discharges vary from 1.54 $m^3.s^{-1}$ to 24.99 $m^3.s^{-1}$.

Table 7.3. Cross-sectional area, maximum depth, minimum, maximum and average velocity, and channel discharge for each profile plotted in autumn.

Date	Profile	Tide	XS Area (m^2)	Maximum Channel Depth (m)	Minimum Velocity ($cm.s^{-1}$)	Maximum Velocity ($cm.s^{-1}$)	Average Velocity ($cm.s^{-1}$)	Channel Discharge ($m^3.s^{-1}$)
12 May 2008	1	Flood	45.45	115	1.30	6.20	4.28	1.62
	2	Ebb	50.75	120	0.70	4.60	2.04	0.93
	3	Ebb	34.85	110	0.60	29.60	9.52	4.21
	4	Ebb	39.75	105	0.00	17.50	8.48	4.37
20 May 2008	1	Ebb	26.07	87	0.40	8.30	5.80	1.68
	2	Flood	21.88	55	2.70	26.00	8.04	1.82
	3	Flood	27.75	80	0.90	18.10	6.80	1.08
	4	Flood	34.50	120	2.20	32.80	12.57	6.33

In Table 7.3 above, the channel cross-sectional area varies from 21.88 m^2 to 50.75 m^2. The maximum channel depth ranges from 55 m to 120 m. In autumn, the flow velocities along the channel range from 0.00 $cm.s^{-1}$ to 32.80 $cm.s^{-1}$. Calculated average channel velocities vary from 2.04 $cm.s^{-1}$ to 12.57 $cm.s^{-1}$, whilst the channel discharges vary from 0.93 $m^3.s^{-1}$ to 6.33 $m^3.s^{-1}$.

Table 7.4. Cross-sectional area, maximum depth, minimum, maximum and average velocity, and channel discharge for each profile plotted in winter.

Date	Profile	Tide	XS Area (m^2)	Maximum Channel Depth (m)	Minimum Velocity ($cm.s^{-1}$)	Maximum Velocity ($cm.s^{-1}$)	Average Velocity ($cm.s^{-1}$)	Channel Discharge ($m^3.s^{-1}$)
26 June 2008	1	Flood	69.46	115	0.10	9.70	3.43	2.78
	2	Ebb	51.15	103	1.70	40.10	10.66	6.51
	3	Ebb	33.75	70	1.30	11.30	5.48	1.98
	4	Ebb	28.80	63	0.70	15.80	8.26	2.52
3 July 2008	1	Ebb	48.28	105	2.40	14.90	8.14	4.07
	2	Flood	30.40	80	3.30	16.90	10.18	3.23
	3	Flood	38.93	70	0.80	9.70	4.92	1.94
	4	Flood	38.00	100	1.40	16.70	10.18	4.64

In Table 7.4 above, the channel cross-sectional area ranges from 28.80 m^2 to 69.46 m^2. The maximum channel depth ranges from 63 m to 115 m. In winter, the flow velocities along the channel range from 0.10 $cm.s^{-1}$ to 40.10 $cm.s^{-1}$. The average channel velocities vary from 3.43

$cm.s^{-1}$ to 10.66 $cm.s^{-1}$, whilst the channel discharges vary from 1.94 $m^3.s^{-1}$ to 6.51 $m^3.s^{-1}$. Generally, for each season, the channel contains a large cross-sectional area and maximum depth during the flood tide, when the wetted perimeter is large due to the incoming tide from the ocean (Dyer, 1986).

Average time-velocity plots were drawn up in order to illustrate how the average channel velocity varies as the tide rises and falls, which are illustrated in Figures 7.3.1 (Page 147) and 7.3.2 (Page 148). Average channel velocities, at the times at which the cross-section was sampled, were superimposed onto the tidal curve provided by SANHO (2008). Maximum and minimum average channel velocities were encountered at different phases of the tide. In general, maximum and minimum average channel velocities illustrate spring-neap and seasonal variations. The occurrences of maximum and minimum average channel velocities are summarized in Tables 7.5 and 7.6 below.

Table 7.5. Temporal occurrences of maximum average channel velocities.

Sampling Date	Maximum Average Velocity
12 January 2008 - 4 days after a spring tide	Profile 2 - Ebb Tide (Peak Low)
11 February 2008 - 4 days after a spring tide	Profile 1 - Ebb Tide (After Mid-Low)
16 February 2008 - 2 days after a neap tide	Profile 6 - Ebb Tide (After Mid-Low)
21 February 2008 - Spring Tide	Profile 1 - Ebb Tide (Peak Low)
12 May 2008 - Neap Tide	Profile 3 - Ebb Tide (After Mid-Low)
20 May 2008 - Spring Tide	Profile 4 - Flood Tide (After Mid-High)
26 June 2008 - Neap Tide	Profile 2 - Ebb Tide (Before Mid-Low)
3 July 2008 - Spring Tide	Profiles 2 and 4 - Flood Tide (After Peak Low and After Mid-High)

Table 7.6. Temporal occurrences of minimum average channel velocities.

Sampling Date	Minimum Average Velocity
12 January 2008 - 4 days after a spring tide	Profile 1 - Ebb Tide (After Mid-Low)
11 February 2008 - 4 days after a spring tide	Profile 3 - Flood Tide (Before Mid-High)
16 February 2008 - 2 days after a neap tide	Profile 3 - Flood Tide (Close to Peak High)
21 February 2008 - Spring Tide	Profile 3 - Flood Tide (After Mid-High)
12 May 2008 - Neap Tide	Profile 2 - Ebb Tide (Before Mid-Low)
20 May 2008 - Spring Tide	Profile 1 - Ebb Tide (Before Peak Low)
26 June 2008 - Neap Tide	Profile 1 - Flood Tide (After Peak High)
3 July 2008 - Spring Tide	Profile 3 - Flood Tide (Mid-High)

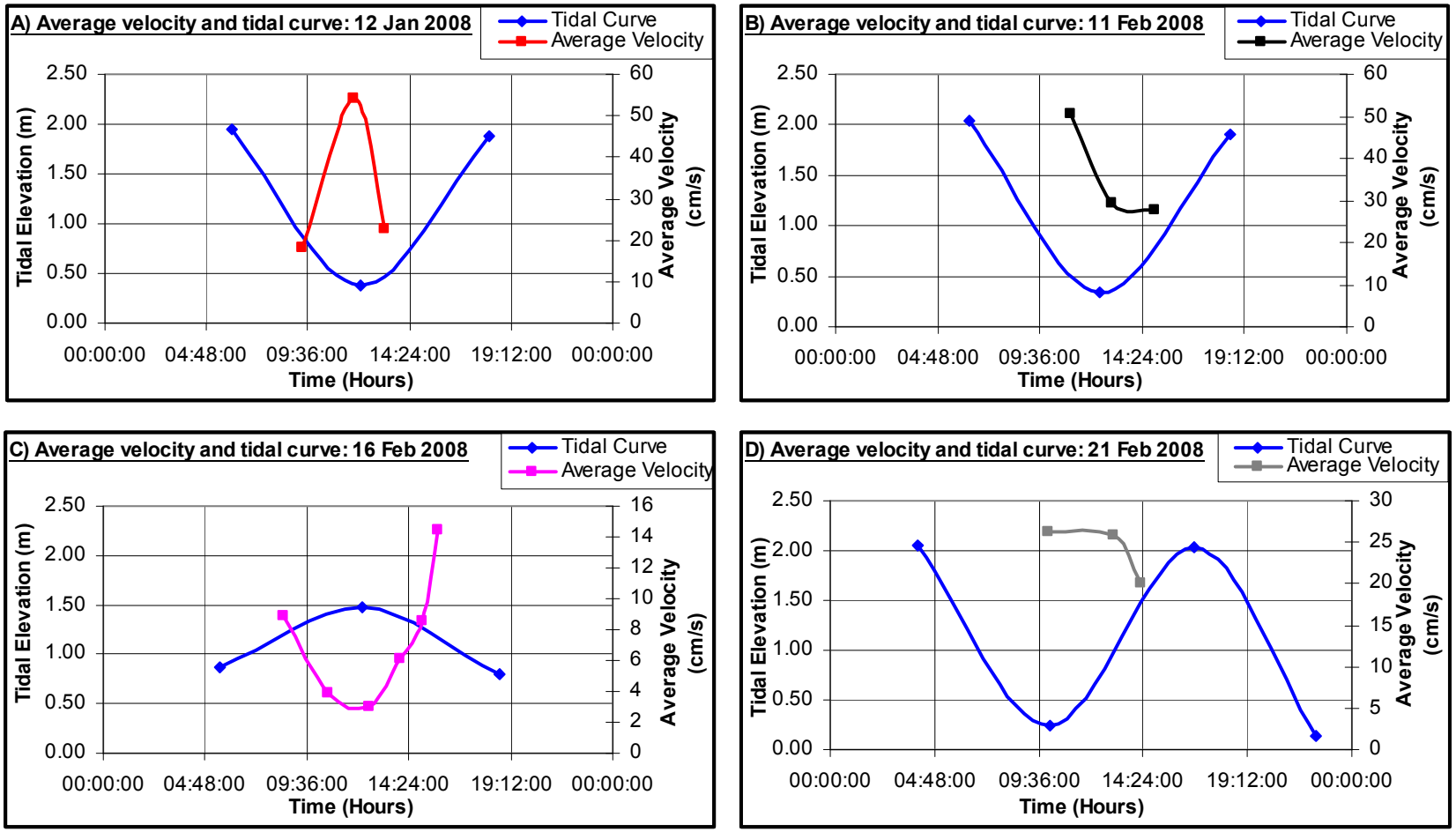

Figure 7.3.1. Average velocity-time plots for each plotted profile on each sample day A) 12 January 2008, B) 11 February 2008, C) 16 February 2008 and D) 21 February 2008.

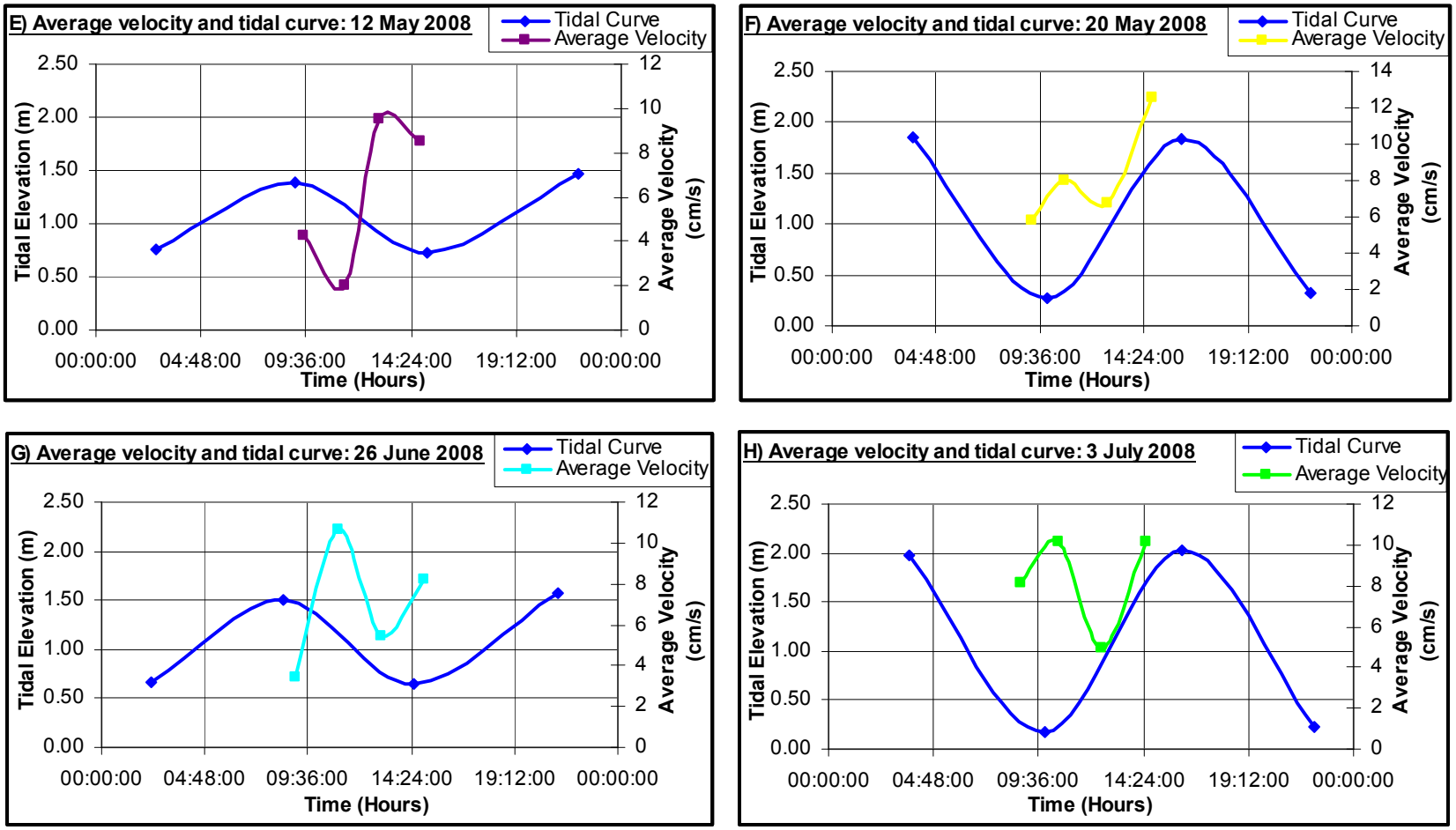

Figure 7.3.2. Average velocity-time plots for each plotted profile on each sample day E) 12 May 2008, F) 20 May 2008, G) 26 June 2008 and H) 3 July 2008.

Table 7.5 (Page 146) shows that in summer, maximum average velocities occur solely on the falling tide or the ebb tide. In autumn and winter, maximum average channel velocities occur both during the ebb and flood tide. Neap and spring tide variations only exist during autumn and winter, as maximum average channel velocities occur during the ebb tide on neap tides and during the flood tide on spring tides. During the falling tide or ebb tides, maximum average channel velocities mainly occur around mid-low tide, however, also tend to occur at peak low tide. Conversely, during the rising tide or flood tides, maximum average channel velocities mainly occur after mid-high tide.

Table 7.6 (Page 146) shows that minimum average channel velocities occur mainly during the flood tide in summer. In autumn and winter, minimum average channel velocities occur during the ebb tide and flood tide, respectively. Spring-neap variations in minimum average channel velocities are not as distinct as in the maximum average channel velocities. During the falling tide or ebb tides, minimum average channel velocities mainly occur around mid-low tide. However, during the rising tide or flood tides, minimum average channel velocities mainly occur around mid-high tide; however tend to occur around peak high tide, as well.

In terms of channel flow velocities, the highest calculated average channel velocities occur in summer and the lowest in autumn. In addition, the second highest average channel velocities are found during winter. This pattern is most probably related to the seasonal distribution of rainfall. The highest maximum average flow velocity is found during summer, more specifically on 11 February 2008, whilst the lowest minimum average flow velocity is found during the neap tide of autumn, which is illustrated in below in Table 7.7.

Table 7.7. Average velocity for the estuary channel during the sampling period.

	Average Velocity ($cm.s^{-1}$)			
Date	**Season**		**Spring/Neap**	
12-Jan-08	Summer	21.35	Four days after spring tide	31.71
11-Feb-08			Four days after a spring tide	36.02
16-Feb-08			Two days after a neap tide	7.46
21-Feb-08			Spring Tide	24.10
12-May-08	Autumn	7.19	Neap Tide	6.08
20-May-08			Spring Tide	8.30
26-Jun-08	Winter	7.66	Neap Tide	6.96
3-Jul-08			Spring Tide	8.35

Throughout the sampling period, average channel velocities were calculated for each sampling day, which is illustrated above in Table 7.7. The calculations reveal that spring tides contain

higher flow velocities than neap tides. Furthermore, sampling four days after a spring tide generated higher and stronger flows than measurements made two days after a neap tide. Therefore, measurements made as the tidal range wanes towards a neap tide display low flow velocities, as opposed to those made on a spring tide or close to a spring tide.

Throughout the sampling period, average flow velocities in the Mgeni Estuary vary from 2.04 $cm.s^{-1}$ to 54.33 $cm.s^{-1}$, measured on 12 May 2008 and 12 January 2008, respectively. However, instantaneous velocity measurements in the Mgeni Estuary vary from 1.93 $cm.s^{-1}$ to 70.70 $cm.s^{-1}$.

Figure 7.4 illustrated below, shows the channel discharge for each sampled profile for each sampling day, throughout the complete sampling period. Throughout the sampling period the channel discharges vary from 0.93 $m^3.s^{-1}$ to 24.99 $m^3.s^{-1}$, measured during the neap tide on 12 May 2008 in autumn and four days after the spring tide on 11 February 2008 in summer, respectively. It is clear that the discharge values illustrate seasonal and spring/neap variations.

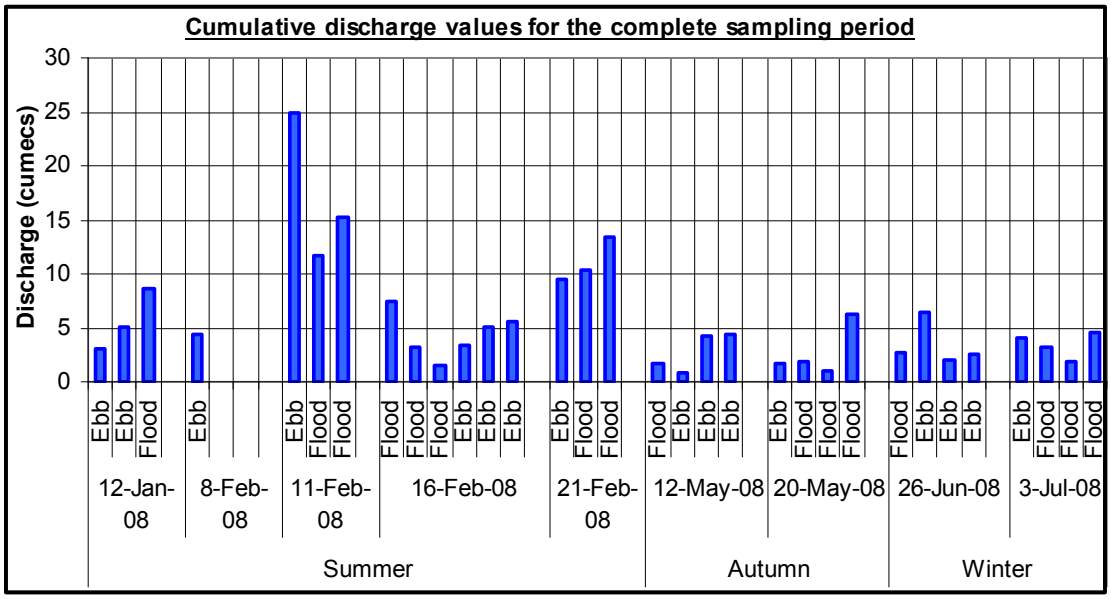

Figure 7.4. Discharge values for the Mgeni Estuary throughout the sampling period.

Seasonally, the channel discharges tend to be largest during summer, successively followed by those measured in winter and finally autumn. Average channel discharges were calculated for each season, revealing values of 8.29 $m^3.s^{-1}$, 2.76 $m^3.s^{-1}$ and 3.46 $m^3.s^{-1}$, for summer, autumn and winter, respectively. Furthermore, throughout the sampling period, channel discharges are greater during spring tides than neap tides. Average channel discharges were calculated for neap tides (including days sampled after neap tides) and spring tides (including days sampled after spring tides) for the complete sampling period. The average neap tide channel discharge equates

to 3.64 $m^3.s^{-1}$, and the average spring tide channel discharge equates to 7.30 $m^3.s^{-1}$. Apart from these variations, the channel discharge varies as the tide rises and falls, within a single tidal cycle on a sampling day. A summary of the temporal occurrence of the maximum channel discharges within each tidal cycle are illustrated below in Tables 7.8.

Table 7.8. Temporal occurrences of maximum channel discharge.

Sampling Date	Maximum Discharge
12 January 2008 - 4 days after a spring tide	Profile 3 - Flood Tide (After Peak Low)
11 February 2008 - 4 days after a spring tide	Profile 1 - Ebb Tide (After Mid-Low)
16 February 2008 - 2 days after a neap tide	Profile 1 - Flood Tide (Before Mid-High)
21 February 2008 - Spring Tide	Profile 3 - Flood Tide (After Mid-High)
12 May 2008 - Neap Tide	Profile 4 - Ebb Tide (Peak Low)
20 May 2008 - Spring Tide	Profile 4 - Flood Tide (After Mid-High)
26 June 2008 - Neap Tide	Profile 2 - Ebb Tide (Before Mid-Low)
3 July 2008 - Spring Tide	Profile 4 - Flood Tide (After Mid-High)

In summer, maximum channel discharges generally occur mainly during the flood tide. However, in autumn and winter, maximum channel discharges occur during both the ebb and flood tides. Spring-neap variations in terms of maximum channel discharges are only clear in autumn and winter, as the maximum channel discharges occur during the ebb tide on neap tides and during the flood tide on spring tides. On the flood tide or the rising tide, maximum channel discharges mainly occur at or around mid-high tide. However, on the ebb tide or the falling tide, maximum channel discharges mainly occur around mid-low tide and peak low tide.

7.2.1. Discussion

- ***Profiles: Channel Area and Depth***

Overall, the plotted profiles illustrate variability in shape, depth and area, as the tide rises and falls. Generally, the profiles display greatest depths within the middle section of the channel, and shallowing along the edges or margins. In most cases, as the tide rises, a parallel increase in cross-sectional area and channel depth is evident, with the opposite taking place as the tide falls on the ebb. This occurs as a result of the large elevated flood tide that enters the estuary from the ocean, which increases the overall water levels in the estuary. However, as the tide falls, especially at peak low tide, the ebb tide drains the back region of the estuary at low levels, which causes the water levels to drop, as well as the cross-sectional area. The cross-sectional channel area tends to be at a minimum during peak low tide on a spring tide, as opposed to neap tides,

due to the large tidal range. In terms of channel depth, the Mgeni Estuary contained a maximum depth (230 cm) in summer and a minimum depth (55 cm) in autumn.

- ***Cross-channel Variations in Average Flow Velocities***

Generally, the flow velocities at each sample point along the channel illustrate variability as the tide rises and falls. However, in most cases, the channel velocities are at a maximum within the middle section of the channel and at a minimum along the channel margins, most probably as a result of friction which reduces the flow velocity. In certain channel profiles, the ebb tidal velocities are higher than the flood tide velocities, with the opposite occurring for remaining profiles. The pattern in which ebb tides contain higher flow velocities than flood tides, suggests that the estuary drains at a faster rate than it floods. There are several reasons attributed to this, which will be discussed below.

- ***Seasonal, Spring-Neap Tide and Tidal Phase Variability in Flow Velocity***

With regards to the temporal occurrence of the maximum and minimum average channel velocities, there seems to be a great deal of variation throughout the entire sampling period. However, certain commonalities and patterns are evident on a seasonal basis. Throughout the sampling period, maximum average channel velocities on the ebb tide occur mainly after mid-low tide and at peak low tide, hence occur on the falling tide nearing peak low tide. Maximum average channel velocities on the flood tide occur mainly after mid-high tide, hence occur on the rising tide nearing peak high tide. Minimum average channel velocities on the flood tide occur mainly around mid-high tide and occur mainly around mid-low tide on the ebb tide. These findings conform to the theories put forward by Pethick (1984); Bird (2000); and Masselink and Hughes (2003), which state that theoretically, at the mouth of an estuary, maximum velocities occur at high water and low water, whereas zero velocities or slack conditions occur at mid-tide, when current reversal occurs (Pethick, 1984; Bird, 2000; Masselink and Hughes, 2003), and tides close to the estuary mouth inlet and the ocean tend to experience slack water closer to mid-tide than those tides further up the estuary (Redfield, 1950 in Pethick, 1984).

In summer, maximum average channel velocities occur solely during the ebb tidal phase and minimum channel velocities mainly occur during the flood tide. This pattern suggests that the estuary channel drains at a quicker pace than it floods, and according to theory, this pattern is termed ebb dominance (Pethick, 1984; Masselink and Hughes, 2003; Beck *et al*., 2004; Beck, 2005). Geyer *et al*. (2001) explain that the maximum velocity of flow in an estuary is very important as it influences and links sediment re-suspension and transport, hence ebb dominance

indicates an overall seaward transport of sediments. In addition, this agrees with the work carried out by Ridderinkhof *et al*. (2000) in the Ems-Dollard Estuary in the Netherlands, Green (2004) in Kosi Bay Estuary in KwaZulu-Natal, Ganju *et al*. (2005) in Browns Island, Suisan Bay in California, and Kitheka *et al*. (2005) in the Tana Estuary in Kenya, in which the mean velocities were greater on the ebb tide than the flood tide.

Maximum average channel flow velocities occur during the ebb tide mainly in summer, as a result of the high amount of rainfall, which in turn generates strong fluvial discharges and currents flowing out to the sea, ultimately enhancing the seaward flowing ebb tide (Ngetar, 2002). Therefore, the ebb tide is particularly enhanced in summer. However, the flood tide contains maximum flow velocities mainly during the spring tides in winter and autumn. This occurs as a result of the decrease in rainfall and fluvial discharge in autumn and winter, which causes the ebb tide to become less dominant as opposed to the flood tide, which increases in intensity and dominates the mouth of the estuary (Ngetar, 2002). Therefore, this enhanced flood tide and marine influence at the mouth during autumn and winter, displays implications for mouth closure, since more marine sediment can be consequently transported into the estuary (Cooper, 2002). This seasonal distribution of rainfall is also related to summer containing the highest average channel velocities. The enhanced marine influence at the mouth of the estuary is also linked to the second highest average channel flow velocities displayed during winter.

Throughout the sampling period, ebb tides generally contain maximum average channel flow velocities, because it constrains and constricts the flow to a small, constricted subtidal channel, travelling towards the open ocean, while draining the shallow back barrier lagoonal region of the estuary (Dyer, 1986; Bird, 2000; Green, 2004). As a result, the flow on the ebb tide is concentrated and intensified within the small channel; hence it reaches maximum flow velocities (Dyer, 1986; 1997; Green, 2004). Comparatively, throughout the sampling period, the flood tide mainly contains minimum flow velocities as a result of it travelling into the estuary from the open ocean as a large, heightened and broad tide that enters a large cross-sectional area, which causes the flow velocity to disperse over the large area and therefore decrease (Dyer, 1986; 1997; Green, 2004). Furthermore, the flood tide decreases in flow velocity because it loses energy as it flows and shoals over flood tidal deltas and sandbars in the mouth (Green, 2004).

The findings of this study illustrate that spring tides display higher average channel velocities than neap tides, which agrees fully with the theoretical concept explained by Bird (2000) and Davis and FitzGerald (2004), which states that spring tides generate stronger and faster currents than neap tides. In conformity with this concept and the findings in the Mgeni Estuary, are the findings of Wright (1990), who recorded maximum flood tidal velocities of 0.70 $m.s^{-1}$ and 0.20 $m.s^{-1}$, and

maximum ebb tide velocities of 0.40 $m.s^{-1}$ and 0.10 $m.s^{-1}$, during a spring and neap tide respectively, in the St. Lucia Estuary in KwaZulu-Natal; Green (2004), who recorded mean spring tide velocities of 31.55 $cm.s^{-1}$ and mean neap tide velocities of 19.03 $cm.s^{-1}$ in the Kosi Bay Estuary, and Kitheka *et al*. (2005) in the Tana Estuary in Kenya.

Beck (2005) found flow velocities to vary between 0.00 $cm.s^{-1}$ and 75.00 $cm.s^{-1}$ in the Goukou Estuary in the Western Cape of South Africa. In general, the velocities within the Mgeni Estuary are somewhat similar to those measured in the Goukou Estuary and St. Lucia Estuary, by Beck (2005) and Wright (1990), respectively.

- ***Seasonal, Spring-Neap Tide and Tidal Phase Variability in Discharge***

Similarly, the channel discharge values display seasonal and spring-neap tidal variations. The highest channel discharges occur in summer, as a result of the seasonal distribution of rainfall and corresponding tidal intensity and regime at the mouth of the estuary, as explained above. Similarly, Ngetar (2002); Zietsman (2004); Stretch and Zietsman (2004); Garden and Garland (2005); and Lawrie (2007), documented a link between flow rates and rainfall, which will be discussed below.

Spring tides generate higher channel discharges than neap tides, as a result of the large average channel velocities and the large tidal range experienced during spring tides (Bird, 2000; Davis and FitzGerald, 2004). Spring and neap tides generally display maximum discharges on the flood tide and ebb tide, respectively, as a result of the greater tidal range during springs than neaps. Consequently, spring tides contain higher water levels and a larger wetted perimeter or cross-sectional area during high water than neap tides, which influences the channel discharge as it is a function of channel area and velocity, which will be discussed further below.

Generally, higher channel discharges enable flushing and erosion of sediments from the estuary to the nearshore zone, resulting in channel scour (Cooper, 2002). However, higher channel discharges on the flood tide allow sediment to be transported into the estuary as well.

- ***Discharge and Average Velocity***

Channel discharge is a function of both average velocity and channel area (Gordon *et al*., 1992). Freeman and Rowntree (2005) explain that the discharge and velocity are clearly and importantly linked. Hence a correlation between these variables was sought through a scatter-plot. Figure 7.5 (Page 155) illustrates the correlation between the average channel velocity and discharge for

each sampling day. A high R^2 value of 0.6821 exists, as well as a strong, positive correlation between the two variables, conforming to Freeman and Rowntree (2005).

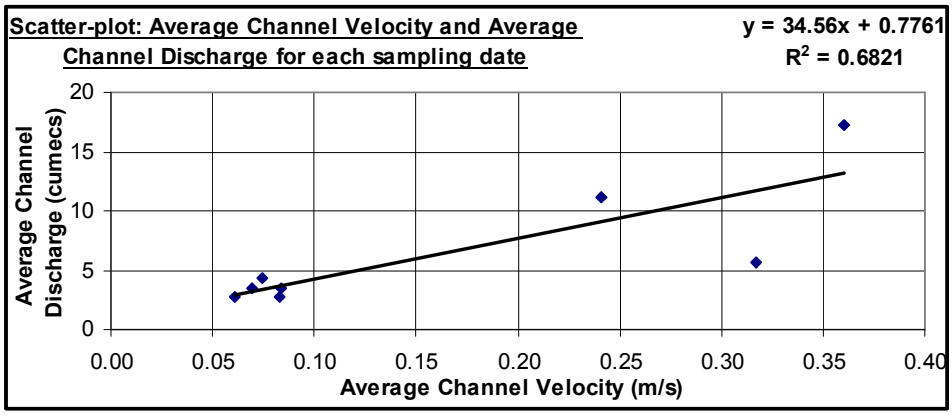

Figure 7.5. Scatter-plot of the average channel velocity and average channel discharge.

- ***Discharge and Rainfall***

As mentioned above, a correlation exists between the channel discharge and the amount of rainfall. Figure 7.6 below and Figure 7.7 (Page 156) indicate the daily rainfall and the total monthly rainfall of Durban, respectively (South African Weather Services (SAWS), 2008), which was extracted from the Virginia Station as it forms the closest station to the study area. From Figure 7.6, it is clear that high rainfall occurred in January 2008, February 2008 and April 2008. With the exception of 08 and 11 February 2008, no rainfall occurred on the actual sampling days, though significant amounts occurred prior to the sampling days.

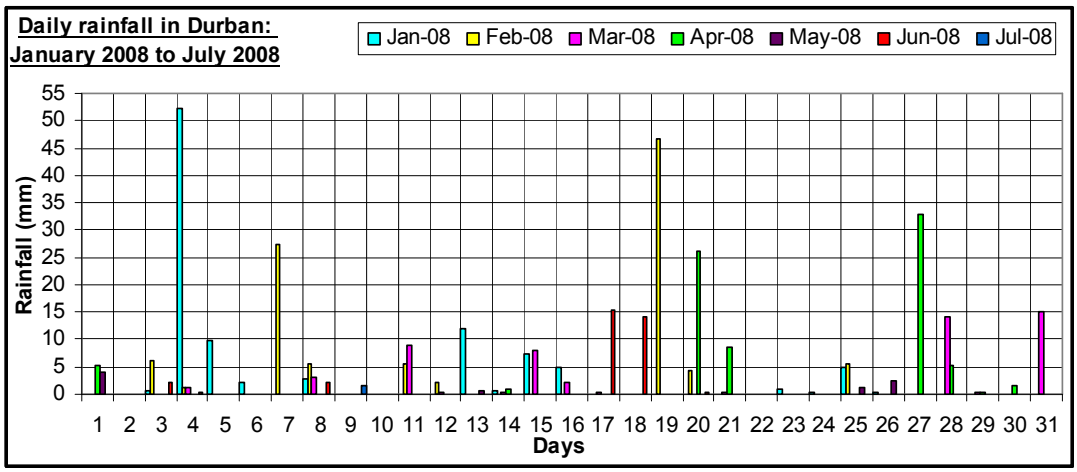

Figure 7.6. Daily rainfall in Durban from January 2008 to July 2008, Weather Station: Virginia (SAWS, 2008).

Figure 7.7 illustrated below, indicates the total monthly rainfall for the Mgeni Estuary from December 2007 to July 2008. Throughout this period, 430.40 mm of rain occurred in the region. The total monthly rainfall decreases from January 2008 to July 2008, displaying a typical seasonal distribution. The highest amounts of rainfall occur in summer, successively followed by autumn and winter. The lowest and highest amount of rainfall took place in July 2008 and February 2008, respectively, the latter of which held a total of 103.80 mm.

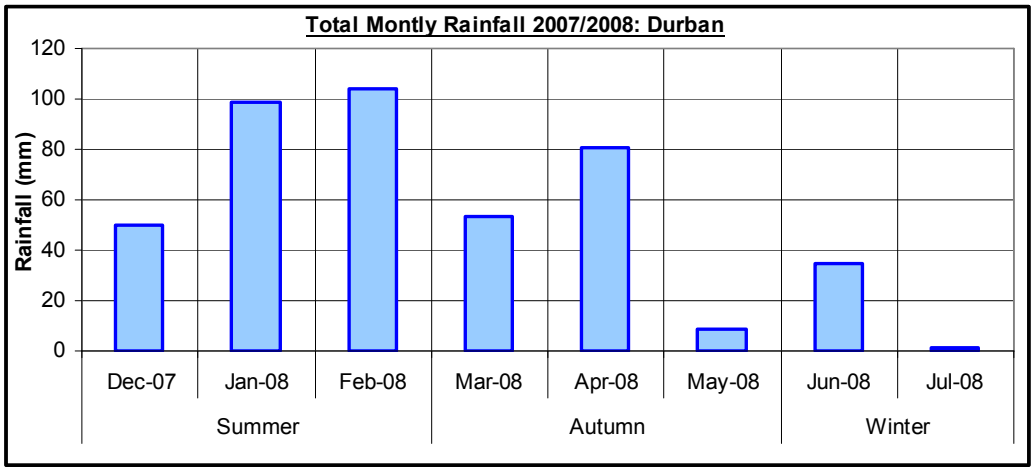

Figure 7.7. Total monthly rainfall in Durban from December 2007 to July 2008 (Weather Station: Virginia) (SAWS, 2008).

As mentioned above, rainfall influences the channel discharge, as it delivers runoff and flow to rivers and estuaries, which in turn influences the channel discharge (Ngetar, 2002). On average, the highest channel discharges, throughout the spring and neap tidal sampling period, occur in January and February 2008. Additionally, it is noticed that these months contain the highest amounts of rainfall, as well. As mentioned above, despite July 2008 containing the lowest monthly rainfall, it does not contain the lowest channel discharge. Therefore, a scatter-plot was established in order to illustrate a link between rainfall and channel discharge.

Figure 7.8 (Page 157) is a scatter-plot of the average monthly channel discharge and the average monthly rainfall. This scatter-plot reveals a high R^2 value of 0.8496, which means that there is a strong correlation between these two variables. Therefore, this scatter-plot illustrates that channel discharge is linked to the amount of rainfall.

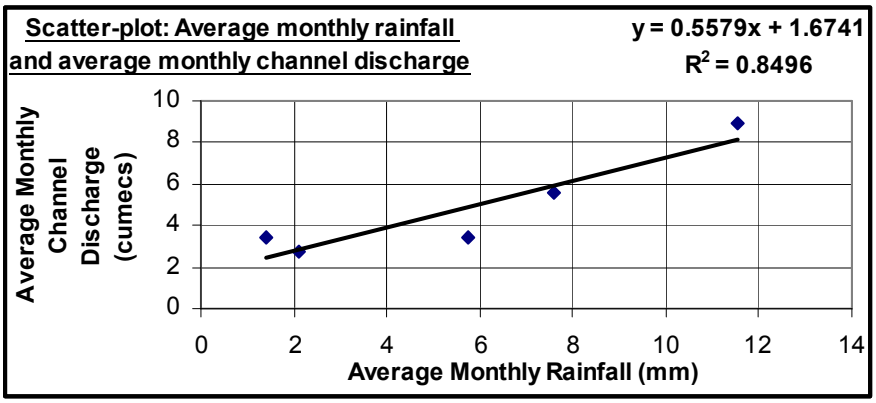

Figure 7.8. Scatter-plot of the average monthly rainfall (January, February, May, June and July 2008) and the corresponding average channel discharge.

As previously explained, the reduced fluvial input and rainfall during autumn and winter, causes the estuary to develop a larger marine influence at the mouth (Ngetar, 2002), which is parallel to the findings in the Mgeni Estuary. The velocity and discharge measurements made during the sampling period, agrees with Ngetar's (2002) concept, as during autumn and winter, the channel velocities and discharges are much greater on the flood tide than the ebb tide, especially during a spring tide. This means that more marine sediment is expected to be introduced into the system during autumn and winter. Therefore, the channel discharges of the Mgeni Estuary are influenced by rainfall, flow velocity, and the influence of tides at the mouth.

- ***Comparisons of Channel Discharge with past studies***

In terms of past research, Zietsman (2004) documented channel discharges varying from 0.20 $m^3.s^{-1}$ to 4.77 $m^3.s^{-1}$ in the Mdloti Estuary, and from 0.17 $m^3.s^{-1}$ to 8.35 $m^3.s^{-1}$ in the Mhlanga Estuary, both located in Durban. Lawrie (2007) measured channel discharges ranging between 0.30 $m^3.s^{-1}$ and 0.80 $m^3.s^{-1}$ in the Mhlanga Estuary. Barnes (1999) measured channel discharges in the Mkuze Wetland ranging from 0.30 $m^3.s^{-1}$ and 3.50 $m^3.s^{-1}$. McCarthy *et al*. (1991) established water discharges ranging between 17.10 $m^3.s^{-1}$ and 143.60 $m^3.s^{-1}$, throughout the fluvial channels of the Okavango Fan in Botswana. It is understood that several factors influence channel discharge, such as the mouth status of the estuary, fluvial input, height above sea level, as well as the extent of the cross-section area. The Mhlanga and Mdloti estuaries contain much lower discharge values than the Mgeni Estuary, mainly because the Mhlanga and Mdloti estuaries are classified as temporarily open and closed estuaries (TOCE) (Whitfield, 2000). This alone, explains the extent and intensity of the estuarine discharge of the Mgeni, especially in summer. Furthermore, the Mgeni Estuary contains much higher discharge values, in comparison to those measured by Barnes (1999) in the Mkuze Wetland. However, it is understood that

wetland and fluvial systems display different flow dynamics in comparison to an estuary; however this apparent difference in discharge values highlights the greatness of the channel discharges generated by the Mgeni Estuary in this study.

On a global scale, Wall *et al*. (2008) recorded a mean daily net channel discharge of 585 $m^3.s^{-1}$, in the Hudson River Estuary in New York. Conversely, Kitheka *et al*. (2005) measured discharges from 60.00 $m^3.s^{-1}$ to 730.00 $m^3.s^{-1}$ in the Tana River Estuary in Kenya. Lin and Kuo (2001) found mean annual discharges of 24.30 $m^3.s^{-1}$ and 48.6 $m^3.s^{-1}$, for two stations along the York River which flows into Chesapeake Bay. Furthermore, Geyer *et al*. (2001) recorded a maximum channel discharge of 1700 $m^3.s^{-1}$ in the Hudson River. In general, the channel discharges measured in various international estuaries are much higher than those measured in the Mgeni. Several factors are attributed to this result, such as the rainfall patterns, run-off-patterns and catchment land-use.

7.3. Suspended Sediment Concentration

Suspended sediment samples were collected at 15 m intervals along the estuary cross-section at 0.8 of the total depth, along each vertical. Extremely fine crystalline filter paper was utilised during the filtration process, in order to seize the finest suspended sediment particles. These suspended sediment particles are generally composed of fine organic matter and clay particles, as well as living planktonic organisms (Dyer, 1986). These suspended sediment concentrations measured at each vertical along the channel width, as well as the average suspended sediment concentrations for each profile are displayed below. The suspended sediment concentrations measured at each vertical along the channel width (instantaneous concentrations) vary across the channel width and between each cross-sectional profile.

Table 7.9 (Page 159) indicates the minimum and maximum instantaneous suspended sediment concentrations measured along each plotted profile for the complete sample period. Throughout the sampling period, the instantaneous suspended sediment concentrations along the cross-sectional channel vary from 6.00 mg/l to 208.00 mg/l, established on the neap tide of 12 May 2008 and the spring tide of 21 February 2008, respectively. Based on this large range in instantaneous suspended sediment concentrations, it is evident that suspended sediments are largely variable in both time and space. However, in most cases the suspended sediment concentrations are greatest within the middle of the cross-sectional profile. Based on the maximum suspended sediment concentrations along each profile, it is clear that the highest values occur during summer.

Table 7.9. Minimum and maximum instantaneous suspended sediment concentrations (SSC) along each plotted profile throughout the sampling period.

Season	Date	Tide	Profile	Minimum SSC (mg/l)	Maximum SSC (mg/l)
Summer	12-Jan-08	Ebb	1	12.00	27.18
		Ebb	2	36.50	90.23
		Flood	3	34.00	72.50
	8-Feb-08	Ebb	1	20.00	32.00
	11-Feb-08	Ebb	1	38.00	64.00
		Flood	2	34.00	38.00
		Flood	3	28.00	32.00
	16-Feb-08	Flood	1	18.00	70.00
		Flood	2	12.00	22.00
		Flood	3	20.00	30.00
		Ebb	4	20.00	34.00
		Ebb	5	12.00	30.00
	21-Feb-08	Ebb	1	72.00	202.00
		Flood	2	60.00	208.00
		Flood	3	26.00	32.00
Autumn	12-May-08	Flood	1	10.00	22.00
		Ebb	2	6.00	12.00
		Ebb	3	12.00	22.00
		Ebb	4	16.00	26.00
	20-May-08	Ebb	1	14.00	26.00
		Flood	2	16.00	36.00
		Flood	3	18.00	26.00
		Flood	4	16.00	24.00
Winter	26-Jun-08	Flood	1	18.00	36.00
		Ebb	2	8.00	16.00
		Ebb	3	16.00	24.00
		Ebb	4	16.00	26.00
	3-Jul-08	Ebb	1	16.00	22.00
		Flood	2	10.00	20.00
		Flood	3	16.00	24.00
		Flood	4	24.00	32.00

Based on the variability of the instantaneous suspended sediment concentrations, the average suspended sediment concentration was calculated for each plotted profile. These average suspended sediment concentrations are displayed in Figure 7.9 (Page 160). The average suspended sediment concentration of each profile varies from 10.40 mg/l to 137.00 mg/l, along Profile 2 plotted on the ebb tide on 12 May 2008, and Profile 1 plotted on the ebb tide on 21 February 2008, respectively. This maximum average suspended sediment concentration is an

extremely large value in comparison to the remaining measured values, which is attributed to the fact that large amounts of rainfall occurred within the study region two days prior to this sampling date, which caused high-flow conditions and increased sediment delivery to the estuary (Cooper, 2002; Kitheka *et al*., 2005).

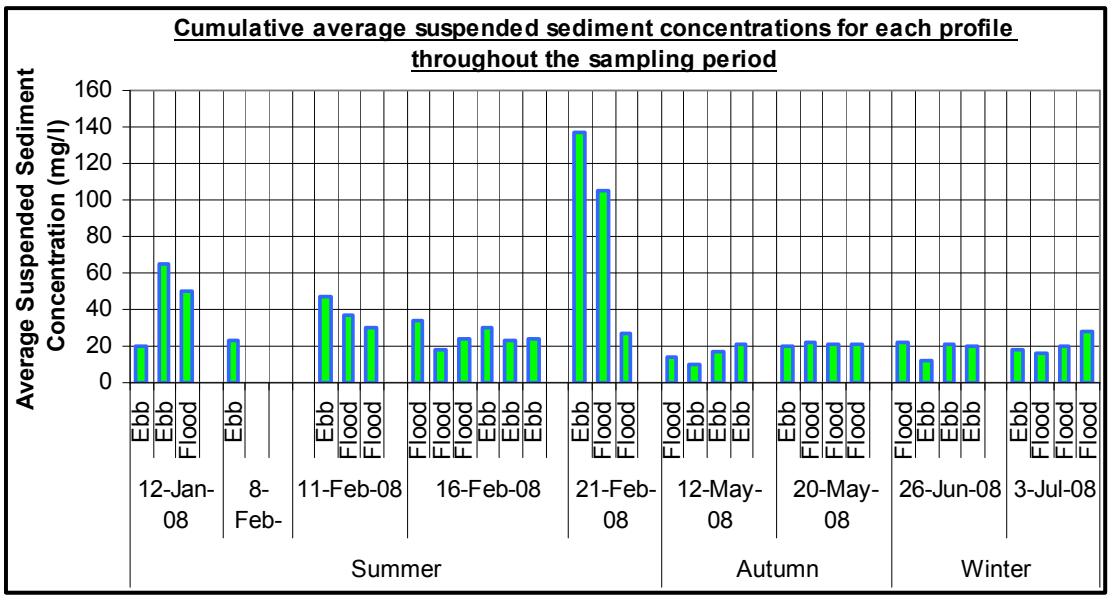

Figure 7.9. Cumulative average suspended sediment concentrations for each profile for the entire sampling period.

From Figure 7.9, it is evident that the highest average suspended sediment concentrations occur in summer, with values mainly rising above 20.00 mg/l. However, the converse is true for average suspended sediment concentrations during autumn and winter, which range below 28.00 mg/l. Therefore, this means that the average suspended sediment concentrations for each profile are higher during summer, in comparison to autumn and winter.

More specifically, average suspended sediment concentrations were calculated for each season, revealing that summer displays the highest seasonal average suspended sediment concentration, followed in descending order by winter and autumn. The average suspended sediment concentrations for summer, autumn and winter are 44.79 mg/l, 18.33 mg/l, and 19.90 mg/l, respectively. This seasonal variability in average suspended sediment concentration is influenced by the distribution of rainfall throughout the sample period.

Average suspended sediment concentrations were calculated for each tidal cycle, in order to illustrate spring-neap tide variability. Average suspended sediment concentrations for each tidal cycle illustrate that neap tides display lower suspended sediment concentrations than spring

tides. Average neap tide (including sampling two days after neap tide) suspended sediment concentrations equate to 20.73 mg/l, whilst average spring tide (including sampling four days after spring tides) suspended sediment concentrations equate to 36.43 mg/l. Hence, throughout the sampling period, spring tides generate higher suspended sediment concentrations.

Another pattern that is highlighted within Figure 7.9 (Page 160) is the variability of the average suspended sediment concentrations as the tide rises and falls within a single tidal cycle. Maximum and minimum average suspended sediment concentrations throughout single tidal cycles were established to illustrate temporal variations in terms of the phase of the tide for the complete sampling period. Tables 7.10 and 7.11 below, illustrate the temporal variations of maximum and minimum suspended sediment concentrations throughout different phases of the tide, respectively.

Table 7.10. Temporal variation of the maximum average suspended sediment concentrations throughout the sampling period.

	Maximum Average Suspended Sediment Concentration
12-Jan-08	Profile 2: Ebb Tide: Peak Low Tide
11-Feb-08	Profile 1: Ebb Tide: After Mid-Low tide
16-Feb-08	Profile 1: Flood Tide: Before Mid-High Tide
21-Feb-08	Profile 1: Ebb Tide: Peak Low Tide
12-May-08	Profile 4: Ebb Tide: Peak Low Tide
20-May-08	Profile 2: Flood Tide: After Peak Low Tide
26-Jun-08	Profile 1: Flood Tide: After Peak High Tide
3-Jul-08	Profile 4: Flood Tide: After Mid High Tide

Table 7.11. Temporal variation of the minimum average suspended sediment concentrations throughout the sampling period.

	Minimum Average Suspended Sediment Concentration
12-Jan-08	Profile 1: Ebb Tide: Subsequent to Mid-Low Tide
11-Feb-08	Profile 3: Flood Tide: Before Mid High Tide
16-Feb-08	Profile 2: Flood Tide: Subsequent to Mid High Tide
21-Feb-08	Profile 3: Flood Tide: Subsequent to Mid High Tide
12-May-08	Profile 2: Ebb Tide: Before Mid-Low Tide
20-May-08	Profile 1: Ebb Tide: Just Before Peak Low Tide
26-Jun-08	Profile 2: Ebb Tide: Before Mid-Low Tide
3-Jul-08	Profile 2: Flood Tide: Just Subsequent to Peak Low Tide

In summer, maximum average suspended sediment concentrations mainly occur along the ebb tide, whilst minimum average suspended sediment concentrations occur mainly along the flood tide. In autumn, maximum average suspended sediment concentrations occur equally on the flood tide and ebb tide, however minimum average suspended sediment concentrations occur completely on the ebb tide. In winter, maximum average suspended sediment concentrations occur completely on the flood tide, whilst minimum average suspended sediment concentrations occur equally on the flood tide and ebb tide.

In terms of tidal phases, maximum average suspended sediment concentrations on the ebb tide occur mainly at or before peak low tide, however maximum average suspended sediment concentrations on the flood tide are more variable, since they occur along the rising tide from after peak low tide to peak high tide. Minimum average suspended sediment concentrations on the ebb tide occur mainly at mid-low tide, whilst minimum average suspended sediment concentrations on the flood tide occur mainly around mid-high tide. Spring-neap variations are mainly clear in autumn and winter, with maximum average suspended sediment concentrations occurring on the flood tide during spring tides.

7.3.1. Discussion

In general, suspended sediment concentrations throughout the sampling period are highly variable and influenced by several factors, with seasonal variability of rainfall being a major factor. As mentioned above, the maximum average suspended sediment concentration was found on a spring tide and during a high-flow event on 21 February 2008, owed to large amounts of rainfall. According to theory, a high flow velocity, seasonal flooding event such as this generally enables channel scouring and flushing of sediments, especially large sediment sizes, out of the estuary into the nearshore zone (Cooper, 2002; Ngetar, 2002), hence maximum suspended sediment concentrations occur on this day. Therefore, the lowest average suspended sediment concentration is found during autumn, as a result of the reduced amounts of rainfall during this season, which is illustrated in Figures 7.6 (Page 155) and 7.7 (Page 156). Therefore, rainfall plays an important role in yielding suspended sediment concentrations. The correlation between rainfall and suspended sediment concentrations will be discussed further below.

- ***Suspended Sediment Concentrations and Rainfall***

Seasonally, the average suspended sediment concentrations are highest in summer, followed successively by winter and autumn. In order to illustrate the influence that seasonal variation of rainfall exerts onto the suspended sediment concentration, the average and total monthly rainfall

were plotted against the average monthly suspended sediment concentrations in a scatter-plot. In Figure 7.10 below, the average monthly rainfall and suspended sediment concentration are plotted against each other, which reveal a R^2 value of 0.6906. When the total monthly rainfall and the average suspended sediment concentration are plotted against each other, a R^2 value of 0.916 is derived. Therefore, a strong, linear correlation is evident in both cases.

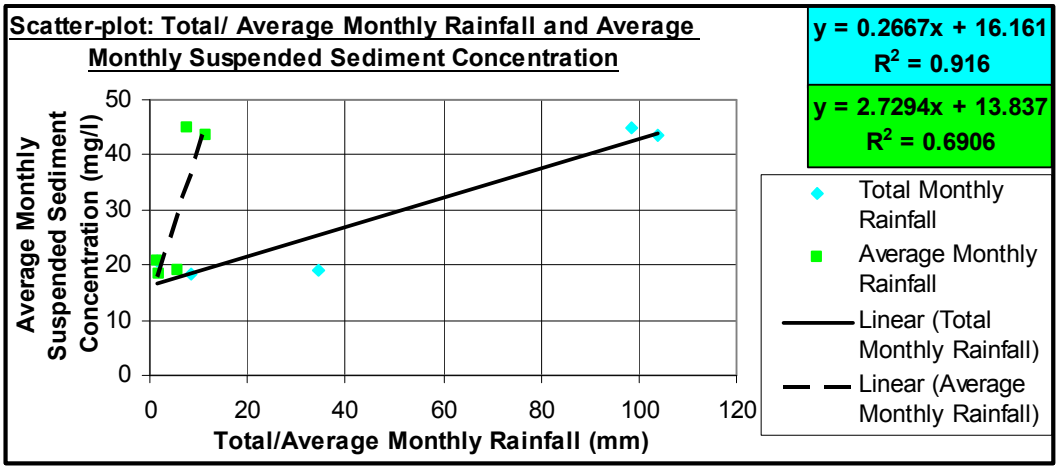

Figure 7.10. Scatter-plot for average and total monthly rainfall against average monthly suspended sediment concentrations throughout the sampling period.

This means that rainfall influences the suspended sediment concentrations, in which increased rainfall results in increased estuarine suspended sediment concentrations. Rainfall drains the catchment and the surrounding regions, and thus increases the runoff and the amount of sediment delivered to the estuary, which ultimately influences the suspended sediment concentrations within the estuary, parallel to the findings of Kitheka *et al*. (2005). However, during the dry months, the sediment within the catchment is not available for transport to the estuary due to less rainfall, which results in lower suspended sediment concentrations (Kitheka *et al*., 2005). Therefore, due to large amounts of rainfall and run-off during summer, the suspended sediment concentrations are consequently high, however as the rainfall wanes towards autumn, the suspended sediment concentrations consequently decrease. Similarly, worked carried out by Chen *et al*. (2006) in the Changjiang Estuary in China, and Wall *et al*. (2008) in the Hudson River Estuary in New York agrees with the findings of this research in the Mgeni Estuary, regarding this seasonal distribution of suspended sediment concentrations, peaking in the wet seasons and falling in the dry seasons.

However, the second highest average suspended sediment concentration occurs in winter, because as the rainfall wanes towards winter, the marine influence at the mouth of the estuary

becomes more evident and strong (Ngetar, 2002; Chen *et al*., 2006), which causes more sediment re-suspension by waves and increased suspended sediment concentrations (Kitheka *et al*., 2005; Theron, 2007), as is evident by the seasonal distribution of suspended sediment in the Mgeni. Therefore, despite the low rainfall in winter, higher concentrations of suspended sediment occur because the estuary mouth experiences stronger marine conditions.

- ***Tidal Phase Variations in Suspended Sediment Concentrations***

Maximum average suspended sediment concentrations mainly occur during ebb tides in summer, equally along flood and ebb tides in autumn and along the flood tides in winter. In summer, the ebb tide dominates maximum suspended sediment concentrations, as a result of the increased and strong fluvial discharge, which consequently decreases the intensity and velocity of the flood tide (Ngetar, 2002), which agrees with the findings of Wall *et al*. (2008) in the Hudson River Estuary. Additionally, during the ebb tide, the estuary drains the back barrier region, and the flow is constricted and concentrated in a small channel (Dyer, 1986; 1997; Green, 2004), which in turn concentrates the suspended sediments yielding a high suspended sediment concentration. Similarly, Wall *et al*. (2008) found higher suspended sediment concentrations on the ebb tide in the Hudson River Estuary.

However, in autumn and winter, maximum suspended sediment concentrations occur on the flood tide, as a result of Ngetar's (2002) and Chen *et al*. (2006) abovementioned concept regarding an increase in marine influence and a stronger flood tide in dry months, when the fluvial discharges are decreased. Flood tides also contain maximum suspended sediment concentrations, as a result of turbulence and mixing generated by wave action at the mouth of the estuary (Kitheka *et al*., 2005; Theron, 2007), especially during spring tides, which agrees with the findings of Chen *et al*. (2006). Therefore, the Mgeni Estuary contains maximum average suspended sediment concentrations mainly on the ebb tide during summer, due to high rainfall, discharges and sediment delivery. The converse is true for autumn and winter, where minimum suspended sediment concentrations occur on the ebb tide, since the flood tide overpowers the ebb tide due to decreased rainfall (Ngetar, 2002, Chen *et al*., 2006).

- ***Spring-Neap Variations in Suspended Sediment Concentrations***

Throughout the sampling period, it is evident that spring and neap tide variations exist in the average suspended sediment concentrations. In the Mgeni Estuary, spring tides generate higher suspended sediment concentrations than neap tides, and this finding is consistent with that of Hossain *et al*. (2004) in Richmond River Estuary in the Australia; Kitheka *et al*. (2005); Chen *et al*.

(2006); Wall *et al*. (2008). The main reason attributed to this is the larger tidal range established during spring tides than neap tides (Hossain *et al*., 2004; Kitheka *et al*., 2005), especially at high water, when the incoming flood tides and waves cause turbulence and increased bed sediment re-suspension (Kitheka *et al*., 2005; Theron, 2007). Hence, this increases the suspended sediment concentrations in the estuary, which is also evident in winter. Therefore, in autumn and winter, spring tides contain maximum suspended sediment concentrations during strong, dominant flood tides which allow more sediment re-suspension due to increased levels in tidal elevation and waves (Kitheka *et al*., 2005; Theron, 2007).

As mentioned previously, during the sampling period, neap tides display lower average channel velocities than spring tides, which according to Dyer (1995); Cooper (2002); Hossain *et al*. (2004) and Kitheka *et al*. (2005), it indicates that the flow during neaps cannot erode and maintain large concentrations of sediment in suspension, as compared to spring tides. Therefore, according to Dyer (1995) and Kitheka *et al*. (2005), neap tides with lower flow velocities enable the deposition of the sediments in suspension. Therefore, once sediments settle on the bed due to low flow velocities on the ebb tide, particularly in autumn, the following incoming flood tide then re-suspends these settled sediments and hence generates higher suspended concentrations due to higher velocities and waves, as documented by Kitheka *et al*. (2005).

- ***Suspended Sediment Concentration, Channel Discharge and Average Velocity***

Since rainfall is a major factor owing to this seasonal variability in suspended sediment concentrations, it is important to make a link to the fluvial discharges. In view of the fact that the Mgeni Estuary contains the highest discharges in summer and the lowest in autumn, similar to the seasonal pattern in average suspended sediment concentrations, it is clear that these variables are correlated. In order to illustrate the correlation between the channel discharges and suspended sediment concentrations, a scatter-plot has been established.

Figure 7.11 (Page 166) indicates a scatter-plot illustrating the correlation between the average monthly discharge and suspended sediment concentration of the Mgeni Estuary. A high R^2 value of 0.736 indicates a strong, positive correlation. Therefore, high concentrations occur during high fluvial discharges. Conversely, low suspended sediment concentrations intersect with low discharge events, such as during winter and autumn. Kitheka *et al*. (2005), found similar discharge-suspended sediment variability in the Tana Estuary in Kenya.

Since the channel discharge is correlated to the suspended sediment concentration, it is likely that the average channel velocity is also correlated to the suspended sediment concentration, as

discharge is a function of channel area and velocity. Therefore, the link between these two variables was sought. Figure 7.12 illustrated below, indicates the correlation between the average monthly flow velocity and suspended sediment concentrations of the Mgeni Estuary measured for the entire sampling period. A high R^2 value of 0.8351 exists between these variables, indicating a strong correlation. Therefore, the faster the flow of the estuary is, the more capable it is of re-suspending and eroding the bed sediment and hence generating high suspended sediment concentrations (Dyer, 1995; Cooper, 2002; Kitheka *et al*., 2005).

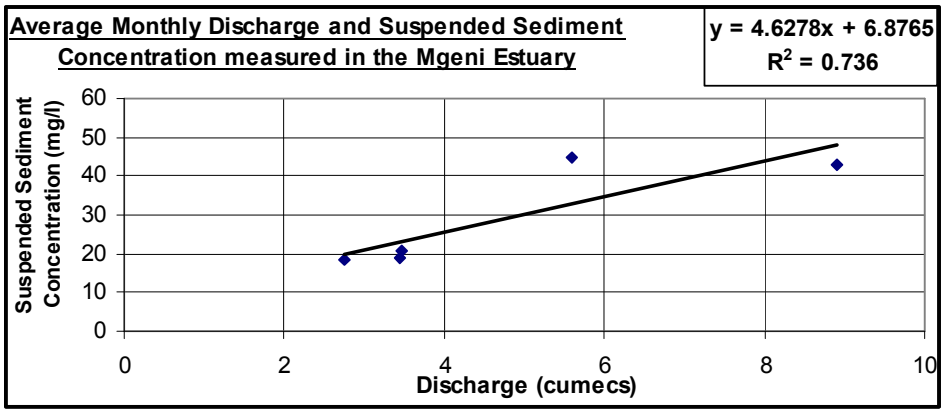

Figure 7.11. A scatter-plot illustrating the correlation between the average monthly discharge and suspended sediment concentrations for the entire sampling period.

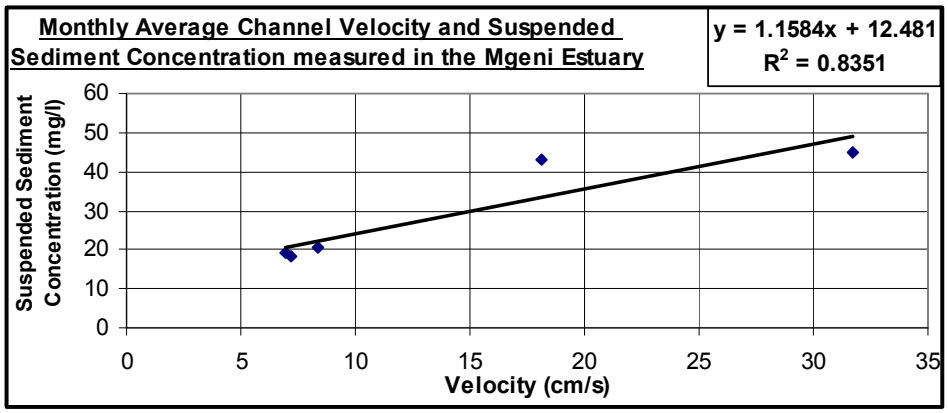

Figure 7.12. A scatter-plot illustrating the correlation between the monthly average flow velocity and suspended sediment concentrations for the entire sampling period.

- ***Comparisons of suspended sediment concentrations to past research***

Comparatively, Dyer *et al*. (2000) established suspended sediment concentrations ranging between 0.00 g/l and 1.00 g/l in the Dollard Estuary in the Netherlands. Similarly, Ridderinkhof *et*

al. (2000) recorded suspended sediment concentrations ranging between 0.20 g/l and 0.60 g/l in the Ems-Dollard Estuary in the Netherlands. Kitheka *et al*. (2005) found suspended sediment concentrations ranging from 0.53 g/l to 1.93 g/l in the Tana Estuary in Kenya. Furthermore, Lindsay *et al*. (1996) found maximum suspended sediment concentrations of 6.00 g/l in the Mfolozi Estuary and < 0.40 g/l in the St. Lucia Estuary, both situated in Northern KwaZulu-Natal. Hossain *et al*. (2004) carried out a study in the Richmond River Estuary in Australia, and found suspended sediment concentrations ranging between 3.14 mg/l and 19.04 mg/l during spring tides, and 1.66 mg/l and 20.51 mg/l during neap tides. Comparatively, Ganju and Schoellhamer (2006) performed a study in the Carquinez Strait in California and measured suspended sediment concentrations varying between 65.00 mg/l and 187.00 mg/l.

Therefore, based on the average suspended sediment concentrations of each plotted profile in the Mgeni Estuary in 2008, some of these concentrations measured in other estuaries across the world are comparatively much higher. The concentrations measured by Lindsay *et al.* (1996), in the St. Lucia and Mfolozi Estuaries, as well as those measured by Dyer *et al*. (2000); Ridderinkhof *et al*. (2000) and Kitheka *et al*. (2005) in various other estuaries are much higher than those measured in the Mgeni. A reason for this is that these estuaries may contain several land use practices that alter the sediment budgets of the estuaries, which is explained in Chapter Four.

In addition, suspended solid concentration data were acquired from Umgeni Water (2008), a water utility company in Pietermaritzburg. This data were used to establish comparisons between the measured suspended sediment concentrations at the mouth of the Mgeni Estuary. The data obtained from Umgeni Water (2008) included monthly suspended solid concentrations recorded at the Inanda Dam Weir, Athlone Bridge and the Ellis Brown Viaduct (M4 Bridge). From this data, the mean annual suspended solid concentrations were calculated for different time periods. The mean annual suspended solid concentrations recorded at the Inanda Dam Weir for the period of 1990 to 2008, range from 5.30 mg/l to 22.38 mg/l.

Furthermore, the mean annual suspended solid concentrations recorded at the Athlone Bridge and the Ellis Brown Viaduct (M4 Bridge), for the period of 1990 to 1998, are displayed in Figure 7.13 (Page 168). The mean annual suspended solid concentrations measured at the Athlone Bridge range from 34.03 mg/l to 75.49 mg/l. The mean annual suspended solid concentrations recorded at the Ellis Brown Viaduct range from 37.44 mg/l to 75.95 mg/l.

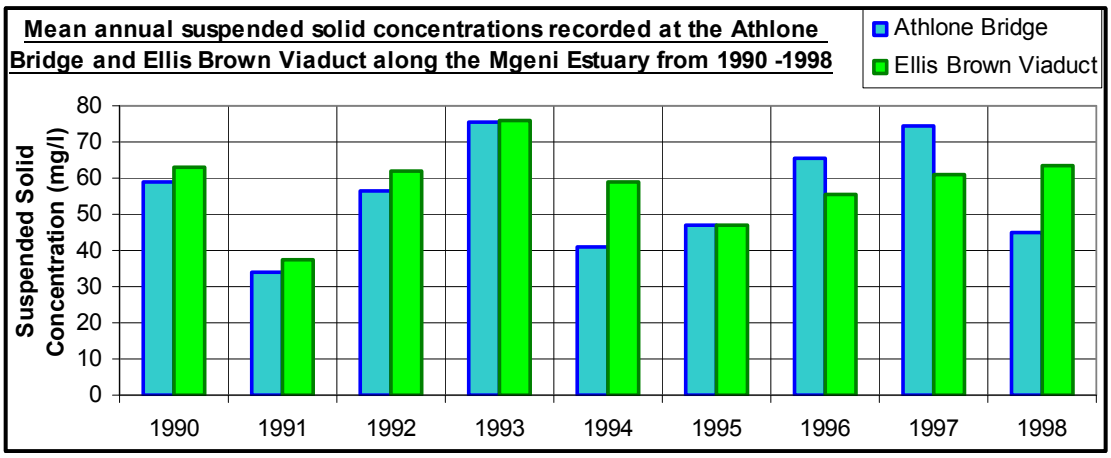

Figure 7.13. Mean annual suspended solid concentrations measured at the Inanda Dam Weir (Data acquired from Umgeni Water: 2008).

Considering that the calculated average suspended sediment concentrations measured at the mouth of the estuary throughout the sampling period vary from 10.40 mg/l to 137.00 mg/l, it is concluded that the concentrations measured at the Inanda Dam Weir, Athlone Bridge and Ellis Brown Viaduct are on average and in general somewhat lower than that recorded at the estuary mouth. From Figure 7.13 it is clear that the mean annual suspended solid concentrations are higher at the Ellis Brown Viaduct than at the Athlone Bridge. This possibly occurs as a result of the proximity of the Ellis Brown Viaduct to the mouth or tidal inlet, where waves and tides enable turbulence and re-suspension of channel bottom sediments (Ngetar, 2002; Kitheka *et al*., 2005; Theron, 2007). The region around the Athlone Bridge on the other hand, is much further away from the inlet of the estuary, which means that the tidal effects are dampened as they travel further landwards. This reason concerning proximity to the inlet corresponds to the low suspended concentrations along the Ellis Brown Viaduct in comparison to the concentrations measured throughout this study in 2008, in which the sampled cross-section was positioned closer to the inlet.

7.4. Suspended Sediment Flux

The suspended sediment flux of each cross-sectional profile was calculated by establishing the product of the cross-sectional channel area, average channel velocity and average channel suspended sediment concentration. Calculated cross-sectional suspended sediment fluxes for each profile throughout the sampling period are displayed in Figure 7.14 (Page 169). Figure 7.14 shows that the cross-sectional suspended sediment fluxes for the complete sampling period vary from 10.77 g/s to 1102.36 g/s, measured on the ebb tide (Profile 2) on 12 May 2008 in autumn, and on the flood tide (Profile 2) on 21 February 2008 in summer, respectively. It is clear that the

cross-sectional suspended sediment fluxes illustrate variability in seasons, spring and neap tides, as well as within each single tidal cycle and tidal phases throughout the sampling period.

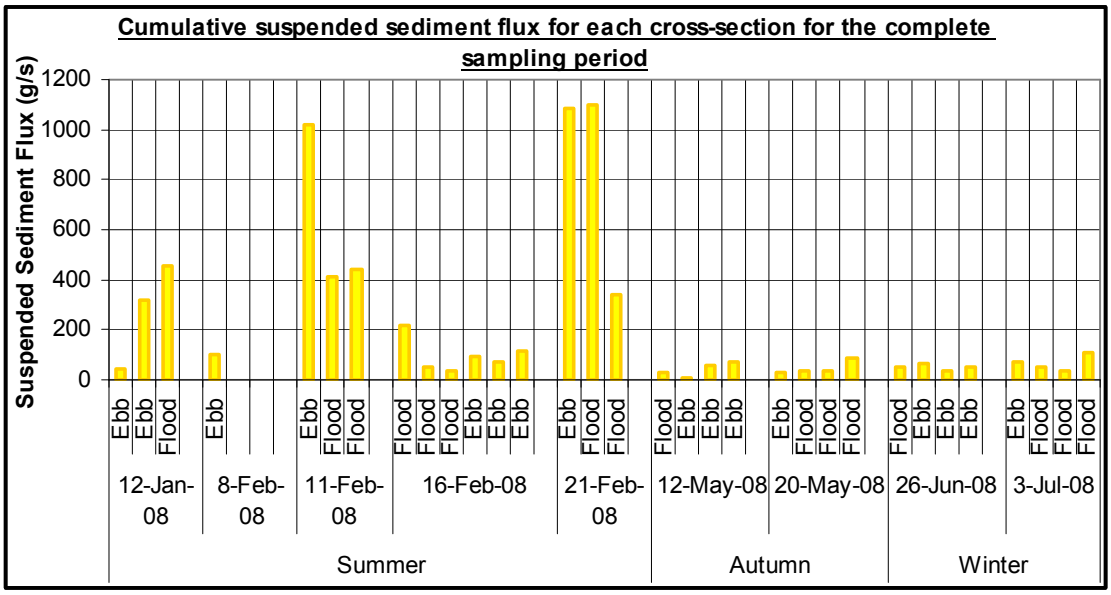

Figure 7.14. Cumulative suspended sediment fluxes calculated for each cross-section plotted throughout the sampling period.

An average cross-sectional suspended sediment flux was calculated for each season, which illustrates that summer displays the highest cross-sectional suspended sediment fluxes, followed in descending order by winter and autumn. Calculated seasonal average cross-sectional suspended sediment fluxes are 368.59 g/s, 45.62 g/s and 59.56 g/s, for summer, autumn and winter, respectively. Therefore, on average, the highest cross-sectional suspended sediment fluxes are generated in summer, whilst the lowest cross-sectional suspended sediment fluxes are generated in autumn. The average fluxes generated during winter are somewhat higher than those generated in autumn.

Additionally, average cross-sectional suspended sediment fluxes were calculated for neap tides and spring tides throughout the sampling period. Neap tides and spring tides display an average suspended sediment flux of 68.37 g/s and 321.21 g/s, respectively. Therefore, neap tides generate lower average cross-sectional suspended sediment fluxes than spring tides.

The cross-sectional suspended sediment fluxes vary within each tidal cycle, as the tide rises and falls. The cross-sectional suspended sediment fluxes for each profile were plotted together with the tidal curves (SANHO, 2008); in order to illustrate how the flux varies as the tide fluctuates. These time-flux and tidal curve graphs are displayed in Figures 7.15.1 (Page 171) and 7.15.2

(Page 172) for the complete sampling period, except for 8 February 2008, since only a single cross-section was sampled due to rainfall. In general, the cross-sectional fluxes display variability as the tide rises and falls within a single tidal cycle.

However, generally the cross-sectional suspended sediment fluxes tend to increase as the tide rises on the rising tide. Only in certain cases, does the cross-sectional suspended sediment flux decrease as the tide rises, such as during 16 February 2008 and 21 February 2008. As previously mentioned, the estuary experienced high-flow conditions during 21 February 2008 due to large amounts of rainfall, which most probably attributes to this pattern. On this day, as the tidal elevation increases towards high water and marine flow travels through the tidal inlet into the estuary, the suspended sediment concentrations began to drop, as a result of mixing of the sediment-laden fluvial flow with the marine flood tide, causing the suspended sediments to disperse over a larger area and ultimately reducing its concentration, as the tide rises.

In winter, the cross-sectional suspended sediment fluxes generally decrease as the tide falls on the falling tide. However, in summer and early autumn, the suspended sediment fluxes tend to increase as the tide falls on the ebb. This is most probably related to the seasonal distribution of rainfall, which ultimately influences the intensity of the ebb and flood tides.

In addition, maximum cross-sectional suspended sediment fluxes were highlighted in order to illustrate positioning along the tidal cycle and phase. Table 7.12 illustrated below, indicates the maximum cross-sectional suspended sediment fluxes and the tidal phases it intersects with for the complete sampling period. Generally maximum cross-sectional suspended sediment fluxes occur during the flood tide on spring tides, and mainly occur during the ebb tide on neap tides, particularly in autumn and winter.

Table 7.12. Maximum cross-sectional suspended sediment fluxes.

Date	Neap or Spring Tide	Maximum Flux	Classification
12-Jan-08	Four days after a spring tide	Flood Tide	Sediment Ingress
11-Feb-08	Four days after a spring tide	Ebb Tide	Sediment Output
16-Feb-08	Two days after a neap tide	Flood Tide	Sediment Ingress
21-Feb-08	Spring Tide	Flood Tide	Sediment Ingress
12-May-08	Neap Tide	Ebb Tide	Sediment Output
20-May-08	Spring Tide	Flood Tide	Sediment Ingress
26-Jun-08	Neap Tide	Ebb Tide	Sediment Output
3-Jul-08	Spring Tide	Flood Tide	Sediment Ingress

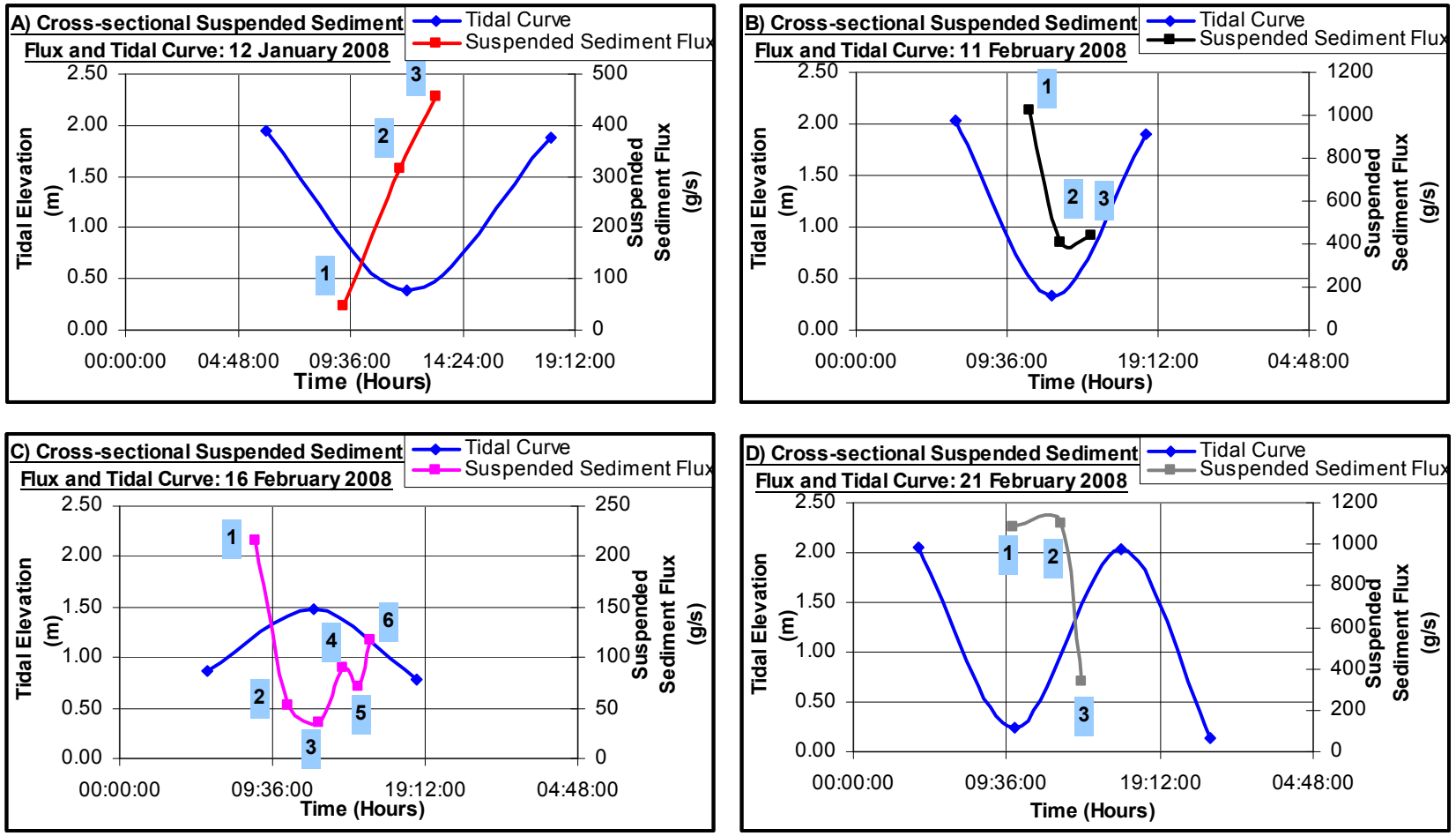

Figure 7.15.1. Tidal Curve and Suspended Sediment Flux for each sampled Cross-sectional Profile on A) 12 January 2008, B) 11 February 2008, C) 16 February 2008, and D) 21 February 2008.

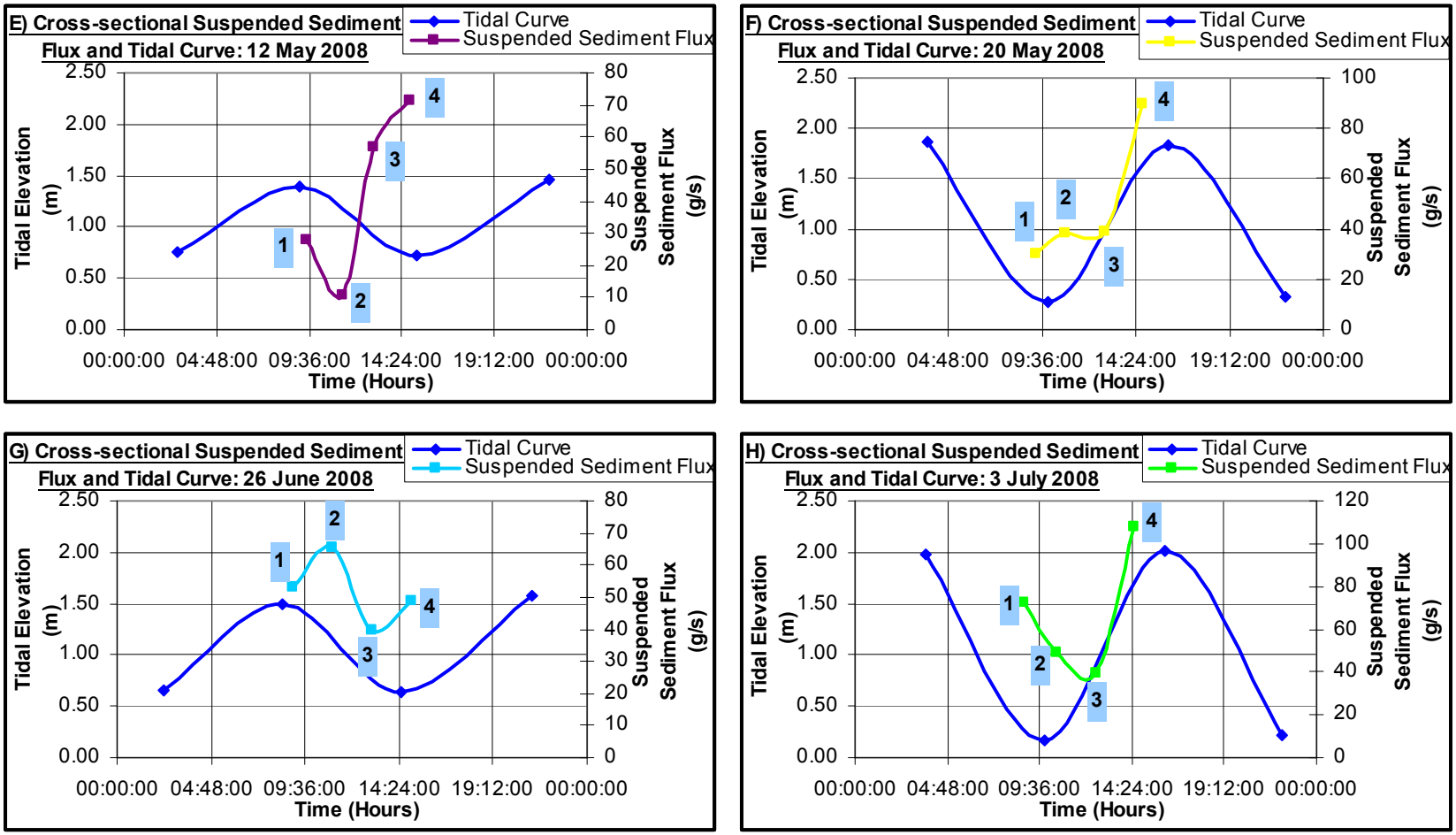

Figure 7.15.2. Tidal Curve and Suspended Sediment Flux for each sampled Cross-sectional Profile on E) 12 May 2008, F) 20 May 2008, G) 26 June 2008, and H) 3 July 2008.

Table 7.12 (Page 170) indicates the maximum cross-sectional suspended sediment fluxes throughout the sampling period. On 12 January 2008, 16 February 2008, 21 February 2008, 20 May 2008 and 3 July 2008, it is clear that the maximum cross-sectional suspended sediment fluxes intersect with the flood tide. Therefore, more suspended sediment is transported through the sampled cross-section into the estuary, in a landward direction. Conversely, on 11 February 2008, 12 May 2008, and 26 June 2008, maximum cross-sectional suspended sediment fluxes occur on the ebb tide, which means that more suspended sediment is transported through the cross-section out of the estuary, in a seaward direction. Therefore, maximum cross-sectional suspended sediment fluxes occur on the flood tide mainly during spring tides, whilst on the ebb tide during neap tides particularly in autumn and winter.

7.4.1. Discussion

- ***Correlation between Suspended Sediment Flux, Velocity, Suspended Sediment Concentration and Discharge***

It has been established that the average channel discharge and average channel velocity; average monthly channel discharge and average monthly suspended sediment concentrations; and average monthly channel velocity and average monthly suspended sediment concentrations are positively correlated to each other. Therefore, since the suspended sediment flux is a function of channel area and channel velocity (ultimately a function of channel discharge) and suspended sediment concentration, it is understandable that these variables are correlated. Therefore, based on these aforementioned correlations, it is likely that higher channel cross-sectional areas, velocities and suspended sediment concentrations increase the cross-sectional suspended sediment fluxes. Similarly, Geyer *et al*. (2001) found that as the suspended sediment concentrations and flow velocities increase, there is a subsequent increase in the sediment flux, which agrees with the findings of this research. In order to illustrate this, a scatter-plot was generated in order to establish a correlation between channel discharge and suspended sediment flux.

Figure 7.16 (Page 174) indicates the correlation between the average monthly channel discharge and suspended sediment flux. A high R^2 value of 0.9464 exists between the two variables, indicating a strong correlation. Since discharge is a function of velocity and cross-sectional area, the suspended sediment flux is therefore linked to these variables as well. Therefore, when the cross-section is relatively large and the velocity is high, the generated suspended sediment flux will be influenced.

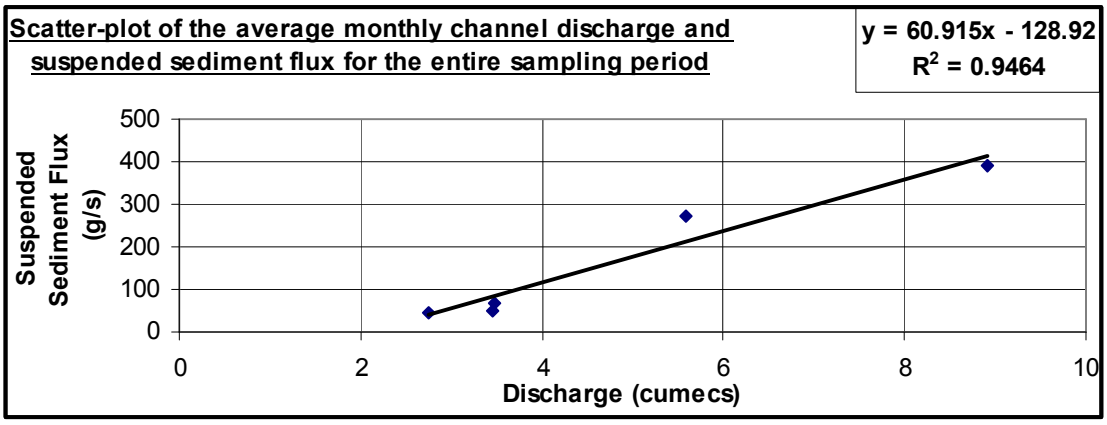

Figure 7.16. A scatter-plot showing the correlation between the discharge and the suspended sediment flux.

- ***Seasonal Variations in Suspended Sediment Flux***

It is clear from Figure 7.14 (Page 169), that the suspended sediment fluxes for each profile are highest during summer. The average suspended sediment flux calculated for each season reveals that summer displays the highest fluxes, followed by winter and autumn. This seasonal variation in fluxes is linked to the seasonal distribution of rainfall and discharge. It has been established that the average monthly channel discharge and the average monthly rainfall are correlated, as well as the average monthly suspended sediment concentration and the average monthly rainfall. Therefore, it is understandable that rainfall is correlated to the suspended sediment flux. Therefore, since more sediment is available during the wet seasons, the suspended sediment concentrations and hence fluxes are increased, with the opposite occurring during the dry seasons (Kitheka *et al*., 2005). However, as mentioned previously, the flood tide becomes more dominant in winter due to a reduced fluvial discharge and ebb tide (Ngetar, 2002), which is responsible for generating slightly higher suspended sediment concentrations and fluxes during this time. Therefore, rainfall and fluvial discharge play an important role in the fluxes and transport of suspended sediment, especially in summer.

- ***Spring-Neap Variations in Suspended Sediment Flux***

On average, the calculated cross-sectional suspended sediment fluxes are much higher during spring tides than neap tides. Furthermore, maximum cross-sectional suspended sediment fluxes occur during the flood tide on spring tides, and mainly occur during the ebb tide on neap tides, particularly in autumn and winter. As mentioned previously, this occurs as a result of greater amounts of re-suspension of the bottom sediment during spring tides as compared to neap tides,

since spring tides display higher average channel velocities than neap tides, and are therefore able to erode and maintain large amounts of sediment in suspension, thereby increasing the suspended sediment concentration (Dyer, 1995; Kitheka *et al*., 2005). Therefore, estuaries are generally well mixed during spring tides, as a result of wave action that enables mixing, however are partially mixed during neap tides (Dyer, 1986; 1995). Therefore, in the Mgeni Estuary, erosion and high suspended sediment fluxes intersect with spring tides, whereas deposition and low suspended sediment fluxes intersect with neap tides.

Similarly, work carried out by Uncles *et al*. (1985) in the Tamar estuary, Dyer *et al*. (2000) in the Dollard Estuary, Geyer *et al*. (2001) in the Hudson River Estuary, and Kitheka *et al.* (2005) in the Tana Estuary, established an increase in suspended sediment flux during spring tides as a result of an increase in wave re-suspension. Therefore, the spring-neap variations in suspended sediment fluxes present in the Mgeni Estuary correspond with the findings of the abovementioned theories and works.

- ***Comparisons of Suspended Sediment Fluxes to other studies***

Based on the fieldwork and analyses performed in the Mgeni Estuary, the suspended sediment fluxes range from 10.77 g/s to 1102.36 g/s. Ganju *et al*. (2005) found suspended sediment fluxes ranging from about -60.00 g/s to 60.00 g/s in Browns Island, a tidal wetland in California. Ganju and Schoellhamer (2006) established total flux values ranging from -400.00 kg/s to 800.00 kg/s, with negative values indicating ebb transport and positive values indicating flood transport, in a tidal strait in California. Additionally, the study carried out by Kitheka *et al.* (2005) in the Tana Estuary in Kenya, concluded a total net cross-sectional flux ranging between 2.00 kg/s and 8.69 kg/s, with a general net transport of sediment out of the estuary. Kao *et al*. (2005) found the suspended sediment load to range from 1 x 10^0 g/s to 1 x 10^8 g/s in mountainous rivers in Taiwan. Beck *et al*. (2004) and Beck (2005) recorded suspended sediment fluxes that range to approximately 25.00 g/s in the Goukou Estuary, with an overall ingress of sediment into the estuary. Gardner and Kjerfve (2006), found a mean suspended sediment flux of -21.28 g/s in Winyah Bay in South Carolina.

Therefore the suspended sediment fluxes recorded in other studies within various estuaries worldwide are much higher in comparison to the suspended sediment fluxes measured in the Mgeni Estuary. This is due to the fact that estuaries are different and contain various factors that influence the concentration and flux of suspended sediment. These factors range from channel area to land use practices in the catchment (Yang *et al*., 2004), as explained in Chapter Four.

However, the suspended sediment fluxes recorded by Beck *et al*. (2004) and Beck (2005), Ganju *et al*. (2005) and, Gardner and Kjerfve (2006) are similar to those measured in the Mgeni Estuary.

- ***Maximum cross-sectional suspended sediment fluxes in terms of tidal phase***

The suspended sediment flux of each cross-section indicates the total amount of suspended sediment that moves through the sampled cross-section per second. Therefore on a flood tide, it is estimated that a mass of suspended sediment travels through the sampled cross-section towards the estuary or into the estuary. Conversely, on an ebb tide, it is estimated that a mass of suspended sediment travels through the sampled cross-section in a seaward direction, out of the estuary. Therefore, on the flood tide it is expected that there is an influx or ingress of suspended sediment, with the opposite being true for an ebb tide, displaying an export of suspended sediment into the nearshore zone. Therefore, an influx of sediment transported into the estuary through the sampled cross-section is indicative of accretion within the estuary. However, an output of sediments from the estuary into the nearshore zone indicates sediment erosion within the estuary and sediment deposition within the nearshore zone.

An output of suspended sediment from the estuary means that more sediment is available and delivered to the nearshore zone, in which it may be transported offshore, alongshore or onshore to form dunes or overwash the barrier to undergo re-distribution into the estuary. Suspended sediment load plays a very important and essential role in the functioning of estuaries and coastlines, as they are understood to accumulate at the mouths of estuaries, to form deltas, as highlighted by Hayes (1979) and Pethick (1984), in Chapter Four. For instance, the barrier extended sandbar present in the inlet of the Mgeni Estuary is considered to have formed as a result of the accumulation of incoming marine-derived suspended and bedload sediments.

During neap tides, maximum suspended sediment fluxes are output from the estuary on the ebb, which may result in channel deepening or erosion, as the suspended sediment is exported from the estuary, which was similarly found in the Tana Estuary by Kitheka *et al*. (2005). However, during spring tides, maximum fluxes are input into the estuary, which may result in increased sedimentation and shallowing, which may in turn lead to mouth closure in winter. Therefore, the Mgeni is an exporter of sediment during neap tides, and a sink for marine sand during spring tides.

Furthermore, the suspended sediments that enter the estuary on the flood tide occur mainly as a result of wave re-suspension of the sediments within the inlet channel and its surrounds (Kitheka

et al., 2005; Theron, 2007). Conversely, the suspended sediment transported out of the estuary may serve several purposes, as follows:

- deposited on the inlet beachface, where it may become available and susceptible to wind transport, for ultimate dune formation,
- transported out of the estuary to great depths further offshore, and
- transported alongshore and ultimately onshore to the beachface, where it may be part of a continuous erosion-accretion cycle within the swash zone or may dry out increasing its susceptibility to wind erosion for dune formation.

7.5. Estuary Bed Sediment: Grain Size Distribution and Statistical Analysis

Bed sediment samples were collected from the estuary bed, simultaneous to the collection of the suspended sediment samples. Estuary bed sediment samples were collected along the vertical sample points along each profile, from February 2008 to July 2008.

7.5.1. Mud Fraction

The sediments within the estuary inlet contain negligible amounts of mud, as a result of strong, fast flowing currents and tides within the inlet, which agrees with the findings of Cooper and Mason (1987) and Cooper (1991a; 1993). Cooper and Mason (1987) recorded that the Mgeni Estuary inlet contained the least amount of mud, as a result of the tides.

7.5.2. Sand Fraction

Sand sized particles can be transported as both suspended and bedload (Tucker, 1981; 1991; Cooper and Mason, 1987; Wright, 1990; Green, 2004). It is understood that sand occupying the estuary bed is derived from several sources, such as from the Beachwood Tidal Creek, marine and offshore environment, as well as the catchment. Sediment samples were collected along the cross-section every two hours, on a spring-neap tidal cycle and seasonal basis. It is evident that the estuary bed sediment illustrates variation in size and texture, as the tide fluctuates.

7.5.2.1. Sand Statistical Parameters

- ***Median Grain Size***

The median grain size of the sediments at each sample point within each sampled channel cross-section varies from 0.19 mm to 0.79 mm. The median grain sizes calculated for each profile

reveals a different trend, ranging from 0.29 mm to 0.42 mm. In terms of the coarsest profile median grain size, 50 % of the sediments along the cross-section are finer and coarser than 0.42 mm. The median grain sizes of the sediments for each sampling day are illustrated below in Figure 7.17, with values varying from 0.29 mm to 0.40 mm.

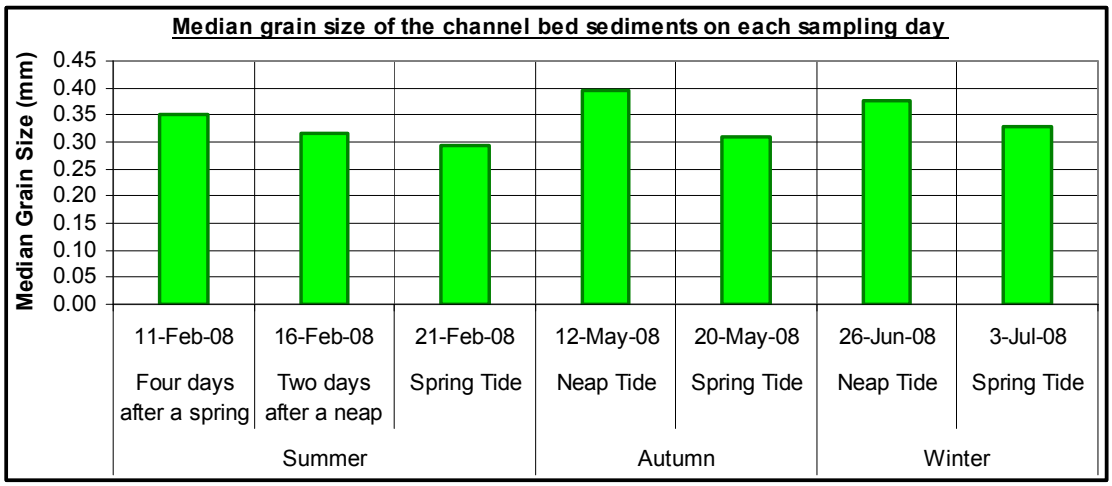

Figure 7.17. The median grain size of the sediments within the sampled cross-section channel bed, for each sampling day.

- ***Mean Grain Size***

Throughout the sampling period, mean grain sizes of the estuary bed sediment at each sample point along the cross-section vary from 0.20 mm to 0.77 mm, which are classified as fine sand and coarse sand, respectively. The finest mean grain size intersects with the spring tide in autumn, and the coarsest mean grain size intersects with the neap tide in autumn. In general, the coarsest sand is restricted to the channel margins of the measured cross-section. Conversely, the finest sand generally occupies the middle of the cross-sectional channel, however shows random variations by being interspersed between coarse sediment.

Mean grain sizes were calculated for each plotted profile, which vary from 0.29 mm to 0.42 mm, and are both classified as medium sand. Figure 7.18 (Page 179) indicates the mean grain size of each plotted profile throughout the sampling period. Therefore, in general the estuary channel bottom consists of medium sand. Generally, the sediments dominating the cross-sectional inlet channel during autumn and winter are coarser than those sediments found in the channel during summer. Seasonal mean grain sizes display values of 0.325 mm, 0.358 mm and 0.355 mm in summer, autumn and winter, respectively. In summer, the mean grain sizes of the sediments along the cross-section are generally coarser on the ebb tide than the flood tide.

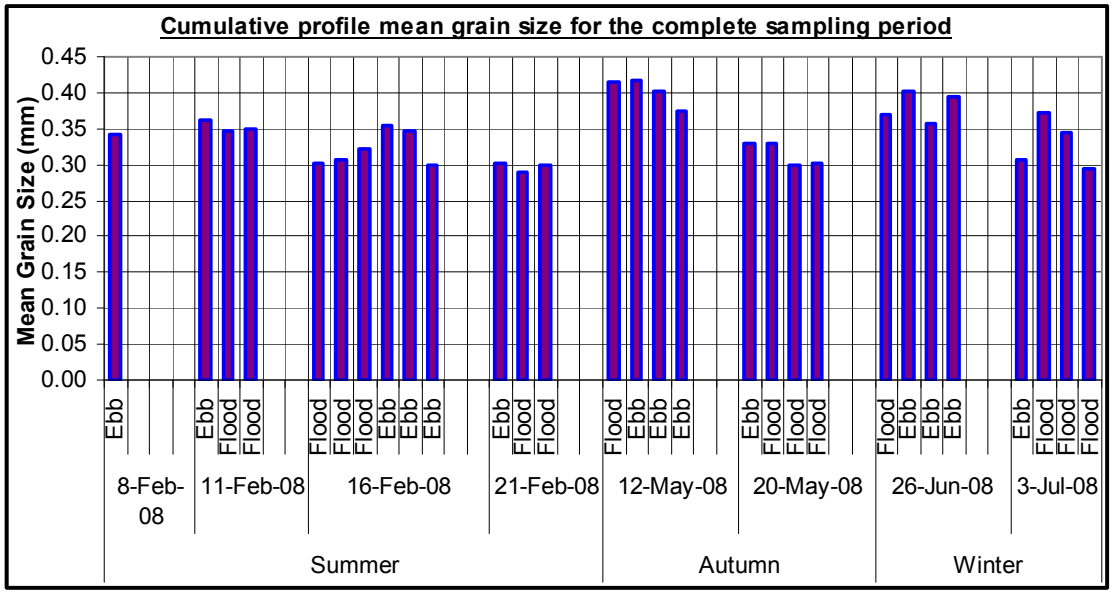

Figure 7.18. Cumulative mean grain size for each profile throughout the sampling period.

On average the estuary bed sediments within the channel contain coarser mean grain sizes during neap tides than spring tides, especially in autumn and winter, as is illustrated in Figure 7.19 below. Figure 7.19 indicates the mean grain size of the sediments found on each sampling day, with values varying between 0.29 mm and 0.40 mm. On average, the coarsest bed sediment is found on a neap tide in autumn, on 12 May 2008, and the finest sediment intersects with a spring tide in summer, on 21 February 2008.

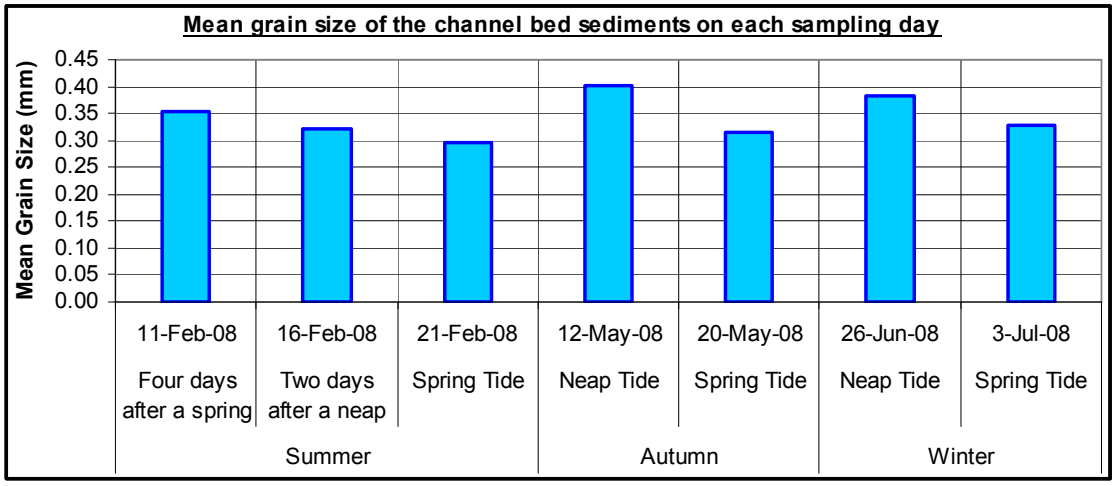

Figure 7.19. The mean grain size of the sediments within the channel bed for each sampling day.

- ***Sorting***

The sorting values of the sediments along the channel bed completely extend well below 0.35 Ø, which is classified as very well sorted. As the tide rises, turns and falls, the sediments along the channel bed are classified as very well sorted.

- ***Skewness***

The skewness of the sediment samples collected along the cross-section throughout the sampling period varies from -0.22 to 0.31, which are classified as coarse skewed and strongly fine skewed, respectively. Coarse skewed sediments intersect mainly with summer; however near symmetrical and fine skewed sediment dominate autumn and winter. Overall, the sediments within the cross-sectional channel bottom are predominantly near symmetrical.

Therefore, the sediments collected along the sampled cross-section illustrate variable skewness ranging from negative to positive, as the tide rises and falls. However, the average skewness of each profile varies from -0.05 to 0.22, which are categorized as near symmetrical and fine skewed, respectively. The average skewness of each profile is illustrated below in Figure 7.20. On average, the profiles display fine skewness on ebb tides, particularly on the neap tide of 16 February 2008. No major difference exists in skewness between spring and neap tides. However, as mentioned above, seasonal variations exist, with coarse skewed sediment dominant in summer.

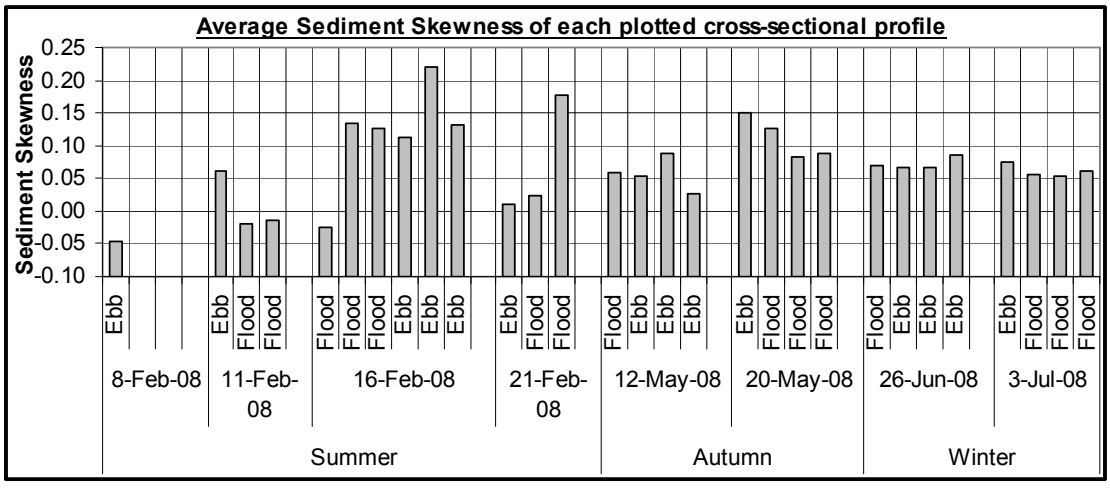

Figure 7.20. Average skewness of each plotted profile throughout the sampling period.

- ***Kurtosis***

The kurtosis ranges from 0.72 to 1.31, which is classified as platykurtic and leptokurtic, respectively. In summer, the sediments mainly display mesokurtic curves, and in autumn and winter, the sediments mainly display mesokurtic and platykurtic curves.

7.5.3. Discussion

- ***Mean Grain Size***

The mean grain size of each bed sediment sample across the estuary cross-section, throughout each profile varies between fine sand and coarse sand. The coarsest sediments generally occupy the channel margins because it is in this region that the flow velocity is minimal. A low flow velocity is capable of transporting fine sediment particles, and conversely large sediment particles require a large flow velocity in order to be transported (Dyer, 1995; Ngetar, 2002; Kitheka *et al*., 2005). Therefore, once the flow velocity decreases, its ability to erode and transport sediment decreases as well (Tucker, 1981; Dyer, 1995; Kitheka *et al*., 2005). Consequently, as the flow velocity and energy decreases or wanes, which in this case occurs along the channel margins, the sediments undergo deposition, with the coarsest particles being deposited first (Tucker, 1981; Dyer, 1995; Cooper, 1991a; Kitheka *et al*., 2005). Therefore, the regions along the channel margins contain the coarsest sediments, as a result of the low flow velocity currents.

The same abovementioned concept applies to the sediments found within the channel bed on a neap tide and a spring tide, since the average velocities of neap tides are lower than spring tides in the Mgeni Estuary. Hence, Figure 7.19 (Page 179) shows that on average the sediments within the channel bed during neap tides are coarser than those sampled during spring tides.

Furthermore, it is clear that mean grain sizes of each profile extend to higher values in autumn and winter, as compared to summer. This occurs because during autumn and winter, the fluvial discharge and fluvial sediment delivery is reduced, however the marine influence at the mouth of the estuary is elevated and enhanced, which results in a more substantial flood tide entering the estuary (Ngetar, 2002). Therefore, this enhanced flood tide transports coarser marine sediments (Tucker, 1981) into the estuary, hence higher mean grain sizes are encountered in winter and autumn, during which the estuary bed is composed of sediment with higher mean grain sizes on the flood tide than the ebb tide. Blackshaw (1985) performed a study in the Mgeni Estuary and the surrounding region, which established that the fluvial sediment comprised a higher percentage of fine particles, as opposed to the beach sand. Therefore, in autumn and winter, the

mean grain sizes of the sediments within the channel bed are coarser than the sediments found during summer. On average, the finest sediment intersects with the high flow event in summer on 21 February 2008, wherein large amounts of catchment derived sediments were delivered to the estuary, which are generally classified as fine grained sediments (Wright, 1990).

On average and throughout the entire sampling period, each profile contains medium sand. Therefore, on average, medium sand dominates the estuary cross-section or estuary channel bottom, as the tide falls and rises. Green (2004) explains that medium sand is generally indicative of sand that has been re-worked from finer regions by the ebb tide. Due to the nearness of the sampled cross-section to the ocean, the sediment sampled is probably predominantly marine-derived (Wright, 1990), which undergoes a continuous cycle of erosion, deposition and transportation. Cooper and Mason (1987) and Cooper (1991a) documented that the sediments within the lower Mgeni Estuary are mainly marine derived from flood tides and barrier overwash. To be specific, the lower 200 m of the Mgeni mouth is composed of high levels of non-cohesive marine sand (Cooper, 1991a). Hence, the coarse sediments found along the channel cross-section are most likely derived from the marine environment by the flood tide and deposited within the estuary as the flood velocities drop (Cooper and Mason, 1987; Cooper, 1991a; Wright, 1990). The fine and medium grained sediments along the cross-section are most probably derived from the catchment and transported into the estuary by the fluvial currents, as well as aeolian sources, as recorded by Wright (1990) in the St. Lucia Estuary and Green (2004) in the Kosi Bay Estuary.

Green (2004) recorded mean grain sizes varying from medium to coarse sand within the Kosi Bay Estuary. Wright (1990) documented that marine sand was dominated by medium grained sand in the St. Lucia Estuary. Wright (1990) additionally found coarse grained sand at the mouth of the St. Lucia Estuary, representative of a channel lag. Grobbler (1987) documented coarse sands dominating specific small regions in the Mdloti Estuary, indicative of washover activity. Furthermore, Grobbler (1987) found on the south coast of KwaZulu-Natal, the uMgababa Estuary mainly contained medium to coarse grained sand, and Cooper (1991a) found that the mouth of the Mtamvuna Estuary on the south coast of KwaZulu-Natal, and the Mhlanga Estuary were dominated by medium grained sand. Blackshaw (1985) established mean grain sizes varying between medium and fine sand in the Mgeni Estuary. Cooper and Mason (1987) studied the sedimentology and characteristics of the Mgeni Estuary and the Beachwood Mangroves, with two cross-sections below the M4 Bridge, which is relevant to this study, and found the mean grain size of the majority of the sediments in the estuary ranged between 0.5 mm and 1 mm, which is classified as coarse sand. However, within the mouth of the estuary, the mean grain size was classified as medium sand, with the head of the estuary being classified as fine sand (Cooper and Mason, 1987), which agrees with the findings of this research.

- ***Sorting***

In general, the sediments throughout each profile, at each sample point, as well as on average, are classified as very well sorted. This pattern owes to the fact that the Mgeni Estuary is a very active zone, particularly along the sampled cross-section. In most cases, the flow of the estuary is strong enough to sort and rework the sediment effectively (Cooper, 1991a; Masselink and Hughes, 2003). Therefore, the sediments within the estuary are very well sorted. The aspect of sediment sorting is explained in detail in Chapter 6. Tucker (1981), points out that sand sized sediment is easily transported and is usually well sorted. Therefore, throughout the sampling period, the mean grain size of the sediments, on average, for each profile is classified as medium sand. Therefore, it is expected that this sediment is easily transported and therefore very well sorted. Furthermore, these estuarine bed sediments are particularly very well sorted, as they are exposed to strong tidal currents, which also change direction as the tide transforms from an ebb to a flood. Green (2004) suggests that the regularity and uniformity of sediment sorting values indicates that the sand is most probably part of a sediment body that is reworked constantly as the sediments exit the estuary on the ebb tide and enter the estuary on the flood tide.

Comparatively, the sorting of the sediments in the St. Lucia Estuary ranged from very well sorted to moderately well sorted (Wright, 1990). Similarly, Green (2004) documented well sorted to moderately sorted sediments within the Kosi Bay Estuary. Blackshaw (1985) found very well sorted to moderately well sorted sediments in the mouth of the Mgeni Estuary. Cooper (1991a) sampled the sediments of the Mgeni Estuary in 1987 after the major flooding event, and established that in general, the sediments were classified as moderately sorted to moderately well sorted. The sediments in the Lovu Estuary ranged between well sorted and moderately sorted (Grobbler, 1987). Similar to the findings in the Mgeni Estuary, Cooper (1991a) classified the sediments within the mouth of the Mtamvuna Estuary on the south coast of KwaZulu-Natal, and the Mhlanga Estuary as very well sorted.

- ***Skewness***

In most cases the sediment skewness, on average for each profile, is classified as near symmetrical. It is noticed that the sediments tend to be fine skewed during the ebb phase of the tide, or close to the ebb tide. This is understandable, because during the ebb phase, the estuary drains fluvial discharge. Fluvial discharge mainly transports fine fluvial sediments (Blackshaw, 1985); out of the estuary, which results in a surplus of fine sediments along the bed, hence it contains positive, fine skewness. Tucker (1981) points out that river sands are generally fine

skewed, therefore the findings in the Mgeni Estuary inlet agrees with this theoretical concept. Sediment skewness is explained in detail in Chapter 6.

Green (2004) documented a similar trend in the Kosi Bay Estuary, whereby the skewness values were mainly classified as near symmetrical. Furthermore, sediment that is near symmetrical, mainly points out that winnowing and lag deposits have not occurred (Green, 2004). Comparatively, Wright (1990) established that the sand in the mouth of the St. Lucia Estuary was classified mainly as near symmetrical, coarse skewed or strongly coarse skewed. However more site specific, Cooper and Mason (1987) found that within the lower reaches of the Mgeni Estuary, the sediment was overall characterised as near symmetrical, which agrees with the findings of this research. Cooper and Mason (1987) established coarse skewed sand located along the intertidal sand bars, with fine skewed sand located within the peripheries of the head of the estuary. Cooper (1991a; 1993) established that the sediments within the upper and lower regions of the Mgeni Estuary, after the 1987 large scale flooding event, were classified as coarse skewed and fine skewed, respectively. Ngetar (2002) found that on average the sediments in the Mgeni Estuary (between the Connaught Bridge and Ellis Brown Viaduct) contained positive, fine skewness. Blackshaw (1985) found positive to negative skewed sediments in the mouth of the Mgeni Estuary. Comparatively, Grobbler (1987) recorded fine to coarse sediment skewness in both the Mdloti and Lovu estuaries, with near symmetrical distributions measured in the uMgababa Estuary. In general, Cooper (1991a) classified the sediments in the mouth of the Mtamvuna Estuary on the south coast of KwaZulu-Natal, and the Mhlanga Estuary as near symmetrical, which agrees with the findings of this research.

- ***Kurtosis***

The calculated average kurtosis values of the estuary bed sediments for each profile ranges between 0.83 and 1.10, which is classified as platykurtic and mesokurtic, respectively. In fact, approximately 93 % of the profiles on average reveal a mesokurtic or normally distributed curve, with the remaining 7 % indicating platykurtic curves. Therefore, this means that on average the profiles mainly illustrate mesokurtic curves that are normally distributed. Comparatively, Ngetar (2002) found that the sediments within the Mgeni contained a leptokurtic distribution. Kurtosis is explained in detail in Chapter 6.

Overall, Cooper (1991a) explains that medium sized sediments that are very well sorted and near symmetrical, is indicative of re-working in a high energy environment. This explanation fits in line with the sedimentary characteristics of the Mgeni Estuary.

- ***Relationship between average channel velocity and bed sediment***

It is understood that sediment grain size is related to flow velocity, such that large velocities are required to transport large sediment particles (Ngetar, 2002). Tucker (1981), points out that sediment is transported in a fluid through suspension and as bedload. Fine suspended sediment remains in suspension through turbulence, whereas coarser sediment particles are transported as bedload along the sediment surface, generally in the form of saltation (Tucker, 1981). Therefore, derived from theory it is understood that smaller flow velocities are able to transport and maintain fine sediment in suspension, whereas larger flow velocities are required to transport coarser material as bedload (Ngetar, 2002). Tucker (1981), points out that the Hjulstrom's diagram illustrates the relationship between flow velocity and grain size. This relationship shows the velocity that is needed in order to establish sediment movement or the critical erosion velocity (Tucker, 1981). Furthermore, it is also understood that large flow velocities may be required to breakdown or erode particles of sediments that are combined, such as clay particles with their cohesive properties (Tucker, 1981).

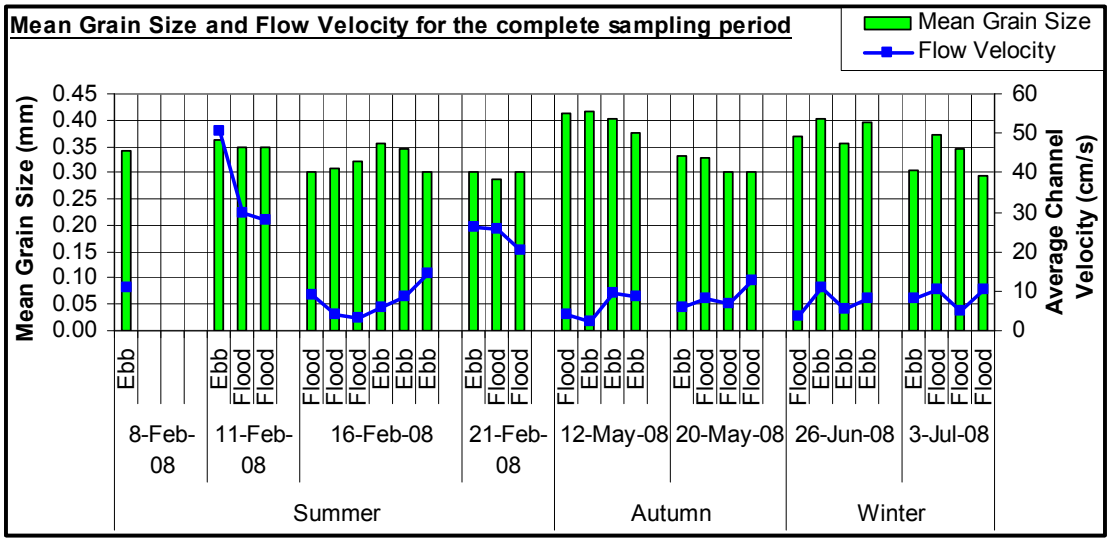

Figure 7.21. Mean grain size and average channel velocity of each profile for the sampling period.

No clear distinct, linear correlation exists between the average channel flow velocity and the mean grain size of each profile. Therefore, the average channel velocity and the mean grain size of each profile, for the entire sampling period, were graphically interpolated in order to illustrate a general trend, as is illustrated above in Figure 7.21. The general pattern indicates that as the average channel velocity decreases on the flood tide, especially in summer, the mean grain size of the sediments along the cross-section tends to increase. However, as the average channel

velocity increases along the falling or ebb tide, such as during the neap tides, the mean grain size of the sediments along the cross-section tends to decrease. As the flow velocity decreases on the flood tide, the channel bed is composed of coarser sediment particles, since the flow is not strong enough to transport these sediments through the cross-section in a landward direction. The converse occurs as the average channel velocity increases on the falling tide. Therefore, this pattern agrees with the abovementioned concepts of Tucker (1981); Cooper (1991a); Dyer (1995); Ngetar (2002); and Kitheka *et al*. (2005).

7.6. Organic Matter Content

Loss on ignition was performed on the estuary bed sediment samples that were collected throughout the sampling period. The percentage of organic matter for each sample point was subsequently calculated, which is presented and discussed below. The average organic content of each cross-sectional profile is displayed below as well. In general, the organic contents illustrate variations within and between each cross-sectional profile.

The organic content of the estuary bed sediment collected along each cross-sectional profile for the complete sampling period, varies from 0.20 % to 0.65 %. This range in organic content of the estuary bed is considered as small, indicating that the sediments occupying the bed are somewhat uniform, in terms of size, composition, sorting and environmental controls, unlike the variation of sediments sampled along the barrier of the Mgeni in the geomorphological study (Chapter 6). In general, high organic contents were found along the margins of the sampled cross-section. Furthermore, an average organic content of 0.40 % was calculated for the estuary bed sediments collected throughout the sampling period. In general, higher organic contents were found within the sediment samples containing high mud contents, however no distinct correlation exists, similar to the findings of Cooper (1991a) in the Mhlanga Estuary. In general, the finer sediment sizes contain higher organic contents; however no clear correlation exists between these two variables.

Average organic contents were calculated for each cross-sectional profile for the complete sampling period, which is displayed above Figure 7.22 (Page 187). Figure 7.22 shows that the average cross-sectional organic contents vary from 0.28 % to 0.48 %, which is also considered a small range in data. On average, the organic contents of the estuary bed sediments, throughout the sampling period, reach higher values during spring tides (including days sampled after spring tides) than neap tides (including days sampled after neap tides). An average organic content of 0.43 % was calculated for the estuary bed sediments collected during spring tides. Additionally, an average organic content of 0.38 % was calculated for the estuary bed sediments collected

during neap tides. Furthermore, average organic contents were calculated for the ebb and flood tides encountered throughout the sampling period. The ebb and flood tides reveal an average organic content of 0.39 % and 0.42 %, respectively. These values indicate that on average, the estuary bed sediments contain higher organic contents on the flood tide than the ebb tide. In relation to the tidal phases, in most cases within each tidal cycle, the average organic content of each profile tends to increase as the tide rises, and decrease as the tide falls. However, in certain cases the average organic content of each profile tends to fluctuate as the tide falls. Seasonally, the estuary bed sediments reveal an average organic content of 0.37 % in summer, 0.42 % in autumn, and 0.43 % in winter. These seasonal averages indicate that the bed sediments contain the highest organic content in winter, and the lowest in summer.

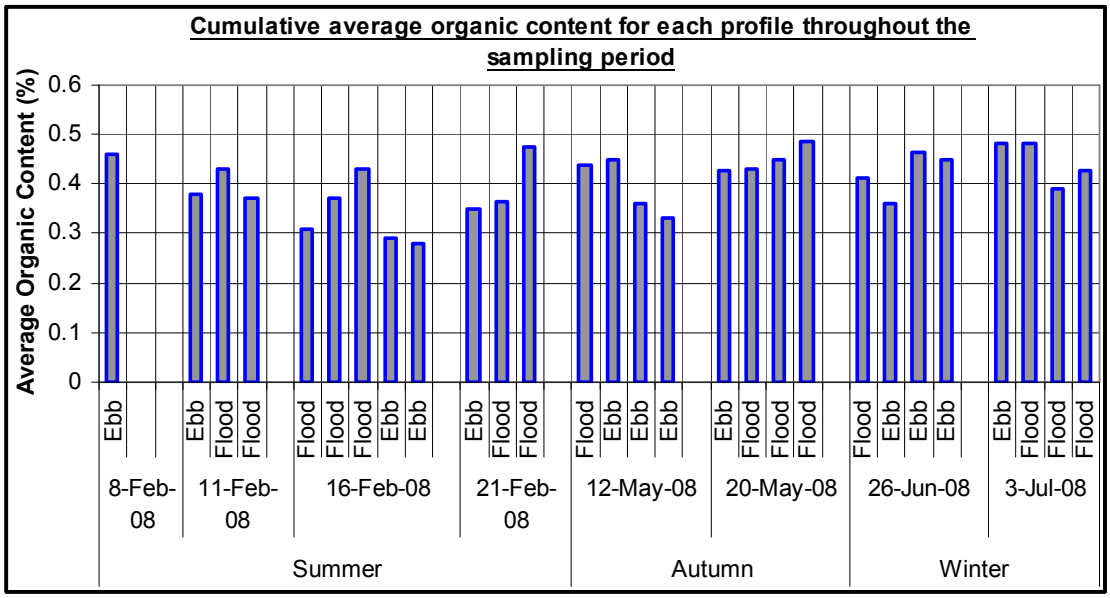

Figure 7.22. Cumulative average organic matter content for each profile measured throughout the sampling period.

7.6.1. Discussion

Based on the range of organic contents of the estuary bed sediments, especially since the maximum percentage of organics is 0.65 %, it derived that the estuary bed sediments occupying the cross-section throughout the sampling period contain very low, minor organic contents. Cooper (1991a) established organic contents between 0.00 % and 42.00 %, in the Mhlanga Estuary, and reaching up to 13.00 % in the Mtamvuna river mouth. Within this research, the surface sediment along the barrier of the Mgeni was sampled as well, in which a maximum organic content of 2.93 % was established in a deep depression in the estuary along Profile C

(Chapter 6). Therefore, based on these comparisons, it is safe to conclude that the bed sediments along the cross-section contain very low percentages of organics.

Similar to the findings of this research, Cooper and Mason (1987) and Cooper (1991a) determined that organic carbon contents of the sediments within the Mgeni Estuary inlet were extremely minor. A possible reason for this is that the cross-section is positioned in a very active, high energy, tide- and wave-influenced, dynamic zone that is constantly changing as sediments, both suspended and bedload, are transported into and out of the estuary, which is not conducive for the settling of mud and organic matter. Based on this, it is understandable that the organic content of the bed sediments within the estuary inlet is remarkably low. Furthermore, the bed sediments throughout the cross-section are composed mainly of medium sand, which is non-cohesive (Schumann, 2003) and contains a low ability to maintain organic matter. Cooper and Mason (1987) assert that in the Mgeni Estuary, the regions dominated by sand generally hold minimal organic contents, which agrees to the findings of this research.

In the previous chapter, is has been established that the percentage of mud in the sediment enhances the percentage of organics, as similarly found by Cooper and Mason (1987) and Grobbler (1987). However, within the estuary bed sediments, no distinct correlation between organic content and mud content exists. Similarly, Cooper (1991a) found no distinct linear relationship between the percentage of mud and organic matter in the sediments in the mouth of the Mhlanga Estuary. This most probably occurs as a result of the inlet containing high energy and a dynamic nature. As found in Section 6.5 in Chapter 6, the calm and stagnant sections of the estuary generally allow mud to settle, which generates and is associated with high organic contents (Cooper and Mason, 1987; Grobbler, 1987).

Furthermore, a possible reason attributed to the lack of a strong correlation between the mean grain size and the percentage organics, is most probably because of the small range in grain size and organic content.

Spring tides display higher organic contents than neap tides, most probably as a result of the greater tidal range associated with the former. Furthermore, spring tides contain higher velocities than neap tides, which indicate that more organic rich sediments are transported to the estuary during spring tides. Seasonal averages of organic content display that summer contains the lowest percentage of organics, whilst winter contains the highest percentages. This pattern suggests that during the dry seasons, the decreased fluvial discharge most probably creates a calmer environment during the ebb, during which fine sediments with substantial mud contents tend to settle and hence increase the organic content.

Therefore, in general, the organic contents within the estuary are remarkably low and contain a small range in percentages. Therefore, the bed sediments along the sampled cross-section of the Mgeni Estuary contain low percentages of organics, as the region is dynamic and very active, which precludes settling, stagnant conditions, and conditions that are conducive to the build up of organic matter.

7.7. Conclusion

The lower region of the Mgeni Estuary can be classified as a very dynamic and active zone that contains high energy levels, which corresponds with the concept put forward by Dalrymple *et al*. (1992). These high levels of energy are sourced from the tides, fluvial currents and waves that enter the estuary, which consequently influences the geomorphology, sediment characteristics and texture, and hydrodynamics of the estuary.

The hydrodynamic study of this research included the measurement of the channel discharge, collection of suspended sediment samples and estuary bed sediment samples. The results obtained were analysed and discussed on a seasonal and spring-neap basis. The plotted channel cross-sections reveal an overall increase in depth and cross-sectional area as the tide rises, with the converse taking place along a falling tide. The cross-sectional area of each profile is at a maximum during the flood tide, when the wetted perimeter is significantly large. Furthermore, maximum depths are almost always encountered in the middle of the channel profile.

Maximum flow velocities mainly occur within the middle of the channel cross-section, whilst minimum velocities occur along the channel margins. The measured flow velocities along each profile were averaged for each sampled cross-sectional profile. Maximum average channel velocities occur along the ebb tide in summer and along the ebb and flood tide in autumn and winter. Minimum average channel velocities occur along the flood tide in summer, the ebb tide in autumn and the flood tide in winter. This pattern is related to the seasonal distribution of rainfall and fluvial discharge, which is dominant in summer and wanes towards autumn and winter, during which the marine influence consequently dominates due a powerful and enhanced flood tide (Ngetar, 2002). On the ebb tide, maximum average channel velocities occur after mid-low tide and at peak low tide, hence on the falling tide close to peak low tide. On the flood tide, maximum average channel velocities occur after mid-high tide, hence on the rising tide close to peak high tide. Minimum average channel velocities occur mainly around mid-low tide on the ebb tide, and around mid-high tide on the flood tide. Overall, the temporal occurrence of maximum and minimum average velocities conforms to the theories outlined by Pethick (1984), Bird (2000) and Masselink and Hughes (2003).

The average channel velocities are higher during spring tides than neap tides, which agree with the theories of Bird (2000) and Davis and FitzGerald (2004), as well as other works. This occurs as a result of the greater tidal range experienced during springs than neaps. The average channel velocities are highest in summer, followed successively by those during winter and autumn. This occurs as a result of the seasonal distribution of rainfall and fluvial discharge, as well as Ngetar's (2002) abovementioned concept.

The channel discharges are highest during summer, followed successively by those during winter and autumn. This seasonal variability in discharge is related to the seasonal distribution of rainfall throughout the sampling period, which was also pointed out by Ngetar (2002); Zietsman (2004); Stretch and Zietsman (2004); Garden and Garland (2005); and Lawrie (2007). A strong link was established between the average monthly rainfall and the average monthly discharge. Despite winter containing the lowest rainfall, it contained the second highest average discharge, as a result of a greater tidal influence at the mouth of the Mgeni (Ngetar, 2002). Furthermore, the channel discharges are higher on spring tides than neap tides, as a result of a greater tidal range evident during springs. Maximum channel discharges mainly occur along the flood tide in summer and during spring tides in autumn and winter, as a result of a greater cross-sectional channel area evident during the flood tide. A strong correlation was established between average channel velocity and average channel discharge. Consequently, channel discharge is influenced by several factors such as rainfall, cross-sectional area and velocity.

The highest suspended sediment concentrations occur in summer, mainly extending above 20.00 mg/l. Average suspended sediment concentrations were calculated for each profile, since the instantaneous concentrations illustrated some degree of variability. The average suspended sediment concentrations were highest during summer, followed successively by those during winter and autumn. This seasonal variation in suspended sediment concentrations is linked to the seasonal distribution of rainfall and fluvial discharges. A strong correlation was documented between the total monthly rainfall and the average monthly suspended sediment concentrations. Furthermore, a strong correlation was documented between the average monthly discharge and suspended sediment concentrations.

Generally, high sediment availability at the beginning of a wet season is evident in the catchments of rivers and estuaries (Kitheka *et al*., 2005); hence high suspended sediment concentrations are evident in summer. However, in winter, the greater influence of tides at the mouth of the estuary (Ngetar, 2002) generally creates and account for a higher average suspended sediment concentration than those calculated for autumn.

In summer, maximum suspended sediment concentrations intersect mainly with the ebb tide, as a result of high amounts of rainfall which drains the catchment and delivers higher amounts of catchment-derived sediment to the coastline. Comparatively, maximum suspended sediment concentrations occur on the ebb and flood tides in autumn, and on the flood tide in winter, which agrees with Ngetar's (2002) abovementioned concept, since a greater tidal influence at the mouth of the estuary causes turbulence and re-suspension of the bottom sediments by waves and tides in the estuary, which increases the suspended sediment concentrations (Ngetar, 2002; Theron, 2007). Higher suspended sediment concentrations occur during spring tides than neap tides, as a result of greater amounts of turbulence and re-suspension of the estuary bottom sediments (Theron, 2007). Furthermore, a strong correlation was documented between the average monthly velocity and suspended sediment concentrations.

The average flow velocity, cross-sectional area and average suspended sediment concentrations were used to calculate the suspended sediment flux. The suspended sediment fluxes were highest during summer, followed by winter and autumn. This seasonal variability is linked to seasonal distribution of rainfall and the consequent marine influence at the mouth of the estuary especially during the dry months, as documented by Ngetar (2002). Spring tides generated higher fluxes on flood tides, as a result of higher tidal elevations which cause greater turbulence and sediment re-suspension (Theron, 2007). Maximum suspended sediment fluxes were encountered on the flood tides during spring tides and, on ebb tides during neap tides, particularly in autumn and winter. The suspended sediment fluxes generally increase along the rising tide. Furthermore, a strong, positive correlation was documented between the average monthly channel discharge and suspended sediment fluxes.

The estuary bed sediments collected along the sampled cross-section in conjunction with the discharge measurements and velocity readings, were analysed for grain size distribution and organic content. The mean grain sizes of each sample collected throughout the sampling period, ranges from fine sand to coarse sand. The coarsest sand dominates the channel margins, whereas the finer sands dominate the middle of the channel. Mean grain sizes were calculated for each profile, which were each classified as medium sand. On average, mean grain sizes are higher during autumn and winter than in summer. Therefore, this seasonal distribution in mean grain size is related to the overall amount of rainfall that occurred throughout the study period, as well as the consequent marine influence at the mouth of the estuary especially during the dry months, as documented by Ngetar (2002). Fluvial discharges, which are high in summer, deliver fine fluvial sediments (Blackshaw, 1985) to the estuary, in comparison to the coarser marine-derived sediment transported into the estuary on the flood tide. Sediments along the estuary bed were coarser during neap tides than spring tides.

The sediments throughout each profile and sampling point along the cross-section are classified as very well sorted. This high degree of sorting owes to the strong energy of the currents and waves that are capable of re-working and sorting the sediments along the bed of the estuary. The average sediment skewness of each profile ranges from near symmetrical to fine skewed. Coarse skewed sediments mainly occur in summer; whilst near symmetrical and fine skewed sediments dominate autumn and winter. The average kurtosis of each profile ranges from platykurtic to mesokurtic, although mainly containing mesokurtic, normally distributed curves.

Furthermore, no strong trend was established between the average flow velocity and the average mean grain size. However, a generalised pattern was evident, where as the average velocity increases on the ebb tide, the mean grain size of the profile decreases, with the converse taking place on the rising flood tide.

In general, the bed sediments contain low, minimal organic contents, most probably as a result of the high energy of the Lower Mgeni, specifically within the vicinity of the tidal inlet, which creates a non-stagnant environment, prohibiting settling and deposition. High organic contents were recorded in the sediments along the channel margins, fine sediments, as well as those that contain high mud contents. The low organic contents of the sediments in the lower Mgeni conform to past research. Furthermore, on average, the bed sediments are dominated by medium sand, which generally do not display an affinity to organic matter, as similarly documented by Cooper and Mason (1987). No clear trend was established between the organic content and the mud content or between mean grain sizes and organic contents. In general, maximum organic contents were associated with flood tides during spring tides and ebb tides during neap tides. On average, the organic contents obtained in summer were lower than those obtained in autumn and winter. Furthermore, organic contents obtained during spring tides were higher than those obtained during neap tides. Therefore, overall, the bed sediments along the cross-section contain low organic contents.

CHAPTER 8:
ESTUARY MOUTH HYDRODYNAMICS AND MORPHOLOGY

On 11 and 16 February 2008, the narrow inlet of the Mgeni Estuary was sampled in order to generate an understanding of the sediment size, suspended sediment concentration and discharge of the channel closer to the ocean. However, it was decided that sampling in such proximity to the open ocean should be discontinued in following fieldtrips, as a result of severely unsafe conditions and due to the risk of damage to the equipment, since the region was sampled by wading and diving. This region is situated approximately 150 m downstream of the abovementioned consistently sampled channel cross-section, schematically shown in Figure 8.1 below. Waves and strong tidal currents are constantly present within this region along the inlet channel cross-section, rendering this region highly turbulent. Cross-sectional profiles were not plotted for the downstream inlet channel, since only a single width and depth reading was made close to the middle of the inlet due to safety constraints, which was used as an average.

Figure 8.1. The position of the mouth inlet cross-section and the established cross-section further upstream (Ethekwini Municipality, 2008).

8.1. Mouth Hydrodynamics and Sediment Characteristics: 11 February 2008

On 11 February 2008, the downstream inlet channel was sampled along Profile 1, after peak low tide along the rising tide and along Profile 2, at mid-high tide. Hence both Profiles 1 and 2 were plotted along the flood tide. Along each of these profiles, three depth and flow velocity measurements were recorded. On this day, the channel covered a width of approximately 10 m. Along Profile 1, the depth of the downstream inlet channel varies from 140 cm to 145 cm, and the

flow velocity ranges from 31.02 cm.s^{-1} to 46.61 cm.s^{-1}. Furthermore, along Profile 1, the inlet channel contains an average depth of 141.70 cm and an average flow velocity of 38.64 cm.s^{-1}. Conversely, along Profile 2, at mid-high tide, the inlet channel contains an average depth of 100 cm, and the flow velocity varies from 57.00 cm.s^{-1} to 70.70 cm.s^{-1}. Additionally, the inlet channel contains an average flow velocity of 65.42 cm.s^{-1} along Profile 2. Therefore, the average inlet channel velocities are greater during mid-tide than along the rising tide after peak low.

In terms of the sediment characteristics, along Profile 1 the suspended sediment concentrations vary from 36.00 mg/l to 40.00 mg/l, with an average concentration of 38.67 mg/l. Comparatively, Profile 2 contains a suspended sediment concentration of 34.00 mg/l. Consequently, the average suspended sediment concentration along Profile 1 is greater than the concentration along Profile 2. Figure 8.2 illustrated below, indicates the sediment characteristics of the inlet channel during 11 February 2008.

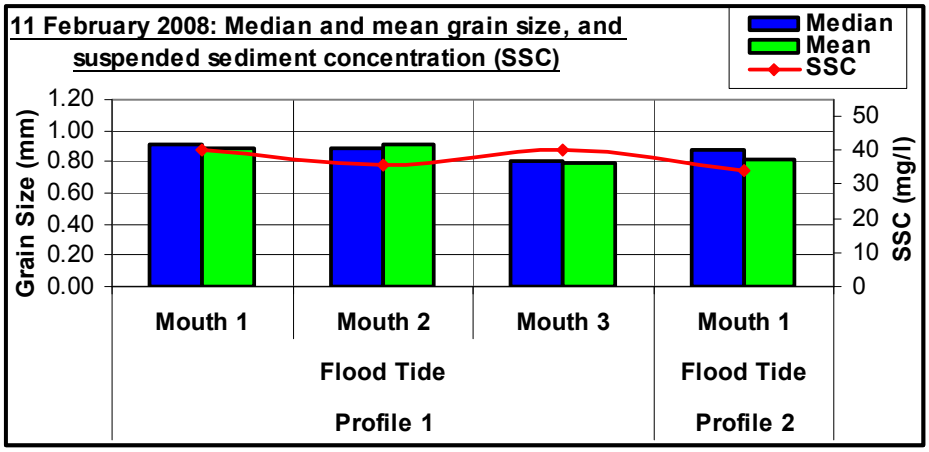

Figure 8.2. The suspended sediment concentrations and the median and mean grain sizes of the estuary bed sediments within the inlet channel on 11 February 2008.

The bed sediments along Profile 1 contain median grain sizes ranging from 0.80 mm to 0.91 mm, with an average value of 0.87 mm. This means that on average, 50 % of the sediments along Profile 1 within the inlet channel are finer and coarser than 0.87 mm. Furthermore, the mean grain sizes along Profile 1 range from 0.79 mm to 0.91 mm, both of which are classified as coarse sand. Profile 1 contains an overall mean grain size of 0.86 mm, which classifies as coarse sand. The sediment sorting values extend below 0.35 Ø, with an average value of -0.86 Ø, which is categorized as very well sorted. In terms of skewness, the sediments along Profile 1 range from coarse skewed to near symmetrical, with an average skewness of -0.08, which is classified as near symmetrical. The calculated kurtosis values along Profile 1 display platykurtic curves. Comparatively, Profile 2 contains a median grain size of 0.88 mm, which means that 50 % of the

sediments along the profile are finer and coarser than this value. The sediments along Profile 2 contain a mean grain size of 0.82 mm (coarse sand), and very well sorted sediments, with a coarse skew and a platykurtic curve.

The organic content of the bed sediments along Profile 1 ranges from 0.20 % to 0.25 %, with an average value of 0.23 %. Profile 2 displays an organic content of 0.30 %. This means that as the tide rises further towards mid-high tide, the organic content of the sediments generally increases.

8.2. Mouth Hydrodynamics and Sediment Characteristics: 16 February 2008

On 16 February 2008, the inlet channel was sampled for a total of four times. This section was sampled during the rising tide close to mid-high tide along Profile 1, during peak high tide along Profile 2, during the falling tide before mid-low tide along Profile 3, and during the falling tide after mid-low tide along Profile 4. Hence, Profiles 1 and 2 were plotted along the flood tide, whilst Profiles 3 and 4 were plotted during the ebb tide.

Along Profile 1, the inlet channel contains an average depth of 160 cm, and flow velocities varying between 9.20 $cm.s^{-1}$ and 20.63 $cm.s^{-1}$. Furthermore, Profile 1 contains an average flow velocity of 16.13 $cm.s^{-1}$. Comparatively, Profile 2 contains an average channel depth of 150 cm, and flow velocities ranging from 7.13 $m.s^{-1}$ to 22.71 $m.s^{-1}$. Profile 2 contains an average flow velocity of 14.05 $cm.s^{-1}$. Along Profile 3, the inlet covers an average channel depth of 110 cm, and contains flow velocities ranging from 59.08 $cm.s^{-1}$ to 94.02 $cm.s^{-1}$. Profile 3 contains an average flow velocity of 76.44 $cm.s^{-1}$. Further readings were taken and along Profile 4, the inlet channel contains an average depth of 140 cm, and flow velocities ranging from 64.29 $cm.s^{-1}$ to 108.09 $cm.s^{-1}$. Profile 4 contains an average flow velocity of 78.45 $cm.s^{-1}$.

In terms of the sediment characteristics, Profiles 1, 2 and 3 contain suspended sediment concentrations of 26.00 mg/l, 14.00 mg/l and 14.00 mg/l, respectively. This indicates a decrease in the suspended sediment concentration as the tide falls. In terms of the estuary bed sediments, Profiles 1, 2 and 3 contain median grain sizes of 0.94 mm, 0.93 mm and 0.88 mm, respectively. The median grain size indicates that 50 % of the sediments along each profile within the mouth are finer and coarser than the median value. Furthermore, Profiles 1, 2, and 3 contain mean grain sizes of 0.90 mm, 0.91 mm and 0.89 mm, respectively, which are collectively classified as coarse sand. Therefore, as the tide rises towards peak high tide from Profile 1 to Profile 2, the mean grain sizes tend to increase. However, as the tide falls towards mid-low tide from Profile 2 to Profile 3, the mean grain size decreases. The sediments along each profile within the inlet channel contain sorting values less than 0.35 Ø, which indicate very well sorted sediments. Each

profile contains negative skewness values ranging from -0.14 to -0.04, with Profiles 1 and 2 containing coarse skewed sediment and Profile 3 containing near symmetrical. Furthermore, each profile contains kurtosis values that represent platykurtic curves. Figure 8.3 below indicates the sediment characteristics of the downstream inlet channel on 16 February 2008.

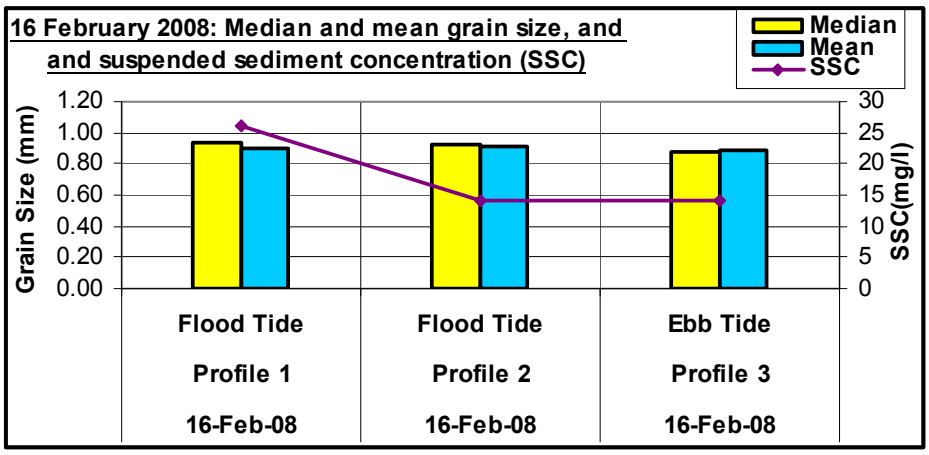

Figure 8.3. The suspended sediment concentrations, and median and mean grain sizes of the estuary bed sediments within the inlet channel: 16 February 2008.

The bed sediments within the inlet channel contain organic contents of 0.15 % and 0.32 % along both Profiles 1 and 2, and Profile 3, respectively. This means that as the tide falls from peak high tide towards mid-low tide, from Profile 2 to Profile 3, the organic content of the estuary bed sediments generally increases.

- ***Discussion***

The bed sediments within the downstream inlet channel of the estuary contain high mean grain sizes classified as coarse sand. The sediments within the lower downstream inlet channel are very much coarser than the sediments along the upper cross-section as discussed in Chapter Seven, as a result of its closeness to the ocean, which results in a strong and dominant flood tide within this region that transports coarse marine sediments (Schumann, 2003) into the estuary and generates strong tidal currents that enable constant sediment re-working and transportation. This results in the collective very well sorted sediments within the inlet channel and predominant negative skewness, ranging between coarse skewed and near symmetrical.

In line with the concepts put forward by Tucker (1981; 1991), Blackshaw (1985), Wright (1990) and Masselink and Hughes (2003), the sediments in the Mgeni are typically dominated by marine sediments, as a result of its uniformity in coarse sediment sizes, very well sorted sediments and

coarse skew. The estuary bed sediments in the inlet channel contain extremely low organic contents, ranging well below 0.32 %, which conforms to the findings of Cooper and Mason (1987) in the Mgeni Estuary, as a result of the strong tidal currents and turbulence within the region. Furthermore, the average suspended sediment concentrations within the downstream inlet channel are fairly lower than those obtained along the sampled cross-section further up the estuary in summer.

8.3. Mouth Morphology

- ***Aerial Photo Analysis***

Aerial photographs of the Mgeni Estuary, spanning from 1999 to 2008 were studied and based on these photographs, a series of six schematic diagrams have been drawn in order to illustrate morphological patterns and features specifically within the mouth, which is illustrated in Figure 8.4 (Page 198). Note that these schematic diagrams are not drawn to scale.

In August 1999, the Mgeni Estuary was separated from the Indian Ocean by a linear, shore-parallel sandy barrier. The barrier remained remarkably linear, lacking cuspate features. However, evidence of slight recurving of the barrier was evident along the inlet beachface on the landward side. This most probably occurred as a result of a large influx and deposition of flood-tide derived marine sediment into the estuary mouth. A narrow, constrained tidal inlet channel was present within the estuary, which consequently widened towards the sea. Additionally, a scour face was present along the barrier inlet beachface, most likely as a result of strong tidal currents that caused erosion along the channel margins.

In August 2003, the Lower Mgeni adopted a similar morphology to that observed in August 1999. However, few changes were noticed, such that the tidal inlet channel was narrower and the recurved spit along the barrier inlet beachface underwent sediment accretion, as it appeared to have increased in size. This is most probably evidence of a dominant influx of marine-derived sediment to the system. Evidence of a possible intertidal sandbar existed just below the M4 Bridge.

In September 2005, the barrier remained linear, however recurving at the tidal inlet, in a landward direction, was more distinct than previous. The tidal inlet channel remained narrow, and the intertidal sand body present below the M4 Bridge in 2003, became more permanent and clear. As Cooper (2001) found that fluvial sediments in river-dominated estuaries characteristically extend towards the barrier, it is therefore possible that this sandbar formed as a result of the

accumulation of fluvial sediments, as well as marine sediments derived from the flood tide and overwash.

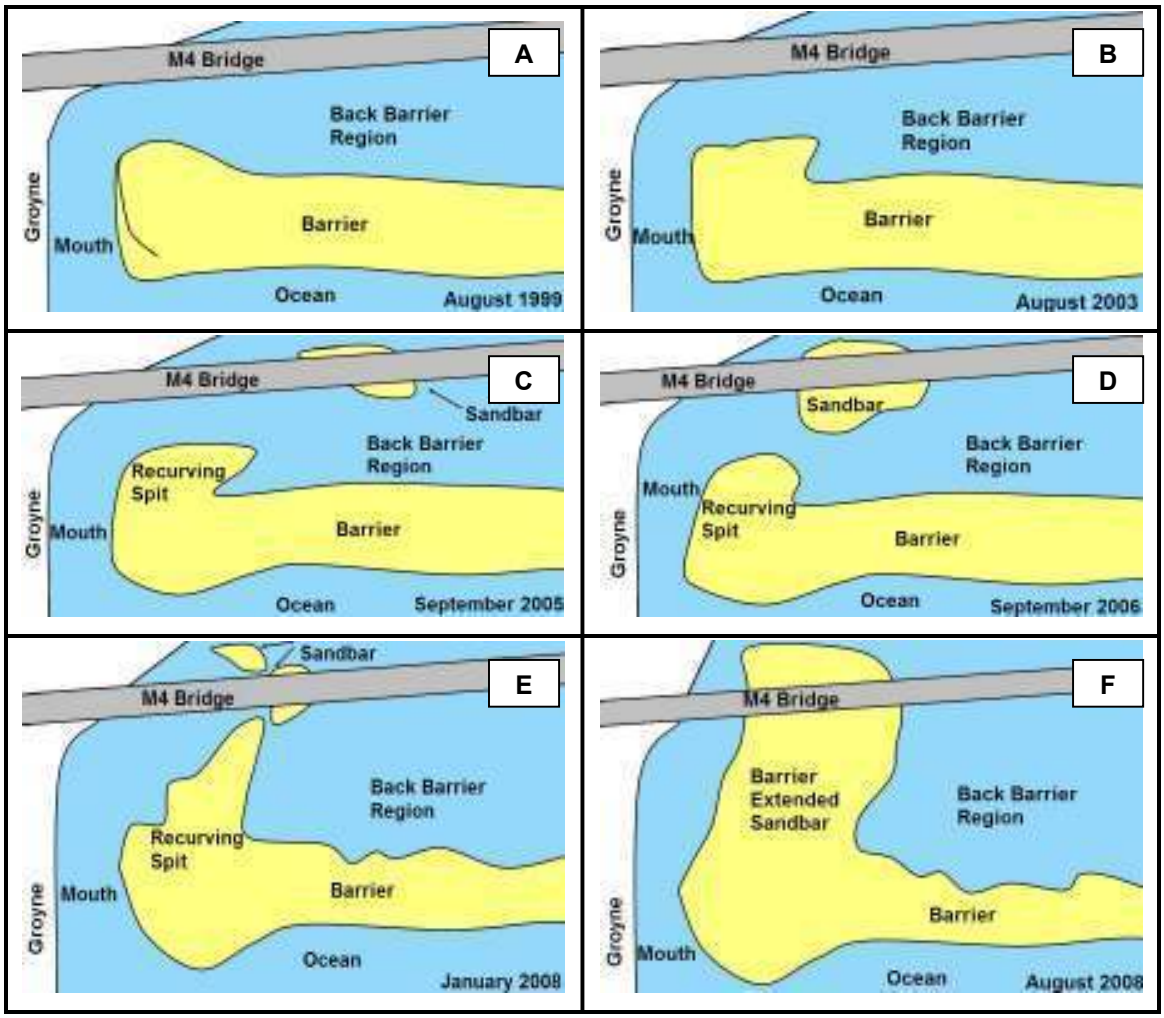

Figure 8.4. Schematic diagrams of the morphology of the Mgeni Mouth A: August 1999, B: August 2003, C: September 2005, D: September 2006, E: January 2008, F: August 2008.

In September 2006, the lower Mgeni contained a similar morphology to that observed in 2005. The tidal channel remained narrow and the recurved section of the barrier remained relatively unchanged in terms of size. Furthermore, sediment deposition on the seaward side of the inlet, along the engineered groyne was evident. The sandbar below the M4 Bridge increased in size and extended further seaward toward the barrier, in comparison to that observed during 2005.

In January 2008, the Lower Mgeni displayed a relatively different morphology, in comparison to that recorded in the past. The inlet channel underwent widening and the barrier had recurved

further landward and extended just before the M4 Bridge. A small sandbar was present underneath the M4 Bridge, in line with the recurved barrier. The landward side of the sandy barrier was outlined by cuspate or curved features, as opposed to the relatively linear pattern recorded in the past. Furthermore, the margin of the barrier lining the inlet channel along the inlet beachface contained a curving or meandering pattern.

In August 2008, the Lower Mgeni displayed a similar morphology to that observed in January 2008. The inlet channel underwent narrowing and the sandbar beneath the M4 Bridge adjoined and amalgamated with the recurving sand barrier, which created a large sandbar that was attached to the barrier, extending landward. This supratidal barrier attached sandbar is termed the barrier extended sandbar, which most probably developed as a result of a higher influx of marine and fluvial sediments to the system. Ngetar (2002) points out that in the Mgeni, fine and coarse sediments transported into the estuary by waves and tides consequently settle at the tip of the flood tide and this results in the accumulation of sediments in this region, mainly in the back barrier region above the M4 Bridge.

Throughout the sampling period, the estuary mouth contained a similar morphology to that recorded during August 2008. Therefore, during the sampling period, the barrier extended sandbar created a calm back barrier region, which included a deep estuary section adjacent to it. However in January 2008, the sandbar and recurved barrier were separated, most probably as a result of a reduction in sediment supply and availability for deposition. Another possible reason for the separation of these two features is the high water levels in the estuary and the large tidal volume derived from the Beachwood Tidal Creek. Therefore, it is predicted that when the tidal volume and estuary water levels are low, it allows the sediment to settle, causing the sandbar and the recurved barrier tend to join creating a large barrier extended sandbar. However, when the tidal volume and estuary water levels are high, there is a build up of water northwards of the barrier extended sandbar, which causes the flow to break through it and move towards the mouth. Based on the work of Harrison *et al*. (2000) and Cooper (2001), due to this accretion linked to the creation of the barrier extended sandbar, it is likely that the Mgeni is also considered as sink for marine sand, as opposed to just being a supplier of sediments to the nearshore zone.

- ***Photographic Analysis***

Throughout the sampling period, photographs were taken of the mouth of the estuary, both from the Blue Lagoon and Beachwood Mangroves regions. This was done to enable a photographic analysis of the mouth of the estuary in terms of the estuarine morphology, and sedimentary

bodies and features. Illustrated below are photographs that were taken of the mouth of the Mgeni Estuary during the sampling period.

As shown schematically in Figure 8.5 below, the mouth of the estuary obtained a broad morphology on 27 July 2006, approximately two days after a spring tide. A small sandbar was present within the mouth of the estuary, positioned just before the M4 Bridge or on the landward side of the inlet. This sandbar is most probably representative of a flood-tidal delta that formed as a result of a large ingress of marine sediments into the estuary. Furthermore, this photograph was taken during winter, which means that the fluvial input to the estuary is relatively low, whilst the flood tide and marine influence is enhanced (Ngetar, 2002). Therefore, it is understandable that this sandbar takes the form of a flood-tidal delta present within the mouth. Furthermore, Cooper (1988) in Cooper (2002) recorded a small flood-tidal delta within the mouth of the Mgeni Estuary. Similarly, Ngetar (2002) recorded a flood-tidal delta behind the barrier of the Mgeni Estuary in 1999 and 2000, and explained its formation as a result of barrier overwash by the incoming flood tide, together with the sediments it transports into the estuary. Furthermore, evidence of barrier recurving on the landward side of the estuary mouth exists. The sandbar below the M4 Bridge was evident on 27 July 2006, as explained above in the aerial photo analysis.

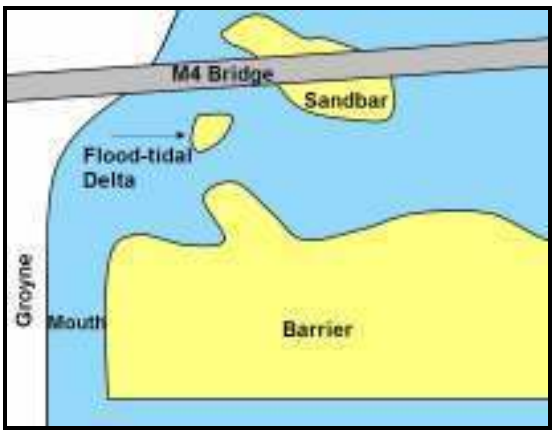

Figure 8.5. Schematic representation of the morphology of the Lower Mgeni: 27 July 2006.

Figures 8.6 A and B (Page 201) shows the Mgeni mouth on 21 March 2007, which consequently intersected with the large-scale storm event during 19 and 20 March 2007. As a result, the barrier of the estuary was almost completely eroded and stretched an estimated 100 m in length. The sandbar beneath the M4 Bridge and the small flood-tidal delta present in July 2006 were absent in March 2007, as a result of the storm erosion. Consequently, the usually small, narrow tidal inlet transformed into a very broad inlet. This enlarged inlet formed a passage for large storm waves, which moved through the estuary. It is unclear how long it took for the barrier of the Mgeni to re-establish itself and redevelop, however in November 2007, when the barrier was surveyed as part

of the geomorphological study (Chapter Six), it had clearly re-formed and the lower Mgeni adopted a morphological plan similar to that depicted in Figure 8.4 F (Page 198). It is believed that this storm event flattened the barrier, which caused it to extend laterally, further inland, additionally owing to the formation of the barrier extended.

Figure 8.6. Lower Mgeni during the large scale storm event on 21 March 2007.

Within the sampling period, the estuary inlet contained a steep scarp or scour face along the inlet beachface, which extended approximately 60 cm in height, and occurs due erosion by tides and waves. In addition, Grobbler (1987) identified a scour face along the mouth of the Mdloti and Lovu estuaries. However, in the Mgeni the scour face was mainly clear during spring tides and was absent during neap tides, as a result of the large tidal range during spring tides, which are capable of significant amounts of erosion (Dyer, 1995; Kitheka *et al*., 2005), as previously discussed. Figure 8.7 below indicates the scarp lining the margin of the inlet beachface.

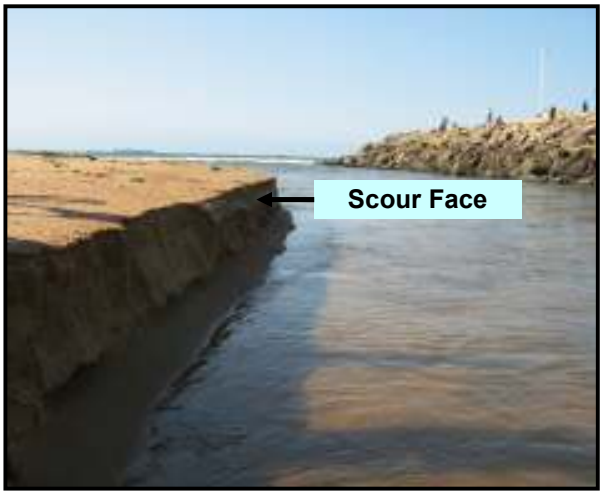

Figure 8.7. Scour face lining the tidal inlet channel of the estuary on 3 July 2008.

Figure 8.8. A merged photograph of the sampled area during the flooding event on 21 February 2008: Spring Tide.

Figure 8.9. A merged photograph of the Lower Mgeni viewed from the Blue Lagoon side on 12 May 2008: Neap Tide.

Figure 8.10. A merged photograph of the Lower Mgeni viewed from the Blue Lagoon side on 20 May 2008: Spring Tide.

Figure 8.8 (Page 202) illustrates the sampled cross-sectional area on 21 February 2008, during which a small scale flooding event took place, as a result of high rainfall. This is evident by the high water levels, which consequently overtopped onto the barrier. Figure 8.9 (Page 202) and Figure 8.10 above shows the mouth of the Mgeni during a neap tide and a spring tide, respectively. During spring tides, the inlet is more defined as a result of the presence of the scour face, as explained above.

8.4. Conclusion

Therefore, the mouth of the Mgeni Estuary can be considered a complex system that undergoes various morphological, hydrodynamic and sedimentological changes. In terms of the hydrodynamics, the downstream inlet channel contains exceptionally high flow velocities, in comparison to the flow velocities recorded further upstream. The inlet channel is dominated by coarse sand that is very well sorted due to strong inlet currents, and mainly coarse skewed, as a result an excess of coarse grained sediments derived from the marine environment. The bed sediments generally contain low organic contents.

In terms of the morphology, the Lower Mgeni has displayed various morphological patterns throughout the period of 1999 to 2008. The lower Mgeni contained a similar morphology from November 2007 through to July 2008. During this period, with the exception of that observed on 19 January 2008, the Lower Mgeni contained a landward protruding barrier extended sandbar. It is believed that the formation of this feature is linked to a high influx of fluvial and marine sediments into the estuary. This barrier extended sandbar originated from the amalgamation of a small sandbar below the M4 Bridge and the landward extending recurved sand barrier.

CHAPTER 9:
CONCLUSIONS

In total, five objectives were presented at the beginning of this study. These objectives worked in conjunction with the aim of the study, which focused on the quantification and assessment of the suspended sediment flux of the Mgeni Estuary, including an investigation of the concomitant implications on the sediment dynamics and geomorphology. Estuaries are important coastal features in terms of environmental, ecological and economic benefits. The sediment supply or output from estuaries into the nearshore zone, particularly bedload, plays an important role in nearshore sediment dynamics, as it aids deposition and accretion.

9.1. Objectives

9.1.1. To quantify the discharge and suspended sediment, input and output from the Mgeni Estuary, during specific conditions, as follows:

- ***mouth state,***
- ***seasonal variations,***
- ***tidal cycles and,***
- ***extreme events (floods and droughts).***

A single cross-section positioned within the tidal inlet of the Lower Mgeni was sampled seasonally and on a spring-neap tidal basis at an approximate 2-hour interval, from 12 January 2008 to 3 July 2008. The channel discharge was quantified using the velocity-area method outlined by Gordon *et al*. (1992), and suspended and estuary bed sediment samples were collected along each channel profile, which formed part of the hydrodynamic study.

- **Mouth State**

Throughout the sampling period, the mouth state of the estuary was classified as open, which indicated that the tidal inlet formed a permanent feature in the estuarine morphology. Therefore, the mouth state of the estuary did not present any variations in terms of the discharge and suspended sediment input and output, as the estuary was open throughout the sampling period.

- **Seasonal Variations**

It is clear that seasonal variations exist in terms of the channel discharges and suspended sediment concentrations, as a result of the seasonal distribution of rainfall. On average, the channel discharges were highest during summer and lowest in autumn. High discharges were established in summer, as a result of the high amount of rainfall. It was established with the use

of scatter-plots, that the channel discharge is positively correlated to rainfall, parallel to the findings of previous studies. Despite the winter months containing the lowest rainfall, it contained the second highest average channel discharges, as a result of the greater flood tidal influence at the mouth of the estuary as explained by Ngetar (2002).

Parallel to the seasonal variations in channel discharge, average suspended sediment concentrations were highest during summer and lowest in autumn. A strong, positive correlation was established between the rainfall and suspended sediment concentrations in the estuary. High amounts of rainfall indicate more catchment draining and a greater delivery of sediments to the coast, however during dry seasons the sediment availability thus decreases (Kitheka *et al*., 2005). Therefore, particularly at the beginning of the wet season, exceptionally high suspended sediment concentrations are evident because large amounts of sediment become available (Kitheka *et al*., 2005). Winter contains a higher average suspended sediment concentration than autumn, as a result of a higher flood tidal influence at the mouth of the estuary as explained above (Ngetar, 2002), which causes more turbulence (Theron, 2007).

- **Tidal cycles**

Conforming to theory and previous works, the channel discharges and suspended sediment concentrations were higher during spring tides than neap tides, throughout the sampling period. This occurs as a result of the greater tidal range during spring tides (Davis and FitzGerald, 2004), which causes greater cross-sectional areas at high water and more turbulence, which increases the discharges and suspended sediment concentrations.

In summer, maximum channel discharges intersected mainly with the flood tide. On the spring tides in autumn and winter, maximum channel discharges occur on the flood tide and on the neap tides in autumn and winter, maximum channel discharges occur on the ebb tide. This occurs as a result of the greater tidal range and cross-sectional area during spring tides, as explained above (Davis and FitzGerald, 2004).

Spring tides in winter and autumn contained maximum concentrations during flood tides, whereas spring tides in summer contained maximum concentrations mainly during ebb tides. The reason for this is that higher rainfall and fluvial discharge occurs during summer, which enhances the ebb tide and suspended sediment concentrations, which is related to the concept explained above by Kitheka *et al.* (2005). Conversely, flood tides during spring tides, being enhanced during low fluvial discharges in winter and autumn (Ngetar, 2002), create more turbulence as a result of waves and tides, which re-suspends the bottom sediments and elevates the suspended sediment concentrations (Theron, 2007).

- **Extreme Event**

The channel discharge and suspended sediment concentrations were measured during an extreme event in the form of a seasonal flooding event, which took place on 21 February 2008. During this time, the estuary received high amounts of rainfall prior to this day. This small-scale seasonal flooding event resulted in the highest cross-sectional suspended sediment concentrations measured throughout the sampling period. Furthermore, high channel discharges were measured on this day, particularly during the ebb tide, as a result of the strong fluvial discharge which consequently accelerated and enhanced the ebb flow on this day due to the river flood.

9.1.2. To assess the contribution of suspended sediment fluxes to the nearshore/beach and estuarine environments, under the specified conditions.

The suspended sediment flux is a function of velocity, cross-sectional area and suspended sediment concentration. The suspended sediment fluxes calculated for each cross-sectional profile plotted throughout the sampling period were found to display spring-neap and seasonal variability. The suspended sediment flux throughout the sampling period ranged from 10.77 g/s to 1102.36 g/s. In terms of seasonal variations, suspended sediment fluxes were highest in summer and lowest in autumn, which is linked to the seasonal rainfall distribution and tidal influence at the mouth of the estuary, as explained above. Furthermore, the suspended sediment fluxes were much higher on spring tides than neap tides, as a result of the greater tidal range and turbulence that occurs with spring tides (Davis and FitzGerald, 2004; Theron, 2007). Maximum suspended sediment fluxes intersect mainly with the ebb tide during neap tides and with the flood tide during spring tides, which means that during neap tides, suspended sediment fluxes are directed seaward on the ebb tide, indicative of an output or export of suspended sediment from the estuary. Therefore, during neap tides it is likely that suspended sediment is transported out of the estuary to the nearshore zone, which results in generalized erosion in the estuary. However during spring tides, suspended sediment fluxes are directed landward on the flood tide, indicative of suspended sediment ingress into the estuary from the nearshore zone, which results in generalized deposition in the estuary. Therefore, the estuary is considered as a sediment exporter during neaps and a sediment sink during spring tides.

9.1.3. To investigate the sediment dynamics of the Mgeni Estuary, in terms of the current velocity, suspended and estuarine bed sediment, hence sediment movement.

Spring-neap and seasonal variations exist for most of the measured parameters throughout the sampling period. On average, the channel flow velocities were highest during summer and lowest

during autumn, which is linked to the seasonal rainfall distribution and tidal influence at the mouth of the estuary, as explained above. Furthermore, channel flow velocities were higher during spring tides than neap tides, as a result of the greater tidal range during springs, as explained above (Davis and FitzGerald, 2004). During both neap tides and spring tides in summer, the average velocities revealed to be highest on the ebb tide. In autumn and winter, maximum velocities intersect with the ebb tide during neap tides and on the flood tide during spring tides. Therefore, during summer and the neap tides in autumn and winter, the ebb tide flows faster than the flood tide, indicating a higher potential for sediments to be transported out of the estuary. However, during spring tides in autumn and winter, there is a greater potential for sediments to be transported into the estuary.

Sedimentologically, the sediments within the tidal inlet of the estuary generally range from fine sand to coarse sand, however on average the estuary bed is dominated by medium sand. The sediments throughout the estuarine cross-section are completely classified as very well sorted, as a result of the strong tidal currents that constantly re-work, transport and sort the sediments within the channel. Furthermore, the profile mean grain sizes displayed higher values in autumn and winter, as compared to summer. No clear relationship was established between the flow velocity and mean grain size of the estuary channel. However generally, as the flow velocity decreases, the estuary bed tends to dominated by coarse sediments, since the flow is not strong enough to transport coarse sediments; hence the sediments are deposited along the estuary bed (Cooper, 1991a).

In terms of sediment skewness, the sediments range from near symmetrical to fine skewed. The sediments are mainly coarse skewed in summer, and between near symmetrical and fine skewed in winter. In terms of kurtosis, on average the sediments in the estuary inlet mainly display mesokurtic curves hence are normally distributed. Parallel to the findings of previous studies, the sediments within the estuary inlet contained extremely low organic contents, as the inlet is a very active zone, dominated by strong tidal currents and waves, which reduces the potential for the sediments to attract and maintain high percentages of organics. Furthermore, in general the bed sediments contain low mud contents, therefore eliminates the affinity to organic matter. Therefore, the sediments within the estuary inlet are classified on average, as medium grained, very well sorted, near symmetrical to fine skewed and mesokurtic, with extremely low organic contents and mud contents.

9.1.4. To determine the sediment and geomorphological characteristics of the estuarine, barrier and coastal environment, through topographical surveying of the barrier environment in order to establish beach profiles, including an analysis of the beach gradient.

Fieldwork for the geomorphological study incorporated seasonal topographical surveying, measurement of beach slope angle and the collection of surface sediment samples. The survey profiles revealed four geomorphic zones including the estuary, lagoonward slope, berm and swash zones (Garden, 2003; Garden and Garland, 2005). Each of these geomorphic zones contains specific sedimentological and geomorphological patterns. Similar to a typical dynamic beach environment, most of the plotted profiles throughout the sampling period, displayed variations in shape and slope, with the progression from the Beachwood Mangroves in the north to the Mgeni mouth in the south. In general, the profiles become flatter and finer from the Beachwood Mangroves towards the Mgeni mouth, conforming to the concept explained by Bascom (1959) and Komar (1998), which occurs as a result of the sheltering nature of the groyne. Both the tidal creek and the mouth of the estuary are classified as sediment sources. Therefore, in certain cases, fining towards the middle of the barrier, away from the sediment sources is apparent. In general, the barrier extended sandbar remained consistent throughout the fieldwork, creating a large depression immediately north of it.

Generally, summer profiles contained lower elevations than the winter profiles. The profiles plotted during autumn formed the transition phase from summer profiles to winter profiles. The summer profiles were classified as storm profiles and the winter profiles were classified as swell profiles, conforming to the concept of Dardis and Grindley (1988). The winter profiles were punctuated with a steep vertical erosion face at the top of the swash zone just below the berm crest, which made these profiles appear much steeper than the summer profiles. Furthermore, the winter profiles contained more distinct berms than the summer profiles.

The estuary zone remained fairly flat or contained a low gradient throughout the sampling period, except in the occurrence of deep depressions, particularly located behind and northward of the barrier extended sandbar. Conversely, the lagoonward slope contained some of the steepest slope angles particularly within summer, whilst the berm was classified as fairly flat, although gently landward dipping in most cases. The swash zone contained relatively steep slopes and contained maximum slope angles in winter and most of autumn and summer.

In terms of the seasonal sediment characteristics, it was found that the sediments within each geomorphic zone were coarsest during summer, as a result of the seasonal distribution of rainfall.

Throughout all four geomorphic zones, the estuary contained the finest sediments, whilst the lagoonward slope contained the coarsest sediments. Furthermore, the lagoonward slope was classed as lag deposit in which the fine particles were winnowed away, leaving behind coarse sediment particles (Garden, 2003). The berm was dominated by medium to coarse sand, although displayed large variations in mean grain size between the sample points. The berm contains slightly coarser sediments than the swash zone.

The sediments within the vicinity of the Beachwood Mangroves Tidal Creek are mainly coarse and coarse skewed. The skewness of the lagoonward sediments is influenced by the estuary sediments, as a result of overtopping. However in general the lagoonward sediments are classified as coarse skewed. Along with the variation in grain size, the berm sediment skewness ranges from coarse skewed to fine skewed. The swash zone is considered as the most complex and energetic geomorphic zone throughout the study area and it is dominated by near symmetrical and fine skewed sediments. The sediments throughout each geomorphic zone and season are classified as very well sorted, as a result of the overall high energy levels throughout the zone, which are capable of sorting and re-working the sediments efficiently. A strong, positive correlation was established between the mean grain size, slope angle and gradient, which conform to the relevant theories outlined in Chapter Three.

Despite the relatively low organic matter contents, the fine grained estuarine sediments contained the highest organic contents, whilst the beach and barrier sediments contained negligible organic contents. This led to an inverse correlation between mean grain size and organic content. High organic contents were restricted to calm, deep regions in the estuary, as well as within the vicinity of the mangroves. Furthermore, a strong, positive correlation was established between the mud content and the organic content.

9.1.5. To study the concomitant implications for coastal and estuarine geomorphology, such as erosion and accretion.

Derived from the geomorphological study, the beach profiles seemed to undergo beach erosion in summer and beach accretion in winter, as a result of storm waves and swell waves in summer and winter respectively, as pointed out by Dardis and Grindley (1988). Therefore, the profiles were steeper and contained a well defined berm in winter than in summer.

Hydrodynamically, the estuary received high amounts of rainfall in summer and low amounts of rainfall in winter. This seasonal rainfall pattern influenced the sedimentary characteristics and patterns within the estuary. Based on the suspended sediment concentrations and estuary bed

sediment, on average the highest concentrations and coarsest sediments occur in summer. Therefore, there is a large potential to supply sediment to the nearshore zone in summer.

Based on the suspended sediment fluxes, the estuary is generally considered as a sediment exporter during neaps and a sediment sink during spring tides. Therefore during neap tides, the estuary tends to deliver more suspended sediment to the nearshore zone, where it may act as a sediment supply to the surrounding beaches or be transported offshore or alongshore, or settle on the beachface where it may dry out and become susceptible to wind transport and consequently transported inland for dune formation. Therefore, during neap tides, suspended sediment is supplied from the estuary to the surrounding nearshore zone, in which it may supplement to the mass of the sediment within this region.

However, during spring tides the estuary is likely to undergo suspended sediment accretion, as a result of greater re-suspension of bottom sediments on the flood tide. Therefore, more sediment is transported and deposited into the estuary during spring tides, in which it may influence the water quality and turbidity of the water column, settle and deposit at the tip of flood tide to create sandbars and deltas, which is evident in the Mgeni as a result of the formation of the barrier extended sandbar or settle in the estuary to be redistributed by the next incoming flood tide. Consequently, the estuary supplies suspended sediment to the nearshore zone during neap tides and undergoes marine accretion during spring tides.

The presence of the Inanda Dam also influences the sediment dynamics, since it reduces the fluvial flow and coarse fluvial sediments supplied to the estuary (Garland and Moleko, 2000; Ngetar, 2002). Based on the suspended sediment fluxes and the morphological assessment of the Mgeni, the system has undergone accretion over the past few years, based on the accretion of flood-tidal deltas, sandbars and eventually the barrier extended sandbar. Therefore, it is possible to consider the Mgeni Estuary not only as an exporter of sediments, but also as a sink for marine sediments (Cooper, 2001).

Furthermore, throughout the sampling study the geomorphology of the Mgeni Estuary remained fairly similar with an open tidal inlet, a sand barrier punctuated with cusps and fans on the estuary side, as well as the presence of a barrier extended sandbar. An open mouth ensures a free exchange of tidally-driven marine flow and fluvial flow, as well as sediments. This open mouth nature of the estuary occurs as a result of the construction of groyne on the south side of the estuary inlet, as well as large fluvial discharges. However, should the fluvial flow decrease rapidly such as in winter, then marine sedimentation and deposition in the estuary mouth may cause mouth closure.

9.2. Limitations and Recommendations

The fieldwork aspect of this research presented a few limitations regarding the fieldwork equipment and access. The Mgeni inlet was accessed via the Beachwood Mangroves, which is managed by KZN Wildlife and is positioned to the north of the barrier. Access was restricted from 8 am to 4 pm, which means that the sampling process had to occur between these times and could not extend any earlier or later. Therefore, sampling during this time mainly ensured plotting of four profiles at two hour intervals. However, if access was granted for longer periods, then the more profiles could have been plotted.

Therefore, although the aims and objectives of this study have been addressed, further monitoring and studying in the Mgeni Estuary is required, considering that it is positioned on the doorstep of Durban and it is a major river and estuarine ecosystem in the province. The aspect of bedload transport should be studied, as bedload does play a large role in influencing the geomorphology of surrounding beaches and the estuary itself. Furthermore, more detailed and longer-period sampling should take place at shorter time intervals, such as hourly intervals. Long-term monitoring of the suspended sediment loads and concentrations should be done, as suspended sediment influences pollution in the estuary, as certain pollutants bind to the sediments, which is a major problem in the estuary.

REFERENCES

Allanson, B. and Baird, D. (1999). Fifteen years on! One hundred and fifty years on! In Allanson, B. and Baird, D. (Eds), *Estuaries of South Africa*, Cambridge University Press, United Kingdom, 1-4.

Allen, J. R. L. (1985). *Principles of Physical Sedimentology*, George Allen and Unwin Publishers, London.

Allen, J. R. L. (1994). Fundamental properties of fluids and their relation to sediment transport processes. In Pye, K. (Ed), *Sediment Transport and Depositional Processes*, Blackwell Scientific Publications, Oxford, 25-60.

Badenhorst, P., Cooper, J. A. G., Crowther, J., Gonsalves, J., Grobler, N. A., Illenberger, W. K., Laubscher, W. I., Mason, T. R., Moller, J. P., Perry, J. E., Reddering, J. S. V. and van der Merwe, L. (1989). *Survey of September 1987 Natal Floods*, South African National Scientific Programmes Report Number 164, 1989, Council for Scientific and Industrial Research (CSIR), Pretoria, South Africa.

Barnes, K. (1999). *Water Chemistry of the Greater Mkuze Swamp System*, Unpublished Honours Thesis, University of Natal, Durban.

Bascom, W. N. (1959). The relationship between sand size and beach-face slope, *American Geophysical Union Trans*., 32 (6): 866-874.

Bascom, W. N. (1960). Beaches, Reprinted from *Scientific American*, W. H. Freeman and Company, California.

Bate, G. C., Whitfield, A. K., Adams, J. B., Huizinga, P. and Wooldridge, T. H. (2002). The importance of the river-estuary interface (REI) zone in estuaries, *Water SA*, 28 (3): 271-279.

Beck, J. S. (2005). *Sediment Transport Dynamics in South African Estuaries*, Unpublished PhD Thesis, University of Stellenbosch, South Africa.

Beck, J. S., Theron, A. K., Kemp, A. Huizinga, P. and Basson, G. R. (2004). *Hydraulics of Estuarine Sediment Dynamics in South Africa: Implications for Estuarine Reserve Determination and the Development of Management Guidelines*, WRC Report No. 1257/1/04, Water Research Commission, South Africa.

Begg, G. W. (1978). *The Estuaries of Natal*, Pietermaritzburg: Natal Town and Regional Planning Report, Volume 41, The Natal Town and Regional Planning Commission, Pietermaritzburg, South Africa.

Begg, G. W. (1984). *The Estuaries of Natal: Part 2*, Pietermaritzburg: Natal Town and Regional Planning Commission, Pietermaritzburg, South Africa.

Bird, E. (2000). *Coastal Geomorphology: An Introduction*, John Wiley and Sons Publishers, Chichester.

Blackshaw, J. A. (1985). *An Analysis of Fluvial and Beach Sediment in the Lower Mgeni River and Immediate Beach Vicinity*, Unpublished Honours Thesis, University of Natal, Durban.

Breen, C. M. and McKenzie, M. (Eds). (2001). *Managing Estuaries in South Africa: An Introduction*, Institute of Natural Resources, Pietermaritzburg.

Breetzke, T., Parak, O., Celliers, L., Mather, A., Colenbrander, D. R. (Eds). (2008). *Living with Coastal Erosion in KwaZulu-Natal: A Short-term, Best Practice Guide*, KwaZulu-Natal Department of Agriculture and Environmental Affairs, Cedara, Pietermaritzburg.

Buller, A. T. and McManus, J. (1979). Sediment sampling and analysis. In Dyer, K. R. (Ed), *Estuarine Hydrography and Sedimentation: A Handbook*, Cambridge University Press, London, 87-130.

Burt, J. E. and Barber, G. M. (1996). *Elementary Statistics for Geographers*, Second Edition, The Guilford Press, New York.

Chen, S., Zhang, G., Yang, S. and Shi, J. Z. (2006). Temporal variations of fine suspended sediment concentration in the Changjiang River estuary and adjacent coastal waters, China, *Journal of Hydrology*, 331: 137-145.

Childers, D. L. and Day, J. W. (1990). Marsh-water column interactions in two Louisiana estuaries I. sediment dynamics, *Estuaries*, 13 (4): 393-403.

Cooper, J. A. G. (1986). *Subaerial Washover Fans in the Beachwood Mangrove Area, Durban*, South African Committee for Oceanographic Research, South Africa.

Cooper, J. A. G. (1990). Ephemeral stream-mouth bars at flood-breach river mouths on a wave-dominated coast: Comparison with ebb-tidal deltas at barrier inlets, *Marine Geology*, 95: 57-70.

Cooper, J. A. G. (1991a). *Sedimentary Models and Geomorphological Classification of River-mouths on a Subtropical Wave-dominated Coast, Natal, South Africa*, Unpublished PhD Thesis, University of Natal, Durban.

Cooper, J. A. G. (1991b). *Shoreline Changes on the Natal Coast: Mkomazi River Mouth to Tugela River Mouth*, Natal Town and Regional Planning Report Volume 77, The Natal Town and Regional Planning Commission, Pietermaritzburg.

Cooper, J. A. G. (1993). Sedimentation in a river dominated estuary, *Sedimentology*, 40: 979-1017.

Cooper, J. A. G. (1994). Sedimentary processes in the river-dominated Mvoti estuary, South Africa, *Geomorphology*, 9: 271-300.

Cooper, J.A.G. (1995a). *Sea Level Rise and its Potential Physical Impacts on the Shoreline of KwaZulu-Natal, Tugela River Mouth to Mtamvuna River Mouth*, Town and Regional Planning Report Volume 80, Town and Regional Planning Report Commission, Pietermaritzburg.

Cooper, J. A. G. (1995b). Lagoons and microtidal coasts. In Carter, R. W. G. and Woodroffe, C. D. (Eds), *Coastal Evolution: Late Quaternary Shoreline Morphodynamics*, Cambridge University Press, Great Britain, 219-265.

Cooper, J. A. G. (2001). Geomorphological variability among microtidal estuaries from the wave-dominated South African coast, *Geomorphology*, 40: 99-122.

Cooper, J. A. G. (2002). The role of extreme floods in estuary-coastal behaviour: contrasts between river- and tide-dominated microtidal estuaries, *Sedimentary Geology*, 150: 123-137.

Cooper, J. A. G. and Mason, T. R. (1987). *Sedimentation in the Mgeni Estuary*, Sedimentation in Estuaries and Lagoons, S.E.A.L Report Number 2, University of Natal, Durban.

Cooper, J. A. G., Wright, I. and Mason, T. (1999). Geomorphology and sedimentology. In Allanson, B. and Baird, D. (Eds), *Estuaries of South Africa*, Cambridge University Press, United Kingdom, 5-25.

Dalrymple, R. W., Zaitlin, B. A. and Boyd, R. (1992). Estuarine facies models: conceptual basis and stratigraphic implications, *Journal of Sedimentary Petrology*, 62 (6): 1130-1146.

Dardis, G. F and Grindley, J. R. (1988). Coastal geomorphology. In Moon, B. P. and Dardis, G. F. (Eds), *The Geomorphology of Southern Africa*, Southern Book Publishers, Johannesburg, 141-174.

Davis, R. A. (1978). Beach and nearshore zone. In Davis, R. A. (Ed), *Coastal Sedimentary Environments*, Springer-Verlag, New York, 237-286.

Davis, R. A. and FitzGerald, D. M. (2004). *Beaches and Coasts*, Blackwell Science Publishing, United Kingdom.

Day, J. H. (1980). What is an estuary? *South African Journal of Science*, 76: 198.

de Boer, H. (17 April 2008). Sewage leak blamed for pollution: Umgeni culvert a “cesspool”, *Daily News*, 2.

Demetriades, N. (2007). *Investigational Report: An inventory of sandmining operations in KwaZulu-Natal estuaries: Thukela to Mtamvuna* [on-line], Marine and Estuarine Research and Consortium for Estuarine Research and Management (CERM), South Africa, http://www.upe.ac.za/cerm/docum.html, Accessed April 2008.

Demetriades, N. (2009). *Management of Estuaries in South Africa: Assessment Workbook*, Management of Estuaries in South Africa Course May 2009, Marine and Estuarine Research, Durban.

Dyer, K. R. (1973). *Estuaries: A Physical Introduction*, John Wiley and Sons, London.

Dyer, K. R. (1979). Estuaries and estuarine sedimentation. In Dyer, K. R. (Ed), *Estuarine Hydrography and Sedimentation: A Handbook*, Cambridge University Press, London, 1-18.

Dyer, K. R. (1986). *Coastal and Estuarine Sediment Dynamics*, John Wiley and Sons, Chichester.

Dyer, K. R. (1994). Estuarine sediment transport and deposition. In Pye, K. (Ed), *Sediment Transport and Depositional Processes*, Blackwell Scientific Publications, Oxford, 193-218.

Dyer, K. R. (1995). Sediment transport processes in estuaries. In Perillo, G. M. E. (Ed), *Geomorphology and Sedimentology of Estuaries*, Elsevier Science, Amsterdam, 423-449.

Dyer, K. R. (1997). *Estuaries: A Physical Introduction*, Second Edition, John Wiley and Sons, Chichester.

Dyer, K. R., Christie, M. C., Feates, N., Fennessy, M. J., Pejrup, M. and van der Lee, W. (2000). An investigation into processes influencing the morphodynamics of an intertidal mudflat, the Dollard Estuary, The Netherlands: I. Hydrodynamics and suspended sediment, *Estuarine, Coastal and Shelf Science*, 50: 607-625.

Ethekwini Municipality, (2008). Aerial Photograph of the Mgeni Estuary, *Ethekwini Municipality Geographic Information Systems [on-line]*, Ethekwini Municipality, Durban, http://citymaps.durban.gov.za/website/master/viewer.htm, Accessed August 2008.

Ezemvelo KwaZulu-Natal Wildlife (EKZNW), (1987). *September 1987 Flood Aerial Photograph of the Mgeni Estuary*, Ezemvelo KwaZulu-Natal Wildlife, Durban.

Freeman, N. M. and Rowntree, K. (2005). *Our Changing Rivers: An Introduction to the Science and Practice of Fluvial Geomorphology*, WRC Report No. TT 238/05, Water Research Commission, South Africa.

Ganju, N. K and Schoellhamer, D. H. (2006). Annual sediment flux estimates in a tidal strait using surrogate measurements, *Estuarine, Coastal and Shelf Science*, 69: 165-178.

Ganju, N. K, Schoellhamer, D. H. and Bergamaschi, B. A. (2005). Suspended sediment fluxes in a tidal wetland: Measurement, controlling factors, and error analysis, *Estuaries*, 28 (6): 812-822.

Garden, S. (2003). *Spit development in a small, subtropical estuary of KwaZulu-Natal, South Africa: the case of Mdloti Estuary*, Unpublished Honours Thesis, University of Natal, Durban.

Garden, S. E. and Garland, G. G. (2005). Spit development in the Mdloti River estuary, KwaZulu-Natal, *South African Journal of Geology*, 108: 257-270.

Gardner, L. R. and Kjerfve, B. (2006). Tidal fluxes of nutrients and suspended sediments at the North Inlet-Winyah Bay National Estuarine Research Reserve, *Estuarine, Coastal and Shelf Science*, 70: 682-692.

Garland, G. and Moleko, L. (2000). Geomorphological impacts of Inanda Dam on the Mgeni estuary, north of Durban, South Africa, *Bull. Eng. Geol. Env*., 59: 119- 126.

Geyer, W. R., Woodruff, J. D. and Traykovski, P. (2001). Sediment transport and trapping in the Hudson River Estuary, *Estuaries*, 24 (5): 670-679.

Gordon, N. D., McMahon, T. A. and Finlayson, B. L. (1992). *Stream Hydrology: An Introduction for Ecologists*, John Wiley and Sons, Chichester.

Green, A. N. (2004). *The Fish Traps and Sedimentary Dynamics of Kosi Bay Estuary, Northern KwaZulu-Natal, South Africa*, Unpublished MSc Thesis, University of KwaZulu-Natal, Durban.

Green, A. N., Garland, G. G. and Diab, R. (2004). Wind characteristics and blowout formation near Mabibi, Northern KwaZulu-Natal, *South African Geographical Journal*, 86 (2): 47-55.

Grobbler, N. G. (1987). *Sedimentary Environments of Mdloti, uMgababa and Lovu Lagoons, Natal, South Africa*, Unpublished MSc Thesis, University of Natal, Durban.

Hardisty, J. (1990). *Beaches: Form and Process*, Unwin and Hyman, London.

Hardisty, J. (1994). Beach and nearshore sediment transport. In Pye, K. (Ed), *Sediment Transport and Depositional Processes*, Blackwell Scientific Publications, Oxford, 219-255.

Harrison, T. D., Cooper, J. A. G. and Ramm, A. E. L. (2000), *Geomorphology, Ichthyofauna, Water Quality and Aesthetics of South African Estuaries* [on-line], State of estuaries report released on the Internet, CSIR and Department of Environmental Affairs and Tourism, South Africa, http://www.deat.gov.za/soer/news/estuary.htm, Accessed March 2007.

Harrison, T. D., Hohls, D. R., Meara, T. P. & Webster, M. S. (2001). *South African Estuaries: Catchment Land-Cover: National Summary Report* [on-line], Division of Water, Environment and Forestry Technology, CSIR and Department of Environmental Affairs and Tourism, South Africa, http://www.environment.gov.za/soer/estuary/summary.pdf, Accessed 2 October 2006.

Haslett, S. K. (2000). *Coastal Systems*, Routledge, London.

Hay, D. (Ed) (2007). *Estuaries and Integrated Development Planning: A Manager's Guide*, WRC Report TT 294/07, Water Research Commission, Pretoria, South Africa.

Hay, D., Huizinga, P. and Mitchell, S. (2005). *Managing Sedimentary Processes in South African Estuaries: A Guide*, WRC Report TT 241/05, Water Research Commission, Pretoria, South Africa.

Hayes, M. O. (1979). Barrier island morphology as a function of tidal and wave regime. In Leatherman, S. P. (Ed), *Barrier Islands*, Academic Press, New York, 1-23.

Heiri, O., Lotter, A. F. and Lemcke, G. (2001). Loss on ignition as a method for estimating organic and carbonate content in sediments: reproducibility and comparability of results, *Journal of Paleolimnology*, 25: 101-110.

Hill, M. (2004). *Coasts and Coastal Management*, Hodder and Stoughton, London.

Hossain, S., Eyre, B. D. and McConchie, D. (2004). Dry season suspended sediment concentration and sedimentation in the Richmond River estuary, northern NSW, Australia, *Australian Journal of Soil Research*, 42: 203-211.

Jaganath, C. (2008). *Aerial Photograph of the Mgeni Estuary: January 2008*, Durban.

Kao, S., Lee, T. and Milliman, J. D. (2005). Calculating highly fluctuated suspended sediment fluxes from mountainous rivers in Taiwan, *Terrestrial, Atmospheric and Oceanic Sciences*, 16 (3): 653-675.

Kienzle, S. W., Lorentz, S. A. and Schulze, R. E. (1997). *Hydrology and Water Quality of the Mgeni Catchment*, WRC Report TT 97/97, Water Research Commission, Pretoria, South Africa.

King, C. A. M. (1972). *Beaches and Coasts*, Second Edition, Edward Arnold, London.

Kinmont, A. (1961). The nearshore movement of sand at Durban. In CSIR (Ed), *Marine Studies off the Natal Coast*, CSIR Symposium S 2, CSIR, Durban.

Kitheka, J. U., Obiero, M. and Nthenge, P. (2005). River discharge, sediment transport and exchange in the Tana Estuary, Kenya, *Estuarine, Coastal and Shelf Science*, 63: 455-468.

Kjerfve, B. (1979). Measurement and analysis of water current, temperature, salinity and density. In Dyer, K. R. (Ed), *Estuarine Hydrography and Sedimentation: A Handbook*, Cambridge University Press, London, 186-226.

Kleinhans, M. G and Brinke, W. B. M. T. (2001). Accuracy of cross-channel sampled sediment transport in large sand-gravel-bed rivers, *Journal of Hydraulic Engineering*, 127 (4): 258-269.

Komar, P. D. (1983). Beach processes and erosion: An introduction. In Komar, P. D. (Ed), *CRC Handbook of Coastal Processes and Erosion*, CRC Press Inc., Florida, 1-20.

Komar, P. D. (1998). *Beach Processes and Sedimentation*, Second Edition, Prentice Hall, New Jersey.

Lapidus, D. F. and Winstanley, I. (1990). Collins Dictionary: *Geology,* HarperCollins Publishers, London.

Lawrie, R. A. (2007). *Modelling of the Water Balance and Nutrient Dynamics of Mhlanga Estuary*, Unpublished MSc (Eng) Thesis, University of KwaZulu-Natal, Durban.

Le Vieux, A. M. (2007). *An Investigation into the Geomorphological Setting of the Mvoti Estuary, KwaZulu-Natal, South Africa*, Unpublished Honours Thesis, University of KwaZulu-Natal, Durban.

Leuci, R. (1998). *An Assessment of Trace Metal Contamination in Sediments of Durban Harbour and Beachwood Mangroves*, Unpublished Honours Thesis, University of Natal, Durban.

Lewis, D. W. and McConchie, D. (1994). *Analytical Sedimentology*, Chapman and Hall, New York.

Lin, J. and Kuo, A. Y. (2001). Secondary turbidity maximum in a partially mixed microtidal estuary, *Estuaries*, 24 (5): 707-720.

Lindholm, R. C. (1987). *A Practical Approach to Sedimentology*, Allen and Unwin Inc., London.

Lindsay, P., Mason, T. R., Pillay, S. and Wright, C. I. (1996). Suspended particulate matter and dynamics of the Mfolozi estuary, KwaZulu-Natal: Implications for environmental management, *Environmental Geology*, 28 (1): 40-51.

Mangelsdorf, J., Scheurmann, K. and Weiss, F. (1990). *River Morphology: A Guide for Geoscientists and Engineers*, Springer-Verlag, Berlin.

Masselink, G. and Hughes, M. G. (2003). *Introduction to Coastal Processes and Geomorphology*, Hodder Arnold, Great Britain.

Mather, A. (2009). *Personal Communication*.

Mather, A., Kasserchun, R. and Wenlock, H. (2003). *City of Durban sand bypass scheme: 20 year performance evaluation*, Conference on Coastal and Port Engineering in Developing Countries, COPEDEC VI, Colombo, Sri Lanka.

McCarthy, T. S., Stanistreet, I. G. and Cairncross, B. (1991). The sedimentary dynamics of active fluvial channels on the Okavango fan, Botswana, *Sedimentology*, 38: 471-487.

McCave, I. N. (1979). Suspended sediment. In Dyer, K. R. (Ed), *Estuarine Hydrography and Sedimentation: A Handbook*, Cambridge University Press, London, 131-185.

M^{c}Cormick, S., Cooper, J. A. G. and Mason, T. R. (1992). Fluvial sediment yield to the Natal coast: A review, *Southern African Journal of Aquatic Science*, 18 (1/2): 74-88.

McKee, L., Ganju, N., Schoellhamer, D., Davis, J., Yee, D., Leatherbarrow, J. and Hoenicke, R. (2002). *Estimates of suspended-sediment flux entering the San Francisco Bay from Sacramento and San Joaquin Delta* [on-line], San Francisco Estuary Institute, California, http://www.sfei.org/rmp/reports/Sediment_loads_report.pdf, Accessed December 2008.

Morant, P. and Quinn, N. (1999). Influence of Man and management of South African estuaries. In Allanson, B. and Baird, D. (Eds), *Estuaries of South Africa*, Cambridge University Press, United Kingdom, 289-320.

Ngetar, N. S. (2002). *Post-dam Sediment Dynamics Below the Inanda Dam at the Mgeni Estuary, KwaZulu-Natal, (South Africa)*, Unpublished MSc Thesis, University of Natal, Durban.

Nikora, V. I. and Goring, D. G. (2002). Fluctuations of suspended sediment concentration and turbulent sediment fluxes in an open-channel flow, *Journal of Hydraulic Engineering*, 128 (2): 214-223.

Perillo, G. M. E. (1995). Definitions and geomorphic classifications of estuaries. In Perillo, G. M. E. (Ed), *Geomorphology and Sedimentology of Estuaries*, Elsevier Science, Amsterdam, 17-47.

Pethick, J. (1984). *An Introduction to Coastal Geomorphology*, Edward Arnold, Great Britain.

Pillay, S. (1981). *An Analysis and Simulation of Correlation Errors in Net Flux Determinations in Salt Marsh Tidal Channel Systems*, Unpublished MSc Thesis, University of South Carolina, United States of America.

Pye, K. (1994). Properties of sediment particles. In Pye, K. (Ed), *Sediment Transport and Depositional Processes*, Blackwell Scientific Publications, Oxford, 1-24.

Ramsay, P. J. (1994). Marine geology of the Sodwana Bay shelf, southeast Africa, *Marine Geology*, 120: 225-247.

Reid, I. and Frostick, L. E. (1994). Fluvial sediment transport and deposition. In Pye, K. (Ed), *Sediment Transport and Depositional Processes*, Blackwell Scientific Publications, Oxford, 89-155.

Reineck, H. E. and Singh, I. B. (1980). *Depositional Sedimentary Environments: With Reference to Terrigenous Clastics*, Second Edition, Springer-Verlag, Berlin.

Ridderinkhof, H., van der Ham, R. and van der Lee, W. (2000). Temporal variations in concentration and transport of suspended sediments in a channel-flat system in the Ems-Dollard estuary, *Continental Shelf Research*, 20: 1479-1493.

Rossouw, J. (1984). *Review of Existing Wave Data, Wave Climate and Design Waves for South African and South West African (Namibian) Coastal Waters*, CSIR Report T/SEA 8401, CSIR, South Africa.

Scharler, U. M. and Baird, D. (2005). The filtering capacity of selected Eastern Cape estuaries, South Africa, *Water SA*, 31 (4): 483-490.

Schoonees, J. S. (2000). Annual variation in the net longshore sediment transport rate, *Coastal Engineering*, 40: 141-160.

Schubel, J. R. (1972). Suspended sediment discharge of the Susquehanna River at Conowingo, Maryland, during 1969, *Chesapeake Science*, 13 (1): 53-58.

Schumann, E. H. (Ed) (2003). *Towards the Management of Marine Sedimentation in South African Estuaries with Special Reference to the Eastern Cape*, WRC Report No. 1109/1/03, Water Research Commission, South Africa.

Schumann, E., Largier, J. and Slinger, J. (1999). Estuarine hydrodynamics. In Allanson, B. and Baird, D. (Eds), *Estuaries of South Africa*, Cambridge University Press, United Kingdom, 27-52.

Selley, R. C. (1982). *An Introduction to Sedimentology*, Second Edition, Academic Press Inc., London.

Selley, R. C. (2000). *Applied Sedimentology*, Second Edition, Academic Press, United States of America.

Smakhtin, V. U. (2004). Simulating the hydrology and mouth conditions of small temporarily closed/open estuaries, *Wetlands*, 24 (1): 123-132.

South African Navy Hydrographic Office (SANHO), (2008). *South African Tide Tables* [on-line], South African Navy, South Africa, http://www.sanho.co.za/tides/tide_index.htm, Accessed 2007-2008.

South African Weather Services (SAWS) (2008). *Virginia (2007-2008) Rainfall*, South African Weather Services, South Africa.

State of Estuaries Report (SOER), (2001). *South African Estuaries: Catchment Land-Cover: Mgeni Catchment Generalized Land-Cover* [on-line], Department of Environmental Affairs and Tourism, South Africa, http://www.environment.gov.za/soer/estuary/catch/mgen.html, Accessed July 2007.

Stretch, D. and Zietsman, I. (2004). *The Hydrodynamics of Mhlanga and Mdloti Estuaries: Flows, Residence Times, Water Levels and Mouth Dynamics*, WRC Report K5/1247, Water Research Commission, South Africa.

Theron, A. (2007). Sediment dynamics. In Whitfield, A. and Bate, G. (Eds), *A Review of Information on Temporarily Open/Closed Estuaries in the Warm and Cool Temperate Biogeographic Regions of South Africa, with Particular Emphasis on the Influence of River Flow on These Systems*, WRC Report No. 1581/1/07, Water Research Commission, South Africa, 24-41.

Thomas, R. B. (1988). Monitoring baseline suspended sediment in forested basins: the effects of sampling on suspended sediment rating curves, *Hydrological Sciences*, 33 (5): 499-514.

Tucker, M. E. (1981). *Sedimentary Petrology: An Introduction*, Blackwell Scientific Publications, Oxford.

Tucker, M. E. (1991). *Sedimentary Petrology: An Introduction to the Origin of Sedimentary Rocks*, Second Edition, Blackwell Scientific Publications, Oxford.

Turpie, J. K., Adams, J. B., Joubert, A., Harrison, T. D., Colloty, B. M., Maree, R. C., Whitfield, A. K., Wooldridge, T. H., Lamberth, S. J., Taljaard, S. and Van Niekerk, L. (2002). Assessment of the conservation priority status of South African estuaries for use in management and water allocation, *Water SA*, 28 (2): 191-206.

Tyson, P. D. & Preston-Whyte, R. A. (2000). *The Weather and Climate of Southern Africa*, Second Edition, Oxford University Press Southern Africa, Cape Town.

Umgeni Water, (2008). *Suspended Solids Concentrations at the Inanda Weir (1990-2008), Athlone Bridge (1990-1998) and Ellis Brown Viaduct (1990-1998)*, Umgeni Water, Pietermaritzburg.

Uncles, R. J., Elliott, R. C. A. and Weston, S. A. (1985). Dispersion of salt and suspended sediment in a partly mixed estuary, *Estuaries*, 8 (3): 256-269.

van Niekerk, L. (2007). Hydrodynamics. In Whitfield, A. and Bate, G. (Eds), *A Review of Information on Temporarily Open/Closed Estuaries in the Warm and Cool Temperate Biogeographic Regions of South Africa, with Particular Emphasis on the Influence of River Flow*

on These Systems, WRC Report No. 1581/1/07, Water Research Commission, South Africa, 5-23.

Wall, G. R., Nystrom, E. A. and Litten, S. (2008). Suspended sediment transport in the freshwater reach of the Hudson River Estuary in Eastern New York, *Estuaries and Coasts*, 31: 542-553.

Wang, Z., Li, L., Chen, D. Xu, K., Wei, T., Gao, J., Zhao, Y., Chen, Z. and Masabate, W. (2007). Plume front and suspended sediment dispersal off the Yangtze (Changjiang) River mouth, China during non-flood season, *Estuarine, Coastal and Shelf Science*, 71: 60-67.

Water Research Commission (WRC), (2002). *State-of-Rivers Report uMngeni River and Neighbouring Rivers and Streams*, WRC Report No. TT 200/02, Water Research Commission, South Africa.

Wells, J. T. (1995). Tide-dominated estuaries and tidal rivers. In Perillo, G. M. E. (Ed), *Geomorphology and Sedimentology of Estuaries*, Elsevier Science, Amsterdam, 179-205.

Whitfield, A. K. (2000). *Available Scientific Information on Individual South African Estuarine Systems* [on-line], Consortium for Estuarine Research and Management (CERM), South Africa, http://www.upe.ac.za/cerm/datab.html, Accessed June 2007.

Woodroffe, C. D. (2002). *Coasts: Form, Process and Evolution*, Cambridge University Press, United Kingdom.

Wright, C. I. (1990). *The Sediment Dynamics of the St. Lucia Estuary Mouth, Zululand, South Africa*, Unpublished MSC Thesis, University of Natal, Durban.

Wright, C. I. (1995). *The Sediment Dynamics of the St Lucia and Mfolozi Estuary Mouths, Zululand, South Africa*, Geological Survey of South Africa, Bulletin 109, Council for Geoscience, South Africa.

Wright, C. I., Miller, W. R. & Cooper, J.A. G. (2000). The late Cenozoic evolution of coastal water bodies in Northern KwaZulu-Natal, South Africa, *Marine Geology*, 167: 207-229.

Yang, C. T. (1996). *Sediment Transport: Theory and Practice*, The McGraw-Hill Companies, Inc., United States of America.

Yang, S. L., Shi, Z., Zhao, H. Y., Li, P., Dai, S. B., and Gao, A. (2004). Effects of human activities on the Yangtze River suspended sediment flux into the estuary in the last century, *Hydrology and Earth System Sciences*, 8 (6): 1210-1216.

Zietsman, I. (2004). *Hydrodynamics of Temporary Open Estuaries, with Case Studies of the Mhlanga and Mdloti*, Unpublished MSc (Eng) Thesis, University of KwaZulu-Natal, Durban.